PHYSIOCHEMICAL CHARACTERISTICS OF CONTROLLED LOW STRENGTH MATERIALS INFLUENCING THE ELECTROCHEMICAL PERFORMANCE AND SERVICE LIFE OF METALLIC MATERIALS

A Dissertation

by

CEKI HALMEN

Submitted to the Office of Graduate Studies of
Texas A&M University
in partial fulfillment of the requirements for the degree of

DOCTOR OF PHILOSOPHY

December 2005

Major Subject: Civil Engineering

PHYSIOCHEMICAL CHARACTERISTICS OF CONTROLLED LOW STRENGTH MATERIALS INFLUENCING THE ELECTROCHEMICAL PERFORMANCE AND SERVICE LIFE OF METALLIC MATERIALS

A Dissertation

by

CEKI HALMEN

Submitted to the Office of Graduate Studies of
Texas A&M University
in partial fulfillment of the requirements for the degree of

DOCTOR OF PHILOSOPHY

Approved by:

Chair of Committee,	David Trejo
Committee Members,	Kenneth Reinschmidt
	Stuart Anderson
	Daren Cline
Head of Department,	David V. Rosowsky

December 2005

Major Subject: Civil Engineering

ABSTRACT

Physiochemical Characteristics of Controlled Low Strength Materials Influencing the Electrochemical Performance and Service Life of Metallic Materials. (December 2005)

Ceki Halmen, B.S., Bogazici University;
M.S., Texas A&M University
Chair of Advisory Committee: Dr. David Trejo

Controlled Low Strength Materials (CLSM) are cementitious self-compacting materials, comprised of low cement content, supplementary cementing materials, fine aggregates, and water. CLSM is typically used as an alternative to conventional compacted granular backfill in applications, such as pavement bases, erosion control, bridge abutments, retaining walls, bedding and backfilling of pipelines. This dissertation presents the findings of an extensive study carried out to determine the corrosivity of CLSM on ductile iron and galvanized steel pipelines. The study was performed in two phases and evaluated more than 40 different CLSM mixture proportions for their corrosivity. An extensive literature survey was performed on corrosion of metals in soils and corrosion of reinforcement in concrete environments to determine possible influential factors. These factors were used as explanatory variables with multiple levels to identify the statistically significant factors. Empirical models were developed for percent mass loss of metals embedded in CLSM and exposed to different environments. The first and only service life models for ductile iron and galvanized steel pipes

embedded in CLSM mixtures were developed. Models indicated that properly designed CLSM mixtures can provide an equal or longer service life for completely embedded ductile iron pipes. However, the service life of galvanized pipes embedded in CLSM should not be expected to be more than the service life provided by corrosive soils.

To my parents, Daniyel and Rebeka Halmen…

ACKNOWLEDGEMENTS

I am grateful to my advisor, Dr. David Trejo, for his support and encouragement throughout my doctoral studies. Although I did not realize it at the time, his persistent demand for excellence and attention in details helped me to perform a high quality research that resulted in this dissertation. The valuable input of my committee members from the Civil Engineering Department, Dr. Kenneth Reinschmidt and Dr. Stuart Anderson are gratefully acknowledged. I would also like to express my gratitude to my committee member, Dr. Daren Cline, for spending a large number of hours to review and improve my statistical analysis.

A special thanks to my former adviser, Dr. Nancy Holland, for her support during my adaptation period in the USA.

Without a doubt it would not be possible to complete this dissertation without the help and support of my colleagues who are also known as the Dr. Trejo Research Group in the Civil Engineering Department. We spent long days and nights in our assigned area in the basement of the old Civil Engineering Building. I would especially like to acknowledge my friends Radhakrishna Pillai, Francisco Aguiniga, Benjamin Schaefer, Michael Esfeller, Aaron Hoelscher, and my late friend Michael Gamble for their help and support.

Like all of the research projects, mine also could not be completed without the help and expertise of our technical staff: Gary Gerke, Scott Cronauer, Kirk Farmer, Jeffrey Perry, Matthew Potter, and Mike Linger. Special thanks to Richard Gehle and Pam Kopf for helping me with all the bureaucratic issues.

I would like to thank all the members of the Hillel organization whom I call my extended family in College Station for their help and support, especially Rabbi Peter Tarlow.

I am grateful to my friends, Jozef Adut, Altug Aksoy, Sualp Aras, Burak and Fusun Meric, Neset Kabbani, Aykut Arac, and especially Celile Itir Gogus who were always there for me during my studies and who endured my endless stories about my experiments. Thank you guys, I could not do it without your friendship and support.

Last but not least, my very special thanks and love to my Mom and Dad who made this whole thing possible with their unconditional love and support. Thanks to my sisters, Elzi and Lina, and to all my family members who believed in me. I hope I can always be worthy of your trust and love.

TABLE OF CONTENTS

CHAPTER Page

CHAPTER Page

LIST OF FIGURES

FIGURE Page

FIGURE Page

FIGURE Page

FIGURE Page

LIST OF TABLES

TABLE Page

TABLE Page

CHAPTER I

INTRODUCTION

Controlled Low Strength Material (CLSM) is a self-flowing cementitious material consisting typically of portland cement, fine aggregates, supplementary cementing materials (SCMs), and water. CLSM as an alternative to conventional, compacted backfill materials has a variety of applications such as conduit bedding, pavement bases, erosion control, bridge abutments, retaining walls, backfilling under foundations, void fill of abandoned tanks, bedding for pipelines and culverts, and backfilling of pipelines. CLSM has several inherent advantages due to its self-leveling characteristics, such as reduced labor and equipment costs, faster construction, and easier placement in inaccessible areas. Also, the use of by-products, such as fly ash and other SCMs, is more environmentally friendly when compared with depositing these materials into landfills.

Although CLSM has shown much promise, the use of CLSM is not as common as would be expected considering the potential benefits. A major challenge in implementing the use of CLSM is the lack of knowledge on the material in the materials and construction fields. Engineers are reluctant to specify CLSM because limited data are available on the corrosion performance of metallic pipe materials embedded in CLSM.

Existing guidelines on the effect of CLSM on the corrosion performance and service life of metallic pipes are not available. Two of the most commonly used existing guidelines for determining the corrosivity of conventional, compacted backfill materials

---

This dissertation follows the style of the *ACI Materials Journal*.

are the ANSI/AWWA C105 method developed by the Ductile Iron Pipe Research Association (DIPRA) and the CALTRANS 643 method developed by the California Department of Transportation. The ANSI/AWWA C105 method assesses the corrosivity of soils for ductile iron pipes and the CALTRANS 643 method estimates the service life of galvanized steel pipes embedded in soils. Both methods do not consider the unique characteristics of CLSM and may not reliably predict the performance of CLSM. Although these prediction methods are not specifically developed for cementitious materials such as CLSM, they are often applied to these materials and often indicate that CLSM could be detrimental to the corrosion performance of metallic pipelines.

An extensive research program has been carried out to extend the knowledge on the corrosivity of CLSM on metallic pipe materials and to establish guidelines and models on the service life estimation of metallic pipelines embedded in CLSM. Ductile iron and galvanized corrugated steel evaluated due to their common use in major water distribution mains, sewer, and storm drains. Electrochemical properties of these materials in CLSM environments were investigated. The study was performed in two phases and evaluated a total of 43 different CLSM mixtures.

The corrosion of ductile iron and corrugated galvanized steel embedded in CLSM was evaluated through mass loss measurements of coupons. Even though examination of corrosion through this method is one of the most time consuming corrosion testing techniques, it is also one of the more reliable techniques available in the literature. In both phases metallic coupons embedded in CLSM mixtures were exposed to different environments for 18 (Phase I) and 21 months (Phase II).

An extensive literature survey was performed to identify influential factors on the corrosion of metallic pipelines embedded in soils and CLSM. Several of these factors were used in designed experiments as variables with multiple levels to determine their significance on the corrosion performance of ductile iron and galvanized steel embedded in CLSM. These factors included cement content, water content, fly ash type, fly ash content, fine aggregate type, fine aggregate content, pH, and resistivity.

Corrosion of metallic coupons embedded in different CLSM mixtures was evaluated in two different environments; distilled water and sodium chloride solution. Chloride ion induced corrosion is accepted as one of the major corrosion processes in cementitious systems. Therefore, the exposure of samples to the two environments with and without the chloride ions and the comparison of results were performed.

The corrosion performance of metals embedded in CLSM when this material was used in conjunction with conventional backfill materials was another important issue observed in the literature. A special experimental setup was designed and used to evaluate the corrosion performance of the ductile iron and galvanized steel coupons that were in contact with CLSM and conventional backfill materials simultaneously throughout their entire exposure period.

Empirical service life estimation models for ductile iron and galvanized steel pipelines embedded in CLSM were developed. The models consider the constituent materials and other characteristics of CLSM mixtures as well as the environmental factors. The service life models developed in this dissertation are the first and only available guidelines for the corrosivity of CLSM on metallic pipelines.

To generate the findings from this research, a comprehensive methodology was followed. The chapters in this dissertation describe critical issues, methodologies, and findings of the research. This dissertation is comprised of seven chapters. A brief summary of each chapter is provided below.

Chapter II summarizes the state-of-the-art and current practice related to CLSM. Typical applications, advantages, and challenges of CLSM are also provided with case histories. Fresh and hardened properties, test methods, and constituent materials of CLSM were discussed in detail. Topics such as CLSM specifications and quality assurance and quality control were also discussed.

Chapter III provides information on principles of electrochemical corrosion processes and a comprehensive review of underground corrosion mechanisms of metallic pipelines. Electrochemical characteristics of ductile iron and galvanized steel are also provided. This chapter also discusses the limited number of preceding studies

found in the literature on the corrosion of metallic materials embedded in CLSM mixtures.

Chapter IV presents the experimental program of the study. The CLSM mixtures used in the two phases of the study and material characteristics of the constituent materials are provided. Information on the testing methods and standards used to evaluate different factors is also provided in this section.

Chapter V presents the data from electrochemical testing and the statistical analysis. The influence of different continuous and classification variables on the percent mass loss of the metallic coupons embedded in CLSM exposed to different environments is discussed. Results are presented and compared with the findings of the previous research on the corrosion of metallic materials embedded in soils. Empirical models were also developed to estimate the percent mass loss of ductile iron and galvanized steel in different CLSM mixtures.

Chapter VI discusses the methodology to calculate probabilistic service life estimates for ductile iron and galvanized steel pipes embedded in CLSM. The information in this chapter will probably be most useful to the practicing engineer. Comparison of developed models with the existing corrosion guidelines for metallic materials embedded in soils was performed. Service life estimates obtained for similar environments using the existing and the developed models were compared.

Chapter VII contains a brief summary of the dissertation and lists the important findings and conclusions.

CHAPTER II

CHARACTERISTICS OF CLSM – BACKGROUND

2.1.Introduction and Definitions

Controlled Low Strength Material (CLSM) is a self-flowing cementitious material typically consisting of small amounts of portland cement, fine aggregates, supplementary cementing materials (SCM), and water. Fine aggregates and the SCMs are also referred to as filler material in the literature and these materials make up the largest portion of the mixture. CLSM is primarily used as a backfill material in lieu of compacted fill (ACI-229 1994). In 1984, The American Concrete Institute (ACI) founded Committee 229 that reports on CLSM applications, developments, material properties, mix proportioning, and construction and quality control procedures (Brewer 1994). The Committee defined the upper limit of compressive strength of CLSM at 28 days as 8.3 MPa (1200 psi) (ACI committee 116R Cement and Concrete Technology). However, when CLSM is used for pipeline backfilling applications the recommended compressive strength range at 28 days is between 0.34 and 0.69 MPa (50 to 100 psi) (Kaneshiro et al. 2001). The low compressive strength is required to be able to easily excavate the material later, if needed.

Many different names, either technically correct or incorrect, were used in the literature for CLSM. CLSM is referred to as controlled density fill, controlled pavement base, controlled structural fill, controlled thermal fill, flowable fill, unshrinkable fill, flowable mortar, flowable fly ash, fly ash slurry, fly ash fill, flowable grout, plastic soil-cement, soil cement slurry, anti-corrosion fill, one-sack mix, K-Krete, M-Crete, and S-Crete. However, ACI committee 229 consistently uses the term Controlled Low Strength Material.

2.2.Historical Development

The historical development of CLSM is reported in detail by Brewer (1994) who himself played an important role in the development of this material. CLSM was developed in the 1970s by engineers from Detroit Edison Company and Kuhlman Corporation as an alternative to conventional backfill. Detroit Edison Company was looking for a possible use of fly ash (a by-product of their energy production) and to reduce their fly ash stockpiling needs. Kuhlman Corporation was looking for extended use of their ready mixed concrete trucks.

Conventional backfilling of all types of excavations are performed using granular materials. Granular materials (soils) are placed, spread, and compacted in thin layers to achieve a specified compaction level. This process is time consuming and difficult and often not properly followed by contractors. Improper compaction of backfill materials causes excessive settlement problems with time. Excessive settlement as a result of poor backfill compaction was reported as an important reason for the deterioration of urban roads in the United States and Canada (Baker and Goodrich 1995). The objective of the initial research supported by Detroit Edison Company and the Kuhlman Corporation was to develop a low strength mixture using fly ash that could be used as an alternative to conventional backfill materials. Low strength was an important consideration in order to be able to re-excavate the CLSM as easily as conventional backfill.

Initial studies at the University of Toledo produced a low compressive strength material containing high volumes of fly ash. The two companies named the new material K-crete and founded K-crete Inc. The company acquired four United States patents for this material. In 1974 K-crete Inc. had several franchises in numerous states and K-crete Inc. of Canada was founded. Currently the patents of the material are assigned to the National Ready Mixed Concrete Association (NRMCA) for general use. Therefore producers and contractors can use this material and similar materials as an alternative to conventional backfill materials.

2.3.Applications

Due to its many inherent advantages, such as easy placement, self compaction, etc., CLSM has found many applications that are well documented in the literature. Many state agencies have published specifications for the use of CLSM for different applications (Riggs and Keck 1998). Main applications of CLSM listed by the NRMCA are:

- Backfilling of sewer trenches, utility trenches, building excavations, bridge abutments, and conduit trenches
- Structural fill for road base, mud jacking, sub footing, floor slab base, and pipe bedding
- Backfilling of void underground structures, such as underground storage tanks, and abandoned sewers
- Slope stabilization and soil erosion control

The use of CLSM for encapsulation of contaminated soil was also documented in the literature (Melton et al. 2005). It was also indicated that appropriate CLSM mixtures can be designed as anti corrosion fill, thermal fill, and pavement subbase (Brewer 1994). Also a survey performed among state agencies found that CLSM was used for bedding applications for granite curbs and as lightweight fill to cover swamp areas (Folliard et al. 1999). The results of the same survey indicated that the relatively high cost of CLSM and lack of knowledge on the use, testing, and performance of CLSM were impediments to its widespread use. Another survey performed in 1995 found that ninety percent of the 3000 ready mixed concrete producers in the United States produce some type of CLSM (EPA 1998).

2.4.Advantages

The advantages of CLSM are well documented in the literature. Although CLSM generally costs more per cubic yard than most soil or granular backfill materials,

its use may result in lower in-place costs due to its many advantages. In 1991 a list of 15 main advantages of CLSM was published (Smith 1991). The list was later adopted by the ACI 229 committee and included in their report on CLSM (ACI 1994). Recently a modified version of the list with 17 items was presented in American Society of Civil Engineers Pipeline Conference in 2001 (Kaneshiro et al. 2001). These advantages are as follows:

1. **Readily available:** Using locally available materials, ready mixed concrete suppliers can produce CLSM to meet most project specifications.
2. **Easy to deliver:** Truck mixers can deliver specified quantities of CLSM to the jobsite whenever the material is needed.
3. **Easy to place:** Depending on the type and location of void to be filled, CLSM can be placed by chute, conveyor, pump, or bucket. Because CLSM is self-leveling, it needs little or no spreading or compacting. This speeds construction and reduces labor requirements.
4. **Versatility:** CLSM mixture proportions can be adjusted to meet specific performance requirements. Mixtures can be adjusted to improve flowability. More fly ash or cement can be added to increase strength and admixtures can be added to adjust setting times and other performance characteristics. Adding foaming agents to CLSM produces a lightweight, insulating fill.
5. **Strength and durability:** Load-carrying capacities of CLSM typically are higher than those of compacted soil or granular fill. CLSM also is less permeable, thus more resistant to erosion. For use as a permanent structural fill, CLSM can be designed to achieve 28 day compressive strength as high as 8.3 MPa (1200 psi).
6. **Excavatability:** CLSM having compressive strengths from 0.34 to 0.69 MPa (50 to 100 psi) can be easily excavated with conventional digging equipment yet is strong enough for most backfilling needs.

7. **Requires less inspection:** During placement, soil backfill must be tested after each lift for sufficient compaction. CLSM self compacts consistently and does not need this extensive field testing.
8. **Allows fast return to traffic:** Because many CLSM mixtures can be placed quickly and support traffic loads within several hours, downtime for pavement repairs is minimal.
9. **Lower settlement:** CLSM does not form voids during placement and does not typically settle or rut under loading. This advantage is especially significant if the backfill is to be covered by a pavement patch. Soil or granular fill, if not consolidated properly, may settle after a pavement patch is placed and form cracks or dips in the road.
10. **Reduces excavating costs:** CLSM allows narrower trenches because it eliminates having to widen trenches to accommodate compaction equipment.
11. **Improves worker safety:** Workers can place CLSM in a trench without entering the trench, reducing their exposure to possible cave-ins.
12. **Allows all weather construction:** CLSM will displace standing water left in a trench from rain or melting snow, reducing the need for dewatering pumps. To place CLSM in cold weather, materials can be heated using the same methods for heating ready mixed concrete.
13. **Reduces equipment needs:** Unlike soil or granular backfill, CLSM can be placed without loaders, rollers, or tampers.
14. **Requires no storage:** Because ready mixed concrete trucks deliver CLSM to the jobsite in the quantities needed, storing fill material on site is unnecessary. Also, there is no leftover fill to haul away.
15. **Makes use of a by product:** Fly ash is a by-product produced by power plants that burn coal to generate electricity. CLSM containing fly ash benefits the environment by making use of this industrial by-product material. Other by-products and waste materials can also be used in CLSM.

16. **Provides homogenous pipe backfill:** CLSM allows for proper structural bedding of pipeline without concerns for hard points, or voids that could compromise the structural design of the pipeline, particularly for flexible pipeline design.
17. **Provides corrosion resistance:** The cementitious backfill purportedly provides a high pH and low permeability environment, therefore resistance to sulfate attack is high and chloride migration is low.

The listed advantages of CLSM were all either observed in case studies for specific CLSM applications or in laboratory experiments performed by various state agencies and research organizations. However, it should be noted that there has been reports contradicting these case studies and research results. Detailed case histories of specific applications and research results are provided in Appendix A.

2.5.Potential Challenges

Although CLSM offers many advantages due to its inherent characteristics and has gained more acceptance in recent years, it has some challenges that are currently preventing its widespread use in the industry.

One of the largest impediments to the widespread use of CLSM is the industry's lack of familiarity with this material. Contractors, owners, engineers, and testing laboratories are not as familiar with CLSM as conventional backfill. Engineers and testing laboratories tend to follow the same ASTM standards used to test concrete to test CLSM (Smith 1991). However, the same ASTM standards may not be applicable to CLSM due to its unique properties, e.g., using a slump cone to test workability of CLSM is not useful. A different test, ASTM D6103, *Standard Test Method for Flow Consistency of Controlled Low Strength Material (CLSM)*, published by ASTM in 1997 is a better method for assessing the flowability of this material. Besides selecting the appropriate testing procedures, there is often confusion regarding who is going to perform the required testing. CLSM is produced using materials similar to those used in

concrete production. However, CLSM is often used as a soil replacement (ACI 1994). Because CLSM is a hybrid material between soils and concrete, it could be tested in geotechnical or concrete testing laboratories. The use of proper equipment for testing is also an important issue, e.g., the compressive strength testing equipment with high ultimate load ratings typically used for concrete cylinders may not provide accurate results for low strength CLSM samples.

The lack of standard testing requirements is another impediment to the use of CLSM. A survey performed in 1999 among state agencies found that only a few CLSM properties are routinely measured by state Department of Transportations (DOT's) and testing laboratories, and even those properties were being measured with various test methods (Folliard et al. 1999). A standard suite of testing procedures for CLSM needs to be developed that will measure all key characteristics of CLSM that will have significant effects on the performance of CLSM in its specific application. As an example, in pipe backfilling applications the preservation of low long-term compressive strength of CLSM is important to allow for easy re-excavation, however, in floor slab base applications the long-term strength gain would be a desired property.

Another challenge associated with CLSM is the lack of construction standards and procedures compared to conventional backfill materials. The ACI 229 report (1994) states that CLSM could displace standing water left in a trench from rain or melting snow and deems dewatering pumps unnecessary. However, contractors have reported that even a small amount of additional water in the trench can cause segregation of some CLSM mixtures (Kaneshiro 2001). Floatation of pipes due to the fluid nature of CLSM is also a construction concern that may require extra pipe fixing measures or placement height limits for CLSM applications (ACI 1994).

One of the most important advantages of CLSM is the ability to use locally available materials and by-products that may not be used in regular concrete production. However, the large variability of the physiochemical characteristics of these non-standard materials can result in large variability in the behavior of CLSM mixtures. Each time a new mixture is proportioned, testing should be performed to examine its

fresh and hardened properties and long-term behavior for the intended application (Adaska and Krell 1992). Standard specifications defining the types of by-product materials for use in CLSM and their effect on the properties of CLSM are lacking (Folliard et al. 1999).

In backfill applications CLSM requires no on site storage or removal of excess material. However, the excavated native soil still has to be hauled away and disposed. Swaffar and Price (1987) also reported that the finished surface of CLSM should not be considered a wearing surface and that the surface will be slippery during rainfall, similar to smooth clay.

Excessive long-term strength gain of CLSM mixtures containing fly ash has been noted in the literature as being a concern. The Tulsa Public Works Department adopted the use of CLSM as standard for backfill of utility trenches. They reported that due to the migration of cement and fly ash to the top of the backfill, a hard crust formation was observed that prevented the excavation of the material using conventional tools and equipment (Balogh 1994). Another study performed in the city of Tulsa, Oklahoma also stated that the 28-day compressive strength of CLSM exceeded the recommended value of 0.41 MPa (60 psi) and this mixture could not be excavated with conventional tools (Landwermeyer and Rice 1997).

There have not yet been many durability problems reported in field applications. However, since durability is a long-term issue, this does not mean that there will not be issues in the future. For example, the use of CLSM in some Canadian municipalities has resulted in deeper frost penetration in the trench backfill and differential heave of the asphalt surface on either side of the trench. Deeper frost penetration puts water service lines and hydrant laterals at risk of freezing. Increasing the depth of water lines is expensive and the differential surface heave causes bumps and cracks in the pavements. Field experiments carried out by the National Research Council (NRC) of Canada in Edmonton indicated that, under freezing conditions, CLSM has a high thermal conductivity but moderate moisture content and, for these reasons, would promote deeper frost penetration (Harry and Baker 1998). Another study performed by the

University of New Hampshire indicated that the top 50 to 150 mm (2 to 6 inches) of the CLSM backfill in the field was susceptible to frost damage. The study recommended the replacement of top 50 to 100 mm (2 to 4 inches) of the CLSM backfill with frost heave compatible base material after the set of CLSM (Gress 1996). The use of foaming agents, increasing the air content of the mixtures to decrease thermal conductivity, use of insulation around the pipes, and the use of lightweight aggregates and bottom ash are among other solutions for freeze thaw resistance stated in the literature.

Different CLSM mixtures were tested in the laboratory and in the field to show that they are less corrosive around metallic pipes compared to conventional backfill materials (Brewer and Hurd 1991, Abelleira et al 1998, Samadi and Herbert 2003). However, the Ductile Iron Pipe Research Association (DIPRA) identified two corrosion related concerns regarding the usage of CLSM around ductile iron pipes (Ductile Iron Pipe News Spring/Summer 1998). Their first concern was with the use of fly ash and the porosity of CLSM. It was thought that CLSM could potentially be corrosive if the porosity of CLSM allows the interface of the CLSM and metal pipe to experience high moisture contents (Bonds 1992). Their second concern was related to the lack of standard construction practices for CLSM applications. It was noted that if ductile iron pipes were not completely encased in CLSM during construction and they were partially exposed to the native soil, this could cause accelerated differential corrosion cells to develop, thus reducing the service life of the pipes. Development of differential corrosion cells would be expected due to the different corrosion potentials of ductile iron in the native soil and in CLSM.

The use of by-products, such ash fly ash, foundry sand, furnace slag, etc. also raises some environmental concerns. Waste materials containing heavy metals and other potentially harmful materials may contaminate the environment and ground water if they leach from CLSM. The two primary recovered materials used in CLSM production are coal fly ash and spent foundry sands. Either Class F or Class C coal fly ash can be used in CLSM. Typically nonferrous foundry sands are classified as hazardous waste due to their lead and cadmium content. Therefore, although the Environmental Protection

Agency (EPA) is willing to develop new markets for the use of waste materials, it limits the use of foundry sands in CLSM only to ferrous foundry sands (Malloy 1998). However, it should be noted that the existence of high values of heavy metals in a waste material is not a reason for rejection alone. The actual leaching of these metals into the environment tested by Toxicity Characteristic Leaching Procedure (TCLP) test (Method 40CFR 261.24) should be used as an acceptance criterion. A study indicated that even though the chemical composition of some fly ashes contained high values of heavy metals, the actual amount of these metals that leached from the CLSM was very low (Folliard et al. 1999).

The ACI committee 229 states that the in-place cost of CLSM is lower compared to conventional backfill materials due to the many advantages of CLSM even though CLSM costs more per cubic yard (ACI 1994). However, a study performed in San Diego, CA stated that the main disadvantage of CLSM is economic and that the material and shipping costs of the fly ash make CLSM more expensive compared to the conventional backfilling methods (Kaneshiro et al. 2001). The cost of CLSM depends on the cost of materials, local availability, the mixing and transportation method, and the methods of placement (Smith 1991). The cost of materials varies with geographical location, time of year, competition, and the amount of work. However, the most important factor affecting the cost of CLSM is the cost of the filler material used in the mixtures (Brewer and Hurd 1991). If locally available inexpensive materials can be used as filler materials to produce the CLSM with required characteristics, together with the advantages such as erosion resistance, minimum testing costs, elimination of hand labor for compaction, narrower trenches, and higher production rates CLSM may result in lower in-place costs. There are many case studies in the literature where the use of CLSM resulted in considerable cost savings (Goldbaum et al. 1997, Sullivan 1997).

2.6.Case Histories and Economics

The use of CLSM as an alternative to conventional backfill materials and its advantages are documented in the literature as case histories. In addition to exhibiting

different advantages of CLSM, the literature also indicates that the use of this material in different parts of the country can result in important cost and time savings, and high quality products for the owners and contractors. The case histories in the literature include the use of CLSM for various applications such as pavement base material, pipe backfill, erosion prevention, bridge rehabilitation, etc. Realized cost savings up to 40 percent (Adaska 1997, Green et al. 1998) were reported in these case histories with CLSM prices ranging from $\$12.4/m^3$ to $\$36.6/m^3$ ($9.5/cy to $28.2/cy) (Brewer 1993). A list of published case histories reporting different applications of CLSM and cost and time savings due to its use are given in Appendix A.

2.7.Fresh and Hardened Engineering Characteristics and Test Methods

The use of CLSM for different applications requires that the proportioning of CLSM mixtures have different fresh and hardened properties. Determination of important characteristics for different applications and specification of appropriate limits and testing methods for those characteristics are very important to implement more use of CLSM. Since CLSM contains cement and exhibits hydration reactions, there is a general tendency to test its characteristics using standards developed for concrete. However, CLSM is a hybrid material that behaves differently in its fresh and hardened states and the use of these standards and equipment developed for testing of concrete may not be appropriate for testing of CLSM. The fresh and hardened properties of CLSM discussed in the literature for various applications are listed below:

2.7.1.Fresh CLSM Properties

2.7.1.1.Flowability

One of the biggest advantage of CLSM compared to conventional backfill materials is its consistency when it is fresh. Due to its flowability, CLSM can be placed quicker and easier compared to conventional backfill materials and requires no compaction or vibration. This reduces labor, increases construction safety, and decreases construction duration. To ensure complete backfill of trenches or voids in

confined spaces with limited effort, the capacity of the CLSM mixtures to flow without segregation needs to be tested.

Consistency is one of the most frequently measured properties of CLSM in current practice, however different testing methods, such as the slump test (ASTM C143) and flow cone test (Corps of Engineers Spec. CRD-C611, or ASTM C939), have been used to measure this characteristic. A CLSM mixture with a slump of 152 mm (6 inch) or less is considered to have a low flowability; a mixture with a slump between 152 and 203 mm (6 and 8 inch) is considered to have medium flowability; and a mixture with a slump of 203 mm (8 inch) or greater is considered to have a high flowability. Several state DOT's have specified the flow cone test for CLSM, and the Florida and Indiana DOT's require an efflux time of 30 ± 5 seconds (ACI 1994). In 1994 ASTM committee D 18 on soil and rock published a provisional test method to measure the flow of CLSM mixtures that gained acceptance and was published as a full ASTM standard in 1996 as ASTM D 6103, *Standard Test Method for Flow Consistency of Controlled Low Strength Material.* The test method uses a 75 x 150 mm (3 x 6 inch) cylinder that is vertically lifted, allowing the CLSM to slump and flow. The final diameter of the CLSM patty is measured twice, perpendicular to each other, and averaged. This average diameter is used as a measure of flowability of the mixture and a diameter of 200 mm or higher is typical of a highly flowable mixtures.

The use of CLSM mixtures with high flowability requires attention to constructability issues such as the hydrostatic pressure exerted by the fresh mixture and the uplift force that can be applied by the CLSM mixture.

Flowability of CLSM mixtures can be affected by CLSM constituents, aggregate gradation and shape, air content, water content, fly ash type, and fly ash quantity. Also the specific method used to perform ASTM D 6103 can affect the measured flow value (Dandria et al. 1997). To achieve the desired flowability for a specific application, trial mixtures should be performed. A study performed on CLSM mixtures containing foundry sand and fly ash determined that the proper amount of fly ash was important in determining the amount of required water and flowability (Bhat 1996). Another study

performed on a CLSM mixture comprised of fly ash, cement, water, and bentonite clay investigated the rheology of the mixture and developed a formula for the spread of CLSM under gravity (Gray et al. 1998). The use of superplasticers was also found to decrease the water requirement of flowable CLSM mixtures (Janardhanam et al. 1992). A comprehensive study performed by Du et al. (2002) reported that certain constituent materials, such as high carbon fly ash, bottom ash, and foundry sand increased the water content of CLSM mixtures for required flowability values and that the increased water content affected the unconfined compressive strength of the mixtures.

2.7.1.2.Segregation and Bleeding

Similar to segregation experienced with some high slump concrete mixtures, high water content requirements for high flowability CLSM mixtures may cause segregation, especially if flowability is primarily produced by the addition of water (ACI 1994). For highly flowable CLSM without segregation an adequate amount of fines should be used in the mixture to provide suitable cohesiveness. Even though non-cohesive materials such as silts have been used up to 20 percent of the total aggregate as fines to provide the required cohesiveness, typically this is obtained with the use of fly ash. In their report the ACI committee 229 (1994) noted that the use of plastic fines such as clay could produce deleterious results, such as increased shrinkage and recommended to avoid the use of plastic materials. Highly flowable CLSM mixtures containing Class F fly ash as high as 910 kg/m^3 (700 lbs/cy) in combination with cement, sand, and water have been reported in the literature (Krell 1989). CLSM mixtures with entrained air were also reported to be less prone to segregation compared to CLSM mixtures that are produced without any air entraining agents (Du 2001). A study performed using the ASTM Test Method C 940, *Standard Test Method for Expansion and Bleeding of Freshly Mixed Grouts for Pre-Placed Aggregate Concrete in the Laboratory*, found that a 30 percent air modified mix had no bleed water, while the non-air modified CLSM mixture yielded 2.4 percent bleed water (Hoopes 1998). A study performed by the City of Tulsa comparing a regular CLSM mixture comprised of cement, sand, fly ash, and water with a quick-

setting CLSM that had increased cement content and an accelerator reported that bleed water was consistently observed at the surface of the regular CLSM while none or only minor amounts of bleed water were observed at the surface of the quick-set CLSM. The study noted that because regular CLSM had lower water content and lower water cement ratio, the bleed water could not be solely explained by the water content of the mixture. The study concluded that the hydration rate was a more important factor in determination of the bleed water (Landwermeyer and Rice 1997).

The quick-set CLSM hydrates more rapidly than regular CLSM which causes water retention and production of hydrated cement paste and other products of hydration. The regular CLSM begins setting in an unusually slow rate due to the low cement content and less of the water is held by the hydration products. A study performed by Du (2001) also noted that bleeding was observed on several different types of CLSM mixtures (air entrained and non-air entrained) and that only flash fill (rapid set) mixtures showed little bleeding. The study also reported that mixtures prepared with bottom ash lacked sufficient fines for workability and were prone to bleeding.

2.7.1.3.Setting and Hardening

The period of time required for the CLSM mixture to go from the plastic state to a hardened state with sufficient strength to support the weight of a person is defined by the ACI committee 229 as the hardening time (ACI 1994). The amount and rate of bleed water and the type and quantity of cementitious material in the CLSM (fly ash, etc.) are very important factors affecting the hardening time of CLSM. Other factors affecting the hardening time according to the ACI committee 229 are: permeability and degree of saturation of surrounding soil in contact with CLSM, fluidity of CLSM, proportioning of CLSM, mixture and ambient temperature, humidity, and the depth of fill. Smith (1991) reported that the hardening time of CLSM mixtures could be as short as one hour, but it generally takes three to five hours under normal conditions. A fast setting CLSM mixture produced with a proprietary product of CTS Cement Manufacturing Company,

called Rapid Set, in Tulsa was reported to exhibit initial setting in 12 to 23 minutes (Pons et al. 1998).

A representative from the Western Washington for Pozzolanic Northwest witnessed the "stomping foot" used on construction sites to determine if the CLSM was sufficiently hard for use as a wearing surface. In this method, a contractor stomps his foot a few times on the CLSM and if his foot does not settle and no water comes to the surface, the final wearing surface can be applied (Hitch 1998). Based on this test method a standardized, similar test method was developed using a "Kelly Ball" that was originally used to measure the slump of concrete. The method was accepted as a provisional test method in 1994 and then accepted as a full ASTM method in 1996 (ASTM D 6024, *Test Method for Ball Drop on Controlled Low Strength Material to Determine Suitability for Load Application)*

ASTM C 403, *Standard Test Method for Time of Setting of Concrete Mixtures by Penetration Resistance*, has also been frequently used to determine the hardening time of CLSM mixtures. The NRMCA (1989) reported that penetration values between 500 and 1500 are normally required to assure adequate bearing capacity. California DOT requires a penetration value of 650 before allowing a pavement surface to be placed (ACI 1994).

The construction industry requires test methods to monitor in-place CLSM as opposed to testing lab mixtures and one such method is the use of a penetrometer on hardened CLSM in the field to monitor field strength (Hitch 1998). Du (2001) used a needle penetrometer, a soil pocket penetrometer, and a pocket vane shear tester to determine the hardening time of different CLSM mixtures. The study reported a good correlation between soil penetrometer values and ASTM C 403 measurements and reported that penetrometer values in the range of 4.3 to 7.4 kPa (0.62 to 1.07 psi) corresponded to the time when the CLSM obtained sufficient strength to support the weight of an average person. Another study performed by Bhat (1996) used a soil pocket penetrometer and reported this value as being 410-450 kPa (59.5-65.3 psi) depending on the person's weight (Bhat 1996). Both studies also reported that the needle

penetrometer was less prone to bleed water effects and that a correlation was observed between needle penetrometer and soil penetrometer values. The soil penetrometer yielded higher resistance values compared to needle penetrometer values at early stages of setting. There was also a limited correlation between the soil penetrometer values and the pocket vane shear tester (Du 2001).

2.7.1.4.Unit Weight

Unit weight of CLSM mixtures were one of the properties occasionally specified in field applications (Hitch 1998). ASTM D 6023, *Test Method for Unit Weight, Yield, and Air Content (Gravimetric) of Controlled Low Strength Material*, accepted in 1996 as a full standard covers the unit weight measurement of CLSM. Du (2001) reported that mixtures containing entrained air and large amounts of fly ash exhibited low density values due to higher water demand of these mixtures to reach required flowability.

Hamilton County engineers in Cincinnati, OH developed an index referred to as removability modulus to assess the excavatability of CLSM mixtures (Du 2001). If this index that is calculated using the dry unit weight and the 30-day unconfined compressive strength of the mixture is equal or less than unity than the CLSM mixture is considered excavatable.

2.7.1.5.Subsidence

Reduction of volume (subsidence) of CLSM mixtures, especially with high water contents, has been reported in the literature. Loss of water through bleeding or absorption into the surrounding environment during the placement of CLSM until it sets is an important consideration to determine the final elevation on which the wearing surface will be placed. In the literature subsidence values of CLSM mixtures up to approximately 1 to 2 percent of the fill depth were reported (Balogh 1994, DiGioia et al. 1992). Du (2001) reported that the use of accelerating admixtures reduced bleeding and slightly reduced subsidence. The same study reported subsidence values ranging from 0.3 to 15.85 mm (0.012 to 0.62 inch) in 600 mm (23.6 inch) total specimen depth.

2.7.2.Hardened CLSM Properties

2.7.2.1.Compressive Strength

As a measure of load carrying capacity the unconfined compressive strength is a critical property of CLSM that has been used to specify CLSM mixtures. CLSM compressive strength of 0.35 to 0.69 MPa (50 to 100 psi) is considered equal to the bearing capacity of a well compacted soil (ACI 1994). Two different sources are believed to contribute to the compressive strength of CLSM: the friction between the particles and the bonding strength due to the hydration processes. The friction between the particles of the fresh CLSM mixture becomes stronger as bleeding occurs leading to a decrease in moisture content. The bond strength due to hydration also develops when the CLSM is in the fresh state and becomes more pronounced after the bleeding has subsided. Strength development due to these sources can be observed in the data obtained by Du (2001). Du (2001) stated that the load deflection curves of CLSM samples at early ages were similar to soils with high ductility and were similar to concrete at later ages with higher strength and brittleness. High amounts of bleeding are expected to result in a more compact structure with higher frictional strength. However, increased bleeding may impede the flowability of the mixtures causing segregation and may cause unacceptable subsidence. Therefore, the drainage condition (permeability of the surrounding soils) in the field affects the early strength development of the CLSM significantly (Bhat and Lovell 1997).

Based on experiments with CLSM mixtures containing waste foundry sand and fly ash Bhat and Lovell (1997) reported that the water cementitious material ratio (w/cm) was the most important parameter affecting the 28-day compressive strength of CLSM and established an indirect relation between compressive strength and the cube of the w/cm. Bhat and Lovell (1997) also reported that a w/cm in the range of 5.8 and 7.4 would result in mixtures with compressive strength in the range of 1.035 MPa to 0.69 MPa (150 to 100 psi). Brewer (1992) reported that the actual cement content would be a

more convenient index compared to w/cm since the compressive strengths reported were insensitive to the w/cm variations at values greater than 3.

Since its acceptance in 1995 ASTM D 4832, *Standard for Preparation and Testing of Controlled Low Strength Material (CLSM) Test Cylinders*, has gained acceptance among state agencies and commercial testing laboratories. The low strength of CLSM mixtures causes some testing challenges such as damaging the test cylinders during stripping of molds or the low accuracy of the results when large-capacity concrete compression machines are used (Folliard et al. 2001). In a comprehensive study, Du et al. (2002) investigated the effects of different test parameters, such as the load rate, curing conditions, drainage conditions, capping materials, and cylinders' size on the compressive strength of CLSM mixtures containing various byproducts and waste materials and developed predictive strength models. Some of their conclusions are as follows:

- Loading rate can affect the compressive strength measurements significantly and a deflection controlled loading rate between 0.042 to 0.16 percent per minute is appropriate for accurate testing.
- Testing equipment with lower ultimate strength capacities yields more repeatable results compared to regular concrete testing equipment.
- Air drying recommended in ASTM D 4832 is not necessary for accurate testing.
- Contact of CLSM samples during curing with standing or dripping water may cause variations in strength.
- Different curing temperatures and humidity values can cause compressive strength to differ by more than an order of magnitude, especially for mixtures containing fly ash.
- Inclusion of Class C fly ash generally results in higher compressive strengths.
- High strength gypsum is an appropriate capping material. Neoprene pads with durometer values less than 50 may also be used if a strength reduction (compared to sulfur capping) less than 20 percent is acceptable.

2.7.2.2.Triaxial Strength and Shear Strength

When shear stresses exceed the shear strength of fill materials soil movements such as landslides may occur (Hoopes 1998). Since CLSM is used as an alternative to granular backfill materials, standard test methods applied to test the suitability of granular backfill materials, such as the triaxial shear strength test or direct shear strength test, were applied to test CLSMs. One study reported that at 3 and 7 days all CLSM mixtures tested for direct shear strength following ASTM D 3080, *Standard Test Method for Direct Shear Test of Soils Under Consolidated Drained Conditions*, performed at least equal to typical compacted soils (Hoopes 1998). The same study reported that the later age shear properties of air modified CLSM were obtained through cohesive properties of the cementitious constituents. Another study performed triaxial shear tests on CLSM specimens following US Army Corps of Engineers (USACE) EM 1110-2-1906, *Laboratory soils testing*, manual (1986) and reported the internal friction angle and the amount of cohesion at 28 days as 30.5 degrees and 875 kPa (127 psi), respectively (Dolen and Benavidez 1998). Du (2001) also performed triaxial shear strength tests on CLSM mixtures and stated that performance of this test using conventional geotechnical equipment was acceptable. In this study measured friction angles for different CLSM mixtures varied from 18.5 to 47.9 degrees and the cohesion values varied from 40.1 to 346.2 kPa (5.82 to 50.21 psi) at 28 days, exhibiting a variation depending on the constituents of the CLSM mixtures. These observed ranges of friction angle and cohesion are similar to dense granular soils. Hoopes (1998) performed triaxial shear strength tests on air-entrained CLSM mixtures at 16 hours, 7 and 28 days. The study indicated that air-entrained CLSM mixtures achieved minimum 38º friction angles at 16 hours. Typical well compacted fill achieves ultimate friction angles in the 30º to 40º range. Although at 16 hours CLSM mixtures exhibited negligible cohesion, their cohesion values increased from 16 hours to 28 days due to the hydration reactions of cementitious constituents further increasing the strength.

2.7.2.3.California Bearing Capacity and Resilient Modulus

California bearing capacity and resilient modulus are two more standard tests used to determine the suitability of conventional granular backfill materials as a base or subbase material. CLSM has been evaluated in the literature by many researchers using the California Bearing Ratio (CBR) for suitability as a subbase or subgrade material. Limited studies have been performed to evaluate the resilient modulus of CLSM mixtures (Du 2001, Abelleira et al. 1998, Landwermeyer et al. 1998).

The CBR value of standard crushed rock measured following ASTM D 1883, *Standard Test Method for CBR (California Bearing Ratio) of Laboratory Compacted Soils*, is 100. Du (2001) reported that all CLSM mixtures included in his study exhibited high CBR values compared to granular conventional backfill materials with the exception of some fly ash mixtures and high air mixtures and the measured values varied between 20 and 216. CBR tests performed by Abelleira et al. (1998) on a CLSM mixture containing only sand and low amounts of cement indicated that the CBR value of the mixture changed from 22.9 (clayey soil) at 3 days to 52.3 at 28 days (graded gravel). Pons et al.(1998) also observed a similar time dependent behavior; at 6 days regular CLSM mixtures exhibited CBR values comparable to a poor pavement subgrade and similar to a Type A aggregate base material at 45 days. The same study indicated that quick-set CLSM would exhibit its long-term CBR value as early as in 24 hours and that it would be comparable to sandy or gravely soils. Both constitute good subgrade materials for pavements (Pons et al. 1998).

Du (2001) measured the resilient modulus of six select CLSM mixtures following AASHTO T 274, *Resilient Modulus of Unbound Granular Base/Subbase Materials and Subgrade Soils (SHRP Protocol P46)*. He concluded that the resilient modulus test was an applicable test method for CLSM using regular soil testing equipment. The resilient modulus values obtained for six CLSM mixtures were an order of magnitude higher than typical soils.

2.7.2.4.Permeability

Permeability of CLSM may be very important for certain applications, e.g., difficulties have been reported in detecting gas leaks in pipelines buried in CLSM mixtures (Folliard et al. 1999). Typical permeability values for CLSM mixtures are in the range of 10^{-3} to 10^{-4} mm/sec ($3.94x10^{-5}$ to $3.94x10^{-6}$ in/sec) and mixtures of higher strength and higher fines content can achieve permeabilities as low as 10^{-6} mm/sec ($3.94x10^{-8}$ in/sec) (ACI 1994). Permeability is increased as cementitious materials are reduced and aggregate contents are increased (particularly above 80 percent) (DiGioia et al. 1992). CLSM mixtures with 21 percent and 30 percent air contents have exhibited permeability values of $1.2x10^{-2}$ and $1.7x10^{-1}$ mm/sec ($4.7x10^{-4}$ and $6.7x10^{-3}$ in/sec), respectively (Hoopes 1998). It was also reported that the w/cm affected the permeability significantly (Du 2001). Generally the lower the w/cm, the lower was the permeability.

The commonly applied method to measure the permeability of CLSM mixtures is the ASTM D 5084, *Standard Test Method for Measurement of Hydraulic Conductivity of Saturated Porous Materials Using a Flexible Wall Permeameter.*

2.7.2.5.Settlement and Consolidation

Reduction of volume of soils due to seepage of water is referred to as settlement. As already mentioned in the subsidence section, CLSM mixtures in their fresh state may loose water to the surrounding soil and through evaporation of bleed water that in turn causes a reduction in volume of in-place CLSM. However, once CLSM begins to set and the hydration processes reach a certain level, a relatively strong and rigid structure develops that reduces the settlement of CLSM to a negligible value. The low settlement is one of the most important benefits of CLSM reported in the literature. A study indicated that in the city of Prescott, AZ over a ten year period the rate of backfill failures due to settlement since the CLSM has been implemented declined to 1 percent from 80 percent (Brinkley and Mueller 1998). Hoopes (1998) reported that the coefficient of volume compressibility of a CLSM mixture with high amount of entrained air was similar to compacted dense gravel fill (Hoopes 1998).

2.7.2.6.Drying Shrinkage

ACI committee 229 (1994) noted that shrinkage and shrinkage cracks do not affect the performance of CLSM and that the typical linear shrinkage for this material is in the range of 0.02 to 0.05 percent. Gandham et al. (1996) also found that the maximum shrinkage and expansion values of CLSM were generally less than the acceptable limit established for concrete. Another study that used the shrinkage-ring method (not adopted as a standard) also reported minimal shrinkage of CLSM (Lucht 1995).

Conventional methods used to measure the drying shrinkage of concrete, such as the ASTM C 426, *Standard Test Method for Linear Drying Shrinkage of Concrete Masonry Units*, may be too harsh for low strength CLSM samples. Du (2001) used a method developed in Germany for flooring applications to measure the shrinkage of CLSM samples and noted negligible shrinkage. However, it was also stated that the applicability of the method, developed for concrete, to CLSM was not certain (Du 2001).

2.7.2.7.Thermal Conductivity

Thermal conductivity of CLSM mixtures is an important property especially for pipe backfilling applications. High thermal conductivity of regular CLSM mixtures has been reported to cause deeper frost penetration compared to conventional backfill materials. This deeper frost penetration can cause freezing of water mains and laterals (Baker and Goodrich 1995). Density, porosity, and the moisture content are important factors affecting the thermal insulation of CLSM mixtures. Dense mixtures, with high amounts of fines and low porosity are good thermal conductors and such mixtures may cause deeper frost penetration. A study that measured the thermal conductivity of air modified CLSM mixtures following ASTM C 518, *Standard Test Method for Steady State Thermal Transmission Properties by Means of the Heat Flow Meter Apparatus*, stated that the thermal conductivity of the oven dry and surface saturated CLSM mixtures were in the range of 0.42 to 0.48 W/mK (2.9 to 3.4 Btu-in/hr-ºF-ft^2) and 0.51 to 0.53 W/mK (3.5 to 3.7 Btu-in/hr-ºF-ft^2), respectively. It also stated that the thermal

conductivity increased to a range of 1.1 to 1.7 W/mK (7.8 to 11.9 Btu-in/hr-F-ft^2) when immersed in water (Hoopes 1998).

The backfill would normally have its highest thermal conductivity when it is frozen and this conductivity is called the frozen thermal conductivity, k_f. The time required for the backfill to freeze depends on the moisture content of the backfill and the latent heat, L. L is the amount of energy released or absorbed during a change of state. The frost penetration depth in the backfill is reported to be proportional to the ratio of the frozen thermal conductivity to the latent heat (k_f/L). A study comparing the k_f/L of CLSM with sand, clay, lightweight aggregate, and bottom ash fill materials reported that CLSM had the highest ratio causing the deepest frost penetration under the same conditions (Baker and Goodrich 1995).

Although regular CLSM mixtures may not be good thermal insulators, CLSM mixtures with low density and high porosity (high air content or light weight aggregates) can easily be designed. Jones and Giannakou (2004) have shown that a cementitious paste including fly ash with preformed foam can be used as a controlled thermal fill. The designed backfill mixtures in the study had densities in the range of 800 to 1600 kg/m^3 (1348 to 1697 lb/cy), flow characteristics of 100 to 300 mm (3.94 to 11.8 in) spread, compressive strength less than 10 MPa (1450 psi), and a thermal insulation performance in the range of 0.2 to 0.6 W/mK (1.4 to 4.2 Btu-in/hr-F-ft^2).

ASTM D 5334, *Determination of Thermal Conductivity of Soil and Soft Rock by Thermal Needle Probe Procedure*, and ASTM C 177, *Steady-State Heat Flux Measurements and Thermal Transmission Properties by means of the Guarded-Hot-Plate Apparatus*, are two methods that can be used to measure the thermal conductivity of CLSM mixtures (Du 2001). Also the 442-1981 Standard of the Institute of Electrical and Electronics Engineers (IEEE) was used to measure the thermal resistivity of CLSM (Ayers et al. 1995).

2.7.2.8.Freezing and Thawing Resistance

Freeze and thaw resistance is one of the important performance parameters of CLSM if it is going to be used in cold climates. At freezing temperatures the water in CLSM mixtures with high permeability values forms ice lenses similar to the frost heave phenomenon of soils. The expansion of water generates an internal hydraulic pressure that can damage the internal structure of the CLSM.

Krell (1989) reported that completely saturated CLSM mixtures exposed to freezing temperatures below -18 °C (-0.4 ºF) broke into pieces about the size of a hand in the laboratory. However, similar CLSM mixtures performed well under freeze-thaw conditions in the field (Krell 1989). Another study performed by the University of New Hampshire indicated that the top 50 to 150 mm (2 to 6 inches) of the CLSM backfill in the field was susceptible to frost damage. The study recommended the replacement of top 50 to 100 mm (2 to 4 inches) of the CLSM backfill with frost heave compatible base material after the set of CLSM (Gress 1996). Hoopes (1998) tested CLSM mixtures for freeze-thaw performance following ASTM D560, *Standard Test Method for Freezing and Thawing Compacted Soil-Cement Mixtures,* and noted that 21 and 30 percent air modified CLSM mixtures performed significantly better than regular CLSM mixtures (1.4 percent entrapped air). However, even the air modified CLSM mixtures had significant volume loss after 12 freeze-thaw cycles (Hoopes 1998). The conditions of the standard freeze and thaw testing method for concrete, ASTM C 666*, Standard Test Method for Resistance of Concrete to Rapid Freezing and Thawing*, was reported to be too severe for the CLSM mixtures (Nantung 1993). Because of the similarity of CLSM and soil-cement ASTM D 560 was used by researchers to test CLSM (Janardhanam et al. 1992, Gress 1996, Hoopes 1998). Du (2001) also used the ASTM D 560 method to evaluate freeze-thaw resistance of different CLSM mixtures without the use of a scratch wire brush on thawed samples. He noted that most of the CLSM mixtures exhibited a weight loss of less than 14 percent the failure criteria stated in the standard. He also

noted that the CLSM mixtures containing foundry sand exhibited much lower freeze-thaw resistance compared to other mixtures (Du 2001).

2.7.2.9.Long-Term Strength Gain and Excavatability

In pipe backfilling applications the limited long-term strength gain of CLSM mixtures is especially important to allow easy re-excavation in case of a future pipe failure. If CLSM gains excess strength and requires effort and time similar to concrete to excavate then the cost and time savings gained during construction may be lost during re-excavation. ACI committee 229 (1994) stated that CLSM with a compressive strength of 350 kPa (50 psi) or less can be excavated manually and that CLSM with compressive strengths between 690 to 1400 kPa (100 to 200 psi) requires heavy equipment, such as backhoes for excavation. Because compressive strength is used as an indicator of excavatability, the long-term strength gain of CLSM mixtures received considerable attention from researchers. Bhat and Lovell (1997) noted that CLSM mixtures containing waste foundry sands exhibited a 30 percent increase of compressive strength from 28 to 91 days. Mullarky (1998) reported that the air and fly ash content of the mixtures were important factors affecting the long-term strength development of the mixtures.

Even though compressive strength was used as a measure of excavatability of the CLSM, it should be noted that there is no clear correlation between these two variables. It was reported that the hand excavation of CLSM mixtures with high quantities of coarse aggregate can be very difficult even at low strengths and that the mechanical excavation of CLSM mixtures with high amounts of fine sand or fly ash can be performed easily even at strengths of 2.07 MPa (300 psi) (Krell 1989).

Engineers in Hamilton County, Cincinnati, Ohio used removability modulus (RE) to assess the excavatability of the CLSM mixtures in their CLSM specifications for backfill applications (HAMCIN 1996). The RE value can be calculated as follows:

$$RE = \frac{w^{1.5} x 104 x C'^{0.5}}{10^6} \qquad (2.1)$$

where:

w: dry unit weight (hardened material) (lb/ft^3)

C' : 30-day unconfined compressive strength (psi)

If the RE value of the CLSM mixture is equal or less than unity then the CLSM mixture is considered to be excavatable. The RE values of hard clay, very stiff clay, and normal weight 20.7 MPa (3000 psi) portland cement concrete are 8, 6.9, and 70.7 kPa (1.15, 1, and 10.26 psi), respectively.

Du (2001) did not find a significant correlation between the compressive strength values of CLSM samples cured in lab conditions and the excavatability of the CLSM cured in the field conditions. He also noted that the correlation between the stiffness of CLSM in the field measured by a Geogauge and the excavability was weak. However, he reported that the Dynamic Cone Penetrometer (DCP) test results showed a good correlation with RE values and that they were successful in estimating the excavability of CLSM mixtures in the field. He also reported that tensile splitting test results gave promising results and suggested further research of this test method for the estimation of excavatability.

2.7.2.10.Leaching and Environmental Impact

Due to the high permeability of regular CLSM mixtures, the use of waste products or by-products in CLSM mixtures requires careful examination of the environmental impact of these mixtures. The two main recovered materials used in the production of CLSM are coal fly ash and spent ferrous foundry sands. In 1992 the Pohlman Foundry in Buffalo, NY attempted to use spent foundry sand in CLSM. As a part of the licensing requirement, the company evaluated the leachate of hazardous materials from the spent foundry sand. Philbin (1997) reported minimal leaching of hazardous materials. The Environmental Protection Agency (EPA) allows the use of coal ash and spent foundry sands in CLSM production (Malloy 1998). Many researchers have investigated the environmental impact of the use of by-products in CLSM mixtures through leachate analysis and found that the toxic contents of the mixtures were below

the EPA leachate standards (Bhat and Lovell 1997, Naik et al. 1998, Gandham et al. 1996).

Trejo et al. (2004) proposed a systematic approach to the determination of the suitability of waste materials for use in CLSM mixtures. They proposed a three step approach: the first step is the chemical analysis of all the raw materials used to produce CLSM and the determination of the heavy metals, such as arsenic, barium, cadmium, etc., following EPA Method 610. The second step consisted of identifying any raw materials that contained heavy metal quantities more than 20 times the TCLP limits following Method 40CFR 261.24. The third step consisted of determining whether the leachate contains heavy metals above the acceptable limits. If any material after encapsulation in CLSM still causes a leachate with heavy metal contents above the TCLP limits, that material should not be used to produce the CLSM mixtures. This three step approach is intended to save time for the practitioners. If a material does not exhibit heavy metal contents above the set limits at any step of the procedure, further testing of the material is not required, thereby minimizing test requirements.

2.8.Materials and Mixture Proportioning

CLSM mixtures are usually produced from small quantities of portland cement, SCMs, filler materials, and water. As mentioned earlier, CLSM mixtures produced for different applications require different characteristics and the amount and type of materials that will be used in CLSM production should be designed to obtain the required characteristics. For applications that may require the excavation of CLSM at a later age the amount and type of cementitious materials should be adjusted to prevent excessive long-term strength gain. Besides the required engineering properties, such as long-term strength gain, flowability, subsidence, hardening time, etc., the cost of the CLSM mixture plays a very important role in the design of CLSM mixtures. When available, the use of locally available materials and waste materials as a filler material can be economically and environmentally advantageous. Of course, in the cases when

waste materials or by-products are used, the environmental impact from using these materials needs to be investigated.

2.8.1.Portland Cement

Together with other SCMs small amounts of portland cement used in CLSM mixtures mainly provides the cohesion and strength of CLSM mixtures (ACI 1994). The amount of portland cement typically constitutes approximately 3 percent of the total CLSM mixture volume (Brewer 1994). Due to the low amount of cement in CLSM mixtures common durability problems, such as alkali-aggregate reaction and sulfate attack, are not considered to be important issues for CLSM mixtures (Du 2001). Therefore, the local availability and cost of cement are the main factors in determining the type of cement to be used in the CLSM. Since Type I/II cement is the most common in most regions of the USA, this type has been widely used. The successful use of Type III cement for high early strength and low subsidence CLSM is also reported in the literature (Landwermeyer and Rice 1997).

2.8.2.Supplementary Cementitious Materials (SCM)

SCMs are materials with pozzolanic properties, such as fly ash, that are used in CLSM mixtures together with portland cement to provide cohesion and strength. Fast setting CLSM mixtures that contained only SCMs as a binder have also been reported in the literature (Trejo et al. 2004).

An early study investigating the applicability of CLSM for backfill applications consisted of high volume fly ash mixtures (Brewer 1994). Fly ash is a by-product of coal burning for energy production. After much research, the use of fly ash replacement of cement in conventional concrete production is a common practice. However, there are requirements, such as carbon content, size distribution, and uniformity requirements as defined in ASTM C618, *Standard Specification for Coal Fly Ash and Raw or Calcined Natural Pozzolan for Use in Concrete*, that need to be satisfied for fly ash to be used in conventional concrete production. Therefore, much of the fly ash produced

cannot be used in concrete. The strict specifications imposed on fly ash for use in conventional concrete may not be required for use in CLSM.

There are two types of fly ash defined in ASTM C 618; Class C and Class F. Fly ash with less than 70 percent SiO_2 and Al_2O_3 resulting in 15 to 35 percent CaO is classified as Class C fly ash. Fly ash with more than 70 percent SiO_2 and Al_2O_3, and lower CaO contents is classified as Class F fly ash. The ASTM C 618 standard also limits the loss on ignition (LOI) to a maximum of 6 percent. Fly ashes with LOI values higher than 6 percent are referred to as high-carbon fly ashes. Class F fly ash has been mostly used in CLSM applications as a binder because of its pozzolanic property. Approximately 8 percent of a typical CLSM mixture is made up by fly ash (Brewer 1994). However, in some applications quantities as high as 1186.5 kg/m^3 (2000 lbs/cy) have been used where fly ash also served as a filler material. Fly ash can improve the flowability of CLSM, decrease bleeding, increase compressive strength, and retard or accelerate setting. The use of high-carbon fly ash has been reported to increase the water requirement of CLSM for a required flowability (Du 2001). Class C fly ash has also been successfully used in CLSM applications. AASHTO specifies the use of Class C fly ash in quantities of up to 207.6 kg/m^3 (350 lb/cy) (AASHTO 1986). Due to its cementitious characteristics Class C fly ash has been reported to cause high early strength values and to increase long-term strength gain in CLSM mixtures. A mixture developed for rapid setting, Flash Fill, contains predominantly Class C fly ash and no cement (Ayers 1995). Like all the ingredients of CLSM mixtures, the amount, type, and quantity of fly ash to be used in the CLSM should be decided based on the required engineering properties of the mixture and the results of trial mixtures.

2.8.3.Filler Materials

2.8.3.1.Conventional Concrete Sand

Conventional concrete sand meeting the requirements of ASTM C 33, *Standard Specification for Concrete Aggregates*, is the most commonly used and most commonly specified filler material for CLSM. The amount of filler material is determined after

considering the cement, fly ash, air, and water content of the mixture. Filler material typically accounts for approximately 72 percent of a typical CLSM mixture (Brewer 1994) and in general the quantities range from 1543 to 1839 kg/m^3 (2600 to 3100 lb/cy) (ACI 1994). The main reason for the use of concrete sand is the availability of this material to the ready mix concrete producers. However, more economical materials, such as waste products or by-products that are locally available to producers may be used to decrease the cost of CLSM. The economic impact of the filler material on the total cost of CLSM is significant because it accounts for the largest percentage of the CLSM. The use of many different materials as filler materials for producing has been reported throughout the literature (Brewer 1994, Larsen 1990).

2.8.3.2.Foundry Sand

Waste foundry sand is one of the fill materials that is used as a low cost filler material in CLSM. The most common casting process used in the foundry industry is the sand cast system. This system uses bonded sand to form molds for ferrous (iron and steel) and nonferrous (copper, aluminum, brass) metal castings. Green sand, the material used for the sand molds of ferrous castings, is the foundry sand that is used in CLSM production. The use of nonferrous sand is not recommended by the EPA due to concerns of potential leaching of phenols and heavy metals (EPA 1998). Green sand consists of high quality silica sand, bentonite (10 percent) clay, water (2 to 5 percent), and sea coal (5 percent). Typically, one ton of foundry sand is required for each ton of iron or steel casting produced and the annual generation of waste foundry sand in the USA is believed to range from 9 to 13.6 million metric tons (Colins and Ciesielski 1994). In 1993 and 1994, CLSM mixtures containing foundry sands were compared with mixtures produced with virgin sands in Ohio and results indicated that characteristics of foundry sand containing CLSM, such as flowability, compressive strength, conductivity, permeability, etc. were as good as the CLSM mixtures produced with virgin sand. As a result of these studies, the County of Hamilton, Ohio approved the use of foundry sand in CLSM applications (HAMCIN 1996). Duritsch (1993) and Stern (1995) presented a

detailed history and technical information regarding the use of foundry sands in CLSM production in Ohio. The Indiana DOT funded a study that concluded that CLSM containing foundry sand settled less than regular CLSM mixtures and that the rate of strength gain was also lower compared to the regular CLSM mixtures (Javed 1994, Javed and Lovell 1995). Another study investigated the engineering properties and cost of CLSM mixtures produced using Class F fly ash and foundry sands and developed step by step procedures for CLSM mixture design (Bhat and Lovell 1996). The same study reported that good performing mixtures containing up to 55.5 percent foundry sand could be produced. Other studies also indicated that mixtures containing foundry sand and Class F fly ash were environmentally acceptable (Javed and Lovell 1995, Bhat and Lovell 1996). Naik and Singh (1997) investigated the effect of fly ash replacement with foundry sands and reported that the minimum hydraulic conductivity was achieved at 30 percent replacement of the fly ash with foundry sand. The study also reported that up to 70 percent of replacement, the hydraulic conductivity values did not change significantly and at 85 percent replacement the conductivity increased dramatically. In 2000 Tikalsky et al. compared the properties of CLSM mixtures containing chemically bonded foundry sand, clay bonded foundry sand, and crushed limestone sand. The study concluded that CLSM mixtures with foundry sands provided similar or better properties compared to mixtures containing crushed limestone sand and that the foundry sand prevented the excess strength gain in the long-term. The study also stated that mixtures containing a combination of chemically bonded foundry sands and fly ash exhibited excellent characteristics and were excavatable.

2.8.3.3.Crushed Limestone Screenings

The International Center for Aggregate Research (ICAR), the National Aggregates Association (NAA), and the National Stone Association (NSA) reported that the fines produced as by-product during aggregate production are one of the largest challenges in the aggregate industry (ICAR 1994). The by-product fines account for 15 to 25 percent of all aggregate production and accumulate in large stockpiles, causing

environmental challenges. In 1996 ICAR identified CLSM production as a possible use of these fines (ICAR 1996). However, most specifying agencies limit the use of fines in CLSM to less than 10 percent because they impede bleeding and therefore the consolidation of CLSM mixtures after placement. Recently developed air entraining admixtures specifically designed for CSLM mixtures can entrain large percentages of stable air bubbles in CLSM that result in air-entrained, workable, excavatable CLSM mixtures with no segregation and limited strength. The use of such admixtures may alleviate the bleeding problem and allow the use of higher amounts of fines in CLSM production. A study performed by Crouch et al. (1998) reported that with the use of air entraining admixtures CLSM mixtures containing up to 21 percent by volume fines that met the NRMCA strength requirements for excavatability and the flowability requirements of the Tennessee DOT. The use of high amounts of fines in CLSM can lower the cost of CLSM for ready mixed concrete producers and the end users and can provide economical and environmental advantages to the aggregate producers.

2.8.3.4.Bottom Ash

Furnaces that burn dry, pulverized coal are one of the most common furnace types used in the coal burning industry. When pulverized coal is burned approximately 20 percent of the unburned material is recovered as bottom ash and collected in a water filled hopper at the bottom of the furnace. Bottom ash is a dark gray, granular, porous, predominantly sand size (smaller than 12.7 mm [0.5 inch]) material. Bottom ash consists of angular particles that usually are well graded. Bottom ash is composed principally of silica, alumina, and iron. Statistics show that 14.5 million metric tons (16 million US tons) of bottom ash were produced in 1996 and approximately 30.3 percent of it was reused (ACAA 1997). Bottom ash was also researched as a possible filler material in the literature.

Naik et al. (1998) tested CLSM mixtures containing fly ash and bottom ash combinations for compressive strength, bleeding, setting and hardening, settlement, length change of hardened CLSM, permeability, mineralogy, and chemical water

leaching. The study reported that well performing, low permeability, expansive CLSM mixtures could be produced that could be used for void filling applications. Won et al. (2004) also performed tests on CLSM mixtures produced with bottom ash as an aggregate. The study investigated the durability characteristics of CLSM mixtures manufactured with bottom ash under various physical and chemical deterioration conditions and reported that long-term compressive strength tests, water permeability tests, repeated freezing and thawing tests, and wetting and drying tests yielded acceptable results. Katz and Kovler (2004) also investigated the use of industrial by-products in CLSM and stated that mixing inert material that initially exhibited very low strength with an active material such as bottom ash, yielded a material with reasonable strength and durability.

2.8.3.5.Other Filler Materials

Advanced coal technology by-products such as limestone injection and fluidized bed combustion ashes have been used in CLSM (Docter 1998). These materials typically show more cementing characteristics and these have been documented by Docter (1998). Colored glass, that could not be recycled by local bottle manufacturers in Boulder, Colorado, was used in CLSM production with good flowability characteristics after being crushed into 12.5 mm (0.5 inch) pieces (Ohlheiser 1998). As a result of this study the Colorado Department of Transportation (CDOT) issued a revision to their structural fill specifications and allowed broken glass to be used as aggregate. Another by-product, phosphogypsum a byproduct of the phosphoric acid production industry was successfully used in CLSM manufacturing (Gandham et al. 1996). There are other potential materials that can be used in CLSM manufacturing in the future, however trial mixtures and testing are required to ensure that these materials provide sufficient engineering properties and are environmentally acceptable.

2.8.4.Coarse Aggregate

Throughout the development of the CLSM mixtures, fine aggregates, especially concrete sands, were used as filler material. The availability of sand to ready mix concrete suppliers and its lower price compared to coarse aggregates in most of the USA is likely the main reason for this. However, in some parts of the country, such as the west coast have equivalent or greater supplies of gravel compared with sands and in those parts the use of gravel in CLSM production can help achieve greater economy (Fox 1989). CLSM produced with gravel was reported to behave similarly to mixtures that use sand as filler material in terms of compressive strength, erosion, flow, permeability, and excavatability. In terms of subsidence they were reported to behave even better. In 1984, the Mount Baker Ridge Tunnel in Seattle, Washington, used 600 m^3 (786 cy) of CLSM produced with 22.2 mm (7/8 in) top-size gravel to fill subsurface tunnels and exploratory shafts. CLSM was placed directly from truck chutes into the shafts and the placement was completed in 4 hours (Fox 1989).

2.8.5.Chemical Admixtures

Since CLSM is being considered as an alternative to usually inexpensive conventional backfill materials, the cost of CLSM is a very important factor and, in general, properties required for specific applications can be obtained without exotic chemical admixtures that can increase the cost of CLSM. However, there are examples of successful applications of CLSM mixtures manufactured with chemical admixtures.

Flow and resistance to segregation are provided by the cementitious materials in CLSM mixtures. The cementitious materials contribute to the cost and long-term strength gain of the mixture. Newly developed, highly potent air entraining admixtures can entrain large percentages of stable air bubbles in the CLSM mixtures. The use of these products can result in excavatable and flowable CLSM mixtures with limited strength and segregation (Crouch et al. 1998). Accelerators and retarders that are usually used for concrete and conform to the requirements of ASTM C 494, *Standard*

Specification for Chemical Admixtures in Concrete, were also successfully used to produce quick-set and delayed set CLSM mixtures.

2.9.Mixture Proportioning

Currently, a standard method for CLSM proportioning similar to that used for concrete proportioning does not exist. CLSM proportioning is mostly done by trial and error until a mixture with the required characteristics for the intended application can be achieved. The versatility of CLSM that allows the use of different materials in CLSM production prevents the establishment of a general mixture proportioning method. Most agencies develop their own CLSM mixture proportions making use of locally available materials and providing the required characteristics, such as flowability, compressive strength, permeability, etc. ACI committee 229 (1994) published a table of previously used mixtures as a guide and starting point for trial mixtures of practitioners. Table 2.1 shows the mixtures published by the ACI committee.

In 2001 Du grouped the used CLSM mixtures in the literature into four main groups, CLSM I through IV. Type I CLSMs are produced with varying cement contents for different applications. Type II mixtures have 4 to 5 percent cement content, good flowability, and are generally used to backfill voids with limited access. These mixtures were reported to achieve compressive strength values as high as 690 kPa (100 psi) at 28 days. Type III mixtures utilize highly potent air entraining admixtures and can have densities as low as 673 kg/m^3 (1134 lb/cy) when used together with foaming agents. Type IV mixtures have high Class C fly ash contents (Du 2001). A recent survey indicated that most DOT's commonly use the Type I and III CLSM mixtures (Folliard et al. 1999). The four basic types of CLSM mixtures are defined in Table 2.2.

Table 2.1--Examples of CLSM mixture designs (ACI 1994)*

Mix	Cement Content	Fly Ash (lb/cy)	Coarse Aggregate (lb/cy)	Fine Aggregate (lb/cy)	Approximate Water Content (lb/cy)	Comp. Strength @ 28 days (psi)
1	50	-	1700[1]	1842[2]	325	60
2	100	300	-	2600	585	-
3	50-100[3]	0-600[4]	-	2750[5]	500 max.	50-150
4	50	300 Class F or 200 Class C	-	2900	375-540	-
5	60	330	-	2860	510	-
6[6]	185	-	-	2675	500	-
7	50 min.	250	-	2910	500 max.	-
8	100	2000 Class F	-	-	665	-
9	50	550 Class F	-[(7)]	-[(7)]	330	-
10	100	250	-	2850	500	-
11	50	250	-	2910	500	-
12	50	600	-	2500	460-540	80
13	60	-	1705 (3/4 in max.)	1977	257[8]	17@1 day
14[9]	50	250	1900 (1 in max.)	1454	270[10]	100
15[11]	50	250	1900 (1 in max.)	1340	255	-
16[12]	98	1366 Class F	-	-	1068	40 (40@56 days)
17[13]	158	1262 Class F	-	-	1052	60 (75@56 days)
18[14]	144	1155 Class F	-	-	1146	50 (70@56 days)

* Table examples are based on experience and test results using local materials. Yields will vary from 27 ft^3. This table is given as a guide and should not be used for design purposes without first testing with locally available materials.

[1]ASTM C33, No. 57, [2]ASTM C33, [3]Quantity of cement may be increased above these limits only when early strength is required and future removal is unlikely, [4]Granulated blast-furnace slag may be used in place of fly ash, [5]Adjust to yield one cubic yard of CLSM, [6]Five to six fluid ounces of air entraining admixture produces 7 to 12 percent air contents, [7]Total granular material of 2850 lb/cy with ¾ in maximum aggregate, [8]Produces 6 in. slump, [9]Produces approximately 1.5 percent air content, [10]Produces 6 to 8 in slump, [11]Produces 5 percent air content, [12]8¾ in. spread ASTM D6103, 0.8 percent air, 93.7 lb/cy density, [13]10½ in spread ASTM D6103, 1.1 percent air, 91.5 lb/cy density, [14]16¾ in spread ASTM D6103, 0.6 percent air, 90.6 lb/cy density.

Table 2.2--Four basic types of CLSM (Du 2001)

Type	Binder	Flow-driving factors	Aggregate
I (K-Krete)	Cement, fly ash	Water, fly ash	Filler*
II (high fly ash)	Cement, fly ash	Water, fly ash	Fly ash
III (high air)	Cement	High air, water	Filler
IV (flash fill)	Fly ash	Water, fly ash	Filler

*Filler includes concrete sand, bottom ash, foundry sand, and high-fine aggregate, depending on the mixture proportions

2.10.Various CLSM Specifications

Even though CLSM mixtures have been produced and used as early as in 1970s, the real development and research of this material started after the foundation of the ACI committee 229 in 1984. At the end of 1995, only one pipe installation standard, ASTM C 12-95, *Standard Practice for Installing Vitrified Clay Pipe*, included flowable fill. To promote the usage of CLSM ACI published four provisional testing methods specifically for CLSM. These were later accepted by ASTM as full standards:

- ASTM D 4832-1996, *Preparation and Testing of Controlled Low Strength Material (CLSM) Test Cylinders*
- ASTM D 6023-1996, *Standard Test Method for Unit Weight, Yield, and Air Content (Gravimetric) of Controlled Low Strength Material*
- ASTM D 6024-1996, *Test Method for Ball Drop on Controlled Low Strength Material to Determine Suitability for Load Application*
- ASTM D 6103-1997, *Standard Test Method for Flow Consistency of Controlled Low Strength Material*

Review of the literature indicates that the development of full specifications for different CLSM applications by state agencies also started in late 1990s. The survey performed by Riggs and Keck (1998) reported that five state agency specifications were developed for different CLSM applications. The states surveyed and issue dates of the

specifications of those states are shown in Table 2.3. As reported by Hitch (1998), both the Ohio Ready Mix Concrete Association and the Ohio DOT played an important role in the development of the CLSM technology and Hamilton County, Ohio prepared a detailed CLSM specification with aiding documents for producers and practitioners (HAMCIN 1996). Also, as a part of the National Cooperative Highway Research Program Project 24-12 a field manual draft containing specifications for different CLSM applications prepared in the AASHTO format was prepared. Kaneshiro et al. (2001) reviewed different state and project specifications developed for CLSM as a part of the City of Sand Diego Water Utilities Capitol Improvements Program (Kaneshiro et al. 2001). Howard (1998) also proposed a specification that can be used for pipeline bedding, gap filler, and embedment applications of CLSM.

Table 2.3--States surveyed and their specification (Riggs and Keck 1998)

State	Specification and Title of Section	Issue Date
Alabama	Section 260 Low Strength Cement Mortar	1996
Florida	Section 121 Flowable Fill	1997
Georgia	Section 600 Controlled Low Strength Flowable Fill	1995
N. Carolina	Controlled Low Strength Material Specification	1996
S. Carolina	Spec 11 Specification for Flowable Fill	1992
Virginia	Spl. Prov. For Flowable Backfill	1991

2.10.1.Materials

Some specifications define locally available materials and approximate quantities to be used in acceptable CLSM mixtures. In many cases materials do not need to meet strict limits applied for concrete production; however some states require the filler materials to meet standard concrete aggregate specifications. Hamilton County specifications and the proposed specification by the NCHRP project do not restrict the materials except requiring them to be tested for environmental and long-term durability

impact if they are going to be used around metallic pipes. Most of the specifications also discuss the use of air entraining and accelerating agents in CLSM mixtures if needed.

2.10.2.Mixture Proportioning

Although some specifications include recommended mixture proportions and materials to be used, all of the specifications require the contractor to submit his/her own mixture proportion and test results for acceptance criteria. It is generally accepted that for a material such as CLSM that may use many locally available, inexpensive materials, waste, or by-products, the use of performance specifications is more logical compared to the use of descriptive specifications.

2.10.3.Acceptance Criteria

The most commonly used acceptance criteria is the compressive strength. However, different testing methods, testing dates, and different limits for excavatable and non-excavatable mixtures can be found. Alabama, Florida, Georgia, Virginia limit the 28-day compressive strength, while North and South Carolina limit the 56-day compressive strength. Hamilton County, OH specifications require cylinders to be tested for compressive strength at 30 and 90 days, while the NCHRP recommended specifications require testing at 28 and 91 days. The 30 and 90 day testing could require testing on weekends which may make it more costly to use.

Hamilton County and the NCHRP draft specifications also require that CLSM mixtures be field tested for flowability before placement and the NCHRP draft specifications also propose sampling for corrosivity and air content of the mixtures. Hamilton County, OH also requires mixtures to be tested for Removability Modulus (RE) that requires yield and dry unit weight data to be submitted for proposed CLSM mixtures. Where gas leaks are possible, odor migration is a concern for the identification of gas leaks, Hamilton County requires the minimum CLSM mixture permeability as tested by ASTM D 5048 to be $1x10^{-4}$ mm/sec ($3.9x10^{-6}$ in/sec).

Many of the published specifications do not address the corrosivity of CLSM for metallic pipes at all. The specification of California DOT Section 19-3.062 published in 1999 specifies a minimum pH and sets limits for chloride and sulfide contents (Kaneshiro et al. 2001). The Hamilton County, OH specification requires that all materials used for CLSM production be evaluated as non-corrosive by appropriate ASTM standards. The specification also requires the evaluation of the final CLSM mixture for corrosivity following ASTM A 674, *Standard Practice for Polyethylene Encasement for Ductile Iron Pipe for Water or Other Liquids* , if it has a resistivity less than 5000 ohm-cm. The specification requires metallic pipes to be encased with polyethylene if the mixture is evaluated as being corrosive following this standard. The NCHRP proposed specification requires the testing of the CLSM mixture for corrosion performance following a specific method proposed in the NCHRP report and designated as AASHTO X 10, *Provisional Method of Test for Evaluating the Corrosion Performance of Metallic Utility Lines Embedded in Controlled Low Strength Material (CLSM) via Mass Loss Testing of Embedded Samples*. The NCHRP draft specification also requires coating or protection of pipes as needed when pipes traverse soil and CLSM.

2.10.4.Trench Width

Trench related accidents each year in the USA account for several hundred deaths and an estimated several thousand people get injured. The majority of these accidents are caused by trench cave-ins (Brewer 1993). To prevent these deaths and injuries the Occupational Safety and Health Administration (OSHA) developed trench excavation and backfilling regulations. Trench related OSHA regulations are reported in 29 CFR, Ch. XVII, 1926-652 between sections (a) and (g). Severe penalties are assessed for willful violation of these regulations and these penalties should be a very important safety consideration for contractors (OSHA 2005).

OSHA (2005) regulations state that each employee in an excavation shall be protected from cave-ins by an adequate protective system designed in accordance with

the OSHA regulations except when excavations are made entirely in stable rock or excavations are less than 1.52 m (5 ft) in depth and examination of the ground by a competent person provides no indication of a potential cave-in. For excavations between 1.5 and 6 m (5 and 20 ft) the design of slopes and configurations of sloping and benching should be selected using one of the four alternatives:

1. Excavations shall be sloped at an angle not steeper than one and one-half (1½) horizontal to one vertical (34 degrees measured from the horizontal),
2. Maximum allowable slopes, and allowable configurations for sloping and benching systems, shall be determined in accordance with the conditions and requirements set forth in the OSHA (2005) document's appendices A and B. (In Appendix A regulations define four types of soil and in appendix B maximum allowable slopes for excavations less than 6 m (20 ft) deep are provided),
3. Designs using other tabulated data, such as tables and charts. At least one copy of the tabulated data that identifies the registered professional engineer who approved the data, shall be maintained at the jobsite during construction of the protective system, and
4. Design by a registered professional engineer.

The table that shows the maximum allowable slopes for excavations less than 6 m (20 ft) are shown in Table 2.4. "Type A" indicates cohesive soils with an unconfined compressive strength of 144 kPa (1.5 ton/ft^2) or greater. Examples of cohesive soils are: clay, silty clay, sandy clay, clay loam, and in some cases, silty clay loam and sandy clay loam. Cemented soils such as caliche and hardpan are also considered Type A. "Type B" soils are cohesive soil with an unconfined compressive strength greater than 48 kPa (0.5 ton/ft^2) but less than 144 kPa (1.5 ton/ft2). Examples of type B soils are: angular gravel, silt, silt loam, sandy loam, and in some cases silty clay loam and sandy clay loam. "Type C" soils are non-cohesive soil with an unconfined compressive strength of 48 kPa (0.5 ton/ft^2) or less, such as gravel, sand, and loamy sand.

Table 2.4--Maximum allowable slopes (OSHA 2005)

Soil or Rock Type	Maximum Allowable Slopes (H:V)[1] For Excavations Less Than 20 Feet Deep[3]
Stable rock	Vertical (90 degrees)
Type A[2]	3/4:1 (53 degrees)
Type B	1:1 (45 degrees)
Type C	11/2:1 (34 degrees)

[1]Numbers shown in parentheses next to maximum allowable slopes are angles expressed in degrees from the horizontal. Angles have been rounded.
[2]A short-term maximum allowable slope of 1/2H:1V (63 degrees) is allowed in excavations in Type A soil that are 12 feet (3.67 m) or less in depth. Short-term maximum allowable slopes for excavations greater than 12 feet (3.67 m) in depth shall be 3/4H:1V (53 degrees).
[3]Sloping or benching for excavations greater than 20 feet deep shall be designed by a registered professional engineer.

Considering the liabilities, risks, and the cost of full compliance with the OSHA regulations (wider trenches, increased excavation, more time and equipment requirements), the value of not having any workers in the trench for compaction of soils can be much better understood. When CLSM is used, trenches can be excavated with vertical walls using a backhoe. A protection box can be used for conduit installation and to make necessary connections, and the trench can be backfilled directly behind the box.

2.10.5.Reduction in Pipe Strength

The pipe material and shape, the support of the material beneath and to the sides of the pipe all affect the maximum loading that pipes are capable of carrying (McCarthy 2002). The bedding under the pipe supports vertical loads, the sidefill prevents pipes from deflecting outward, and the haunch zone is a part of both sections (Figure 2.1). Good support in the haunch zone is very important to carry vertical loads and to prevent lateral deformations. The difficulty of filling and compacting conventional backfill materials in the haunch zone causes large variability in support in this area. However, CLSM can easily flow into this zone and provide uniform and continuous support to the pipe. Generally, if the bedding and backfill are shaped to the contour of the pipe, better support and higher permissible loads are obtained.

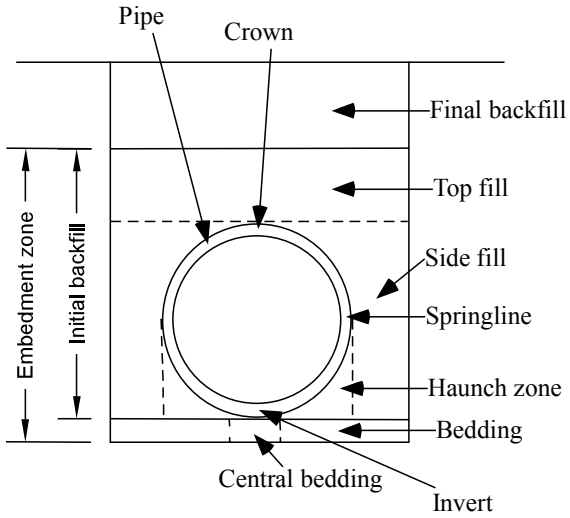

Fig. 2.1--Terminology for pipe and soil zones (McGrath and Hoopes 1998).

The available load bearing capacity of rigid pipes is typically determined using three-edge bearing test load. However, the three-edge bearing test represents a severe loading condition and generally buried pipes are capable of supporting greater loads than determined by the test based on the quality of their beddings and backfill. A study performed at the Iowa Engineering Experimental Station, Iowa State College, classified soil beddings (Marston Spangler bedding classifications) for pipes and determined their load factors, L_f (Spangler 1941). L_f is the ratio of permissible field load to three-edge bearing test load. L_f values greater than unity indicate that the magnitude of the allowable field loading is greater than that for the test load (McCarthy 2002). The Marston Spangler classifications are (Du 2001):

- Class D (Impermissible bedding): Little or no effort is taken to shape the bedding to fit the invert of the pipe or to fill the haunch zone. Backfill is partially compacted.
- Class C (Ordinary bedding): Earth bedding is pre-shaped to fit the invert of the pipe for a width of at least 50 percent of the pipe diameter. The pipe is

surrounded to a height of at least 0.15 m (0.5 ft) above its crown by granular materials that are shovel placed and shovel tamped to completely fill all spaces under and adjacent to the pipe.

- Class B (First class bedding): The pipe is placed on bedding made out of fine granular materials. The bedding is shaped to fit the invert of the pipe with a template for a width of at least 60 percent of the pipe diameter. The pipe is surrounded to a height of at least 0.3 m (0.98 ft) above its crown by granular materials that are carefully placed to completely fill the haunch zone and the sidefill area. Granular materials are thoroughly compacted on each side and under the pipe in thin layers not exceeding 0.15 m (0.5 ft) in thickness.

In addition to the Marston Spangler classifications, there are Standard Installation Direct Design (SIDD) models that were recently adopted by ASCE and AASHTO (McGrath and Hoopes 1998). SIDD differentiates between four types of backfill designs. Type I is a carefully haunched and densely compacted backfill. Type II is a slightly lower quality installation that is approximately equivalent to Class B Marston Spangler bedding. Type III is roughly equivalent to Class C and Type IV is roughly equivalent to Class D Marston Spangler bedding. SIDD Type I installation has well graded sand as a bedding and sidefill and SIDD Type III has low consistency silts.

A study performed by McGrath and Hoopes (1998) compared the L_f values for air entrained CLSM mixtures at 16 hours, 7 days, and 28 days. The study concluded that although the strength and stiffness of air modified CLSM increased with time, CLSM provided good pipe support as early as 16 hours after placing the material. Table 2.5 shows the L_f values for CLSM mixtures at different ages and the load factors for different backfill classifications.

Table 2.5--Comparison of load factors (McGrath and Hoopes 1998)

Backfill		Load factor
CLSM	16 hours	1.8
	7 days	2
	28 days	2.5
Marston Spangler	Class B	1.9
	Class C	1.5
	Class D	1.1
SIDD	Type I	2.3
	Type II	1.7

2.10.6.Placement

Some states, such as South Carolina, allow the placement of CLSM in rain and also allow the placement of CLSM in standing water assuming that it will displace the standing water. Hamilton County and the NCHRP draft specifications also allow the placement of CLSM into standing water, however the NCHRP draft proposed specification does not allow the placement if the standing water represents more than approximately 5 percent of the total volume of CLSM. The NCHRP specification does not allow the placement of CLSM under rain unless approved by the engineer.

Virginia and Alabama require a minimum temperature of 10 °C (50 ºF) and 1.6 °C (35 ºF) for the placement of CLSM, respectively. Virginia also requires protection against freezing of CLSM for 24 hours after placement, while Georgia requires protection for 36 hours. Hamilton County specifications do not specify protection, however the specification states that the mixture shall not be placed on frozen ground and that the mixtures shall be protected from freezing. The NCHRP draft specification also requires a minimum of 10 °C (50 ºF) ambient temperature and requires protection against freezing for 36 hours. Besides the protection against freezing none of the specifications require any special curing treatment for CLSM.

All specification allow direct placement of CLSM into the trenches and Hamilton County and the NCHRP draft specifications do not allow compaction or vibration. The

Hamilton County, OH specification requires vertical wall containments to prevent excess flow of CLSM in long trenches and the NCHRP draft specification limits the allowable flow to 20 m (65.6 ft) from the discharge location. The NCHRP draft specification also requires the CLSM mixture to be placed in 30 minutes after the end of mixing. The draft NCHRP and the Hamilton County, OH specifications both require the CLSM to be brought up to the lines or limits shown on the plans uniformly. For underwater placement applications Florida specifically requires the use of a tremie.

South Carolina discusses the issue of subsidence and the NCHRP draft specification requires the placement of a final lift account for estimated subsidence in cases where subsidence effects on the final grade are critical.

Several state specifications and the Hamilton County, OH specification warn contractors against floating of pipes during the backfilling of trenches with CLSM. Virginia directs the pipes to be secured by some means, such as soil anchors to prevent misalignment. The NCHRP draft proposed specification states that for projects in which no pipe bedding is in place the appropriate horizontal and vertical alignment of pipes and fixtures prior to and during the placement should be ensured and maintained until such time as the CLSM has set to sufficient strength to hold the pipes in place. The specification requires the use of straps, soil anchors, or other approved means of restraint.

2.10.7.Opening to Traffic

Many of the state agency specifications recommend a minimum waiting time before the placement of a wearing surface or opening of the backfill to traffic. The waiting times are based on the setting times of their recommended mixtures. Alabama allows the use of accelerators to reduce the opening time to 12 hours, while Georgia, Virginia, and North Carolina do not discuss the issue. South Carolina recommends waiting periods in the range of 8 to 20 hours and requires the contractor to use a steel plate on CLSM if rutting is likely or if the backfill is opened to traffic in less than 8 hours (Rigs and Keck 1998). Florida requires construction to stop until the CLSM

mixture reaches a penetration strength of 414 kPa (60 psi) measured following ASTM C 403, *Test Method for Time of Setting of Concrete Mixtures by Penetration Resistance*. Hamilton County, OH requires a minimum load bearing strength of 137.9 kPa (20 psi) measured with a penetrometer using the 28.5 mm (1.124 inch) diameter head following ASTM D 1558, *Standard Test Method for Moisture Content Penetration Resistance Relationships of Fine-Grained Soils*. The Hamilton County specifications also state that when CLSM is used to backfill trenches under pavement within the public right-of-way a fast setting mixture shall be used. The specification defines a fast setting mixture as a mixture that will reach the required 137.9 kPa (20 psi) load bearing strength within two hours. The NCHRP draft specification does not define a minimum waiting time or minimum strength requirement but states that CLSM bearing strength should be checked and approved before application of any loads.

2.10.8.Measurement and Payment

The NCHRP recommended specification and the Hamilton County, OH specification both concur that the measurement shall be based on the payment lines indicated on the plans. The Hamilton County specification warns that the volume of CLSM is greater in plastic state compared to the hardened state and the NCHRP draft specification requires the payment to be based on the hardened state of CLSM. Both specifications agree that no payment shall be made for additional material required due to over excavations and that the payment shall be per unit volume of in place material including all costs for furnishing, all materials, equipment, and labor.

2.11.Quality Assurance and Quality Control

American Association of State Highway and Transportation Officials (AASHTO) Quality Assurance Guide Specification defines quality assurance as actions necessary to provide adequate confidence that a product will satisfy a set of given requirements for quality. A survey performed among the State DOTs indicated that half of the states had quality assurance programs for CLSM within their materials department

(Folliard et al. 1999). Since many locally available materials from different sources can be used in CLSM production, the uniformity of the materials should be controlled. Changes in the characteristics of waste or by-products used in the CLSM production can have significant effects on important CLSM characteristics such as flowability, strength, excavability, and other critical characteristics.

2.12.Challenges and Further Research Needs

As mentioned earlier, the foundation of the ACI committee 229 in 1984 was an important step in the development and research of the CLSM. Since then considerable amount of research has been performed and published on important characteristics of CLSM and the ACI committee 229 is in the process of updating its report on CLSM. However, one very important property of CLSM, its corrosivity for metallic pipes, especially when produced using different by-products, has not been investigated. Some researchers indicated that due to the high pH value of cementitious CLSM mixtures, these mixtures should be expected to protect metallic materials embedded in them against corrosion (Brewer 1994). However, currently there are only three limited studies in the literature that actually tested the corrosion of steels in CLSM mixtures (Howard 1998, Abelleira et al. 1998, Samadi and Herbert 2003). These studies were limited in the number of mixtures, materials, samples, and the types of metals they considered. The reference to ASTM A674 that is used for soils, to measure the corrosivity of CLSM mixtures for ductile iron in Hamilton County specifications also shows that engineers still tend to use test methods developed for different materials to test CLSM. Use of these test methods for corrosivity measurements may not necessarily be appropriate for CLSM.

More detailed information on corrosivity of CLSM mixtures, factors that are likely to affect the corrosivity of CLSM, and existing corrosion research is provided in Chapter III.

CHAPTER III

UNDERGROUND CORROSION OF FERROUS MATERIALS

3.1.Corrosion Principles and Mechanisms

Corrosion is broadly defined as the deterioration of materials due to reactions with their environments. The most well known case of corrosion is the corrosion of metals in aqueous solutions where refined metals return to their native states as oxides or salts through interaction with their environment. Corrosion of metals is an electrochemical process that involves exchange of electrons. This process converts chemical energy into electrical energy and consists of one or more electrodes (metals) and/or one or more electrolytes. Figure 3.1 shows the basic corrosion process for metals in aqueous solutions. The area of the metal at which the chemical reduction occurs is referred to as the cathode. The area where oxidation occurs is referred to as the anode. At the anodic site the metal atoms are transferred to the solution as positively charged metal ions and the net oxidation reaction is $M \rightarrow M^{m+} + me$. The electrons liberated from the anodic reaction are picked up and consumed at the cathodic site and the net reduction reaction is $X^{x+} + xe \rightarrow X$. The size of the anodic and cathodic areas in a corrosion process may vary from few atoms to hundreds of square meters. When the anodic and cathodic sites are indistinguishably small and close to each other and undergo reversals with time uniform corrosion occurs. When the areas are identifiable and they do not change over time localized corrosion occurs.

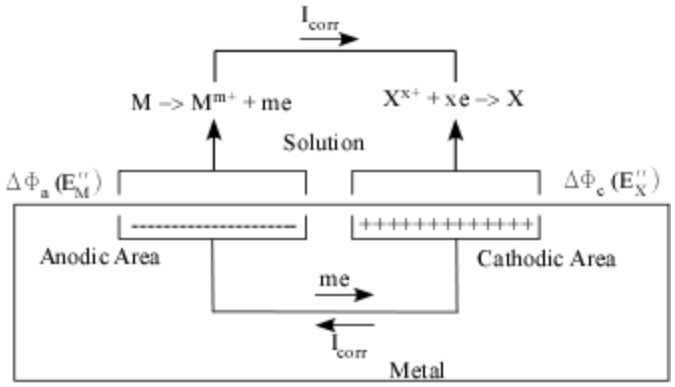

Fig. 3.1--Basic corrosion processes (Stansbury and Buchanan 2000).

The reduction reactions are dependent mainly on the pH and aeration state of the electrolyte. In acidic and basic environments the corrosion of metals is sustained at the simplest case with the reduction of hydrogen (H^+) and water (H_2O), respectively. In aerated environments the reduction of dissolved oxygen increases the rate of corrosion. Table 3.1 shows the possible reduction reactions based on the environment. Also other species in solution can affect the corrosion of metals by affecting the thermodynamic driving forces or by affecting the kinetics of the several corrosion reaction steps. Complexing agents in solution can react and reduce the concentration of free metal ions and make it thermodynamically more favorable for metal ions to pass into solution. On the contrary, species in solution can also form insoluble precipitates with metal ions on the surface of the metal. These precipitates can form protective diffusion barriers and decrease the corrosion rates.

Table 3.1--Reduction Reactions for Different Solutions

Solution	Low Oxygen Solutions	Oxygen Containing Solutions (aerated)
Acidic	$2H^+ + 2e^- \rightarrow H_2$	$2H^+ + ½O_2 + 2e^- \rightarrow H_2O$
Neutral/Basic	$2H_2O + 2e^- \rightarrow H_2 + 2(OH)^-$	$H_2O + ½O_2 + 2e^- \rightarrow 2(OH)^-$

Due to the transfer of ions and electrons at the anode and the cathode, differences in electrical potential develop between the metal and the solution. The potential difference at the anode, $\Delta\phi_a$, is the difference of potential between the metal phase and the solution phase at the anode as shown:

$$\Delta\phi_a = \phi_{M,a} - \phi_{S,a} \tag{3.1}$$

where the subscripts M and S designate the metal and solution phases. Similarly the potential difference at the cathode, $\Delta\phi_c$, is defined as shown:

$$\Delta\phi_c = \phi_{M,c} - \phi_{S,c} \tag{3.2}$$

Coupled, these potential differences build an electrochemical cell in which electrons flow from the anode to the cathode in the metal and the current flows from the cathode to the anode as shown in Figure 3.1. In the solution current flows from the anode to the cathode due the potential in the solution above the anode being higher than that above the cathode; $\phi_{S,a} > \phi_{S,c}$. The driving potential difference for the current in the solution, $\Delta\phi_S$, can be shown as:

$$\Delta\phi_S = \phi_{S,a} - \phi_{S,c} = (\phi_{M,a} - \Delta\phi_a) - (\phi_{M,c} - \Delta\phi_c) \tag{3.3}$$

Following Ohm's law, the corrosion current can be calculated by dividing the driving potential difference between the cathode and the anode by the resistance as shown:

$$I_{corr} = \frac{\Delta\phi_c - \Delta\phi_a}{R_S + R_M} \tag{3.4}$$

where:

I_{corr} is the corrosion current

R_S and R_M are the resistances of the solution and metal paths

Also the tendency for the electrochemical reactions to occur can be related to the interface potential difference and can be determined by the Gibb's free energy equation as shown in Equation 3.5. If the driving potential difference between the cathode and the anode is positive, the Gibb's free energy change will be negative indicating that the reactions will take place.

$$\Delta G = -(\Delta\Phi_c - \Delta\Phi_a)nF \tag{3.5}$$

where ΔG is the change in free energy, n is the number of electrons transferred in the reaction, and F is Faraday's constant (~96500 C).

However, observations have shown that the potential difference at the anode and the cathode are not constant values but functions of the current density. For uniform corrosion the anode current density, i_a, can be calculated by dividing the corrosion current by the area of the anode, A_a. Similarly, the cathodic current density, i_c, can be calculated by dividing the corrosion current by the area of the cathode, A_c. As a function of the current density the potential difference at the anode and at the cathode can be shown as:

$$\Delta\phi_a(i_a) = \Delta\phi'_a + \eta_a(i_a) = \Delta\phi'_a + \eta_a\left(I_{corr}/A_a\right) \tag{3.6}$$

$$\Delta\phi_c(i_c) = \Delta\phi'_c + \eta_c(i_c) = \Delta\phi'_c + \eta_c\left(I_{corr}/A_c\right) \tag{3.7}$$

where $\Delta\phi'_a$ and $\Delta\phi'_c$ are the equilibrium half cell potentials that are the potential differences at the anode and at the cathode when the individual interfaces are at equilibrium, that is, no net transport of ions and electrons occur. The potential difference at the anode and the cathode during corrosion is the equilibrium half-cell potential plus a term, $\eta(i)$, representing the shift in potential difference resulting from

the current density. The shift is referred to as overpotential. Substituting Equations 3.6 and 3.7 into 3.4 the corrosion current can be shown as:

$$I_{corr} = \frac{\Delta\phi_c - \Delta\phi_a}{R_{total}} = \frac{\left[\Delta\phi_c' + \eta_c\left(I_{corr}/A_c\right)\right] - \left[\Delta\phi_a' + \eta_a\left(I_{corr}/A_a\right)\right]}{R_{total}} \tag{3.8}$$

Since η_a is always positive and η_c is always negative, the expression in Equation 3.8 indicates that for the current to flow in the direction shown in Figure 3.1 the equilibrium half cell potential of the cathode must be greater than the equilibrium half cell potential of the anode. However, the corrosion rate is a function of the kinetic mechanisms of the physical, chemical, and electrochemical processes occurring at the cathode and anode and does not depend only on the relative positions of the equilibrium half cell potentials. The expression also shows that the corrosion current is inversely related to the total resistance (R_{total}), that is, if during the corrosion high resistance interface films form on the metal surface the total circuit resistance will increase, decreasing the corrosion rate.

Faraday's law establishes the relationship between the corrosion current density and other expressions of corrosion rate, such as corrosion intensity (*CI*) and the corrosion penetration rate (*CPR*). Each ion formed by the detachment of a metal atom from the surface contributes the charge of m electrons to the corrosion current, where m is the number of electrons left by each atom. The charge of an electron, q_e, is -1.6×10^{-19} Coulomb. If W is the mass loss of metal due to corrosion in t seconds, then the number of moles of metal lost in one second can be found by W/Mt , where M is the atomic mass of the metal. The corrosion current (I_{corr}), generated by the transfer of metal atoms into the solution can be calculated as shown:

$$I_{corr} = \frac{WN_0}{Mt} mq_e \tag{3.9}$$

where I_{corr} is the corrosion current and N_o is Avogadro's number (6.02×10^{23}). The charge of one mole or Avogadro's number of electrons is Faraday's constant (F=96,485 Coulomb/mol). By solving Equation 3.9 for *W/t* and dividing it by the area of the anode (A_a) an expression for the corrosion intensity (*CI*) in units of mass-loss per unit area per unit time can be established as shown:

$$CI = \frac{M\left(I_{corr} / A_a\right)}{m\left(N_0 q_e\right)} = \frac{Mi_{corr}}{mF} \tag{3.10}$$

The corrosion penetration rate (*CPR*) can be calculated by dividing the expression shown in Equation 3.10 by the density of the material, ρ, as shown:

$$CPR = \frac{Mi_{corr}}{mF\rho} \tag{3.11}$$

Table 3.2 shows expressions for the *CI* and *CPR* in different units.

Table 3.2--Faraday's Law Expressions

Expression	Unit	Formula
CI	g/m^2y	$0.327\frac{Mi_{corr}}{m}$
CI	mg/cm^2y	$0.0327\frac{Mi_{corr}}{m}$
CPR	μm/y	$0.327\frac{Mi_{corr}}{m\rho}$
CPR	mm/y	$0.327\times10^{-3}\frac{Mi_{corr}}{m\rho}$
CPR	mpy	$0.0129\frac{Mi_{corr}}{m\rho}$

Note: M, g/mol; m, oxidation state or valence; ρ, g/cm^3; icorr, mA/m^2; y, year; and mpy= mils (0.001 in.) per year

3.2.Underground Corrosion of Metallic Pipes

Many metals, such as iron, used in underground construction applications form a protective passive film of oxide immediately upon being exposed to air. At room temperature, the passive film of iron oxide can provide considerable protection against corrosion. Corrosion of iron and other metals in underground applications at normal or moderate temperatures is due to the formation of an electrochemical cell as explained in the previous section. Two electrically connected points with a potential difference and immersed in an electrolyte build an electrochemical cell. Electrons flow from the anode through the metal to the cathode and ions flow through the electrolyte completing the circuit. Anode corrodes through the loss of metal ions to the electrolyte and the corrosion at the cathode is either completely prevented or slowed down. Although the theory is simple the correlation of this theory with actual corrosion of metallic materials used in underground construction is complicated due to many factors that singly or in combination affect the corrosion reactions (Romanoff 1957). These factors determine the rate and the type of electrochemical corrosion, such as uniform or localized corrosion.

Electrochemical cells fall into three general classes: galvanic cells, concentration cells, and electrolytic cells (AWWA 2004). Galvanic cells form when dissimilar metals are electrically connected in a homogenous electrolyte. Concentration cells form when a metal is submerged in a non-homogenous electrolyte. Electrolytic cells are similar to galvanic cells but they form in the presence of an outside source of electrical energy (stray currents, etc.).

3.3 Common Forms of Corrosion Encountered on Buried Metallic Pipelines

This section will provide information on the commonly observed forms of corrosion of metallic pipelines embedded in backfill materials. Some corrosion forms such as the stray current corrosion, although important, will not be discussed because the rate and occurrence of these corrosion forms are not related to the type of backfill (soil or CLSM).

3.3.1.Uniform Corrosion of Metallic Pipe

Constant, regular removal rates of metal atoms from the overall surface of the metallic pipe is defined as uniform corrosion. Moist earth serves as an electrolyte for the transport of ions. This type of corrosion is the most common and costly corrosion phenomena, however it is usually associated with atmospheric corrosion of metals (Trejo 1997). Because for uniform corrosion to occur, the metallurgical composition of the metal must be uniform and the exposure conditions must be homogeneous over the whole surface. Anode and cathode areas are typically very small, indistinguishable, and reversible. Oxidation and reduction reactions occur uniformly over the surface and can significantly affect the integrity of large portions of the metallic pipe. Formation of a thin passive iron oxide layer on the pipe surface may decrease the corrosion rate considerably.

3.3.2.Pitting Corrosion

Pitting corrosion is a type of localized corrosion. Formation of stable local anode and cathodes due to many different reasons may lead to localized pitting corrosion. Stagnant solution conditions and the presence of halide ions, such as fluoride, chloride, bromide, and iodide, can cause pitting corrosion.

The mechanisms of pitting are not well understood, however there are many theories on the initiation and growth of pits. One of the commonly cited theories is the chloride ion dissolution theory (Brown 1995). This theory suggests that chloride ions replace hydroxyl ions at the passive layer solution interface to form a metal chloride that is soluble in water. Chloride ions will keep dissolving the passive layer until pitting of the underlying metal initiates. Jones (1982) noted that the chloride ions commonly interact with the passive layer at surface heterogeneities and/or at inclusion sites. Janik-Czakor et al. (1975) also noted that the accumulation of chlorides at certain areas of the metal surface lead to the formation of high chloride, low pH micro environments that leads to pit initiation.

Figure 3.2 shows the detail of a pipe wall at an anode undergoing pitting corrosion. The acid-chloride solution in the pit accelerates the dissolution of the metal and concentrates the chloride ions in the pit. An insoluble tubercle of $Fe(OH)_3$ collects at the pit mouth when Fe^{++} diffuses out of the pit and oxidizes to $Fe3^{+}$. In many soils (especially dry soils) the barnacle like scab will seal the pit preventing transfer of Fe^{++} but is porous enough to permit the ingress of more chloride ions, thereby sustaining a high acid chloride solution in the pit. This causes the development of a potential difference between the interior and exterior of the pit and generates a galvanic cell which accelerates the corrosion process (Trejo 1997). One weakness of the chloride ion dissolution theory is that it predicts continuous growth of pits once they are formed, however this is not the case, some pits cease to grow (Brown 1995).

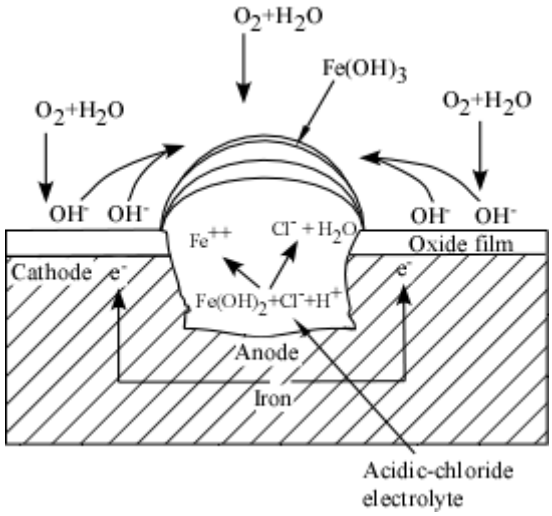

Fig. 3 2--Development of a pit in a ferrous material.

3.3.3.Corrosion Due to Dissimilar Metals

Dissimilar metals submerged into the same electrolyte will have different potential differences forming an electrochemical cell. Two such cases are shown in

Figures 3.3 and 3.4. In Figure 3.3 a brass valve is the protected cathode and the steel pipe is the anode submerged in soil. Since the cathode area is much smaller than the anode area the corrosion intensity of the anode should be low. In Figure 3.4 a galvanic cell is formed with the installment of a new piece of pipe in an old line. Because the old pipe sections have a protective layer built on their surface the new pipe will act as an anode and will corrode based on the corrosivity of the soil and the anode to cathode area ratios.

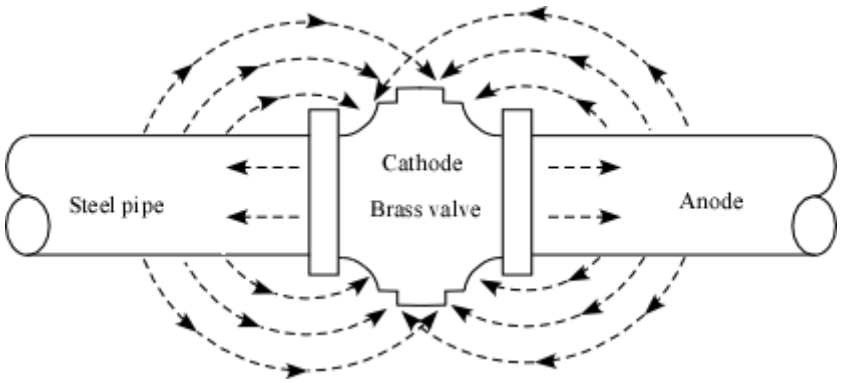

Fig. 3.3--Corrosion caused by dissimilar metals in contact (AWWA 2004).

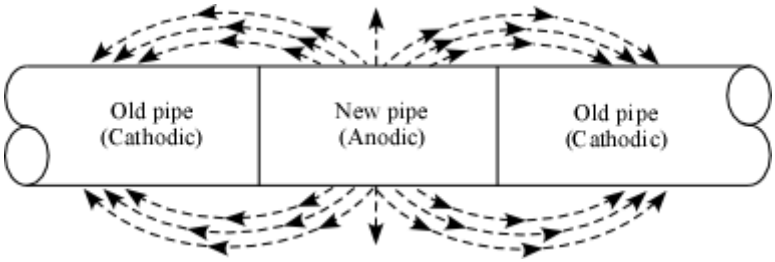

Fig. 3.4--Corrosion due to dissimilar metals (AWWA 2004).

3.3.4.Corrosion Due to Dissimilar Surface Conditions

Scratches or imperfections caused by pipe wrenches, threads, or other damage around coupled areas as shown in Figure 3.5 can cause potential differences to develop. A galvanic corrosion cell with different potentials develops and electrons start to flow from the scratches to the intact parts of the pipe where they are consumed by different reduction reactions. The very small anode to cathode ratio causes the damage due to the galvanic corrosion to be very severe in most cases. The large cathode area will force the corrosion density at the anode to be very high since the corrosion current at the anode and cathode have to be equal. As noted earlier corrosion density is directly related to the corrosion penetration rate or the corrosion intensity.

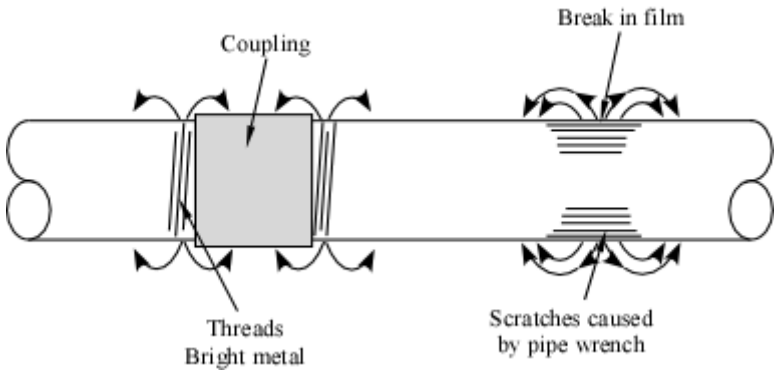

Fig. 3.5--Corrosion caused by dissimilarity of surface conditions (AWWA 2004).

3.3.5.Corrosion Due to Dissimilar Soils

Research indicates that potential differences develop between the areas on metallic pipes that are in contact with dissimilar soils forming electrochemical cells. Hoar and Farrer (1961) reported that the corrosion potential of pipes embedded in different soils could be as much as 90 mV and likely even higher. More recently Levlin (1996) reported that the difference between steel sheets embedded in a clay material and

a sandy, clayey, gravel material was twice as much as that reported by Hoar and Farrer (1961). The same study also reported that the corrosion current between the cathode and anode was as high as 200 μA for a cathode to anode ratio of one and as high as 850 μA for a cathode to anode ratio of 10. Figure 3.6 shows a metallic pipe embedded in clay that goes through a sandy loam column. Sections of the pipe in sandy loam are cathodes and will be protected by the corrosion of the section embedded in the clay. Availability of higher amounts of oxygen to the section of the pipe will increase the reduction reaction rate and cause this section to be cathodic (and more alkaline) compared to the sections of the pipe embedded in clay.

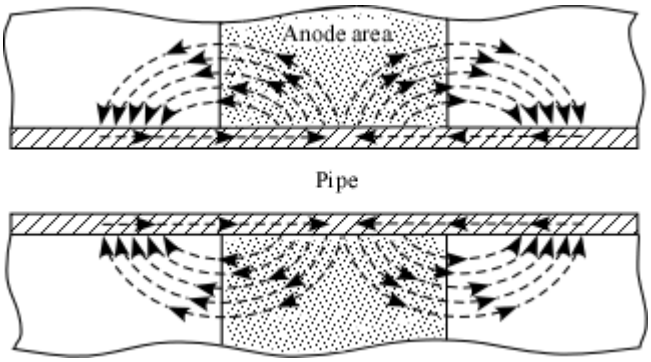

Fig. 3.6--Corrosion caused by dissimilar soils (AWWA 2004).

3.3.6.Corrosion Due to Differential Aeration of Soil

Romanoff (1957) reported on several large scale studies performed at the National Bureau of Standards (NBS) on galvanic corrosion caused by embedded steel samples in different environments. Studies investigated the influence of soil aeration on corrosion and reported that the mass loss was low in soils with good aeration and high in poorly aerated soils. Figure 3.7 shows an example of a corrosion cell established due to differential aeration. Soil throughout the depth of the ditch is uniform but the pipe rests on heavy, moist, undisturbed soil at the bottom of the ditch while the remainder of the

pipe circumference is in contact with drier and more aerated soil backfill. Improper bedding can cause extensive corrosion of the narrow strip at the bottom of the ditch in contact with the moist soil.

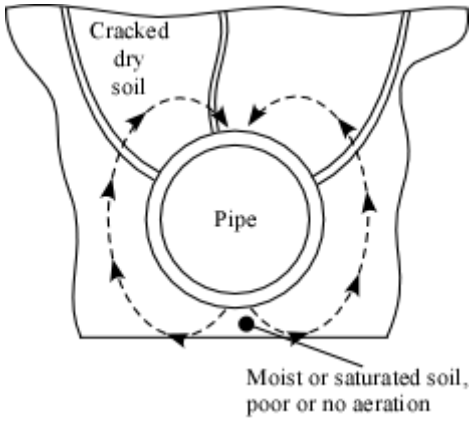

Fig. 3.7--Corrosion caused by differential aeration of soil (AWWA 2004).

3.3.8.Microbial Corrosion

Certain sulfate reducing bacteria that can exist at anaerobic conditions at the pipeline surface consume hydrogen in the process. The consumption of hydrogen causes depolarization of cathodic areas and leads to more rapid corrosion of the metal by galvanic corrosion cells. Anaerobic corrosion of pipelines is usually encountered in water saturated areas, such as areas in close proximity of rivers, lakes, oceans, or areas with poor drainage and stagnant water (Hamilton 1985). Hadley (1939) reported that corrosion due to sulfate reducing bacteria was especially damaging in swamps and low lands when the pH of the soil pore water was between 6.2 and 7.8.

The main effect of sulphate reducing bacteria on cast iron is graphitization. The iron is dissolved away leaving the pipe consisting only of a soft graphitic residue. Corrosion of aluminum and copper containing alloys due to the sulphate reducing bacteria have also been reported. Pitting corrosion of steel pipes due to sulphate reducing bacteria is another common observation. In these cases the pits are open and

filled with soft black corrosion products in the form of iron sulphides (Puckorius 1983, Stoecker 1984, Tatnall 1981). The most significant effect of sulfate reducing bacteria on corrosion was observed in the corrosion of pipe joints calked with sulfurous materials (Starkey and Wight 1945).

Starkey and Wight (1947) and Costanzo and McVey (1958) investigated methods on in-situ determination of anaerobic corrosion. The oxygen reduction (Redox) potential of a soil is an indication of the reducing and oxidizing qualities of the soil and it may be used as an indication of the probable degree of the presence of biochemical corrosion activity. The redox potential is measured between a clean platinum electrode and a saturated calomel reference electrode. The values shown in Table 3.3 can be used as a guide to the possible corrosion severity (NCHRP 1998).

Table 3.3--Redox potential evaluation guide

Redox values	Possible corrosion severity
<100 mV	Severe
100-200 mV	Moderate
200-400 mV	Slight
>400 mV	None

3.3.9.Stress Corrosion Cracking (SCC)

SCC is the caused by the combined action of tensile stress and corrosive environment. The required tensile stresses may be in the form of directly applied stresses or residual stresses that are introduced as a result of cold deformation and forming, welding, heat treatment, machining, and/or grinding. Buried pipelines can be subjected to environmental abuse, external damage, coating disbondments, inherent mill defects, soil movements/instability, and third party damage. An appropriate combination of environment, stresses (hoop and/or tensile and fluctuating stresses) and material type can cause SCC.

Two types of SCC is generally observed in pipelines; high pH SCC (9-13) and near neutral pH SCC (5-7). The high pH SCC caused numerous failures in the USA in the early 1960's and 1970's and near neutral pH SCC failures were recorded in Canada in mid 1980's to early 1990's (corrosion doctors 2005). High pH SCC is usually observed in gas transmission pipelines and occurs in a relatively narrow potential range (-600 to -750 mV vs. $Cu/CuSO_4$) in the presence of a carbonate/bicarbonate environment. SCC initiates at a minimum temperature of 40º C (104 ºF) in the inter-granular cracking mode, however growth rates were observed to decrease exponentially with increasing temperature. In the carbonate/bicarbonate environment a thin protective oxide layer forms around the crack which breaks due to changes in loading or cyclic loading and leads to crack propagation. Near neutral pH SCC is a transgranular crack observed in diluted groundwater containing dissolved CO_2. A cyclical load is required for crack initiation and sulfate reducing bacteria exacerbates the cracking propagation.

3.3.10.Crevice Corrosion

Crevice corrosion is a localized form of corrosion associated with stagnant microenvironments that tend to occur in crevices, such as under gaskets, washers, fastener heads, surface deposits, disbonded coatings, lap joints, and clamps. Limited oxygen diffusion into the crevice sets up a differential aeration cell between the crevice and the external surface. Reduction of oxygen cannot be sustained in the crevice which causes the crevice to be an acidic, anodic environment. Build up of aggressive species such as chloride ions in the crevice can exacerbate the corrosion. Figure 3.8 shows the stages of a typical crevice corrosion process.

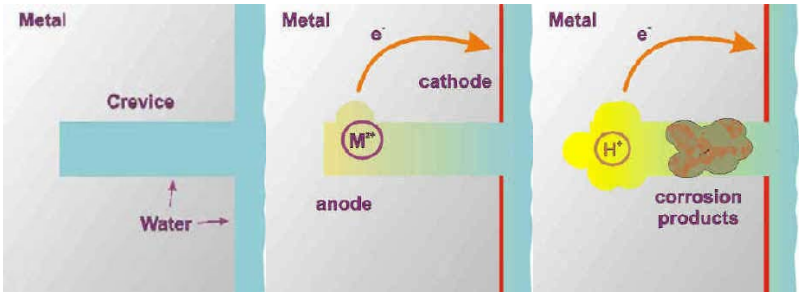

Fig.3.8--Propagation of crevice corrosion.

3.4.Factors That Affect Underground Corrosion

Important factors affecting the corrosion of metallic underground structures were grouped into four interrelated main groups by Romanoff (1957): aeration, electrolyte, structure-environment homogeneity, measurement methods. Brief discussions of these factors are provided in the following section.

3.4.1.Aeration

Aeration factors are all of the factors that affect the access of oxygen and moisture to the buried metal. Aeration factors depend on the physical characteristics of soils such as the particle size, particle size distribution, and specific gravity that affect the size and continuity of pore space. Local differences in oxygen concentration around the pipe can occur due to differences in packing of the soil or the moisture content. Areas of the pipe exposed to lower oxygen concentration will be anodic compared with the areas with higher oxygen concentration. Drying and wetting cycles of the soils have an important affect on the aeration factors. Soils, particularly clays, decrease in volume when dried and increase in volume when wetted. Drying shrinkage soils can create cracks that are effective channels for the oxygen to reach buried pipelines.

3.4.2.Electrolyte

In underground corrosion moist soil is the electrolyte that allows electrochemical corrosion by allowing the flow of current between anodic and cathodic areas. In addition to hydrogen and hydroxyl ions from the water itself the electrolyte also contains

and a variety of cations and anions. The amount and type of the ions depend on the soluble salts dissolved in the electrolyte. The number and type of the ions in the electrolyte determine the characteristics of the electrolyte such as resistivity, alkalinity, and acidity of the electrolyte and the chemical reactions between the primary products of corrosion and the electrolyte. Dissolved sulfate and chloride ions in the electrolyte can build soluble corrosion products with metal ions disturbing protective passive layer (Stansbury and Buchanan 2000). Dissolved ions in the electrolyte can also affect the corrosion without reacting with metal ions, e.g., soluble calcium bicarbonate can form insoluble cathodic deposits (calcium carbonate) due to the increase of alkalinity in the vicinity of the cathode. The soluble ions that need determination for corrosion studies area typically chlorine, sulphate (SO_4), nitrate (NO_3), phosphate (PO_4), calcium, and sodium (Compton 1981).

The overwhelming majority of studies indicate that the resistivity of the electrolyte is the major controlling parameter for corrosion except for areas with severe microbiological activity (Williams 1982). Studies have shown that single-probe measurements are unreliable and the Wenner Four-Electrode Method should be used (Palmer 1989).

Although the resistivity may be measured at grade, ASTM G57, *Standard for Field Measurement of Soil Resistivity Using the Wenner Four-Electrode Method*, recommends resistivity measurements to be obtained from the pipe ditch since at-grade measurements can miss contamination effects. In deicing salt areas, chloride contamination is the main factor affecting the soil corrosivity. Chloride ions decrease the resistivity and break down the passive layer. The NBS test data show that the least corrosive soils have high resistivities and low soluble salt concentrations and that for soils with resistivity values higher than 3000 ohm-cm, soluble ion concentrations were neglible (Romanoff 1957).

Acidity or alkalinity of soils as indicated by the pH value is generally considered a factor affecting the corrosion of metallic underground pipelines. Soils with pH values lower than 4 or higher than 8.5 are considered potentially corrosive. However,

examination of a simplified Pourbaix diagram shown in Figure 3.9 shows that iron can be immune (non corrosive), passive (corroding very slowly), or actively corroding depending on its potential at these pH values. Although most soils in the eastern US are acidic due to leaching of acid rain to the soil, observation of natural soils with a pH lower than 4 is rare without severe industrial contamination. Research performed on the corrosion of carbon steel and metallic coated carbon steel pipes in Swedish soils has also shown that the corrosion rate is in general higher in soils having a low pH, both on carbon steel panels and zinc-coated panels (Camitz and Vinka 1989). However, other researchers have suggested that although pH measurements may be useful in identifying unusual soil conditions, in most cases they are only significant in distinguishing between otherwise similar soils (Palmer 1989). ASTM G51, *Standard Test Method for Measuring pH of Soil for Use in Corrosion Testing*, requires the measurement of soil pH either in situ or immediately after a sample is collected from the field.

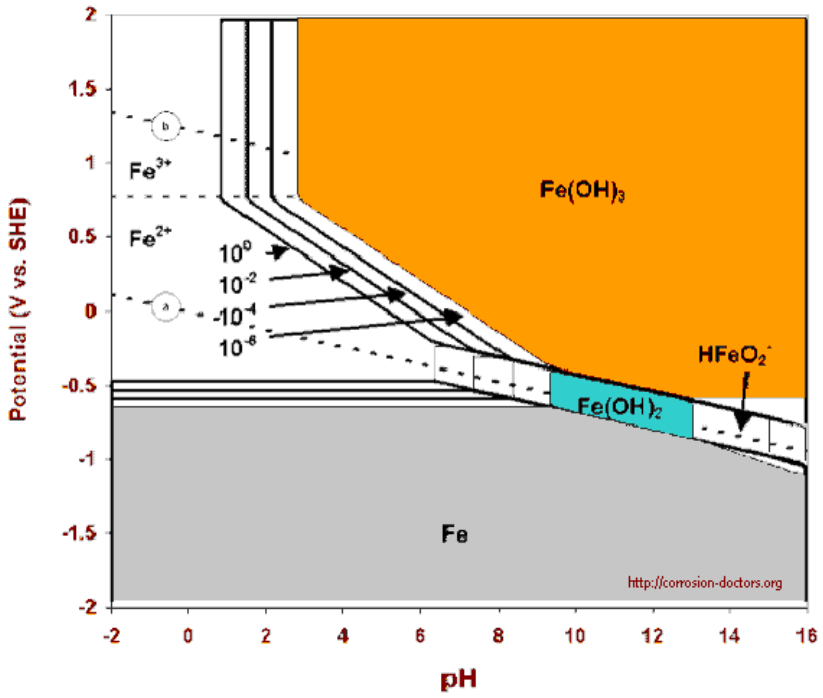

Fig. 3.9--Pourbaix diagram for corrosion of iron (Stansbury and Buchanan 2000).

3.4.3.Structure-environment Homogeneity

Variation of potential over different surface areas of metallic pipelines in the solution is the main cause of electrochemical corrosion. Any factor that can disturb the homogeneity of the underground structure and its environment can cause potential differences. These factors include, but are not limited to dissimilar metals, dissimilar soils, presence of impurities, intermetallic compounds, variation in the supply of oxygen and moisture, etc. The amount of corrosion current that flows due to the variations of potential depends on the electrical characteristics of the electrolyte and polarization at the metal surfaces. The potential differences and the amount of current can change over time due to changes in total resistance caused by accumulation of reaction products. Polarization of surfaces due to hydrogen and hydroxyl ions and local ion deficiencies due to chemical reactions within the electrolyte can also change the potential differences and the amount of corrosion current. Another important factor is the anode to cathode area (A_a/A_c) ratio. The damage to the anode gets larger with the decrease of A_a/A_c for the same potential difference and the same corrosion current because of the increase of corrosion current density.

Another factor noted in the literature that can cause differential potentials to develop is the long-line currents. The long-line currents enter the earth from an anode, enter the pipe at a cathodic site, are transferred long distances along the pipelines, and leave the pipe at an anodic site. These long-line currents are usually observed in cross-country pipelines and there are different suggestions for their origin in the literature (Romanoff 1957).

Improper backfilling of trenches after the lowering of the pipelines is another factor that influences underground corrosion. Placement of excavated soil that consists of a mixture of different soil layers into trenches, without proper wetting or compaction, can cause differential potentials due to earlier defined factors or their combinations.

3.4.4.Measurement Methods

Research has shown that there are so called statistical factors that affect the corrosion data. Logan (1939) has concluded that the observed maximum pit depth in pipeline investigations will increase with increase in the surveyed pipe area. This can cause different pitting factor values to be reported for the same pipe. Pitting factor is the ratio of the observed maximum pit depth to the average depth of pits observed in the surveyed area of the pipe.

3.5.Corrosion of Ferrous Materials in Cementitious Systems

To evaluate the important factors that may influence the corrosion of ductile iron and galvanized steel pipe embedded in CLSM, evaluation of important factors influencing the corrosion of metallic materials in concrete is necessary. Because CLSM contains much lower cement contents compared to regular strength concrete, it is not considered prone to some important durability problems of concrete such as alkali silica reactions or sulfate attack. However, due to the hydration of low amounts of cement and other pozzolanic materials CLSM still exhibits an alkaline environment even though it is lower than concrete. Because of this similarity evaluation of important characters influencing the corrosion of reinforcement in concrete are discussed in the following section.

In good quality concrete steel is unlikely to corrode even if sufficient moisture and oxygen are available due to the spontaneous formation of a thin protective oxide film (passive film) in the highly alkaline pore solution environment (Elsener 2002). However, active corrosion of steel in concrete can occur due to the presence of chlorides in the surroundings of the steel or due to the drop in pH induced by carbonation of concrete cover, providing the concrete is moist enough (Andrade and Alonso 2001, Rodriguez et al. 1996).

Soluble chloride ions in the concrete can be added to the fresh concrete with an admixture, with the mixing water, or with aggregates. Chloride ions can also be introduced into the hardened concrete from the environment due to the application of

deicer salts, sea water exposure, or other exposure conditions. Cement paste has the ability to chemically and physically bind a portion of the chloride ions but the unbound chloride ions are transported into the concrete. The rate of unbound chloride ion transport into the concrete depends on many factors such as the pore size, pore distribution, type of cations present, temperature, mix proportions, and material compositions (Trejo 1997). Once chlorides reach the steel-concrete interface it is believed that they break down the protective passive layer on the surface of the steel. There are two theories for the breakdown of the passive layer by chloride ions. The oxide-film theory states that chloride ions increase the permeability of the passive layer by either penetrating the oxide film through pores or defects or by colloidally dispersing the oxide film (Uhlig and Revie 1985). The adsorption theory states that in competition with the oxygen and hydroxyl ions, chloride ions adsorb on the metal surface and increase the ease in which metal ions go into solution (Kabonov et al. 1947). Tuutti (1982) developed a schematic model for the corrosion process of steel in concrete due to chloride ingress with two separate steps; the initiation period and the propagation period. Later, another study modified Tuutti's model to represent the initiation stage as a function of material selection, mixture proportion, and the degree of damage of the hardened concrete (Mehta 1994).

The high alkalinity of concrete pore solution is due to the $Ca(OH)_2$ produced by the hydration of the portland cement paste. As CO_2 permeates into the concrete (carbonation) it first reacts with the calcium-hydroxide to produce calcium carbonate and then calcium carbonate reacts with CO_2 and H_2O to produce calcium bicarbonate as shown (Trejo 1997);

$$Ca(OH)_2 + CO_2 \rightarrow CaCO_3 + H_2O \tag{3.12}$$

$$CaCO_3 + CO_2 + H_2O \rightarrow Ca(HCO_3)_2 \tag{3.13}$$

Although the formation of calcium carbonates through the reaction of CO_2 with calcium hydroxides improves the impermeability of concrete at the earlier stages of

carbonation, permeability increases with increasing carbonation at later stages due to the formation of soluble calcium bicarbonates (Mehta 1991). The alkalinity of the pore solution decreases in the parts of the concrete penetrated by the carbonation front due to the decrease in the calcium hydroxide concentration. When the carbonation front reaches the hydrated cement paste-steel interface the passive film becomes unstable and breaks down leading to the corrosion of steel.

Use of sound materials, proper mixture proportioning, admixtures, proper placement, and curing procedures were all investigated for their effects on the mitigation of carbonation and chloride induced corrosion. Ho and Lewis (1987) investigated the use of chemical admixtures, fly ash, different curing conditions, and different water-cement ratios for their effects on carbonation and reported that water-cement ratio was the most important controlling factor for the carbonation.

3.6.Corrosion Inspection Techniques for Metallic Pipelines

Failure of metallic water distribution pipelines and transmission lines due to corrosion is very common and their inspection for damage is very difficult due their location below ground. General techniques used by water utilities to assess the condition of their underground systems are failure records, leak detection, and water audits. The biggest disadvantage of these methods is that a problem can only be detected after the pipes have failed. However, since the call for new inspection techniques research by the American Water Works Association Research Foundation (AWWARF) in 1992, new methods have been developed that allow the utilities to prevent pipe failures instead of just reacting to them (Jackson et al. 1992). Some of the general and newly developed inspection techniques are:

- Zone water audits
- Sonic-acoustic leak detection
- Remote field inspection (hydroscope)
- Magnetic flux leakage
- Ultrasound

- Soil corrosivity measurements
- Half cell potential measurements
- Metallic coupons

Zone water audits are an easy way of testing parts or whole of a distribution system. The test compares the minimum nightly flow rate per person per household and a target value that represents the background leakage. The difference between the two indicates the water consumption at night in the monitored part of the system. The standard all nighttime industrial and consumer household usage is then subtracted from the total consumption to find the amount that was lost through breaks and leaks of the system. The method is inexpensive and it can cover large areas of a city quickly. It also allows for a comparison of water losses between individual districts (Sullivan 1990). However, the method does not provide the precise location of leaks and requires isolation of zones. This method can be very useful as a screening process for other techniques and additionally it can be used to evaluate the effectiveness of repair programs by evaluating the before and after repair losses.

Sonic and acoustic leak detection methods use electronic hearing enhancement tools to listen to distinctive sounds produced by the leaks in the pipelines (AWWA 1990). Sonic methods use stethoscopes or listening horns and acoustic methods use geophones or hydrophones placed against the hydrants or on the ground above the pipeline to pick up leak sounds. Correlation software can be used to find approximate locations of the leaks. Studies have shown that leaks in all sizes of service lines with flow rates from 1 to 4000 L/min (1057 gal/min) can be detected. Recently, a new system was developed in the United Kingdom to perform leak detection on large diameter pipelines (Makar and Chagnon 1999). A buoyant hydrophone with a parachute like tail is placed into the pipe to be carried with the water flow. Later, the tail is collapsed and the probe is wound back to the entry point listening and detecting the leaks inside the pipe (Figure 3.10). Because this is a new technology, the percentage of leaks missed by the sonic or acoustic leak detection methods is currently unknown. However,

it should be noted that this method is a reactive control method, i.e., it can detect damage only after pipe damage has occurred.

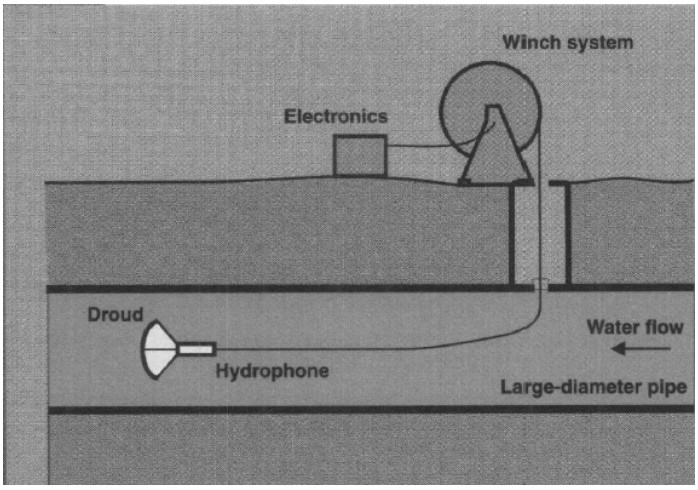

Fig. 3.10--Acoustic leak detection system (Makar and Chagnon 1999).

Remote field inspection is an electromagnetic, nondestructive evaluation technique that has historically been used for heat exchangers and oil well casings (Mackintosh et al. 1996, Schmidt et al. 1989). The method uses a circular emitter coil to generate an alternating magnetic field that is transported to a pickup unit through the pipe wall. The strength of the field fades during the transport based on the thickness of the pipe wall. This characteristic allows damage, such as corrosion pits, wall thinning, and some forms of cracking, to be detected. A recent study concluded that a commercial tool was able to locate and size corrosion pits of more than 3600 mm^3 (0.22 in^3) in volume with an accuracy of ± 0.55 m (± 1.8 ft) (McDonald and Makar 1996). Although this method is more expensive than water audits and leak detection per unit pipe inspection, it is the only method that can detect damage and pitting in pipes before they leak.

The magnetic flux leakage method uses a magnetic field that travels along the pipe wall and exits the pipe wall wherever a corrosion pit or similar defect is present

The magnetic field is established by an arrangement of magnets and sensors placed inside the pipes that can detect the leakage field. The most significant limitation of this method is that it requires the tool to be in direct contact with the pipe wall, which makes it unusable for lined pipelines.

The ultrasound method uses a beam of sound energy with a high frequency (Gas. Res. Inst. 1996). The beam travels into the object to be inspected and is reflected whenever there is a change in the density of the material such as a crack or a corrosion pit. Although not commonly used, ultrasonic tools are commercially available for inspecting oil pipelines (Birks and Green 1991). Tuberculation, that may build up outside the metallic pipelines, can hinder the effective use of ultrasound equipment by causing the ultrasonic beam to be scattered before it enters the pipe material (Makar and Chagnon 1999).

Two complementary techniques; soil corrosivity analysis and half-cell potential measurements can locate areas in which metallic pipes are susceptible to corrosion. A soil analysis can identify areas where corrosion cells can easily develop. The most widely used soil analysis method for material and protective measures selection is ANSI/AWWA C105/A21.5, *American National Standard for Polyethylene Encasement of Ductile Iron Pipe Systems*. This method is based on the measurement of five soil properties; resistivity, pH, redox potential, sulfide content, and moisture levels. Each of the measured characteristics is evaluated using a point rating system and if the total number of points of the soil is 10 or more, the soil is considered to be corrosive for gray or ductile cast-iron pipe. Table 3.4 shows the rating system of the AWWA analysis. Soil resistivity is considered as the most important parameter among the five parameters used by the method and many researchers have indicated direct correlations between the resistivity and observed corrosion activity (Palmer 1989, Edgar 1989, Logan and Koenig. 1939). Based on the importance of the soil resistivity a method was developed that estimates the soil corrosivity based solely on resistivity measurements as shown in Table 3.5 (Palmer 1989). Bernard (1981) also described a statistical probability method for determination of soil resistivity.

Table 3.4--Assigned points for soil characteristics (ANSI/AWWA C105/A21.5)

Soil Characteristics	Points
Resistivity--ohm-cm (based on single probe at pipe depth or water saturated soil box)	
<700	10
700-1000	8
1000-1200	5
1200-1500	2
1500-2000	1
>2000	0
pH	
0.0-2.0	5
2.0-4.0	3
4.0-6.5	0
6.5-7.5	0*
7.5-8.5	0
>8.5	3
Redox potential	
>+100 mV	0
+ 50 to + 100 mV	3.5
0 to + 50 mV	4
Negative	5
Sulfides	
Positive	3.5
Trace	2
Negative	0
Moisture	
Poor drainage, continuously wet	2
Fair drainage, generally moist	1
Good drainage, generally dry	0

*If sulfides are present and low or negative redox potential results are obtained give 3 points for this range.

Table 3.5--Soil corrosiveness based on resistivity

Soil Corrosiveness	Resistivity (ohm-cm)
Very low	10000>R>6000
Low	6000>R>4500
Moderate	4500>R>2000
Severe	2000>R

Studies performed by the NBS have reported observation of abrupt discharges of current from the pipe sections that were in soils of low resistivity and observations of unchanged currents or current collections in the pipe sections that were in soils with moderate or high resistivity (Romanoff 1957). A combination of half cell and line current measurements in areas of corrosive soils can locate the corrosive areas on existing pipelines.

Another inspection technique uses small iron or steel plates (coupons) buried at arbitrary intervals near a pipeline at the pipe depth to determine the rate of corrosion to be expected on the pipeline. Coupons may be extracted at different time intervals and examined for corrosion. A number of cases of close agreement between pipe service life and predictions based on the use of coupons are cited in the literature (Kane et al. 2005).

It should be noted that the periodic inspection of a pipeline using one or a combination of the methods described above is impractical due to the number and extent of the examinations necessary to obtain the representative data. In 1923 a statistical study to estimate the average condition of a pipeline concluded that the line should be inspected at equally spaced points and the longest distance between inspection points should be 610 m (2000 ft) (Gill 1923). In 1939 another statistical study of pit depths on several hundred miles of pipelines reported the effect of different factors on the inspection results such as space interval between the inspected sections, the number of inspection points, starting location, size of the inspected area, etc (Logan and Koenig 1939). The study concluded that a pipeline should be inspected at equally spaced intervals and that the number of inspections should be determined based on the required precision. The study also concluded that as long as the length of inspection intervals was within 1.6 km (1 mile), the starting point on the line did not have a significant effect and that the size of the inspected area is also not significant as long as the number of inspections was sufficiently large (at least one 6 m [20-ft] joint per 1.6 km [mile]). Researchers of the same study also suggested that the number of total inspections may be reduced by first identifying different types of soils traversed by the pipeline and by making only a sufficient number of inspections in each soil to establish its corrosiveness.

In spite of all the research and proposed inspection methods the American Petroleum Institute (API) and the Interstate Commerce Commission (ICC) decided to use an empirical standard for determining pipeline service life based on the experience of the engineers and the age of the line (ICC 1937).

3.7.Ductile Iron Pipe Corrosion

Ductile iron (DI) is a high carbon, cast ferrous material. DI pipe was cast experimentally in 1948 and was introduced to the marketplace in 1955. Since then DI has been the industry standard for more than four decades for transporting raw and potable water, sewage, slurries, and process chemicals. DI pipe is the successor of gray cast iron pipe that was introduced into the United States market in 1817. Today more than 590 U.S. cities have Gray Iron distribution mains in continuous service for more than 100 years.

Gray Iron and DI have similar chemical properties and similar amounts of carbon that affects the machinability and the corrosion resistance of both materials. In gray cast iron most of the carbon is present in the form of a continuous network of flake graphite platelets that are dispersed throughout the metal matrix. Mechanical properties of gray cast iron, such as its relative weakness and lack of ductility, are due to the form of this matrix. DI differs from Gray Iron in that its graphite is spheroidal, or nodular, instead of the flake form found in Gray Iron due to the addition of an inoculant (e.g. magnesium) to molten iron during manufacturing. Figure 3.11 shows the graphite structures of DI and gray cast iron. Since DI consists of a near single-phase ferrous material with only minor discontinuities due to the graphite spheroids, its mechanical strength and ductility are close to that of steel. Although DI is produced with a low cost foundry manufacturing process it has similar mechanical properties to steel.

Fig. 3.11--Photomicrographs showing the graphite structure (DIPRA 2003).

There is a notable lack of consistent opinions on issues such as failure mechanisms, corrosion resistance, and optimal corrosion control methodologies for buried ductile and gray cast iron. This is evident in the 1992 NACE International Report from Task Group T-10A-21 on Corrosion Control of Ductile and Cast Iron Pipe (NACE 1992). There are two major controversies; the first is on the relative service life expectancy of ductile and gray cast iron when exposed to underground conditions, the second is on the relative effectiveness of loose polyethylene encasement system, which is a corrosion control method that is widely used for ductile and gray cast iron pipe but rarely used for other types of pipes.

Although the Ductile Iron Pipe Research Association (DIPRA) claims that DI has better corrosion resistance than gray cast iron because of the spheroidal morphology of the graphite nodules there are conflicting reports on the topic (DIPRA 2003). LaQue (1995) suggested that the interconnected and overlapping flakes of graphite in gray iron could cause a greater depth of penetration of corrosion along the graphite flake boundaries. This suggestion was supported by another study investigating the corrosion of ductile iron pipe exposed in field installations. The study reported that DI was less susceptible to deep localized pitting compared to gray iron because of the "spreading out" of corrosion over the surface of the metal due to the spheroidal graphite structure

(Fuller 1981). Another study comparing the corrosion of adjacent DI and gray iron mains reported that DI was better compared to gray iron due to a lower pitting rate, greater strength, and greater ductility (Ferguson and Nicholas 1992). However, Cox stated that the flake graphite matrix in gray cast iron served as a highly effective diffusion barrier to impede both the access of aggressive species to the corrosion interface of the ferrite phase and to retain the corrosion products within the matrix (Cox 1983). Impeding the transport of the corrosion products out of the material matrix is believed to stifle the subsequent corrosion activity. Investigation of cast iron water mains in England that were constructed in the early part 1900s showed that although there was a substantial reduction in residual pipe wall thickness over large areas of piping there were no leaks and the service life of pipelines was considerably extended compared to the service life of uncoated steel or ductile iron pipes exposed to the same environment.

The flake graphite containing corrosion products have considerable mechanical strength that can contribute to the long service-life of unprotected gray iron pipes in corrosive environments. The strength and adhesion of the flake graphite containing corrosion products of gray iron is believed to be better when compared to the corrosion products of DI due to their difference in microstructure and composition. The corrosion products of gray iron are tightly bound together and to the pipe metal substrate by the residual flake graphite structure and the remaining eutectic network. The eutectic network in the case of phosphorus rich gray iron is made out of the more corrosion resistant phosphide eutectic. In the case of ductile iron the spheroidal graphite nodules are easily detached and there is negligible phosphide eutectic because of the lower levels of phosphorus necessary to achieve the essential spheroidal graphite structure during the manufacturing process (De Rosa and Parkinson 1985, Fitzgerald 1984a, Nicholson 1991, Cox 1983). There are also other studies that concluded that the corrosion resistance of ductile and gray cast iron were not significantly different (NACE 1992, CIPRA 1964, King et al. 1986, Sears 1964, Romanoff 1968, Smith 1968, Gummow 1984, De Rosa and Parkinson 1985). LaQue (1995) reported that gray iron and DI specimens exposed to

abnormally corrosive environments of clay soil in two European beaches exhibited similar corrosion resistance.

3.7.1.Mechanisms of Corrosion

Although it is generally accepted that the mechanisms of external corrosion of ductile iron are similar to those of steel, DI does not fail in the same way or at the same rate as pipe made out of other materials (Fitzgerald 1984b). Corrosion as graphitization is an important external corrosion mechanism for cast gray iron and DI (LaQue 1995, Romanoff 1968). Graphitization usually occurs at soil conditions with appropriate pH, dissolved salts, and organic content for favoring anaerobic bacterial growth. The result is a matrix of iron oxides with distributed residual graphites. As noted earlier in the case of DI, the function of these graphite containing corrosion products as a diffusion barrier is not certain. Subsequent pipe failures occur due to mechanical stresses or hydraulic shocks, such as roadwork, transport damage, or ground movement.

Pitting corrosion is one of the primary failure mechanisms reported for DI pipes. A report prepared by the NRC of Canada on water main breaks during 1992 and 1993 from 21 Canadian cities reported that break rates for DI pipe in 1992 and 1993 were 9.3 breaks/100 km/year (15 breaks/100 mile/year) and 9.8 breaks/100 km/year (15.8 breaks/100 mile/year), respectively (Rajani et al. 1995). Between 76 percent and 78 percent of the ductile iron pipes failed as a result of holes or pits. Another survey performed in England reported that the primary mode of failure for unprotected ductile iron was pitting and the average pitting corrosion rate was in the range of 0.5 to 1.5 mm/year (20-60 mils/year) with values up to 4.0 mm/year (160 mils/year) in some instances (De Rosa and Parkinson 1985). It is generally believed that the rate of external pitting on unprotected ferrous materials is governed by the environment and not by the type of material.

As stated earlier the most commonly used method to assess the corrosivity of an environment for DI pipe is the ANSI/AWWA C105/A21.5 method. Figure 3.12 shows the typical range of average pitting rates of DI at different soil resistivity values

measured from DI pipes with ages of 15 years or younger (Shreir 1963). Since the wall thickness of DI pipe is as much as 50 percent less than that of gray iron pipe the discrepancy between the pitting rates may explain the observed early corrosion failures of DI pipes as reported by Gummow (1984), and De Rosa and Parkinson (1985).

In Scarborough, Ontario DI pipes installed in 1965 exhibited corrosion failures in just seven years and a subsequent study showed that pipes with smaller diameters (thinner walls) were responsible for the largest number of the failures (Doherty 1989). De Rosa and Parkinson (1985) also pointed out the importance of the presence of surface oxides on the localized corrosion of DI pipes. Damage to the annealing oxide scale, especially at the sites corresponding to the reverse peen marks on the external surface of DI pipe can expose bare metal substrate that leads to the formation of galvanic corrosion cells due to dissimilar metals with large cathode to anode ratios.

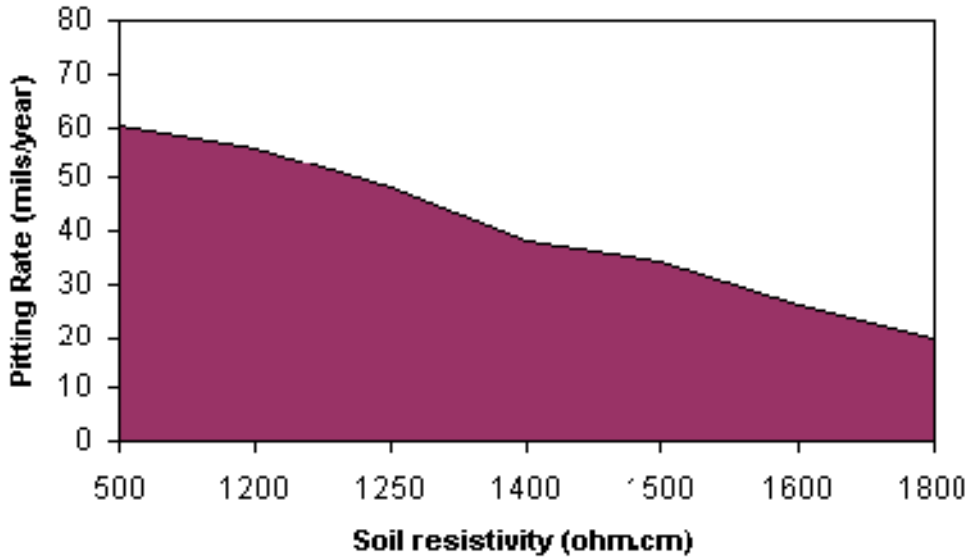

Figure 3.12--Pitting rate at different soil resistivity values (Vrabs 1972).

The service piping used in North America is almost exclusively copper and the galvanic corrosion of DI pipes in contact with copper pipes due to dissimilar metals is

another observed external corrosion mechanism of DI pipes. In 1980 6.2 percent of the 42 water main failures/100 km (62 mile) in Calgary resulted from attack to service saddles that were joined to copper service lines (Caproco 1985). Also, 80 percent of the 23 failures of the DI mains in Bayside, Wisconsin between 1972 and 1976 occurred within 1 m (3 ft) of a copper service pipe or a copper bond strap (Stetler 1980).

A study that exposed blast cleaned cast gray and DI pipe specimens to soils with sulfate reducing bacteria determined that they can suffer extensive corrosion by microbiological activity (King et al. 1986). Both types of pipes corroded at similarly high corrosion rates of 1.27-1.52 mm/year (50-60 mils/year). De Rosa and Parkinson (1985) also reported that DI pipe coated with mill scale corroded with a rate of 1 mm/year (40 mils/year) in soils with sulfate reducing bacteria.

Modern ductile iron pipe are manufactured in 5.5 and 6.1 m (18 and 20 ft) nominal lengths and rubber gaskets are utilized for some joint systems (AWWA 1996). Joints with rubber gaskets offer resistance that may vary from a fraction of an ohm to several ohms and make the pipeline electrically discontinuous. Although this makes the corrosion due to stray currents very difficult, it also makes the line unsuitable for cathodic protection.

3.7.2.Corrosion Protection of Ductile Iron Pipe

Although DIPRA (1997) has reported that the majority of soils found in North America are not corrosive to gray or ductile cast iron and pipes in these soils do not need corrosion protection, there are contradictory opinions on the subject. In their statement DIPRA noted that the soils that were deemed corrosive in their 1956 and 1957 surveys were not considered corrosive anymore based on their 10 points system.

Polyethylene (PE) encasement of DI pipes in corrosive soils is the most recommended protection method by DIPRA. The method was first used in 1950s and was then incorporated in many standards in the US, Japan, UK, Germany, Australia, and international ISO standards. The method requires the encasement of DI pipes in either loose 200 microns (8 mil) low density polyethylene or loose 100 microns (4 mil) high

density cross laminated polyethylene. Advantages of PE encasement are listed as being relatively inexpensive, easy to install, no maintenance or monitoring required, and it is easy to repair if damaged. A 1972 paper by Smith reported that in 20 years no failure of pipe protected with PE encasement was observed (Smith 1972). Case history reports published by DIPRA indicated minimum attack to DI pipes installed in the United States with PE encasement (Horton 1988, Stroud 1989, DIPRA 1997). However, in most of these reports case histories for DI Pipes covered time periods of 6 to 21 years only in soils with resistivity values of 310 to 4000 ohm-cm. A more recent study analyzing the data of the DIPRA database concluded that PE encasement is very effective as a corrosion control system in all soils tested, except in unique severe environments (Bonds et al. 2005).

It should be noted that there are strong disagreements about the benefits of PE encasement. A study reported that bolts made out of 0.5 percent copper content cast iron and used in PE wrapped joints that were buried in the Atlantic City tidal marsh lost an average of 28.9 to 33.1 grams (1 to 1.2 ounce) per year. This significant corrosion rate was attributed to the forcing of water into the void between the PE and the pipe by tidal action (Lisk 1997). Another study performed for Calgary, Canada in 1975 also reported that loose PE encasement was not protective and wrapped pipes and fittings could be severely corroded (Hawn and Davis 1975). Vrabs (1972) performed a study on buried pressurized steel drums and also reported that PE encasement was not a reliable corrosion barrier.

One of the arguments against the use of PE encasement was that the loose PE jacket could easily be damaged, resulting in holidays, rips, and tears during handling, pipe laying, and backfilling operations and that such defects could lead to accelerated corrosion of the pipe in their vicinity by admitting environmental water into the interface between the PE film and the pipe surface. However, a study performed by DIPRA examining 1379 specimens and inspections involving more than 300 different soils concluded that the corrosion rates of iron pipe at damaged areas in PE encasement are not greater than those of non-encased iron pipes (Bonds et al. 2005). DIPRA (1997) did

not recommend PE encasement as the sole protection method in areas where high density stray currents may be present. DIPRA also suggested that PE encasement alone might not be able to protect the pipelines in continuously saturated soils and that it could be used in conjunction with cathodic protection systems (Lisk 1997).

Another recent study concluded that while PE encasement is a cost effective and technically sound method for the corrosion protection of DI pipe, cathodic current can improve the effectiveness of PE encasement and that the methods are not exclusive and can be used in combination (Kroon et al. 2005). This is contradictory to the statement in the NACE report that the use of PE films can restrict the subsequent use of cathodic protection (NACE 1992). Another problem of PE reported in the literature is that PE exhibits significant softening at temperatures over 82 ºC (180 ºF) and will melt around 104 to 110 ºC (219 to 230 ºF) (DIPRA 1997).

Cathodic protection can be used to slow or prevent the corrosion on DI pipelines. Cathodic protection systems reverse the electrochemical corrosive force by creating an external circuit between the pipeline to be protected and an auxiliary anode (sacrificial metal). An auxiliary anode can be immersed in water or buried in the ground at a predetermined distance from the pipe (AWWA 2004). Two methods of cathodic protection are available for generating a protective current. The first method uses a sacrificial anode material such as magnesium or zinc to create a galvanic cell. The electrical potential generated by the cell causes current to flow from the anode to the pipe and to return to the anode through a simple connecting wire as shown in Figure 3.13. This system is generally used to apply small amounts of current at a number of locations, most often on coated pipelines in lightly or moderately corrosive soils. It is practical to use zinc anodes only in low resistivity soils or where only a small cathodic protection current is required since Zinc has a lower corrosion potential and therefore a lower current output. Magnesium anodes have a larger protection current output and can be used over a wider range of soil resistivity values and to protect larger pipe sizes.

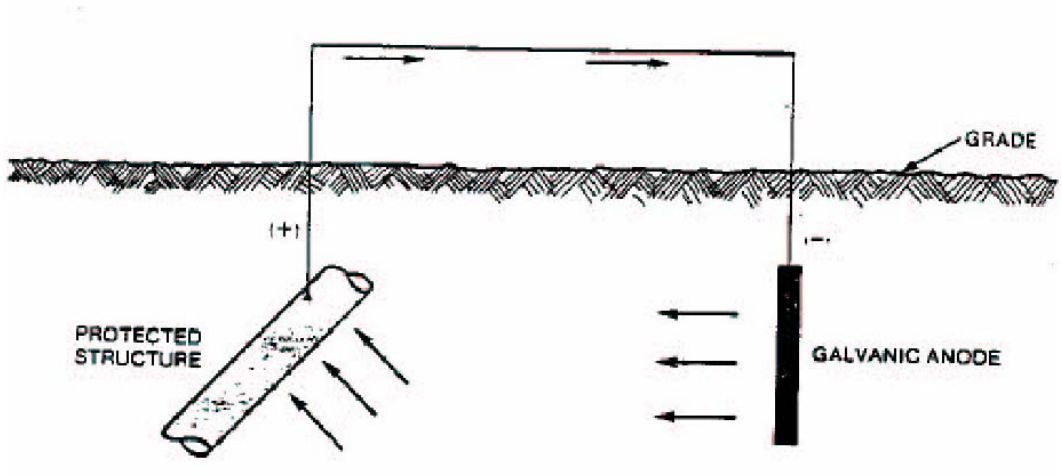

Fig. 3.13--Galvanic anode type cathodic protection (AWWA 2004).

The second method of cathodic protection commonly referred to as impressed current method uses an external DC power supply to energize the circuit. The pipe is connected to the negative terminal and a relatively inert anode is connected to the positive terminal. This method is generally used to supply large amounts of currents at relatively few locations. The basic criterion for adequate cathodic protection of water mains is generally taken as the application of a protection current from the anodes equivalent to 10 mA/m^2 (0.93 mA/ft^2) of pipe surface (Doherty 1989). A recent study on DI pipes concluded that a 75 percent reduction in the corrosion rate or four times the life extension of DI pipe can often be realized with 0.07 V or less of polarization (Kroon et al. 2005). The same study also concluded that the 0.07 V of polarization can be achieved at a current density of 0.1 μA/cm^2 (100 μA/ft^2). Various case histories have also shown that cathodic protection was an effective corrosion control method for DI pipelines (Caproco 1985, Stetler 1980, Doherty 1989, Green and De Rosa 1994). A study comparing the cost of cathodic protection and PE encasement for a 100 year service life of 1.6 km (1 mile) of 762 mm (30 in) DI pipe (assuming PE encasement is sufficiently intact after installation and provides effective corrosion prevention) concluded that the installation cost of the cathodic system was 18 times the cost of

purchasing and installing the loose PE encasement (Craft 1995). The same study also concluded that the operating costs of the cathodic system were 370 times as much as the PE encasement and 6 times the initial purchasing cost of the DI pipe. Using Rossum's (1969) pit depth calculations Spickelmire (2002) also concluded that in aggressive soils, DI with only PE encasement will have a shorter life than DI with cathodic protection and either PE encasement or tight-bonded coatings.

Another corrosion control method that can be applied to DI pipes is the application of an additional bonded coating. DI pipes have a standard asphaltic shop coating and typical annealing oxide that provide some degree of corrosion protection. However, the application of dielectric coatings is not preferred by the industry due to their high costs and due to the following factors (Kroon et al. 2005):

- Abrasive blast surface preparation negates the protective effects of the asphaltic shop coating and the annealing oxide and the measured resistance to earth of shop coated pipe is 1.4 to 1.5 times greater than that of uncoated pipe.
- Because of the peen pattern and the annealing oxide proper surface preparation and coating adhesion is very difficult
- Blisters and slivers can appear on the pipe during blasting
- Many pipe installation contractors and inspectors are not familiar with the proper method of handling coated DI pipe
- Field coating procedures for joints and repairs are difficult
- Coating has a limiting impact on the joint configurations and joint tolerances of field cut pipes.

More recently developed coating systems such as the 100 percent solids polyurethane coatings have also been reported to be successful in corrosion protection. They have been reported to have good chemical resistance, impact resistance, resistance to cathodic disbondment, and abrasion resistance. Polyurethane (100 percent solids) coating was used in combination with sacrificial magnesium anode cathodic protection on a 305 mm (12 in), 9.7 km (6 mile) DI pipeline in San Diego, CA. The coating system

had an efficiency of 99.66 percent and the actual current requirement of the pipe was three times less than the design value (Guan 1995).

3.7.3.Service Life Estimation

Even though the DIPRA website reports a 100 year service life for the cast iron pipes that are predecessors of DI pipes there is no commonly used service life estimation method for DI pipes embedded in different backfill materials. As mentioned earlier the ANSI/AWWA C105/A21.5 uses a 10 point evaluation system to evaluate the corrosivity of soils and requires the encasement of ductile iron pipes in PE when embedded in soils deemed corrosive following this method. But the method does not provide a guideline to estimate the service life of DI pipelines embedded in corrosive soils with or without the PE encasement.

3.8.Galvanized Corrugated Steel Pipe Corrosion

Corrugated Steel Pipe (CSP) was first introduced into the construction industry in 1896 and its basic metal composition, corrugation patterns, and coatings have had many revisions since then. General life expectancy of CSP varies between 10 and 35 years before complete perforation of the metal. CSP is usually fabricated in 6 and 7.3 m (20 and 24 ft) lengths and derives most of its inherent strength from the corrugations formed into the metal sheets at the time of fabrication.

The chemical compositions and microstructures of DI and gray cast iron are different from carbon steel that is commonly used for steel pipes. Steel has a lower carbon content, often forming pearlitic-ferritic microstructure. The ferrite portion of the steel is subject to all the corrosion failure mechanisms described for the DI pipes except the graphitization due to its lower carbon content. A study performed by Horn (1993) noted that steel has less inherent corrosion resistance than DI in buried pipeline applications. Also, the superiority of the resistance to atmospheric corrosion of cast irons compared to carbon steel is widely accepted (LaQue 1995). In contrast, based on the results of a study performed by the U.S. NBS and a British research sub-committee

of the Institute of Civil Engineers it was concluded that with the exception of expensive stainless steels, the corrosion perforation rate of different materials mainly depended on the type of soils and not on the type of material (Mailliard 1985). Evans (1960) also concluded that steel and cast iron corroded at similar rates and that if their thicknesses were the same, steel would probably outlive the iron. Pennington (1966) also worked with steel, gray cast iron, and DI and concluded that for a given thickness when buried bare in soil, steel performed the best among the three. However, in larger commercial sizes, gray cast iron was the only type that did not require an external coating for a service life of 50 years (Pennington 1966). Pennington (1966) also concluded that DI and steel would have about the same service-life in severely corrosive soils, although the DI pipe exhibits greater pitting rates compared to steel or gray cast iron. It should be noted that the wall thickness of DI pipe is as much as 50 percent thinner than gray cast iron pipe for equivalent nominal diameter and is typically only slightly thicker than or equal to the thickness of steel pipe that would be used for similar service (Gummow 1984). Table 3.6 shows the available gage numbers of CSP in the industry and their corresponding wall thickness.

Table 3.6--Conversion of nominal gage to thickness

Gage No.	16	14	12	10	8
Uncoated Thickness (inch)	0.0598	0.0747	0.1046	0.1345	0.1644
Galvanized Thickness (inch)	0.064	0.079	0.109	0.138	0.168
Galvanized Thickness (mm)	1.63	2.01	2.77	3.51	4.27

To provide a longer service-life all CSP have a metallic coating for corrosion protection. When the applied coating does not provide the required service life or is not appropriate for the operational environment, an alternate coating system can be applied.

CSP coatings can be classified into two broad categories, metallic and non-metallic coatings. Commercially available metallic coatings include zinc (galvanized) and aluminum coatings. Non-metallic coatings used on CSP include asphalt, cementitious materials, polymerized asphalt, precoated polymer, and aramid fiber bonded asphalt coatings (NCSPA 2000).

The hot dip galvanizing process (batch galvanizing) produces a zinc coating on iron and steel by immersion of the material in a bath of molten zinc metal. The material to be coated is first cleaned to remove oils, greases, soils, mill scale, and rust. The cleaning process includes a degreasing step, followed by acid pickling to remove scale and rust, and fluxing to apply a protective surface to inhibit oxidation of the steel before dipping into the molten zinc. When the material is dipped in molten zinc, the zinc flows into recesses and other difficult to reach areas for better protection against corrosion.

The batch hot dip galvanized coating is metallurgically bonded to the steel substrate and consists of a series of zinc-iron alloy layers with a surface layer of zinc as shown in Figure 3.14. The strength of the tightly adherent bond is in the range of several thousand pounds per square inch (1 psi = 6.8 kPa). The standard coating thickness for CSP following ASTM A929, *Standard Specification for Steel Sheet, Metallic Coated by the Hot Dip Process for Corrugated Steel Pipe*, is 600 g/m^2 (2 oz/ft^2), 85 μm (3.3 mils).

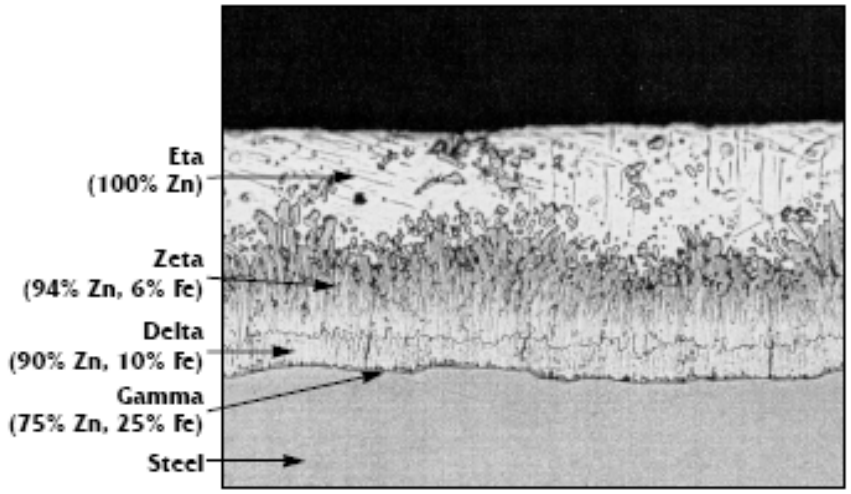

Fig. 3.14--Photomicrograph of batch hot dip galvanized coating (AGA 2000).

Typically the Gamma, Delta, and Zeta layers are harder than the underlying steel. The hardness of the inner layers provides protection against abrasion and the eta layer provides impact resistance through its ductility. Hardness, ductility, and adherence of the galvanic coating protect the CSP against damage caused by rough handling during transportation and handling (AGA 2000).

The zinc coating protects the steel by two mechanisms; by providing a diffusion barrier against oxygen and moisture and by protecting the underlying steel as a sacrificial anode. If the pH of the environment is between 12.2 ± 0.1 and 13.3 ± 0.1, zinc is covered with a thin, compact film of calcium hydroxyzincate [$Ca(Zn(OH)_3)_2 \cdot 2H_20$] that passivates and prevents the corrosion of steel (Macias and Andrade 1987a). If the pH of the environment exceeds 13.2 then zinc is in the active state and undergoes generalized corrosion. Finally, if the pH is between 11 and 12 zinc is covered with a porous, scarcely adhesive film of ZnO that provides no protection (Macias and Andrade 1987b).

Any coating that provides a barrier to the moisture and oxygen in the air will help protect the carbon steel from corrosion. However, if the barrier is damaged with a scratch or surface imperfection corrosion can initiate. When zinc coating is damaged

because zinc is more active than the carbon steel (has a greater tendency to give up electrons), zinc acts as a sacrificial anode and protects the steel. The rate of zinc depletion is relatively slow when the pH of the environment is between 4 and 13. The cathodic protection provided by galvanizing is shown in Figure 3.15.

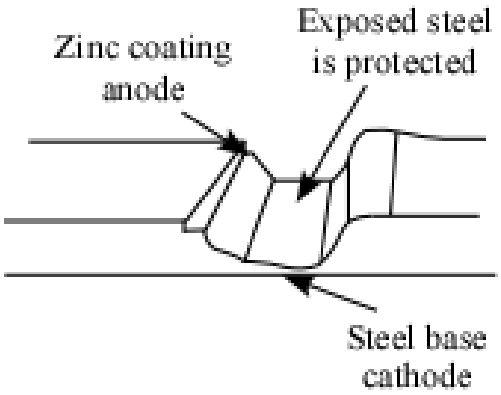

Figure 3.15--Cathodic protection provided by the zinc coating (AGA 2000).

A study performed by the NBS that started in 1937 using 1½" (38 mm) steel pipe with a nominal 3 oz./ft^2 (5.3 mil) zinc coating indicated that the galvanized coating will prevent pitting of steel in soil, just as it does in atmospheric exposure (Romanoff 1957). The same study showed that even in instances where the zinc coating was completely consumed, the corrosion of the underlying steel was much less than that of bare steel specimens exposed to identical conditions. Another study performed by the Corrpro Companies in 1986 found that for CSP external corrosion was generally not the limiting factor (Corrpro 1991). The study stated that 93.2 percent of plain galvanized installations had a service life in excess of 75 years and 81.5 percent had a service life in excess of 100 years. The same study also reported that the soil moisture content primarily affected the activity of the chloride ions present and the chloride's acceleration of the corrosion. The chloride ions did not have a significant effect on the corrosion rate of the zinc coating where the soil moisture content was below 17.5 percent.

The most common method to determine the service life of galvanized CSP is to use the American Iron and Steel Institute (AISI) chart shown in Figure 3.16 (HTF 2002). This chart predicts a variable service life based on pH and resistivity of water and soil. The chart is based on 16 gage galvanized CSP with 610 g/m2 (2 oz/ft2) coating and can be applied to other thicknesses with the appropriate factor. The AISI chart was developed from a chart originally prepared by the California Department of Transportation (Caltrans) (Caltrans 1993). The Caltrans study of durability was based on life to first perforation in culverts that had not received any special maintenance treatment. Many state agencies have defined and use their own failure criteria for their specific type of systems and geography and they use their own service life methods, usually similar to the Caltrans method. More detailed information on the service life estimation methods is provided in Chapter VI, service life of metallic pipes in CLSM.

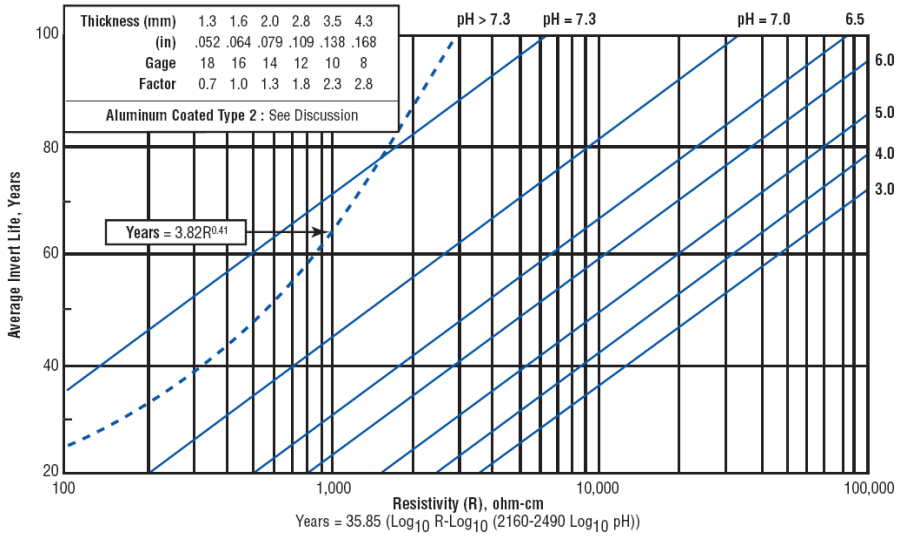

Figure 3.16--AISI chart for estimating average service life for galvanized CSP.

3.9.Corrosion of Metals in Controlled Low Strength Materials

Although CLSM has shown much promise, the use of CLSM is not as common as would be expected considering the potential benefits. Detailed information on the material characteristics and its potential benefits in different applications was provided in Chapter II. A major challenge in implementing the use of CLSM is the lack of knowledge on the material in the materials and construction fields. Engineers are reluctant to specify CLSM because limited data are available on the corrosion performance of metallic pipe materials embedded in CLSM. Existing guidelines on the effect of this material on the corrosivity and service life of pipes are not available. Existing guidelines for determining the corrosivity of soils such as the ANSI/AWWA C105 method discussed earlier do not consider the unique characteristics of CLSM and may not reliably predict the performance. Although these prediction methods are not specifically developed for cementitious materials such as CLSM, they are often applied to these materials and they often indicate that CLSM could be detrimental to the corrosion performance of metallic pipelines.

As noted earlier, research is needed to determine the corrosion performance of metallic pipe embedded in CLSM. The high pH of the pore solution in cementitious materials and the reduced permeability and diffusivity of these cementitiouos materials, when compared with conventional backfill materials, provides improved corrosion protection for embedded metallic materials. But, these characteristics have not yet been considered in existing CLSM guidelines and standards. As such, there is a need to either validate the applicability of existing guidelines and standards for the corrosion performance and protection of pipe embedded in soils for pipes embedded in CLSM or to develop new, more appropriate guidelines for the corrosion performance of metallic pipelines embedded in CLSM.

The ANSI/AWWA C105/A21.5 method used to assess the corrosivity of the soils for ductile iron pipes by assigning different points to certain properties of soils and the AISI method used to assess the service life of galvanized CSP consider the resistivity,

pH, redox potential, sulfides, and moisture of soils. Both methods accept low resistivity as an indicator of corrosivity. However, Abelleira et al. (1998) found that CLSM saturated with corrosive water had a resistivity of approximately one third of the resistivity of sand, even though the corrosion rate was almost negligible for the steel samples embedded in the CLSM. As such, resistivity alone may not necessarily be a significant indicator of corrosion performance for metallic pipes embedded in CLSM.

The pH of the environment is also considered an important factor affecting the corrosivity of the environment. For soils with pH values greater than 8.5, the ANSI/AWWA standard notes that these soils are generally quite high in dissolved salts, resulting in lower resistivity values and higher assigned point values. But, the high pH of the CLSM results from the hydroxyl ions and alkalis present in the pore solution and not from dissolved salts. It has been well documented that high pH pore solutions result in stable, protective, passivating oxide films on iron products (Broomfield 1997). Thus, assigning 3 points for high pH values is probably not applicable for CLSM backfill.

Samadi and Herbert (2003) tested the corrosion of steel coupons embedded in sand and CLSM exposed to tap water and to corrosive water and noted that the CLSM was continuously more alkaline than the sand. The study also reported that CLSM with higher resistivity was less corrosive and the corrosion rate of the CLSM vs. that of encasement sand was 0.76 μm/y vs 6.35 μm/y (0.03 mpy vs. 0.25 mpy), respectively. Samadi and Herbert (2003) also noted that although the corrosion rates of the coupons were changing at the beginning of the exposure period, they gradually leveled off.

Two other soil characteristics identified by the methods used to assess the corrosivity of soils are oxidation-reduction (redox) potential and the sulfide content of the soil. Because most CLSM mixtures are purposely designed for low strength, CLSM mixtures typically exhibit relatively high porosity and permeability values, providing oxygen relatively easy access to the internal CLSM microstructure. The presence of sulfides indicates that sulfate-reducing bacteria could be present. The availability of free sulfides (and sulfates) is expected to be low in the CLSM pore structure, indicating the presence of sulfate-reducing bacteria would be unlikely.

The final soil characteristic considered by the corrosion assessment methods of soils is the moisture content. Bonds (1992) found that the moisture content of CLSM can increase by 4 orders of magnitude from a dry to saturated state. Although resistivity may not be a parameter that can solely predict the corrosion of pipe embedded in CLSM, water is necessary for corrosion reactions and moisture availability could influence the corrosion activity of the pipe. Completely dry conditions will eliminate corrosion. Higher moisture contents can lead to higher corrosion activity and the ANSI/AWWA standard allocates 2 points for continuously wet conditions.

As noted earlier one of the most common corrosion failure modes encountered on buried metallic pipelines is the corrosion due to dissimilar environments (soils). In many instances when CLSM is used in the field, it may not be possible to embed a pipe entirely in CLSM. This could occur when a pipe undergoes localized repair or replacement and CLSM is used as a bedding and backfill material for the repaired area (scenario 1), when a pipe lateral crosses a trench that is to be backfilled with CLSM (scenario 2), or when CLSM is used only as a bedding material and conventional fill materials are used as the backfill material (scenario 3). Figure 3.17 shows these possible scenarios. In these scenarios, different environmental conditions around metallic pipes could generate galvanic corrosion cells that could lead to accelerated, localized corrosion and reduced life expectancies of the pipelines. Concern about the development of galvanic corrosion cells due to potential difference on ductile iron pipes in contact with CLSM and soils simultaneously has also been expressed by the DIPRA (1994).

Engineers commonly use the ANSI/AWWA standard and the California 643 Method, or its modified version the AISI method, to determine the corrosivity of soils for metallic pipe applications. Engineers also use these standards for evaluating the corrosivity of other materials and other applications. Because CLSM is a cementitious material, these standards for evaluating soils are likely not applicable for this material. However, engineers currently have no guidance on how to evaluate the corrosivity of CLSM for pipe applications and these standards are commonly used. Because these standards are likely not applicable for CLSM, they may be limiting the use of CLSM for

backfill applications. As a result, this dissertation developed a research program to evaluate the effect of CLSM on the corrosion performance of ductile iron pipe and galvanized steel and also to evaluate the potential impact of exposing these materials simultaneously to two different environments, CLSM and soils.

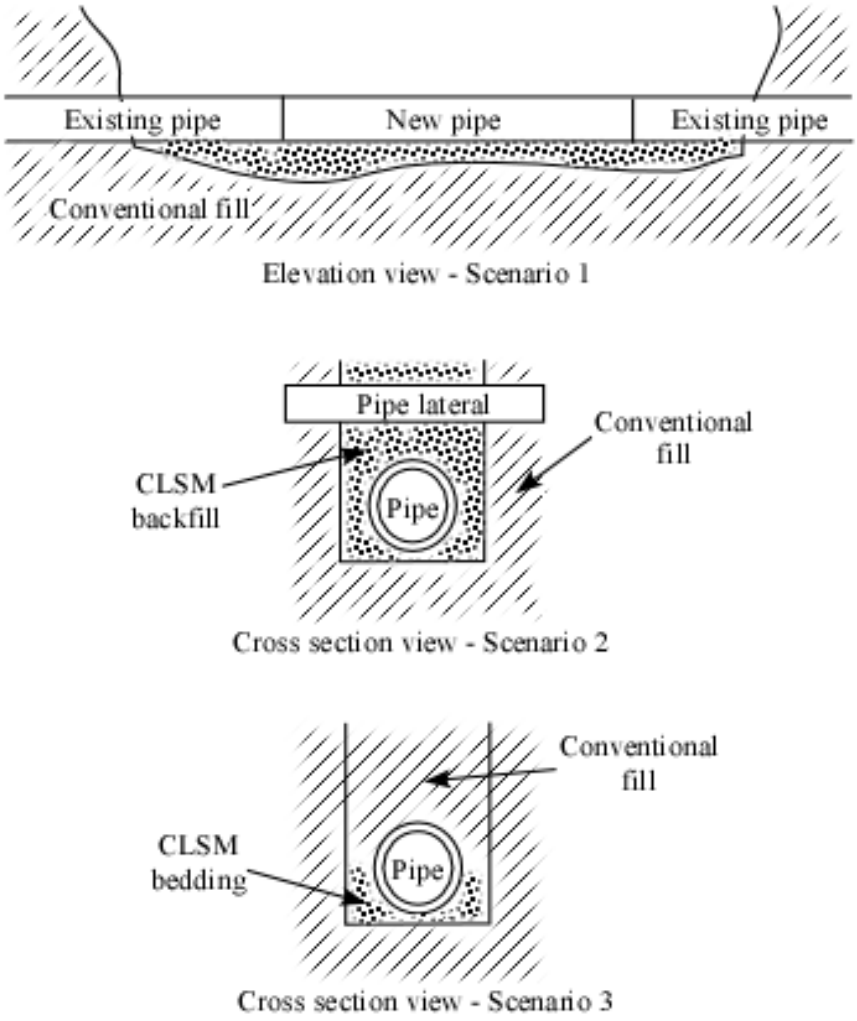

Fig. 3.17--Various scenarios where pipe cannot be completely embedded in CLSM.

CHAPTER IV

EXPERIMENTAL PROGRAM

An extensive study was performed to evaluate the corrosion performance of metals embedded in different CLSM mixtures. DI and galvanized corrugated steel were selected for evaluation because of their common occurrence in current major water distribution and sewage systems. The study was performed in two phases and evaluated a total of 43 CLSM mixtures. The characteristics of the CLSM mixtures such as pH, electrical resistivity, fly ash type, fine aggregate type, cement content, water cementitious materials ratio were examined for their influence on the corrosion of the DI and galvanized steel.

The corrosion of DI and corrugated galvanized steel was evaluated through mass loss measurements of coupons. Even though examination of corrosion through the evaluation of mass loss of metallic coupons is one of the most time consuming corrosion testing techniques, it is also one of the most reliable techniques available in the literature. In two phases metallic coupons were exposed to different environments for a total of 39 months.

Corrosion of metallic coupons embedded in different CLSM mixtures was evaluated in two different environments; distilled water and sodium chloride solution. Chloride ion induced corrosion is accepted as one of the major corrosion processes in cementitious materials in the literature, therefore the exposure of samples to two environments with and without the chlorides and the comparison of results was very important.

The corrosion performance of metals embedded in CLSM when this material was used in conjunction with conventional backfill materials was another important concern observed in the literature. A special experimental setup was designed and used to evaluate the corrosion performance of the ductile iron and galvanized steel coupons that

were in contact with CLSM and conventional backfill materials simultaneously throughout their entire exposure period.

4.1.Sample Fabrication

To evaluate the corrosion performance, metallic coupons machined from ductile iron and galvanized steel pipes were embedded in CLSM and soils and tested in two conditions; uncoupled and coupled. Figure 4.1a and 4.1b shows the samples for both uncoupled and coupled conditions.

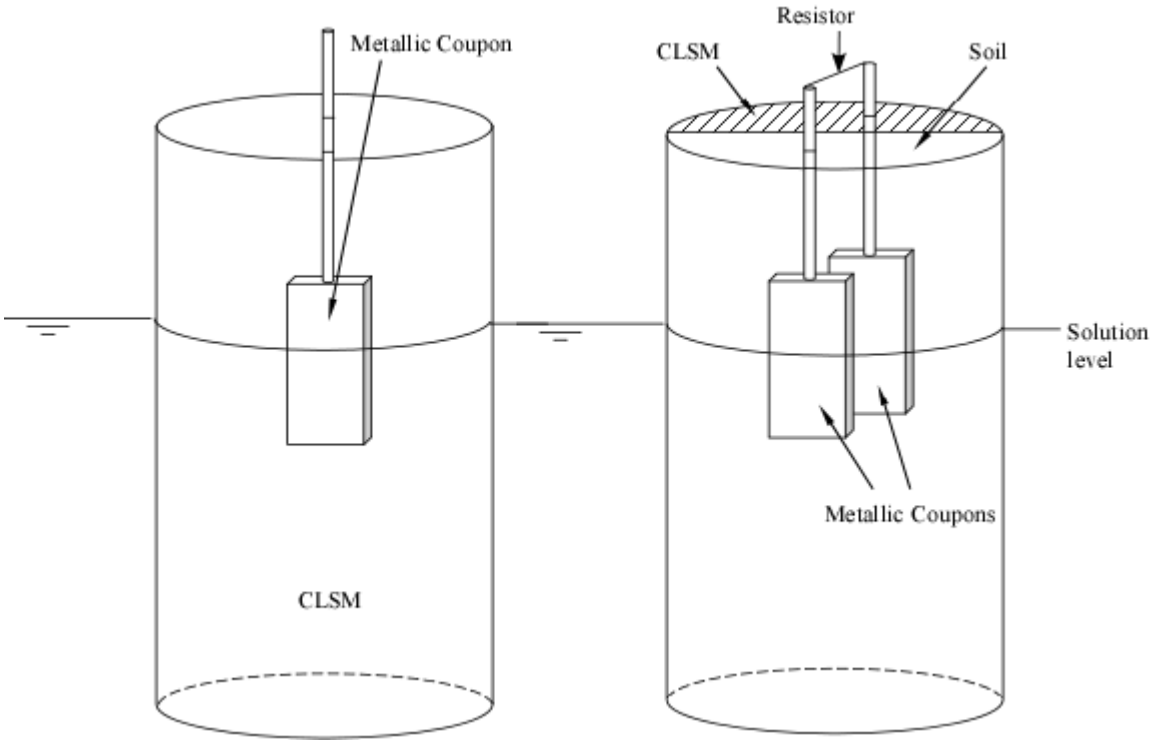

Fig. 4.1 a) Uncoupled sample b) Coupled sample.

Metallic coupons in the uncoupled state were embedded in 75 x 150 mm plastic cylinders containing CLSM and exposed to a chloride solution or distilled water

environment. The center of the metallic coupon was placed at the center of the cylinder, 50 mm (1.96 in) from the top surface. Because CLSM is a low strength material, care was taken not to damage the samples after casting. Precutting the plastic cylinders longitudinally and taping these cuts closed prior to casting minimized damage for the uncoupled specimens. After curing, the plastic cylinder was separated from the CLSM to allow for the direct exposure of the CLSM to the environment. The CLSM cylinders were not removed from the plastic cylinders in order to prevent possible damage to the low strength CLSM samples.

To evaluate the impact of embedding ductile iron and galvanized steel in different environments (coupled state) on the corrosion performance of these materials, metallic coupons were embedded in 100 x 200 mm (4 x 8 in) plastic cylinders as shown in Figure 4.1b. Note that one metallic coupon was completely embedded in the CLSM and the other coupon was completely embedded in the soil. These coupons were electrically coupled with a 10 ohm resistor soldered to the top of the connector rods. To cast a coupled sample, the cylinder was laid on its side. A 38 x 100 mm (1.5 x 4 in) plexiglass sheet was glued to the top of the cylinder, covering one-half of the top opening. A 3 mm (0.12 in) diameter threaded connector rod, connected to the metallic coupon, was attached to the plexiglass with one nut on each side of the plexiglass to secure the rod in place. The hole in the plexiglass was drilled such that the coupon would have 5 mm (0.2 in) of CLSM cover (i.e., offset 7 mm [0.28 in] from the center of the cylinder) when the sample was cast on its side. The top of the metallic coupon was embedded to a depth 98 mm (3.86 in) below the top of the cylinder. After the metallic coupon was secured, the CLSM was placed in the cylinder lying on its side. The sample was then covered with wet burlap for 1 day and then cured in an environmental chamber. After curing, sand or clay was placed in three equal layers and compacted in the remaining cylinder not filled with CLSM. A metallic coupon was placed opposite the coupon embedded in the CLSM, 5 mm (0.2 in) from the face of the CLSM. Six holes (4 mm [0.16 in] diameter) were drilled at 15 mm (0.6 in) above the bottom of each cylinder and the holes were wrapped with a filter paper that would allow the chloride solution or

distilled water to enter into the cylinders but would prevent the soils from being washed out of the cylinders. Control samples were similar to the uncoupled samples, but metallic coupons were completely embedded in sand.

Ductile iron coupons, 13x24x4 mm (0.5x1x0.16 in) in size, were machined from a 300 mm diameter commercially available ductile iron pipe (AWWA C151, Grade 60-42-10) and zinc galvanized steel coupons, 13x24x3.5 mm (0.5x1x0.14 in) in size, were machined from a 300 mm (11.8 in) diameter zinc galvanized steel culvert (uncoated thickness approximately 3.40 mm [0.13 in]). To better represent the actual corrosion performance of the pipe material, care was taken during the sample fabrication to minimize damage to the "as received" mill scale on the samples. The cut edges were coated with low viscosity, two part epoxy to prevent corrosion on the edges.

All samples were covered with wet burlap for 1 day after casting and then cured for 27 days following ASTM C192/C192M-02, *Standard Practice for Making and Curing Concrete Test Specimens in the Laboratory*, in a curing room with a temperature of 23 ± 2°C (73.4 ± 4 ºF) and a relative humidity greater than 98 percent. Later, samples were exposed to a 3.0 percent sodium chloride solution or distilled water. The liquid level was maintained at a level of 90 mm (3.54 in) throughout the test program.

4.2.Experimental Design

The laboratory study was performed in two phases. In the first phase study more CLSM mixtures were evaluated with a lower number of samples per mixture and in the second phase a lower number of CLSM mixtures were evaluated with a higher number of samples per mixtures. This provided for a better statistical analysis. In both Phases I and II, uncoupled and coupled samples were prepared and tested.

4.2.1.Phase I Investigation

The influence of thirty different CLSM mixtures and one sand type (control sample) on the corrosion performance of metals was evaluated. The mixture proportions and fresh CLSM characteristics are shown in Table 4.1a in SI units and in Table 4.1b in

english units. Eight mixtures were duplicated to evaluate the repeatability of the test results. Repeated mixtures are identified with an "R" next to their mixture number. A liquid air entraining agent (AEA) specifically designed for CLSM was used in mixtures 16 through 23 and mixture 26. Mixtures 26, 27, and 28 contained a liquid, non-chloride, accelerating admixture meeting ASTM C494, *Standard Specification for Chemical Admixtures for Concrete*, Type C requirements. In the first phase study only ductile iron coupons were evaluated. Three coupled and uncoupled samples for each of the thirty-eight CLSM mixtures and five control samples were fabricated. All of the samples were exposed to 3.0 percent sodium chloride solution for 18 months. The control samples and the soil section of coupled samples were filled with a sand meeting the "graded sand" requirements of ASTM C778, *Standard Specification for Standard Sand*.

4.2.2.Phase II Investigation

Thirteen CLSM mixtures were cast to evaluate the corrosion of metals embedded in CLSM. The proportions of CLSM mixtures and their unit weights are shown in Table 4.2a in metric and Table 4.2b in english units. Small case letters added to the mixture names indicate separate batches. The corrosion performance of ductile iron and galvanized steel coupons were evaluated. A minimum of five coupled and five uncoupled samples were prepared for each of the thirteen CLSM mixtures. Over 1000 samples were evaluated in the second phase study. Half of the samples were exposed to 3.0 percent sodium chloride solution and the rest were exposed to distilled water for 26 months. One of the two types of soils (sand or clay) was used to fill the soil section of each coupled sample. The sand met the "graded sand" requirements of ASTM C778. The clay used was obtained from the National Geotechnical Experimentation Site located on the Texas A&M University Riverside Campus. The plastic and liquid limits of the clay were 20.9 percent and 53.7 percent, respectively, and the hydraulic conductivity coefficient was measured as $5x10^4$ m/yr.

Table 4.1a--Phase I CLSM mixture proportions and fresh characteristics (metric)

Mix No	Cement Content (kg/m^3)	Fly Ash Type	Fly Ash content (kg/m^3)	Fine Aggregate Type	Water Demand (kg/m^3)	Flow (mm)	Total Bleeding (%)	Air Content (%)	Fresh Unit Weight (kg/m^3)
1	30	Class C	180	CS	211	200	-	0.9	1965
1R	30	Class C	180	CS	206	210	2.08	0.9	1974
2	60	Class C	180	CS	206	200	2.45	0.95	2108
2R	60	Class C	180	CS	206	250	0.21	0.5	2291
3	60	Class C	360	BA	577	180	4.32	1.65	1754
3R	60	Class C	360	BA	541	200	2.58	2.1	1997
4	30	Class F	360	CS	220	200	0.39	2.2	2199
4R	30	Class F	360	CS	220	220	2.92	1.8	2211
5	60	Class F	180	BA	600	180	5.84	2.5	1739
5R	60	Class F	180	BA	600	160	7.2	1.4	1887
6	30	HC	360	CS	315	200	2.26	1.3	2103
7	30	Class F	180	FS	501	200	0.57	2.1	1817
8	60	HC	180	FS	532	240	1.04	3.3	1647
9	60	Class F	360	FS	520	200	0.54	2.5	1684
10	30	HC	180	BA	628	140	4.81	2	1681
11	60	HC	360	BA	573	230	6.42	1.7	1743
12	30	Class C	360	BA	572	220	3.64	2.7	1774
13	60	Class C	360	FS	499	200	0	1.8	1902
14	60	Class F	360	CS	216	220	1	1.3	2174
15	30	Class C	360	FS	486	200	0.13	2.75	1741
16	30	None	0	CS	295	200	2.33	16	1922
16R	30	None	0	CS	295	190	2.35	15.5	1874
17	30	None	0	BA	582	130	4.35	20	1447
18	60	None	0	CS	200	220	0.7	16.5	1836
19	30	None	0	BA	492	130	1.08	25	1385
20	60	None	0	BA	525	130	3.41	18.5	1485
20R	60	None	0	BA	525	130	1.44	15.5	1511
21	30	None	0	CS	170	180	0.62	25.5	1789
22	60	None	0	CS	131	200	0.05	26.5	1748
22R	60	None	0	CS	136	180	0.43	25.5	1802
23	60	None	0	BA	454	140	1.3	28.5	1382
24	60	Class F	1200	None	486	240	2.25	2.8	1635
25	60	HC	1200	None	853	240	7.38	1.3	1322
26	60	None	0	CS	136	170	0	25.5	1802
27	60	Class F	1200	None	486	230	1.28	0.7	1638
28	60	Class F	180	CS	220	200	1.33	1.4	2182
29	60	None	0	FS	373	230	0.28	2.6	1812
30	30	None	0	FS	414	200	0.4	2	1789

CS – concrete sand, BA – bottom ash, FS – foundry sand, HC – high carbon

Table 4.1b--Phase I CLSM mixture proportions and fresh characteristics (English)

Mix No	Cement Content (lb/cy)	Fly Ash Type	Fly Ash content (lb/cy)	Fine Aggregate Type	Water Demand (lb/cy)	Flow (mm)	Total Bleeding (%)	Air Content (%)	Fresh Unit Weight (lb/cy)
1	51	Class C	303	CS	356	200	-	0.9	3312
1R	51	Class C	303	CS	347	210	2.08	0.9	3327
2	101	Class C	303	CS	347	200	2.45	0.95	3553
2R	101	Class C	303	CS	347	250	0.21	0.5	3862
3	101	Class C	607	BA	973	180	4.32	1.65	2956
3R	101	Class C	607	BA	912	200	2.58	2.1	3366
4	51	Class F	607	CS	371	200	0.39	2.2	3707
4R	51	Class F	607	CS	371	220	2.92	1.8	3727
5	101	Class F	303	BA	1011	180	5.84	2.5	2931
5R	101	Class F	303	BA	1011	160	7.2	1.4	3181
6	51	HC	607	CS	531	200	2.26	1.3	3545
7	51	Class F	303	FS	844	200	0.57	2.1	3063
8	101	HC	303	FS	897	240	1.04	3.3	2776
9	101	Class F	607	FS	876	200	0.54	2.5	2838
10	51	HC	303	BA	1059	140	4.81	2	2833
11	101	HC	607	BA	966	230	6.42	1.7	2938
12	51	Class C	607	BA	964	220	3.64	2.7	2990
13	101	Class C	607	FS	841	200	0	1.8	3206
14	101	Class F	607	CS	364	220	1	1.3	3664
15	51	Class C	607	FS	819	200	0.13	2.75	2935
16	51	None	0	CS	497	200	2.33	16	3240
16R	51	None	0	CS	497	190	2.35	15.5	3159
17	51	None	0	BA	981	130	4.35	20	2439
18	101	None	0	CS	337	220	0.7	16.5	3095
19	51	None	0	BA	829	130	1.08	25	2334
20	101	None	0	BA	885	130	3.41	18.5	2503
20R	101	None	0	BA	885	130	1.44	15.5	2547
21	51	None	0	CS	287	180	0.62	25.5	3015
22	101	None	0	CS	221	200	0.05	26.5	2946
22R	101	None	0	CS	229	180	0.43	25.5	3037
23	101	None	0	BA	765	140	1.3	28.5	2329
24	101	Class F	2023	None	819	240	2.25	2.8	2756
25	101	HC	2023	None	1438	240	7.38	1.3	2228
26	101	None	0	CS	229	170	0	25.5	3037
27	101	Class F	2023	None	819	230	1.28	0.7	2761
28	101	Class F	303	CS	371	200	1.33	1.4	3678
29	101	None	0	FS	629	230	0.28	2.6	3054
30	51	None	0	FS	698	200	0.4	2	3015

CS – concrete sand, BA – bottom ash, FS – foundry sand, HC – high carbon

Table 4.2a--CLSM mixture proportions and unit weights (metric)

Mix	Cement Content (kg/m^3)	Fine Aggregate Content (kg/m^3)	Fine Aggregate	Fly Ash Content (kg/m^3)	Fly Ash Type	Water Content (kg/m^3)	Flow (mm)	Air Content (%)	Unit Weight (kg/m^3)
A1a	63	0	None	1200	F	184	209	1.5	1605
A1b	63	0	None	1200	F	432	203	1.3	1591
A1c	63	0	None	1200	F	515	200	1	1605
A2a	0	1500	CS	206	C	134	200	1.5	2177
A2b	0	1500	CS	206	C	200	305	0.6	2180
A3a	30	1500	CS	0	None	98	178	30	1602
A3b	30	1500	CS	0	None	118	200	25	1695
A3c	30	1500	CS	0	None	111.7	200	29	1593
A4a	15	1500	CS	180	F	190	216	1.5	2194
A4b	15	1500	CS	180	F	204	229	1.3	2169
A4c	15	1500	CS	180	F	196	216	1.5	2167
A5a	30	1500	CS	180	F	184	203	2	2185
A5b	30	1500	CS	180	F	188	203	2.3	2163
A5c	30	1500	CS	180	F	170	225	1	2177
A6a	15	1500	CS	180	HC	190	210	2	2115
A6b	15	1500	CS	180	HC	224	203	2	2097
A6c	15	1500	CS	180	HC	216	206	1	2084
A7a	30	1500	CS	180	HC	232	203	2.3	2099
A7b	30	1500	CS	180	HC	232	203	1.3	2111
A7c	30	1500	CS	180	HC	214	206	1.8	1978
A8a	15	1500	CS	180	C	168	216	4.8	2155
A8b	15	1500	CS	180	C	168	216	1.8	2220
A8c	15	1500	CS	180	C	174.4	200	1.5	2179
B10a	30	1500	BA	180	C	318	175	1.5	1852
B10b	30	1500	BA	180	C	318	200	2	1848
B4a	30	1500	CS	180	C	186	216	4.8	2170
B4b	30	1500	CS	180	C	144	216	1.3	2225
B4c	30	1500	CS	180	C	184	200	1.8	2228
B6a	30	1500	CS	180	HC	472	209	2.3	1753
B6b	30	1500	FS	180	HC	494	203	1.8	1765
B6c	30	1500	FS	180	HC	524	200	1.5	1750
B7a	30	1500	FS	180	C	484	222	1.5	1795
B7b	30	1500	FS	180	C	426	229	3	1848
B9a	15	1500	BA	180	HC	324	165	1.8	1821
B9b	30	1500	BA	180	HC	324	145	2.8	1760

CS - concrete sand; BA - bottom ash; FS - foundry sand; HC - high carbon; "-" indicates data not obtained. All CLSM mixtures containing fine aggregate had 1500 kg/m^3 of fine aggregate. Because flow was the key parameter and the amount of water influenced the amount of flow, all mixtures volumes may not be exactly 1 m^3.

Table 4.2b--CLSM mixture proportions and unit weights (English)

Mix	Cement Content (lb/cy)	Fine Aggregate Content (lb/cy)	Fine Aggregate	Fly Ash Content (lb/cy)	Fly Ash Type	Water Content (lb/cy)	Flow (mm)	Air Content (%)	Unit Weight (lb/cy)
A1a	106	0	None	2023	F	310	8.2	1.5	2705
A1b	106	0	None	2023	F	728	8.0	1.3	2682
A1c	106	0	None	2023	F	868	7.9	1	2705
A2a	0	2528	CS	347	C	226	7.9	1.5	3669
A2b	0	2528	CS	347	C	337	12.0	0.6	3675
A3a	51	2528	CS	0	None	165	7.0	30	2700
A3b	51	2528	CS	0	None	199	7.9	25	2857
A3c	51	2528	CS	0	None	188	7.9	29	2685
A4a	25	2528	CS	303	F	320	8.5	1.5	3698
A4b	25	2528	CS	303	F	344	9.0	1.3	3656
A4c	25	2528	CS	303	F	330	8.5	1.5	3653
A5a	51	2528	CS	303	F	310	8.0	2	3683
A5b	51	2528	CS	303	F	317	8.0	2.3	3646
A5c	51	2528	CS	303	F	287	8.9	1	3669
A6a	25	2528	CS	303	HC	320	8.3	2	3565
A6b	25	2528	CS	303	HC	378	8.0	2	3535
A6c	25	2528	CS	303	HC	364	8.1	1	3513
A7a	51	2528	CS	303	HC	391	8.0	2.3	3538
A7b	51	2528	CS	303	HC	391	8.0	1.3	3558
A7c	51	2528	CS	303	HC	361	8.1	1.8	3334
A8a	25	2528	CS	303	C	283	8.5	4.8	3632
A8b	25	2528	CS	303	C	283	8.5	1.8	3742
A8c	25	2528	CS	303	C	294	7.9	1.5	3673
B10a	51	2528	BA	303	C	536	6.9	1.5	3122
B10b	51	2528	BA	303	C	536	7.9	2	3115
B4a	51	2528	CS	303	C	314	8.5	4.8	3658
B4b	51	2528	CS	303	C	243	8.5	1.3	3750
B4c	51	2528	CS	303	C	310	7.9	1.8	3755
B6a	51	2528	CS	303	HC	796	8.2	2.3	2955
B6b	51	2528	FS	303	HC	833	8.0	1.8	2975
B6c	51	2528	FS	303	HC	883	7.9	1.5	2950
B7a	51	2528	FS	303	C	816	8.7	1.5	3026
B7b	51	2528	FS	303	C	718	9.0	3	3115
B9a	25	2528	BA	303	HC	546	6.5	1.8	3069
B9b	51	2528	BA	303	HC	546	5.7	2.8	2967

CS - concrete sand; BA - bottom ash; FS - foundry sand; HC - high carbon; "-" indicates data not obtained. All CLSM mixtures containing fine aggregate had 1500 kg/m^3 of fine aggregate. Because flow was the key parameter and the amount of water influenced the amount of flow, all mixtures volumes may not be exactly 1 m^3.

4.3.Material Characteristics

4.3.1.CLSM

The CLSM mixtures used in the research program contained portland cement, fly ash, water, and fine aggregates. The materials and the mixture proportions selected for this study were based on a survey of current practice; in addition, an experimental design software was used to select the actual mixtures from a range of possible mixtures to allow for subsequent interpolation and extrapolation of research findings (Folliard et al. 1999). Mixtures differed in the quantity of cement, the type of fine aggregate, and the type and quantity of fly ash used. Water was added to each mixture to achieve a flow of approximately 200 mm (7.9 in). Flow was measured following ASTM D 6103-97, *Standard Test Method for Flow Consistency of Controlled Low Strength Material (CLSM)*.

ASTM Type I cement and laboratory tap water was used for all the mixtures. The chemical composition of the cement used in the research is shown in Table 4.3.

Table 4.3--Chemical composition of Type 1 Portland cement

Chemical compound	% by weight
Silicon Dioxide, SiO_2	21.0
Aluminum Oxide, Al_2O_3	4.9
Iron Oxide, Fe_2O_3	2.3
Calcium Oxide, CaO	64.8
Magnesium Oxide, MgO	1.7
Sodium Oxide, Na_2O	0.3
Compound composition	
C_3S	62.0
C_2S	13.0
C_3A	9.0
C_4AF	7.0

Three fly ashes were included in the study, including one Class C and one Class F fly ash (based on ASTM C 618, *Standard Specification for Coal Fly Ash and Raw or Calcined Natural Pozzolan for Use as a Mineral Admixture in Concrete*). The third fly ash had a loss-on-ignition (LOI) value of over 14 percent and is referred throughout this dissertation as a "high-carbon" fly ash. The high-carbon ash exceeds the 6 percent maximum LOI value specified in ASTM C 618. The chemical compositions and LOI values of the fly ashes and foundry sand used in the research are shown in Table 4.4. High-carbon off-spec fly ashes are often not used in conventional concrete because they increase the water requirement and admixture dosage, especially air-entraining agent dosage. However, these ashes are acceptable and widely used for CLSM, which is desirable as a low strength material.

Table 4.4--Chemical composition of fly ashes and foundry sand

Chemical compound	Percent by weight			
	Class F Fly Ash	Class C Fly Ash	High-Carbon Fly Ash	Foundry Sand
Silicon Dioxide, SiO_2	55.24	34.40	47.29	85.20
Aluminum Oxide, Al_2O_3	29.43	20.20	19.53	3.92
Iron Oxide, Fe_2O_3	5.19	5.76	5.21	3.46
Total (SiO_2+ Al_2O_3+ Fe_2O_3)	89.86	60.36	72.03	92.58
Calcium Oxide, CaO	1.59	26.73	6.01	0.79
Magnesium Oxide, MgO	0.93	5.15	2.05	0.58
Sodium Oxide, Na_2O	0.24	1.58	2.47	0.98
Potassium Oxide, K_2O	2.18	0.36	0.83	0.17
Titanium Dioxide, TiO_2	1.44	1.32	0.75	0.21
Manganese Dioxide, MnO_2	0.03	0.06	0.04	0.11
Phosphorus Pentoxide, P_2O_5	0.28	1.08	0.40	0.00
Strontium Oxide, SrO	0.10	0.39	0.31	0.01
Barium Oxide, BaO	0.07	0.60	0.30	0.07
Sulfur Trioxide, SO_3	0.38	1.98	0.38	0.20
Loss on Ignition (LOI)	2.90	0.37	14.44	
Specific Gravity	2.41	2.51	2.09	

Concrete sand, bottom ash, and foundry sand were used as fine aggregates. Fine aggregate gradations were determined following ASTM C 136, *Standard Test Method for Sieve Analysis of Fine and Coarse Aggregates*. The bottom ash was slightly coarser and the foundry sand was finer than the limits imposed by ASTM C 33, *Standard Specification for Concrete Aggregates*. Figure 4.2 shows the gradation curves of the fine aggregates and the ASTM C 33 limits. The absorption capacities and specific gravities of the constituent materials were determined following ASTM C 128, *Standard Test Method for Density, Relative Density (Specific Gravity), and Absorption of Fine Aggregate*. The chemical composition of the foundry sand is shown in Table 4.4. The absorption capacities, specific gravities, and fineness modulus of fine aggregates are shown in Table 4.5.

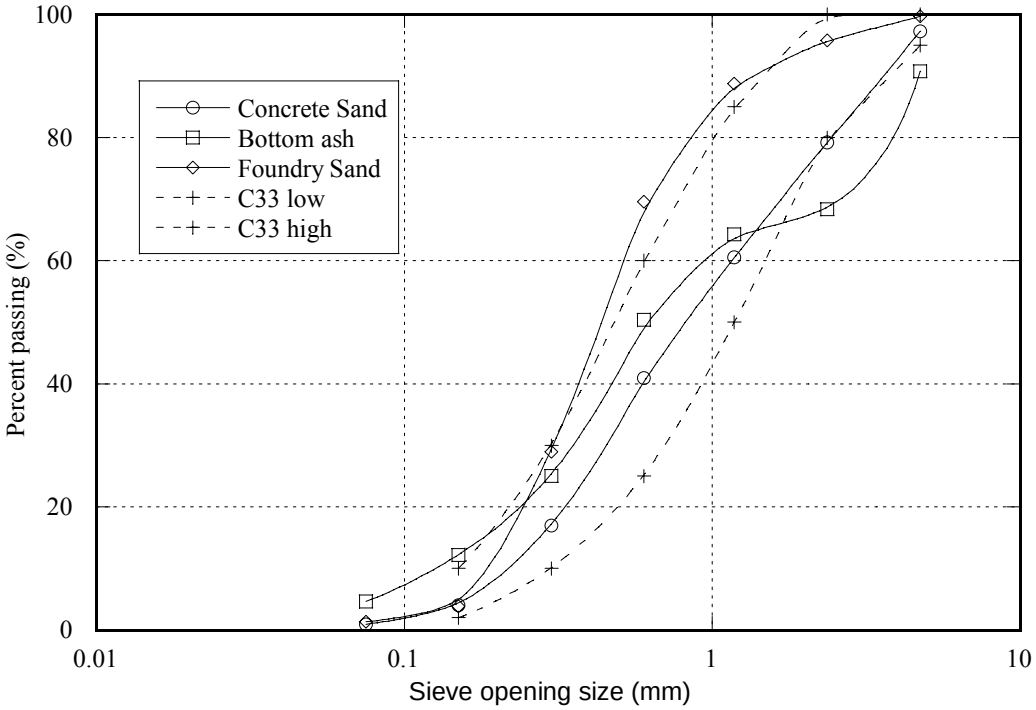

Fig. 4.2--Gradations of the fine aggregates.

Table 4.5--Material characteristics of fine aggregates

Material	Type	Specific Gravity	Absorption (%)	Fineness Modulus
Fine Aggregate	Concrete Sand	2.60	1.00	3.00
	Foundry Sand	2.36	5.60	2.14
	Bottom Ash	2.28	8.90	2.89

The air-entraining agent (AEA) was a viscous solution of organic compounds specifically designed for use in CLSM. The average specific gravity of the agent is 1.0 and the average total solids are 95 percent. The admixture is capable of entraining stable air contents ranging from 15 to 35 percent. The accelerating agent was a liquid non-chloride admixture conforming to the requirements of the Type C group of ASTM C 494, *Standard Specification for Chemical Admixtures for Concrete*. The average specific gravity of the accelerating agent is 1.34 and the average total solids are 41.5 percent.

4.3.2.Ductile Iron and Galvanized Steel

The corrosion current (I_{corr}) and the corrosion potential of the specific ductile iron and galvanized steel specimens used in this study were also evaluated in a simulated solution with similar alkalinity to the CLSM pore solution. CLSM pore solution has a pH value lower than concrete pore solution that typically has a pH greater than 13. Using the Tafel extrapolation technique with a potentiodynamic scan of ±300 V about the corrosion potential the corrosion potential (E_{corr}) and the exchange current density (i_{corr}) were calculated. A slow scan rate of about 600 mV/h was used to determine the i_{corr}. Figure 4.3 shows the potentiodynamic scan of the galvanized steel coupon in simulated solution that has a pH of 10. The analysis shows that the current exchange density is approximately 1.76×10^{-3} A/cm^2.

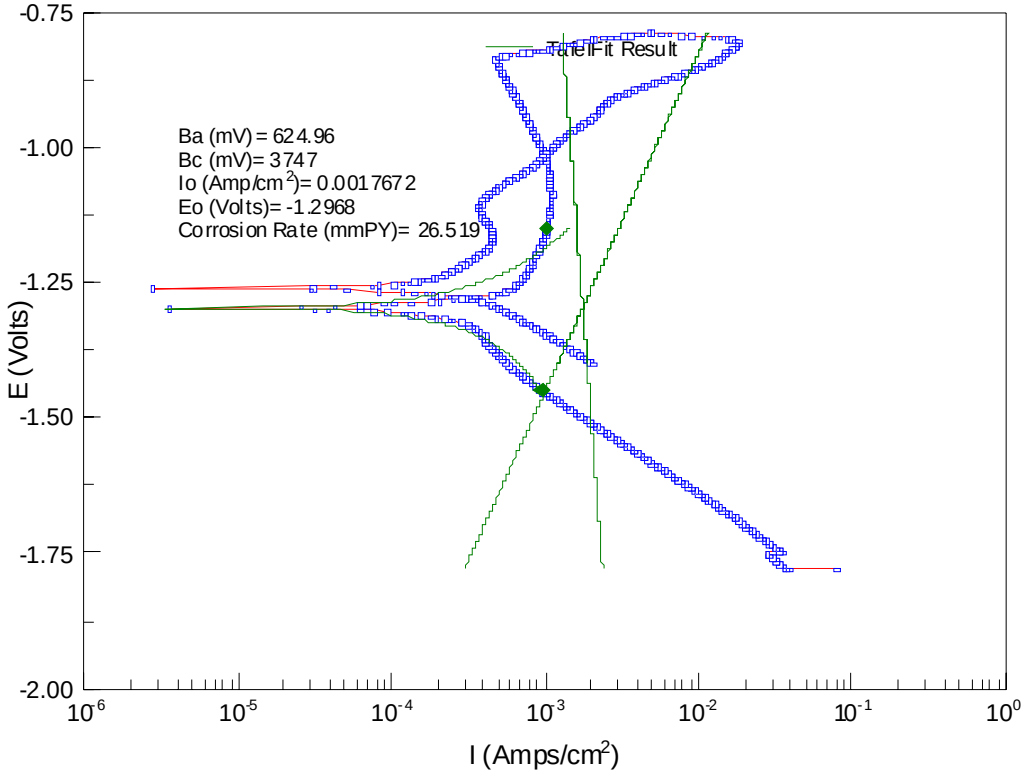

Fig. 4.3--Potentiodynamic scan of galvanized steel coupon.

Figure 4.4 shows the potentiodynamic scan of the DI coupon in simulated solution that has a pH of 10. The analysis shows that the current exchange density is approximately 3.56×10^{-6} A/cm^2.

The curves obtained from the potentiodynamic scanning of the DI coupons and the galvanized steel coupons indicate that corrosion of galvanized steel coupons can be expected to be greater in CLSM environment which typically exhibits a pH value between 9 and 11.

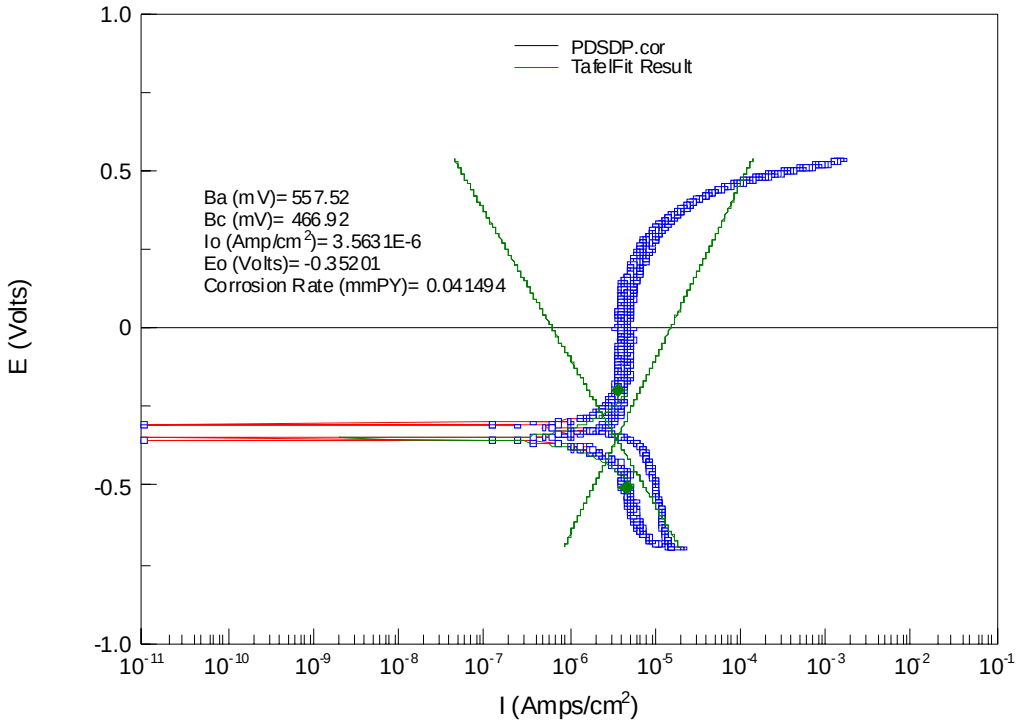

Fig. 4.4--Potentiodynamic scan of DI coupon.

4.4.Testing Methods

4.4.1.Mass Loss Testing

In both phases, metallic coupons were removed from the samples at the end of the exposure period and were evaluated for mass loss following ASTM G1, *Standard Practice for Preparing, Cleaning, and Evaluating Corrosion Test Specimens.* Ductile iron coupons were cleaned using cleaning procedure C.3.5 and galvanized steel coupons were cleaned using cleaning procedure C.9.5. In the case of coupled samples, only the coupons embedded in the sand were evaluated for mass loss as it was determined early in this study that this would be the anode. The coupon embedded in the CLSM on these samples exhibited limited corrosion, if any. Evaluation of the coupons was based on the

amount of mass loss resulting from corrosion divided by the original mass of coupons resulting in percent mass loss values.

4.4.2.Resistivity

In the first phase study, the resistivity of the CLSM and sand were evaluated using a resistivity box (or soil box) as described in ASTM G57, *Standard Test Method for Field Measurement of Soil Resistivity Using the Wenner Four-Electrode Method*. Resistivity measurements were obtained from saturated samples at 182 days after casting. These samples were cast at the same time with the corrosion samples (i.e., the CLSM came from the same batch for both sample types). In the second phase study, the resistivity of CLSM and soils were not measured from separately cast samples, but from each of the actual exposed uncoupled and coupled samples following ASTM G57. Four stainless steel pins were used as electrodes instead of a soil box with a soil resistance meter to measure the resistance of cylindrical CLSM samples as shown in Figure 4.5. The electrodes were placed at an equal distant of 25.4 mm (1 in) from each other, measuring the resistance of CLSM at a depth of 25.4 mm (1 in).

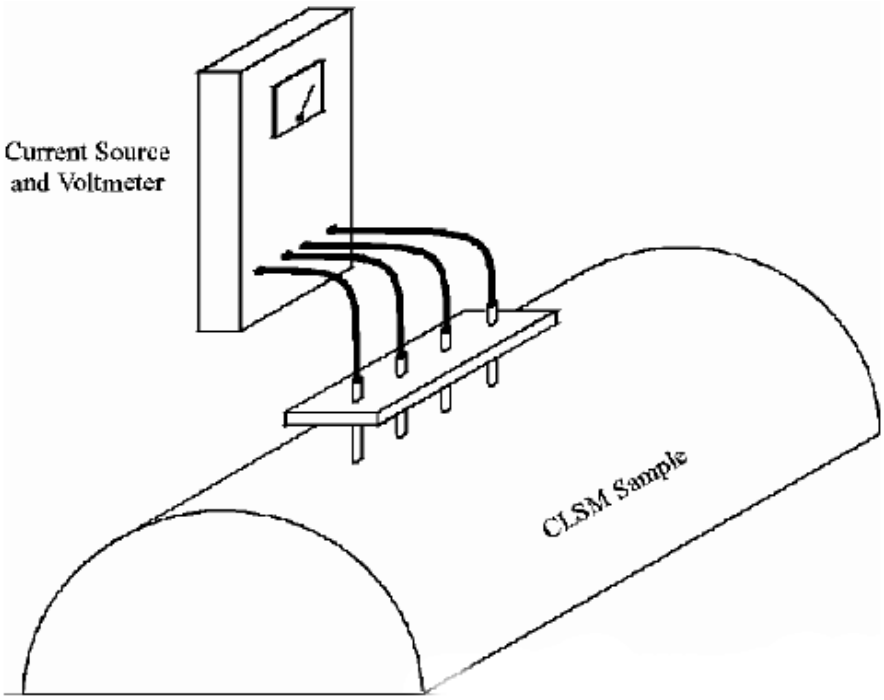

Fig. 4.5--Resistivity measurements with Wenner Four-Electrode method.

4.4.3.Alkalinity

In the first phase study two 50 x 100 mm (2 x 4 in) cylinders were cast for each CLSM mixture at the same time as the corrosion samples were cast to evaluate their pH. At 182 days after casting, the CLSM cylinders were removed from the curing room and their pore water solution was extracted using an MTS compressive strength testing machine with an ultimate capacity of 445 MN (100,000 kips) and immediately evaluated for pH. In the second phase study, 1:1 by weight of CLSM and distilled water solutions were prepared from each exposed uncoupled and coupled sample to evaluate for pH. In both phases, a pH combination electrode connected to a benchtop multimeter with a precision of 0.01 was used to measure pH. In the second phase, the pH of soil samples used in the coupled samples was also determined using 1:1 by weight distilled water

solutions. Because only one type of clay and only one type of sand was used in the samples, only randomly selected soil samples from coupled samples exposed to the chloride and distilled water environments were collected and tested. One soil pH value was determined for each type of soil exposed to each type of environment in a coupled sample.

4.4.4.Chloride Content

In the second phase, a test method developed under the Strategic Highway Research Program to rapidly determine the chloride content of mortars and concrete was used to determine the chloride content of the CLSM and soil samples that were exposed to the chloride solution (Cady and Gannon 1992). The most common method to determine the chloride content of concrete and cementitious materials is the ASTM C1152, *Acid-Soluble Chloride in Mortar and Concrete* method. However, this method uses a labor and time intensive potentiometric titration procedure to determine the chloride content of samples. A study was performed and the chloride content of selected CLSM samples were measured using the ASTM method and the rapid chloride content method to validate the applicability of this method by showing that the results of the two methods were highly correlated.

The correlation coefficient between the chloride content readings from the titration method and the rapid method of CLSM samples was 0.976 and was statistically significant. The rapid chloride content measurement method was applied on 3 g (0.1 ounce) of CLSM samples. Table 4.6 shows the parameter estimates and their significance obtained through regression analysis between the titration method and rapid method results. The intercept was not statistically significantly different from zero and the slope was less than 1 and it was significantly different from 1. Figure 4.6 shows the fitted regression model and, 95 percent confidence limits of the estimated means, and the 95 percent confidence limits of the individual predictions. The residuals were independent from the chloride content values and there were no influential observations.

Table 4.6--Parameter estimates and their significance

Parameter	DF*	Estimate	Std. Error	t-stat	Pr.> $\|t\|$
Intercept	1	0.0613	0.0454	1.350	0.2000
Slope	1	0.707	0.0437	16.19	0.0000

*DF : Degrees of freedom

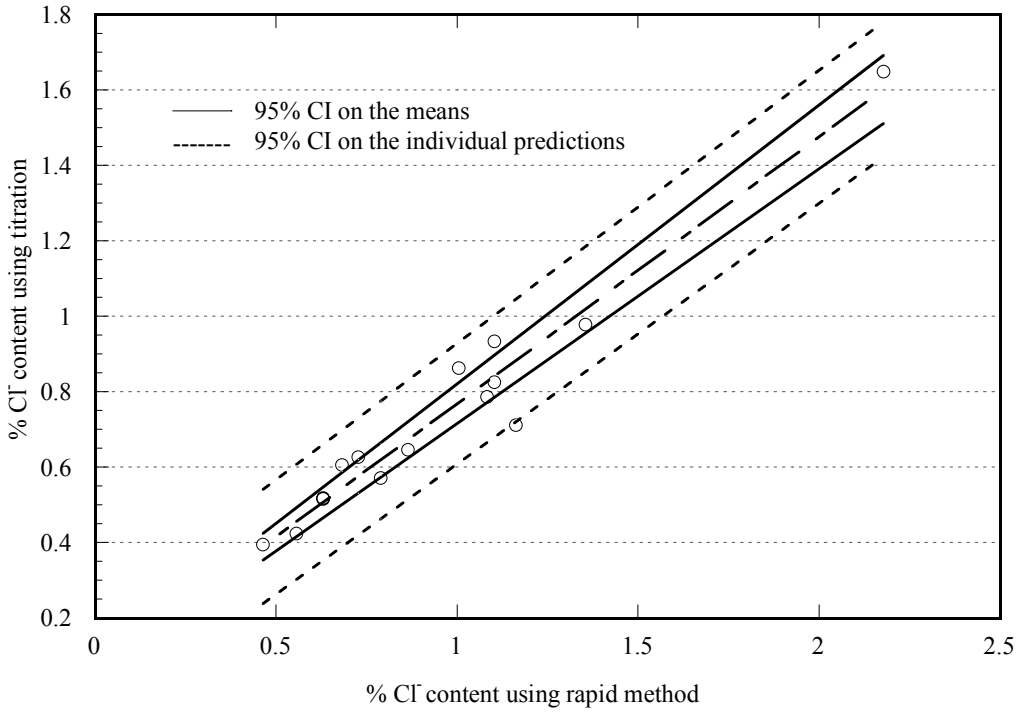

Fig. 4.6--Fitted regression model and the 95% confidence limits.

Testing methods used in this study were discussed and explained in this chapter. All of the selected methods are commonly used standard testing methods in the corrosion research except the rapid chloride content determination method. However, the correlation of this rapid method with the standard ASTM method was evaluated and the rapid method was found to be an acceptable alternative. The data obtained from this test and its statistical analysis is provided in Chapter V.

CHAPTER V

RESULTS AND DISCUSSION*

The results and the statistical analysis of the uncoupled and coupled samples for the two phases of the research project are provided in four separate sections as follows; Phase I - Uncoupled samples, Phase I - Coupled samples, Phase II – Uncoupled samples, and Phase II – Coupled samples.

5.1.Phase I – Uncoupled Samples

The percent mass loss values of the DI coupons embedded in CLSM and exposed to two different environments (distilled water, chloride solution) were determined following ASTM G1, *Standard Practice for Preparing, Cleaning, and Evaluating Corrosion Test Specimens.* The box plot showing the distribution of the average percent mass loss values of the ductile iron samples is shown in Figure 5.1. It can be seen that samples 21 and 23 are extreme outliers, i.e., the difference between the 75th quartile of the data and these samples is larger than three times the interquartile range of the data. Because these mixtures are not significantly different from the others and these results seem to be an anomaly, these data were not included in the Phase I screening section statistical analysis. In Phase II, where higher numbers of samples were produced, a detailed statistical analysis was performed. The resistivity and pH values for the CLSM mixtures at 182 days are shown in Table 5.1.

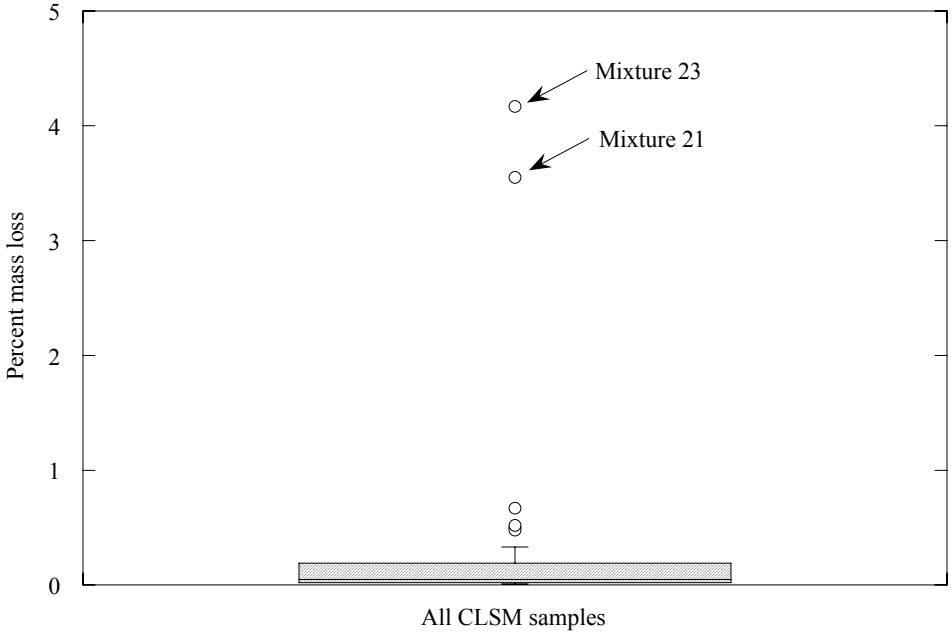

Fig. 5.1--Phase I percent mass loss of ductile iron coupons.

Table 5.1--Phase I resistivity and pH of CLSM mixtures at 182 days

Mixture	pH	Resistivity (Ω-cm)	Mixture	pH	Resistivity (Ω-cm)
1	11.4	2593	15	8.63	2122
1R	10.33	3484	16	11.32	1834
2	9.8	2855	16R	9.8	2881
2R	11.9	3882	17	11.01	2310
3	11.65	2698	18	11.93	4128
3R	11.58	3248	19	12.64	7072
4	11.12	--	20	12.89	5291
4R	11.2	8487	20R	12.97	8644
5	11.24	--	21	12.53	7387
5R	12.25	12,573	22	12.3	8120
6	8.7	10,478	22R	12.3	3824
7	10.8	3196	23	11.4	3536
8	11.18	3222	24	11.53	1582
9	11.1	1441	25	12.93	1048
10	11.28	1781	26	9.07	3091
11	11.3	3468	27	13.03	3065
12	11.58	4086	28	12.65	6287
13	10.1	5605	29	11.28	3143
14	11.4	12,049	30	11.2	1624

A multiple regression and analysis of variance was performed with the average percent mass loss data of the thirty-six CLSM samples as the response variable. However, the data were transformed by taking the logarithm of the data after evaluating the residuals of different models for a better analysis. Cement content, fine aggregate type, fly ash type, resistivity, pH, and w/cm were taken as the explanatory variables. The first model used to evaluate the results considered only the main effects, i.e., interactions between the explanatory variables were initially assumed to be negligible. The p-value for the overall model was 0.0002 and the coefficient of multiple determination (R^2) was 0.76, i.e., 76 percent of the observed variation in the data are attributable to variation among predictions based on the fitted model. The probability of occurrence of such a proportion is less than 1 percent if there is no relation between the response variable and the explanatory variables. Thus, there is strong statistical evidence that the logarithm of the percent mass loss data are related to the explanatory variables in the model. However, the significance analyses of the estimated explanatory variable coefficients show that only the coefficients for the fly ash type and fine aggregate type are significant at the 90 percent confidence level.

Comparison of all possible main effect models for the maximum adjusted R^2 and minimum mean sum of error (MSE) indicates that the best model to predict mass loss of ductile iron pipe completely embedded in CLSM has three explanatory variables; fly ash type, fine aggregate type, and w/cm as shown below:

$$\log_{10}(\%mass\,loss) = 0.056 - \gamma - \lambda + 0.0312\frac{w}{cm} \tag{5.1}$$

where, γ is 1.13, 1.068, 1.313, and 0.0 for bottom ash, concrete sand, foundry sand, and no fine aggregate, respectively, and λ is 0.467, 0.614, 0.688, and 0.0 for Class C, Class F, high-carbon, and no fly ash, respectively. The logarithm of the percent mass loss data is the response variable. The adjusted R^2 for this second model is 67 percent and its MSE is 0.0916. Appropriate coefficients should be used to predict the percent mass loss of a specific mixture.

Figure 5.2 shows the observed values plotted against the predicted percent mass loss values obtained from the model shown in Equation 5.1. The residual plot shows that residuals are independent of the values of the predictor variables. There are no influential observations, i.e., there are no data points that solely have a large impact on model properties. The coefficients for the fine aggregate type and the fly ash type are significant at the 95 percent confidence level and the coefficient for the w/cm is significant at the 89 percent confidence level.

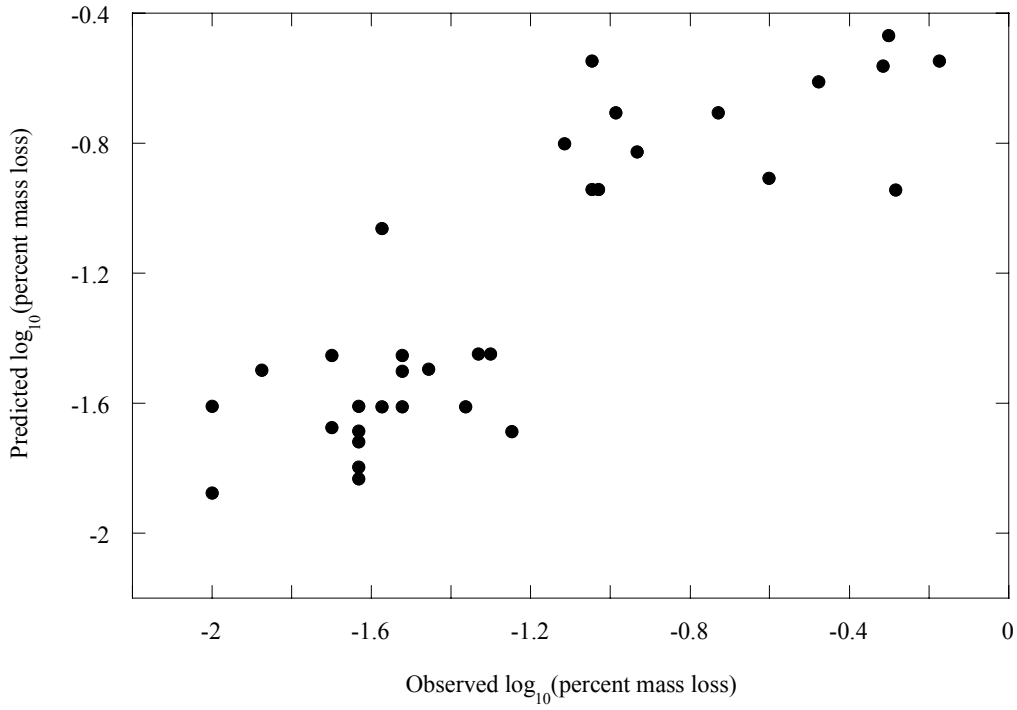

Fig. 5.2--Predicted versus observed mass losses for three explanatory variables; fly ash type, fine aggregate type, and w/cm.

5.1.1.Percent Mass Loss versus Resistivity

Many field investigations on the corrosion of metals embedded in soils have reported that resistivity is a major controlling parameter affecting corrosion activity of the embedded metal (Spickelmire 2002, Kozhushner et. al. 2001). An exception to this is when severe microbiological activity is present (Palmer 1989). Figure 5.3 compares the mean percent mass loss of the coupons embedded in the thirty-six different CLSM mixtures with the resistivity of the CLSM mixtures measured at 182 days. Prior corrosion research in soils reported non-linear relationships between mass loss and resistivity (Edgar 1989, Palmer 1989) as follows:

$$Mass\ Loss = \alpha \cdot r^{-\beta} \tag{5.2}$$

where r is the resistivity (Ω-cm) and α and β are constants. However, the evidence for such a non-linear relationship for the CLSM data shown in Figure 5.3 is very weak.

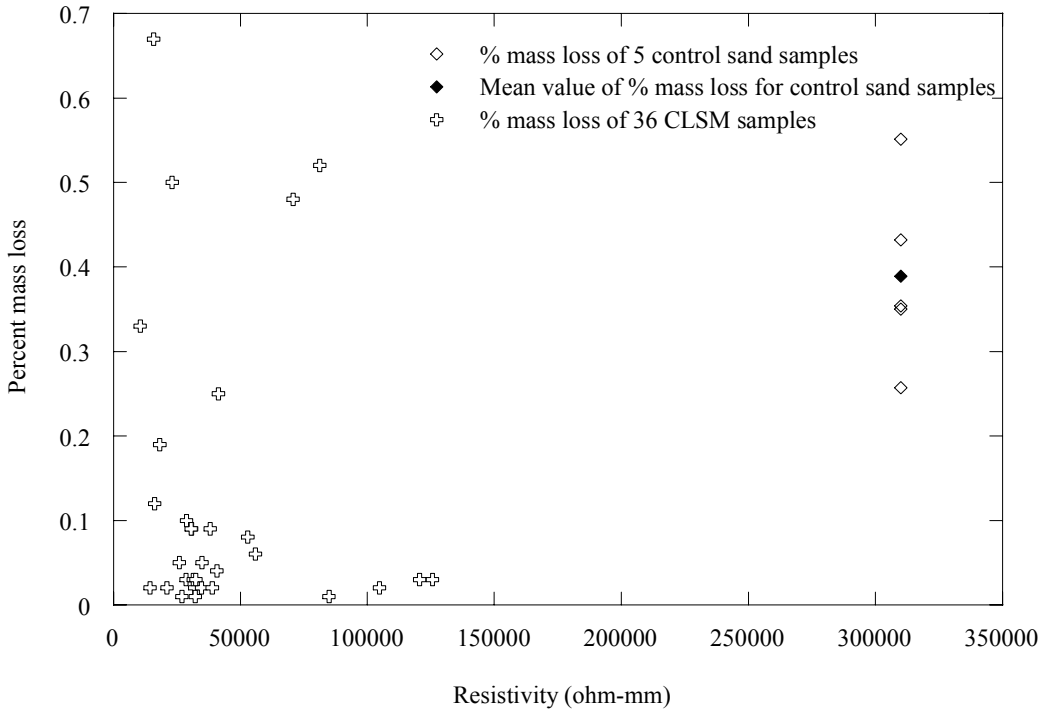

Fig. 5.3--Percent mass loss values versus resistivity.

Figure 5.3 also shows the percent mass loss values of the control group (i.e., the ductile iron samples embedded in standard sand). The average percent mass loss for the control group was 0.39 percent. The control sand exhibited a resistivity of 3.1×10^4 Ω-cm. Ductile iron pipe embedded entirely in CLSM exhibited lower corrosion activity than the ductile iron samples embedded in the control sand even though the resistivity of the control sand material was higher than the resistivity of all the CLSM mixtures. Although it is reported throughout the literature that corrosion rates are inversely proportional to the material resistivity, resistivity alone may not be a reliable indicator of corrosion potential for ductile iron pipes embedded in CLSM. These results agree with earlier research by Abelleira et al. (1998), which reported that resistivity is not a good measure of the potential corrosivity for CLSM.

The non-linear relationship shown in Equation 5.2 implies a linear relationship between the natural logarithm of the mass loss and the natural logarithm of resistivity as shown below:

$$\ln(Mass\ Loss) = \ln(\alpha) - \beta \ln(r) \tag{5.3}$$

The correlation coefficient (R) between the natural logarithm of percent mass loss of the coupons embedded in CLSM and the natural logarithm of resistivity values is only 0.084 and α and β are 0.87 and 0.21, respectively.

It should be noted that in the Phase I study the resistivity of the CLSM was measured on samples exposed to standard curing conditions. The resistivity of these samples may not represent the actual in place resistivity of the exposed samples. In Phase II of this research program, the resistivity was measured from the actual exposed samples and was found to be a significant factor. The difference in measurement techniques is believed to be the reason for the different results obtained in the statistical analysis. The resistivity measured from a separate sample cast in a soil box could be a better indicator of the inherent resistivity property of the CLSM mixture. However, the actual resistivity of the CLSM in exposed conditions will depend on many factors such as soluble salt concentration and the saturation level. The finding of this study that resistivity is a statistically significant factor, indicates that the mass loss data of coupons was better correlated to the actual resistivity values measured from the exposed samples. Edgar also found that the corrosion of galvanized culverts in the field was much better correlated to the field resistivity measurements than the saturated soil resistivity measurements using a soil box (Edgar 1989). He suggested that the difference in correlations could be due to the different saturation levels of the soil box testing and the field conditions throughout the service life of the pipes.

5.1.2.Percent Mass Loss versus Fly Ash Type

Some utility agencies have voiced concern regarding the use of fly ash in CLSM and how it influences the corrosion performance of their pipes. In some cases, utility agencies do not allow the use of fly ash in CLSM, even though there have been no documented studies addressing the influence of fly ash in CLSM on the corrosion performance. Thus, there is a need to document the corrosion performance of pipes embedded in CLSM containing fly ash.

It has been well established that SCMs react with calcium hydroxide to form calcium silicate hydrates. This delayed reaction between the siliceous mineral admixture and the calcium hydroxide consumes the calcium hydroxide, resulting in a reduction of the pH pore solution (Diamond 1981, Holden et al. 1983). Because a reduction in the pH could result in higher corrosion activity, fly ash may be detrimental to the corrosion performance of pipe embedded in CLSM containing fly ash. Byfors (1987) reported that the addition of 40 percent fly ash to a concrete mixture resulted in the reduction in the pore solution pH, which reduced the chloride threshold level to approximately half of that of the corresponding mixture without fly ash. But, the addition of fly ash to a cement-based system also results in a refined pore structure and typically, reductions in the diffusivity, permeability, and porosity. Cao et al. (1994) reported that fly ash blended cement pastes showed superior passivation characteristics over longer-terms.

Figure 5.4 compares the pH values of CLSM samples with and without fly ash. Tukey's comparison at a 90 percent level indicates that there is no statistical evidence of a difference among true pH means of the different fly ash types.

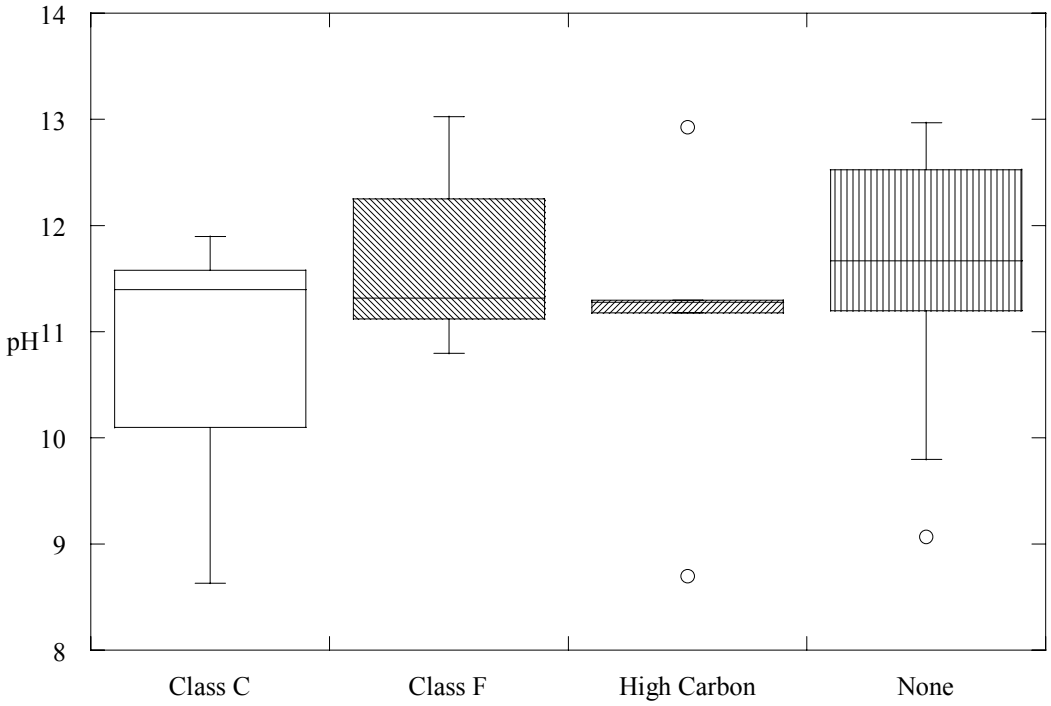

Fig. 5.4--Distribution of pH of pore solution values for CLSM mixtures with different types of fly ashes.

Figure 5.5 shows the influence of fly ash type on the logarithm of the mass loss of the ductile iron pipe embedded in the various CLSM mixtures. The figure shows that the addition of fly ash reduces the logarithm of the percent mass loss of the ductile iron samples resulting from chloride-induced corrosion. Statistically, there is no significant difference at the 95 percent confidence level between the logarithm of the mean percent mass losses of the coupons embedded in the CLSM mixtures containing class C, class F, and high carbon fly ashes. However, the logarithm of the mean percent mass loss of mixtures without fly ash is statistically significantly higher than the mixtures with fly ash. This indicates that the benefits of the fly ash on the microstructure and long-term passivation characteristics, as reported by Cao et al. (1994), likely has a more significant impact on corrosion performance than the relatively limited reduction in pH.

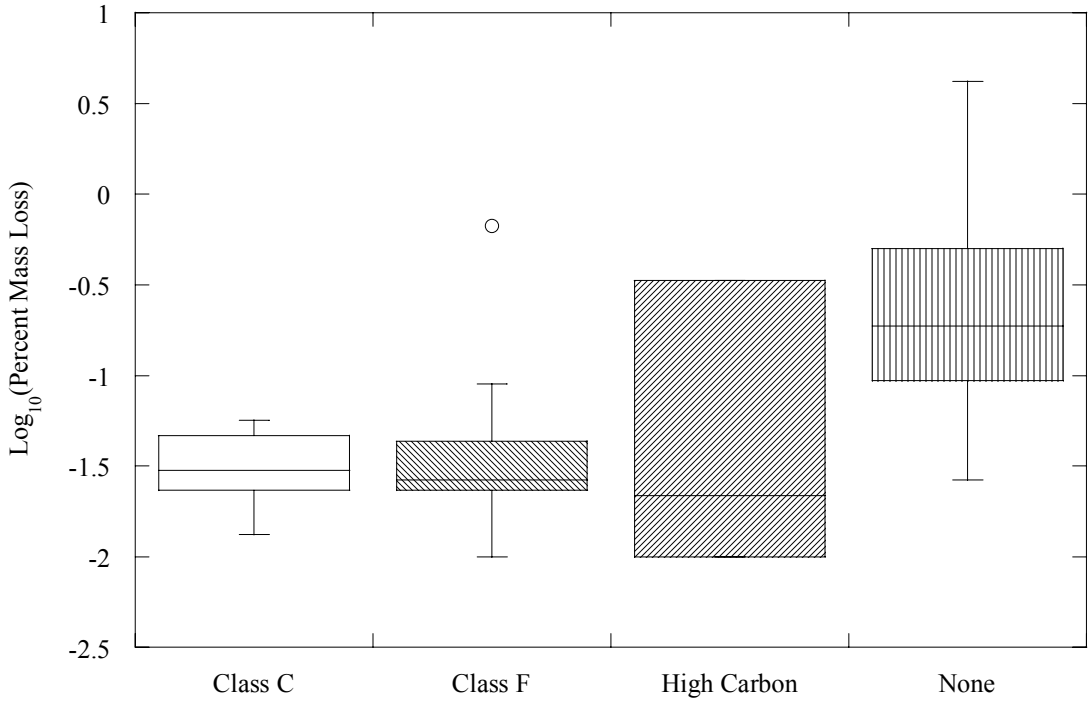

Fig. 5.5--Distribution of percent mass loss values for coupons embedded in CLSM with different types of fly ash.

5.1.3.Percent Mass Loss versus pH

The hydration process of cementitious materials results in a high pH pore water solution. It has been well established that this high pH solution results in the formation of a passive, protective film on the surface of steel (Broomfield 1997). From Table 5.1, it can be seen that the pH of the CLSM mixtures is generally higher than 10. The mean pH of the pore solution from the CLSM mixtures evaluated in this study was 11.35. The pH of the control sand pore solution used in this study was 7.46. Because the pH of the CLSM pore solution is higher than the pH of the control sand pore solution, it would be

expected that the CLSM would provide more protection against corrosion than the control sand.

Figure 5.6 shows the mass loss as a function of pH for both the samples embedded in CLSM and in the control sand material. Although pH is expected to decrease the corrosion performance of the ductile iron pipe, the results do not indicate a significant decrease in the percent mass loss as a result of the increased pH. As such, the pH of the pore solution alone does not seem to reliably estimate the corrosion performance of ductile iron pipe embedded in CLSM. Prior research in soils has also stated that in most cases pH is only significant in distinguishing between otherwise similar soils (Palmer 1989).

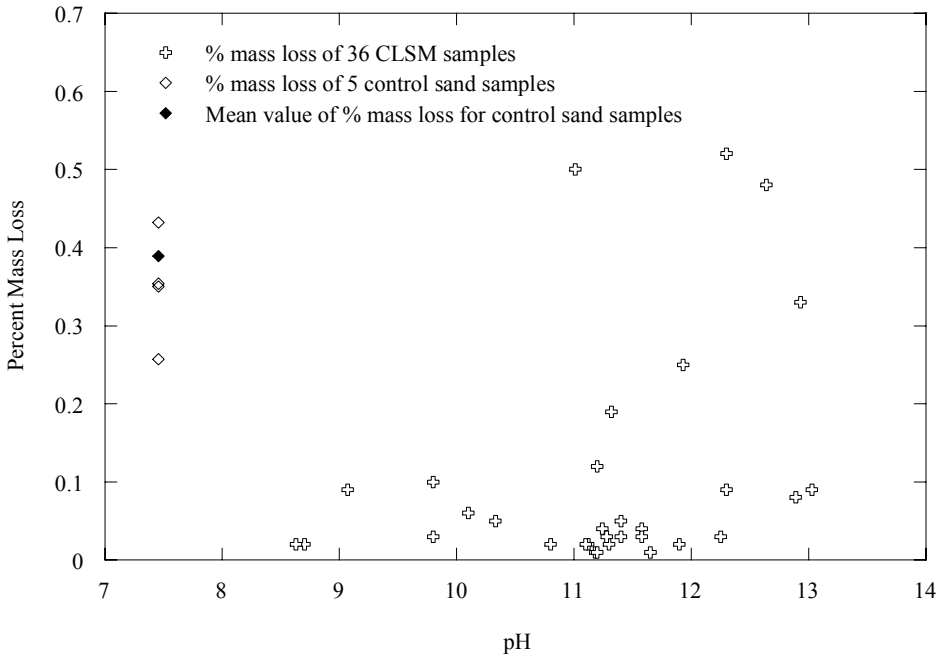

Fig. 5.6--Percent mass loss from corrosion as a function of pore solution pH.

5.1.4.Percent Mass Loss versus Aggregate Type

A wide selection of materials can be used in CLSM as fine aggregates. CLSM producers have successfully used many locally available materials; however, conventional concrete sand is the most commonly used aggregate (Folliard et al. 1999). Foundry sand is another material used successfully in CLSM (Bhat and Lovell 1997, Stern 1995). The Federal Highway Administration (FHWA) issued a report that covers in detail the use of foundry sand in CLSM (Chesner 1998). EPA has also recognized foundry sand as a suitable material for CLSM (EPA 1998). Bottom ash, a by-product of coal combustion, has also been successfully used in CLSM (Naik et al. 1998).

A statistical analysis of the data obtained in this study indicates that the fine aggregate type used in a CLSM mixture has a significant effect on the percent mass loss data. Figure 5.7 shows the logarithm of the percent mass loss distribution by fine aggregate type. Tukey's comparison at a 95 percent confidence level indicates that the mean logarithm of percent mass loss data for mixtures containing bottom ash, concrete sand, and foundry sand are statistically not different from each other. However, the mean logarithm of percent mass loss data for the coupons embedded in mixtures without fine aggregates is statistically different and higher than the other mixtures containing fine aggregate.

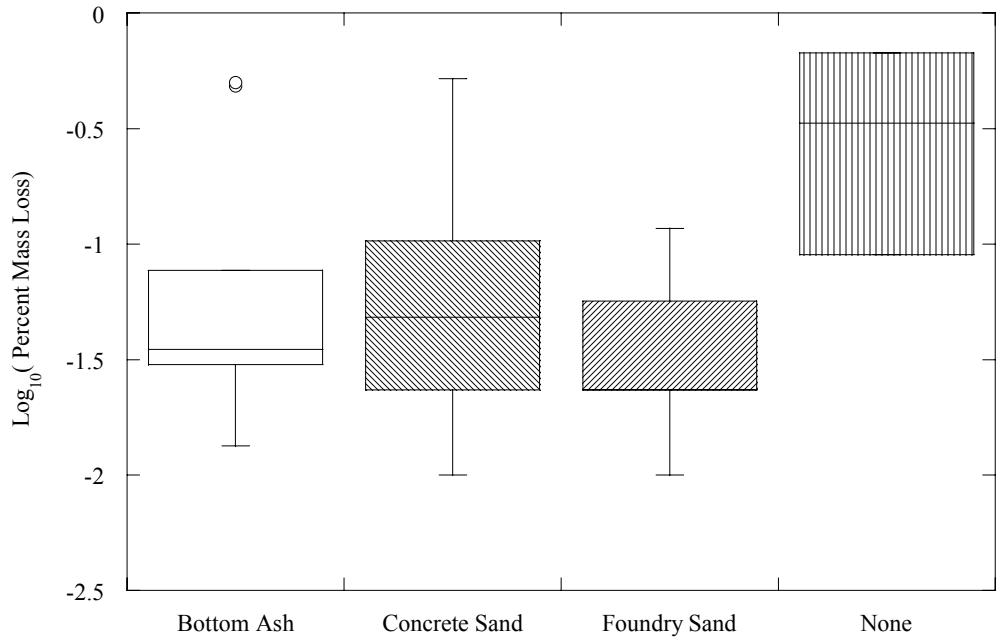

Fig. 5.7--Logarithm of mass loss versus aggregate type.

Previous research investigating the pore structures of mortars has shown that increasing fine aggregate volume concentration caused the porosity of mortar specimens to decrease linearly while increasing their density for all curing periods up to 6 months (Okpala 1989). Following the same logic, the decrease in percent mass loss could be due to reductions in the diffusivity, permeability, and/or porosity of the CLSM mixtures containing fine aggregates. This study indicates that as long as CLSM contains a fine aggregate the percent mass loss of the embedded pipe will be lower when compared with CLSM mixtures containing no fine aggregates.

5.1.5.Percent Mass Loss versus Cement Content

The amount of cement used in CLSM mixtures is very low compared to the amount of water used. The statistical analysis indicates that the cement content had no significant effect on the percent mass loss of the ductile iron coupons embedded in the

CLSM mixtures. However, the ratio of the amount of water to the amount of cement together with fly ash (i.e., cementitious materials content) had a more significant effect on the percent mass loss data.

5.1.6.Percent Mass Loss versus w/cm

For conventional concrete, it has been well established that as the w/cm decreases (within reason), the strength increases and the diffusivity, porosity, and permeability decreases. Other characteristics are also improved. Thus, for uncracked concrete, as the w/cm ratio is decreased, corrosion of embedded steel would be reduced due to the improved concrete characteristics. For CLSM, the w/cm is typically very high. The influence of w/cm for CLSM mixtures on the corrosion performance of ductile iron pipe has not been reported. Figure 5.8 shows the logarithm of the percent mass loss of the ductile iron pipe embedded in the CLSM as a function of the w/cm of the CLSM mixtures containing fly ash and fine aggregates. As with the other plots of mass loss in this section, the outliers are not included in the analysis. It can be seen that the percent mass loss slightly increases with increasing w/cm.

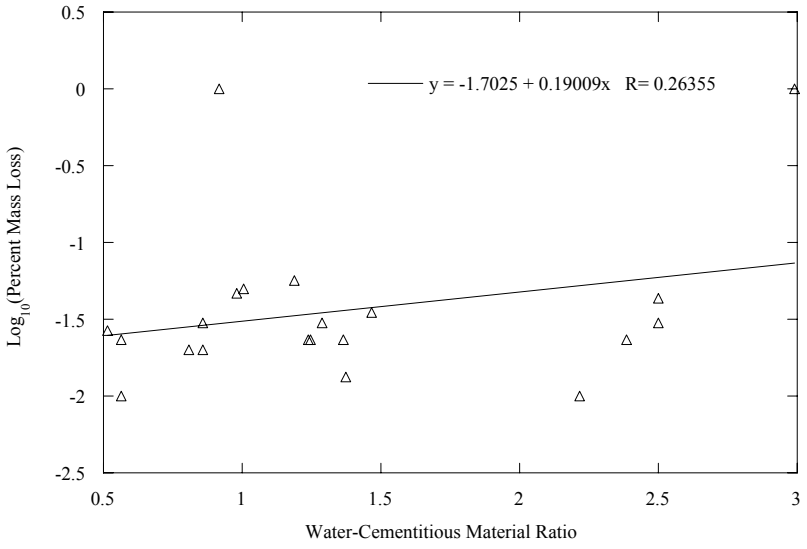

Fig. 5.8--Percent mass loss versus w/cm.

5.2.Phase I – Coupled Samples

To evaluate the mass loss (i.e., corrosion performance) of the coupled ductile iron coupons embedded in both CLSM and sand, a similar statistical analysis as described in Phase I – Uncoupled samples was performed. The effects of cement content, fine aggregate type, fly ash type, resistivity, pH, and water-cementitious materials ratio (i.e., the explanatory variables) on the average percent mass loss of the ductile iron specimens embedded in sand were evaluated. The average percent mass loss (i.e., the response variable) was transformed by taking its logarithm to satisfy the assumption of normal distribution of residuals. Figure 5.9 shows the histogram of the transformed percent mass loss values for the ductile iron coupons embedded in the sand of the galvanically coupled samples after the transformation. The p-value for the normality test after the transformation was 0.83, indicating a high likelihood of this distribution being normal.

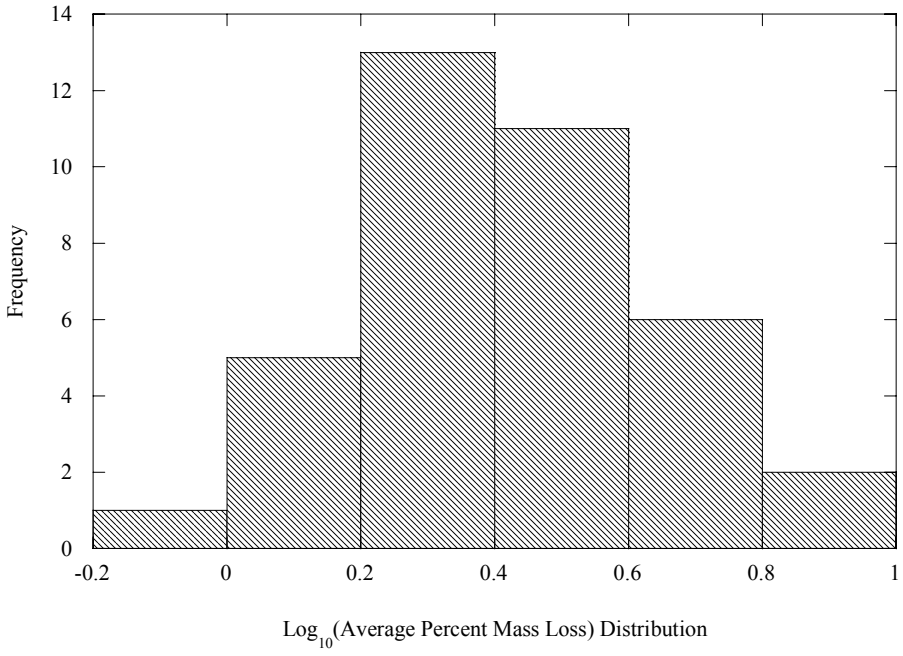

Fig. 5.9--Histogram of the transformed percent mass loss of coupons embedded in sand section of coupled samples.

An initial model for predicting percent mass loss was developed and used in the multiple regression analysis that considered only the main effects of the explanatory variables, i.e., the interactions between the explanatory variables were assumed to be negligible. This initial model, considering all six explanatory variables, was determined to be statistically insignificant (as such it is not shown here). This indicated that the response variables alone, considering no interactions, used in this model could not explain the variance of the average percent mass loss values. Models considering all possible interactions between the six explanatory variables were then tested. Similar to the initial results, none of the models was statistically significant. These analyses indicated that a good prediction of percent mass loss using the explanatory variables was not possible for ductile iron pipe embedded in two different environments (i.e., galvanically coupled).

Examination of the percent mass loss values for the ductile iron specimens embedded solely in CLSM from the Phase I – Uncoupled samples indicated that the percent mass loss values were related to three CLSM characteristics; fly ash type, fine aggregate type, and the water-cementitious materials ratio. These ductile iron specimens from the Phase I – Uncoupled samples study likely corroded due to the formation of micro-galvanic corrosion cells on the surface of the single coupon because the anode and cathode were contained on a single coupon. These corrosion cells typically form due to differences of the metal surface or as a result of local differences in the CLSM environment directly adjacent to the ductile iron coupons. However, the major driving force of the corrosion of ductile iron specimens coupled in two different environments was likely a result of macro-galvanic corrosion cells formed due to the potential difference between the ductile iron specimens. Micro-galvanic cells likely had some effect on the corrosion, but it is believed that these effects were less significant when compared with the macro-galvanic effects. Because the sand and CLSM environments are significantly different, a corrosion potential difference sufficient to increase the corrosion activity was likely. For the Phase I – Coupled samples, this potential difference had a much more significant impact on the corrosion performance than the

cement content, fine aggregate type, fly ash type, resistivity, pH, and w/cm of the CLSM mixtures.

5.3.Comparison of Phase I Uncoupled and Coupled Samples

The first part of the study found that there was a statistically significant difference in the percent mass loss of ductile iron coupons embedded in CLSM mixtures containing fly ash and fine aggregates when compared with CLSM mixtures not containing these materials. Figure 5.10 compares the logarithm of the distribution of percent mass loss of uncoupled samples (specimens embedded only in CLSM), coupled samples (specimens embedded in sand and connected to identical samples embedded in CLSM), and the control group (specimens embedded only in sand). These distributions are grouped by fly ash type. It can be seen that the coupling of the ductile iron coupons has a significant impact on the percent mass loss, whereas the effect of fly ash type was insignificant. Figure 5.11 shows the same comparison grouped by the fine aggregate type. As with the fly ash type, the effect of fine aggregate type is insignificant when compared with coupling of the ductile iron samples.

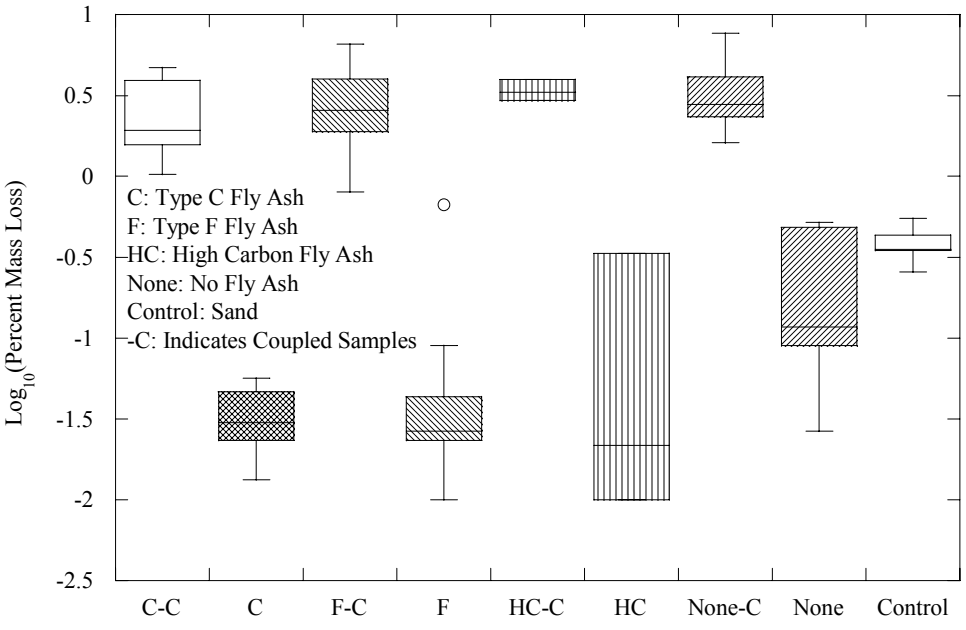

Fig. 5.10--Uncoupled versus coupled log mass loss versus CLSM mixtures containing fly ashes.

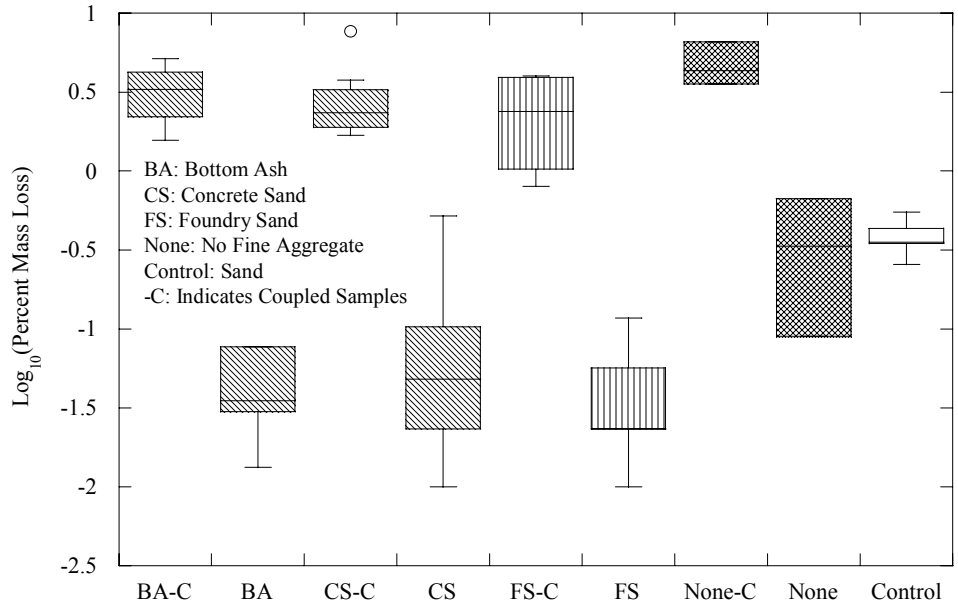

Fig. 5.11--Uncoupled versus coupled log mass loss versus CLSM mixtures containing various fine aggregate types.

Both figures indicate that the percent mass loss of ductile iron specimens embedded in sand and CLSM can be expected to be significantly larger than the specimens completely embedded in CLSM and the control group samples.

Embedding ductile iron pipes in different bedding or backfill materials could lead to higher corrosion activity, which is similar to the earlier research finding that soils with significantly different characteristics could also result in accelerated corrosion. However, because there is a significant reduction in corrosion activity for metallic pipe samples completely embedded in CLSM, with good engineering, the formation of galvanic couples in the field could be prevented. These methods could include wrapping of pipe laterals that traverse trenches that are to be filled with CLSM, wrapping the repaired pipe in polyethylene or another protective material, using dielectric pipe fittings or couplers to prevent the formation of a galvanic cell, ensuring that pipes are not placed directly on native soils, and other standard methods. Good engineering practice, as has been practiced with conventional soil bedding and backfill materials, can lead to increased use of CLSM such that owners and contractors can achieve faster construction, minimal trench settlement, and reduced corrosion activity of pipelines embedded in CLSM.

5.4.Phase II – Uncoupled Samples

Figure 5.12 shows the box plot with the distribution and the median of the percent mass loss data of the 361 galvanized steel and ductile iron coupons embedded in CLSM mixtures exposed to distilled water and chloride solution.

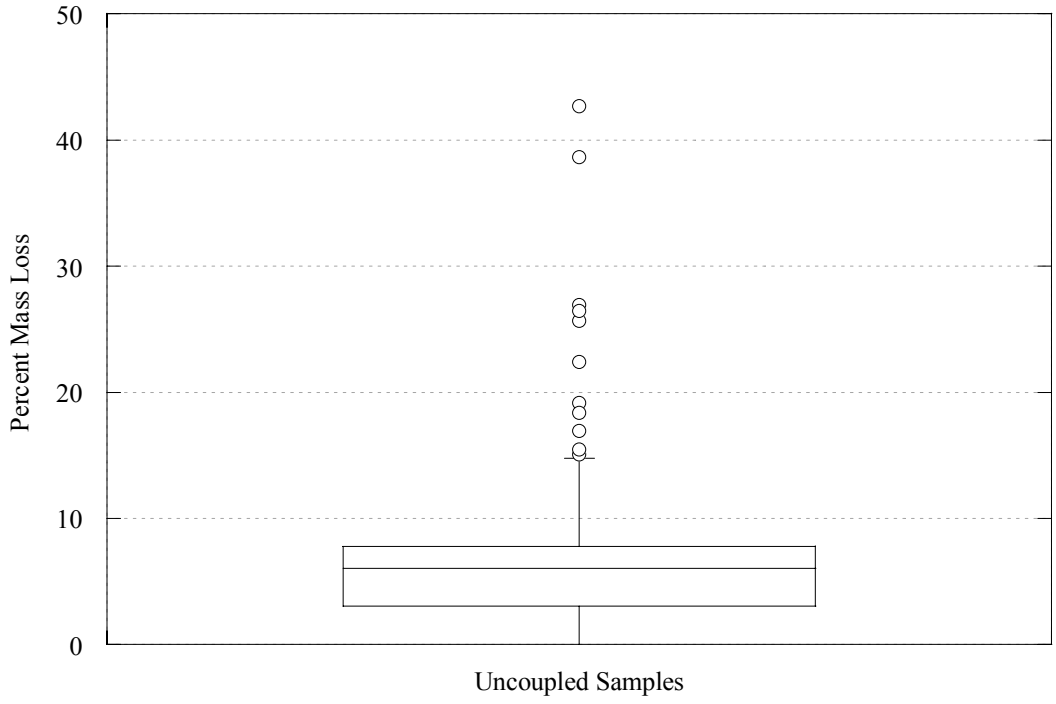

Fig. 5.12--Percent mass loss distribution of metallic coupons.

Table 5.2 shows the correlation coefficients and their significance between the continuous explanatory variables and the response variable (percent mass loss). The significance value of each correlation coefficient is shown below the correlation coefficient. The explanatory variable pH had the largest significant correlation with the response variable, and the correlation coefficient is significant.

Table 5.2—Phase II uncoupled samples correlation table

	Mass loss	pH	log10(Resistivity)	Water/cementitious material	Cement content
Mass loss	1.000	-0.400	-0.042	0.328	0.126
		<0.0001	0.435	<0.0001	0.018
pH	-0.400	1.000	-0.141	-0.134	0.222
	<0.0001		0.008	0.012	<0.0001
log10(Resistivity)	-0.042	-0.141	1.000	-0.083	-0.161
	0.435	0.008		0.121	0.003
w/cm	0.328	-0.134	-0.083	1.000	-0.040
	<0.0001	0.012	0.121		0.452
Cement content	0.126	0.222	-0.161	-0.040	1.000
	0.018	<0.0001	0.003	0.452	
Percent chloride	0.108	-0.006	-0.746	-0.068	0.128
	0.043	0.912	<0.0001	0.203	0.016

Multiple regression and analysis of variance were performed on the data. The percent mass loss data were used as the response variable and the environment, fine aggregate type, fly ash type, resistivity, pH, metal type, w/cm, percent chloride content, and cement content were used as the explanatory variables. Different possible models consisting of main effects and single interaction effects of the explanatory variables were applied to the data to find the best parsimonious model. Different models were compared using their adjusted coefficient of multiple determination (R^2) and root mean square values. Models were applied to the observed percent mass loss values, to their square root transformation, and to their logarithm. Trials indicated that a logarithmic transformation was more effective in decreasing the observed dependence of variability of residuals on the values of response variable. Among the models examined for the logarithm of percent mass loss values (LPML), the following model had the highest adjusted R^2 value and smallest root mean square error:

$$\log_{10}(\%mass\,loss) = 1.844 + \alpha + \beta + \gamma + (\delta + \kappa)\cdot\log_{10}(resistivity) + \varepsilon\cdot pH + \phi + (\tau + \omega)\cdot\frac{w}{cm} + \varphi + \eta + \lambda + \sigma \quad (5.4)$$

The adjusted R^2 of this model is 69 percent and the root mean square error is 0.27. It should be noted that the best models for the same criteria obtained for different transformations of the response variable were very similar to this model. The model includes:

- The main effects of classification variables; environment (α), fine aggregate type (β), fly ash type (γ), and metal type (Φ).
- The main effects of continuous variables; logarithm of electrical resistivity (δ), pH (ε), and water cementitious material (w/cm) ratio (τ).
- The interaction effects of classification variables with classification variables; fine aggregate type with metal type (φ), fly ash type with metal type (η), and environment with metal type (λ). Fly ash type with environment (σ).
- The interaction effect of a classification variable with a continuous variable; logarithm of electrical resistivity with metal type (κ) and w/cm with metal type (ω).

Table 5.3 shows the results of the multiple regression analysis and Table 5.4 shows the analysis of variance table. Table 5.3 shows that the probability of getting an F-statistic higher than the one calculated is almost zero. This indicates that some linear function of the parameters is significantly different from zero and thereore indicates that the overall model was statistically significant. The analysis of variance was used to detect which model factors had an effect on the LPML that was significantly greater than the background level of noise. The probability values calculated for the different factors of the model in Table 5.4 indicate that all of the factors had a statistically significant effect on the LPML.

Table 5.3—Phase II uncoupled samples multiple regression analysis

Source	DF[1]	SS[2]	MS[3]	F-statistic	Pr > F
Model	23	58.46	2.542	33.13	0
Error	336	25.78	0.0767		
Total	359	84.24			

[1]Degrees of freedom, [2]Sum of squares, [3]Mean square

Table 5.4--Analysis of variance table (uncoupled)

Source	**DF[1]**	**SS[2]**	**MS[3]**	**F-statistic**	**Pr > F**
fly ash	3	6.078	2.026	26.41	0
fly ash*metal type	3	5.684	1.895	24.7	0
fine aggregate	3	4.452	1.484	19.34	0
environment	1	3.128	3.128	40.77	0
environment*fly ash	3	3.702	1.234	16.08	0
pH	1	2.11	2.11	27.5	0
metal type	1	2.101	2.101	27.38	0
fine aggregate*metal type	3	2.22	0.74	9.647	0
log(Resistivity)*metal type	1	1.655	1.655	21.57	0
log(Resistivity)	1	1.603	1.603	20.89	0
environment*metal type	1	1.538	1.538	20.05	0
w/cm	1	0.722	0.722	9.416	0.0023
w/cm*metal type	1	0.634	0.634	8.266	0.0043

[1]Degrees of freedom, [2]Sum of squares, [3]Mean square

The studentized residuals (residuals divided by their standard error) of the data points were examined to see if there were any outliers. There was only one data point with a studentized residual greater than 3, which indicated that this point was an outlier.

The Dffits statistic was calculated for all the data points. The Dffits *statistic* is a scaled measure of the change in the predicted value for the i^{th} observation. For linear models,

$$F_i = \frac{\hat{\mu}_i - \hat{\mu}_{(i)}}{s_{(i)}\sqrt{h_i}} \tag{5.5}$$

where $\hat{\mu}_{(i)}$ is the i^{th} value predicted without using the i^{th} observation, $s_{(i)}$ is the root mean square error, and the h_i is the leverage of the observation. Leverage values are the diagonals of the hat matrix, H, calculated as:

$$H = X * inv(X' * X) * X' \tag{5.6}$$

where X is the data matrix with a column of 1s for the intercept, X' is the transpose of the X matrix, and inv() is the inverse of the enclosed quantity. Large absolute values of F_i indicate influential observations. A general cutoff to consider is 2. In this case there were no influential observations.

Figures 5.13 and 5.14 show the residuals plotted against the predicted values of LPML and against their normal quantiles.

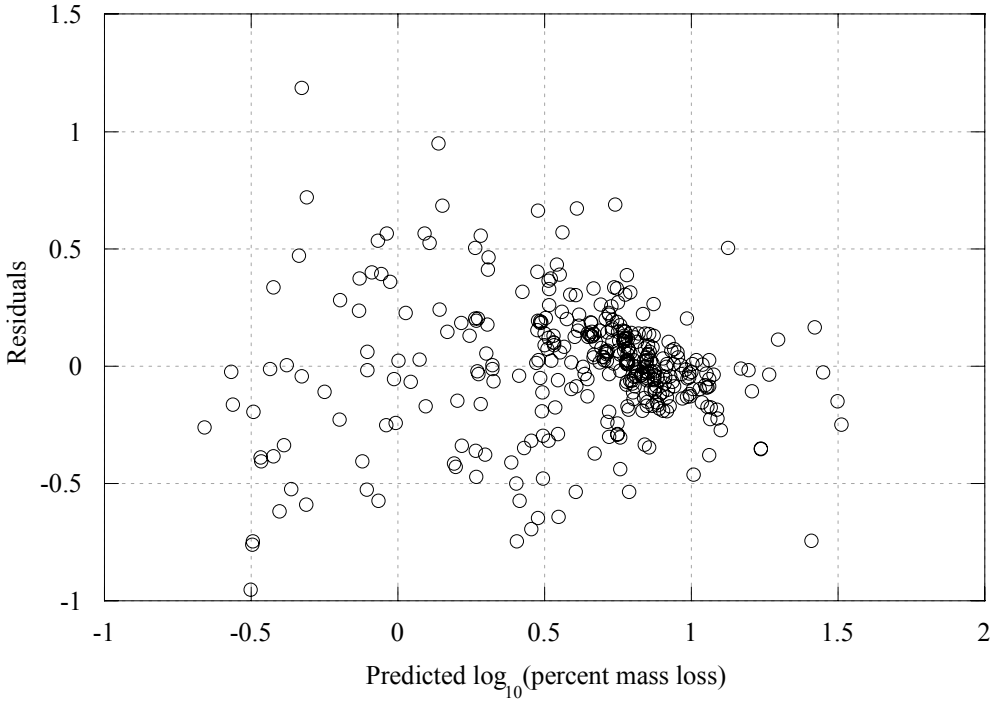

Fig. 5.13--Residuals vs. predicted LPML values.

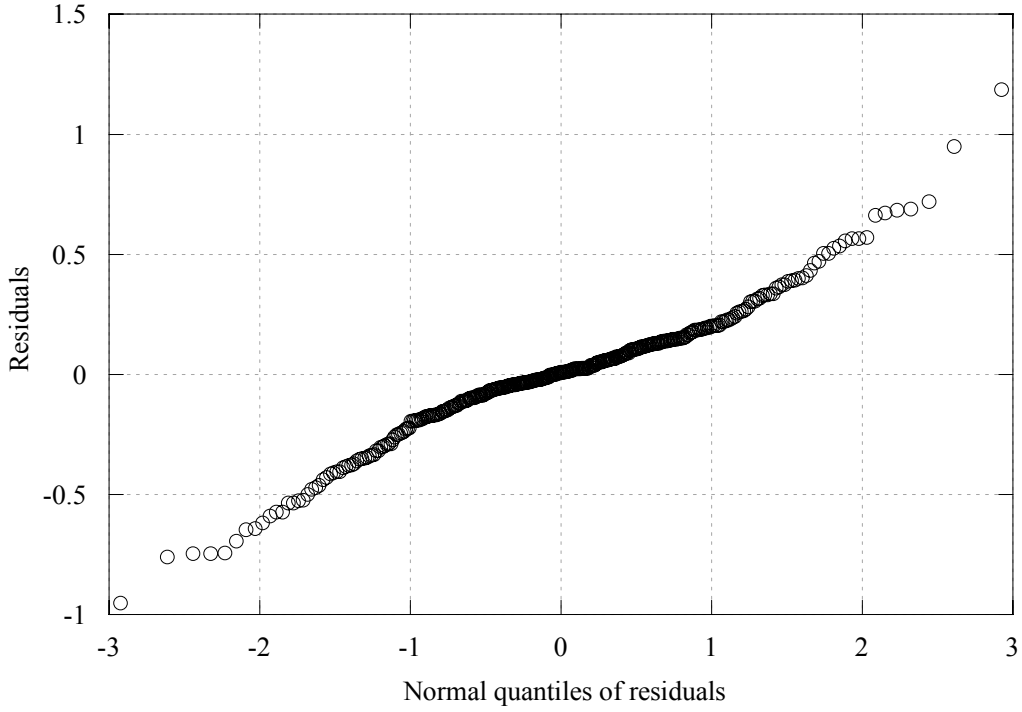

Fig. 5.14--Residuals vs. their normal quartiles.

The wedge shape in Figure 5.13 and the heavy tails observed in Figure 5.14 indicated that the variance of residuals depended on the mean response. This does not satisfy the assumptions of regression analysis.

Also the degree of non-constant variance of the residuals relative to the predicted LPML was tested using a Chi-square test. A large chi-square value, with a small probability, indicates that the assumption of constant variance of the residuals is not tenable. The test uses the squared, scaled residuals from the analysis as the dependent variable in an analysis of variance (ANOVA) with the predicted LPML value as the predictor variable. The scaling of the squared residuals consists of dividing each by the error sum of squares which is itself divided by the number of observations. The regression sum of squares is divided by 2 to produce the chi-square statistic. The probability is obtained from the chi-square distribution with the normal degrees of freedom for the predictor variable. The value of the chi-square statistic was 119.65 with

probability close to 0, which indicated that the assumption of constant variance of the predicted LPML should be rejected.

Figures 5.15, 5.16, and 5.17 show the residuals plotted against the three continuous variables of the model; logarithm of resistivity, pH, and w/cm, respectively. These figures also show the same non-constant variance of the response variable, LPML.

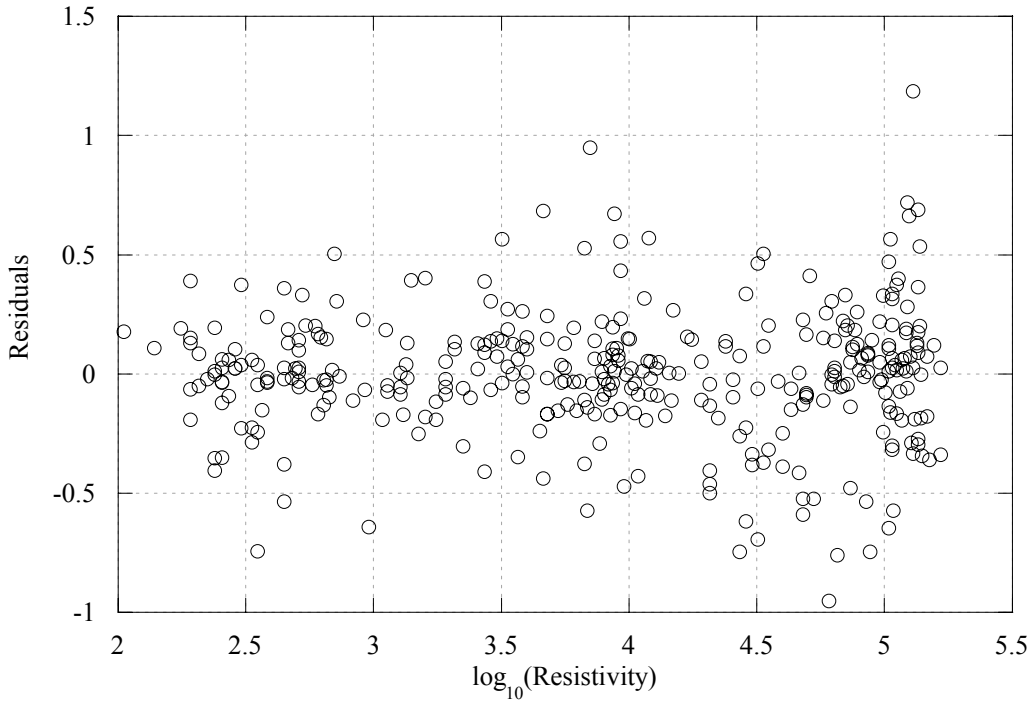

Fig. 5.15--Residuals vs. the logarithm of resistivity.

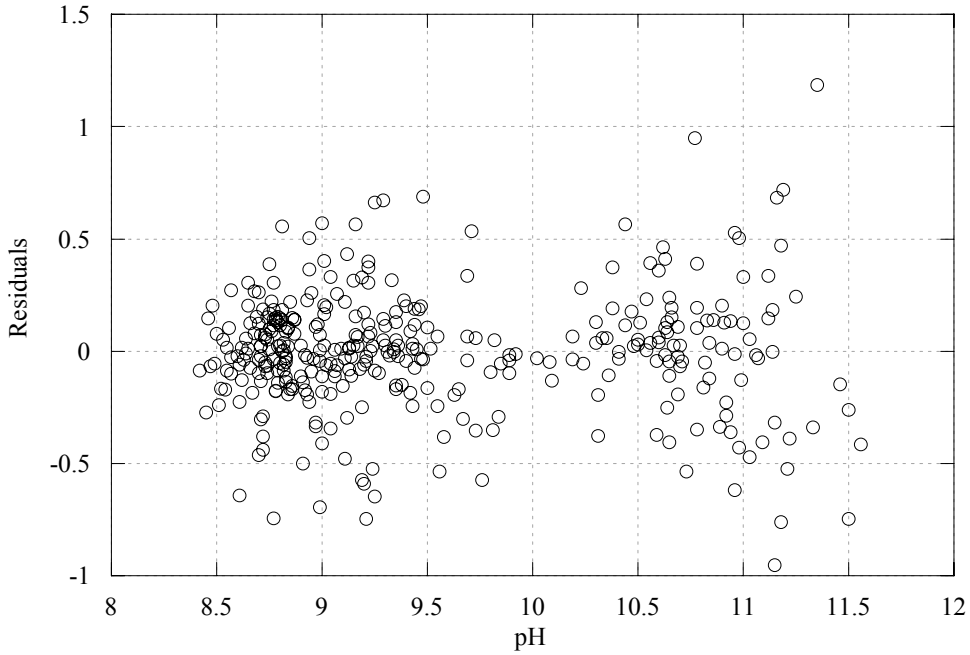

Fig. 5.16--Residuals vs. the pH.

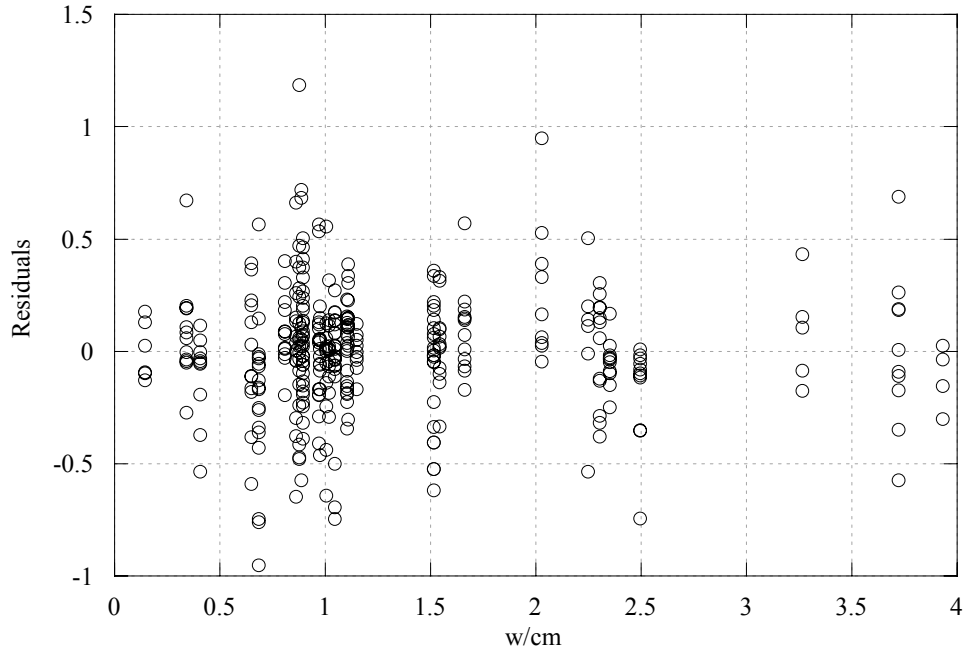

Fig. 5.17--Residuals vs. the water cementitious materials ratio.

Since the assumption of constant variance was not satisfied a weighted regression analysis was performed. The factors that had the biggest effect on the LPML values were the environment and the metal type. Figure 5.18 shows the residuals separated by these two variables. The variances of these four groups were 0.075, 0.01, 0.17, and 0.054 for ductile iron in chloride, galvanized steel in chloride, ductile iron in distilled water, and galvanized steel in distilled water, respectively. The reciprocals of variances of these four groups were used as a weight variable for the weighted regression analysis.

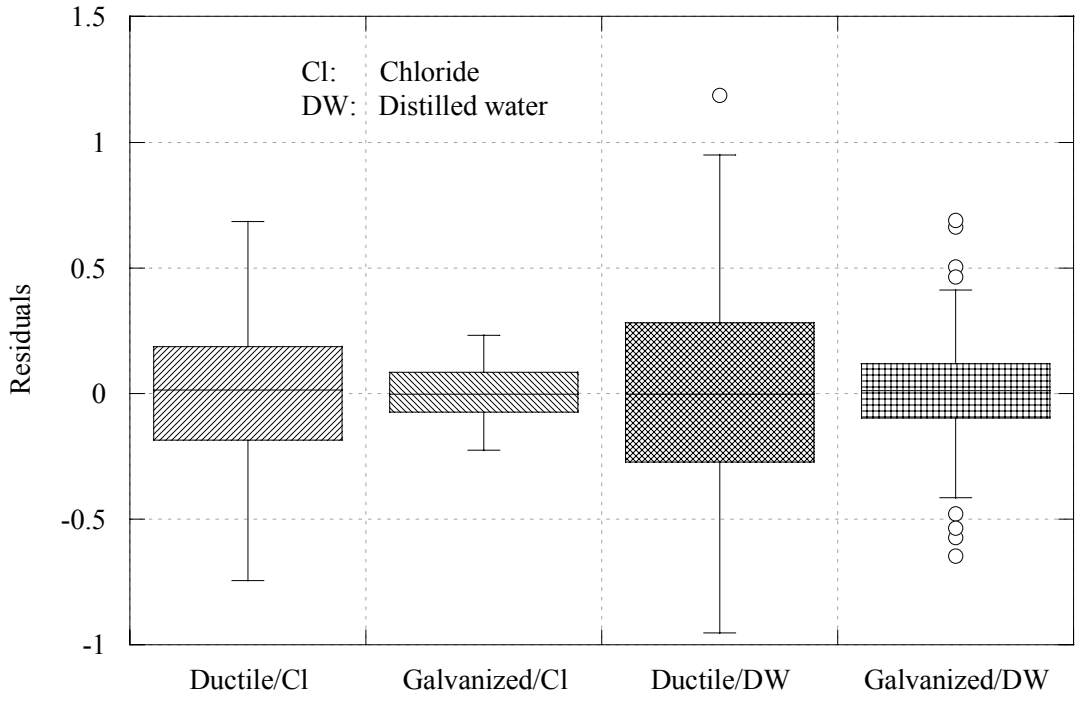

Fig. 5.18--Residuals separated by environment and metal type.

Figure 5.19 shows the studentized residuals of the weighted regression analysis plotted against the predicted LPML values. The studentized residuals do not exhibit the wedge shape shown in Figure 5.13 when plotted against the predicted LPML values. Figure 5.20 shows the studentized residuals plotted against their normal quantiles and

Figure 5.21 shows their histogram. Both figures indicate that the normality assumption of residuals was satisfied much better compared to the earlier regression analysis.

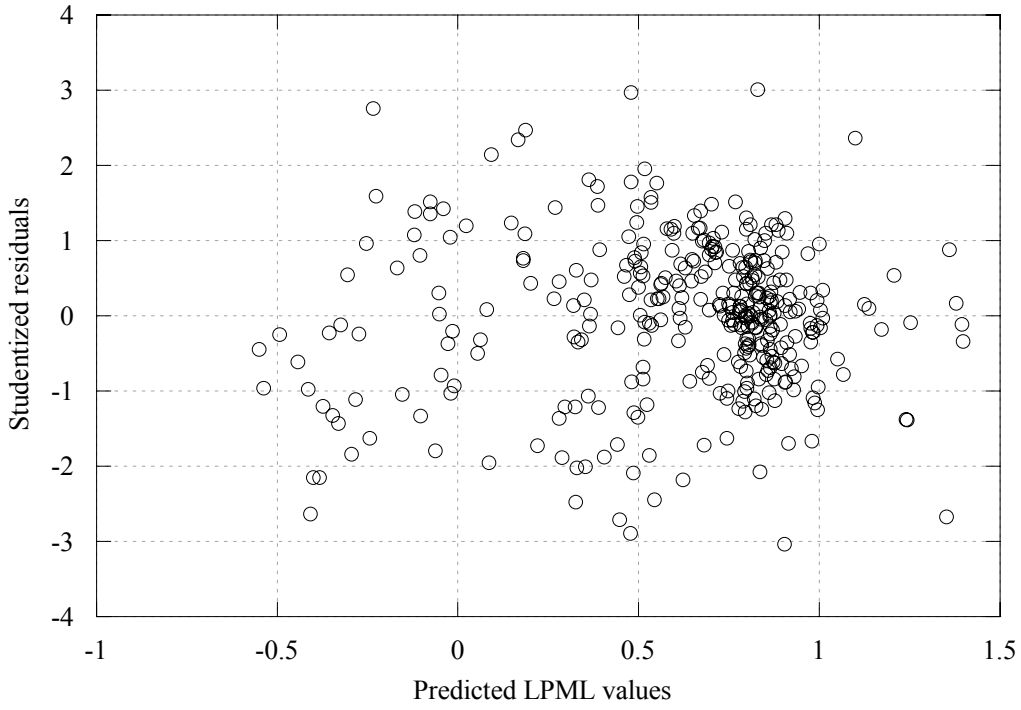

Fig. 5.19--Studentized residuals vs. predicted LPML values.

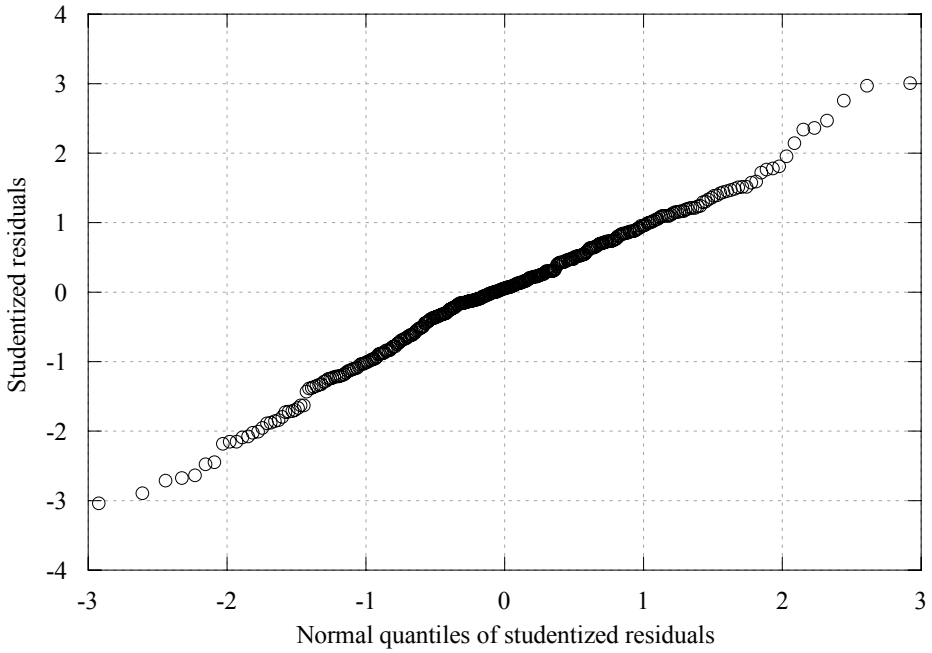

Fig. 5 20--Studentized residuals vs. their normal quantiles.

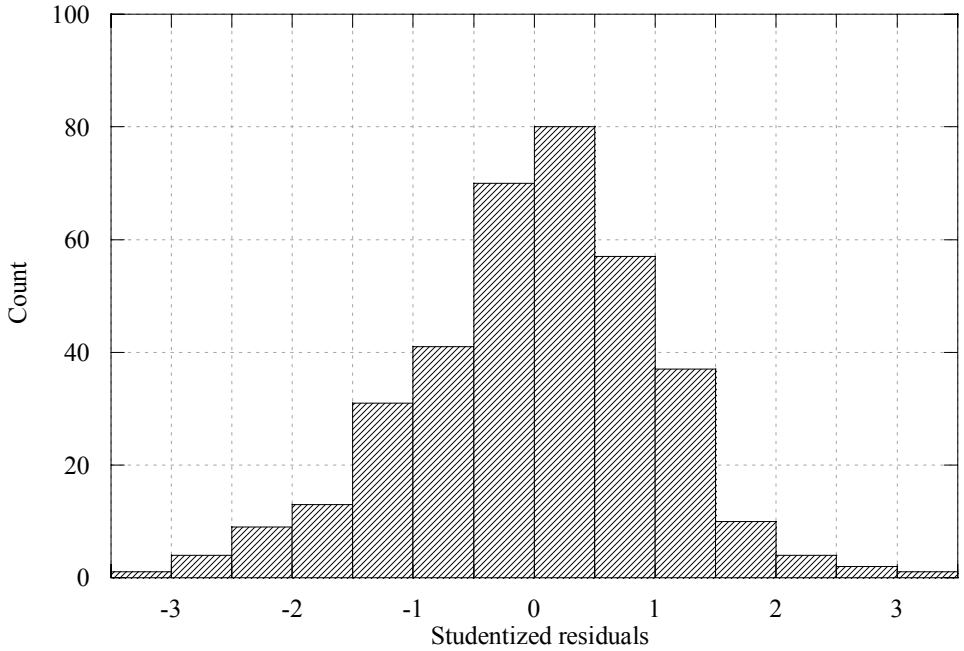

Fig. 5.21--Histogram of the studentized residuals.

Figures 5.22, 5.23, and 5.24 show the studentized residuals plotted against the three continuous variables; logarithm of resistivity, pH, and w/cm. These figures also do not indicate any dependency of studentized residuals on the continuous variables.

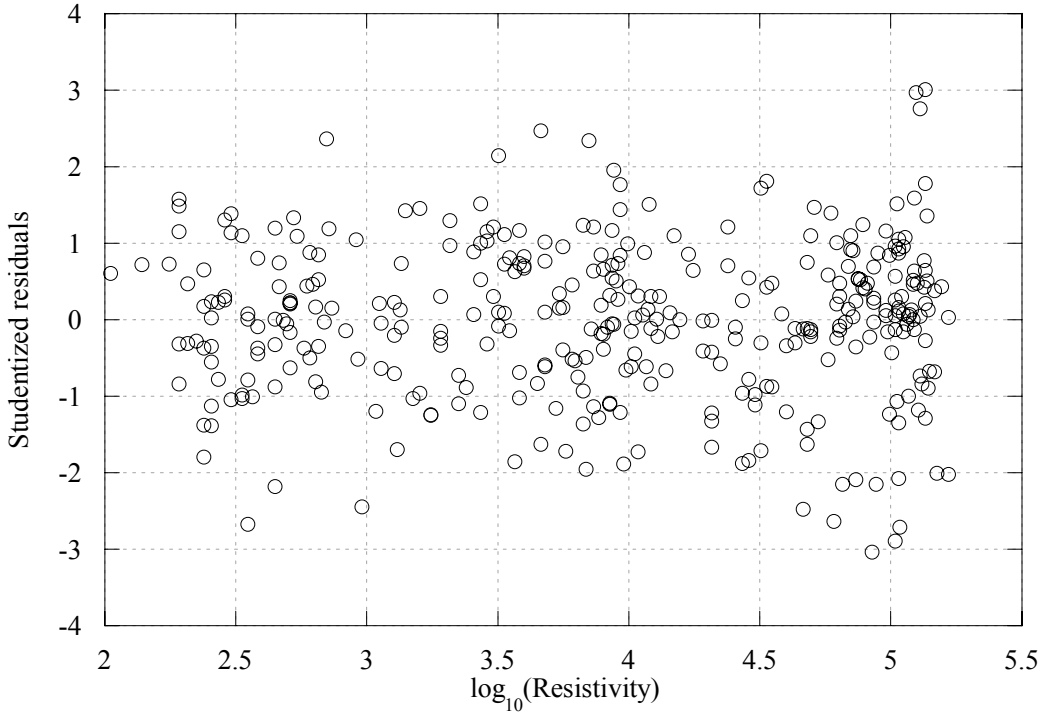

Fig. 5.22--Studentized residuals vs. the logarithm of resistivity.

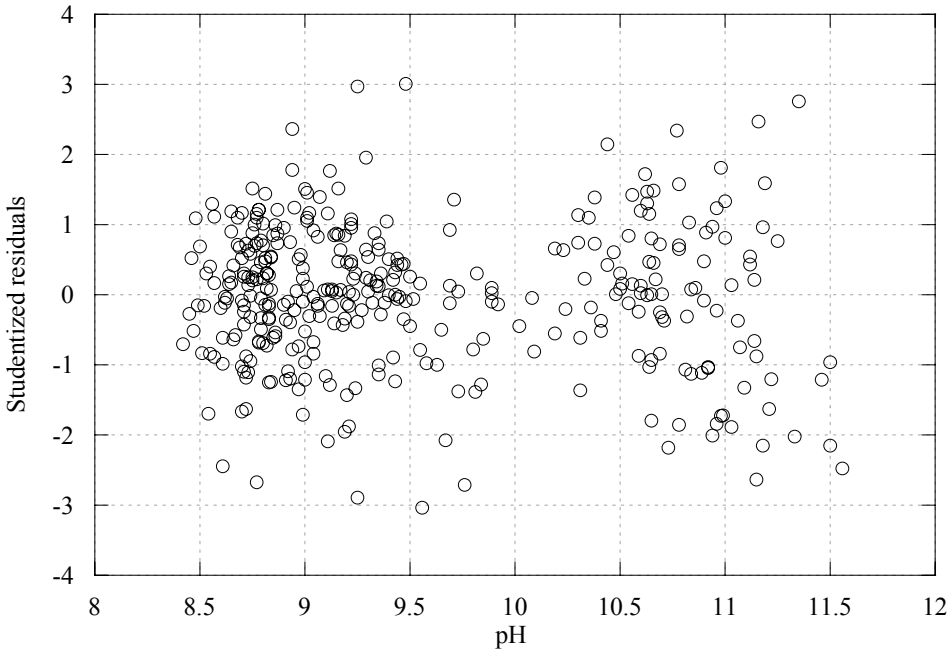

Fig. 5 23--Studentized residuals vs. the pH.

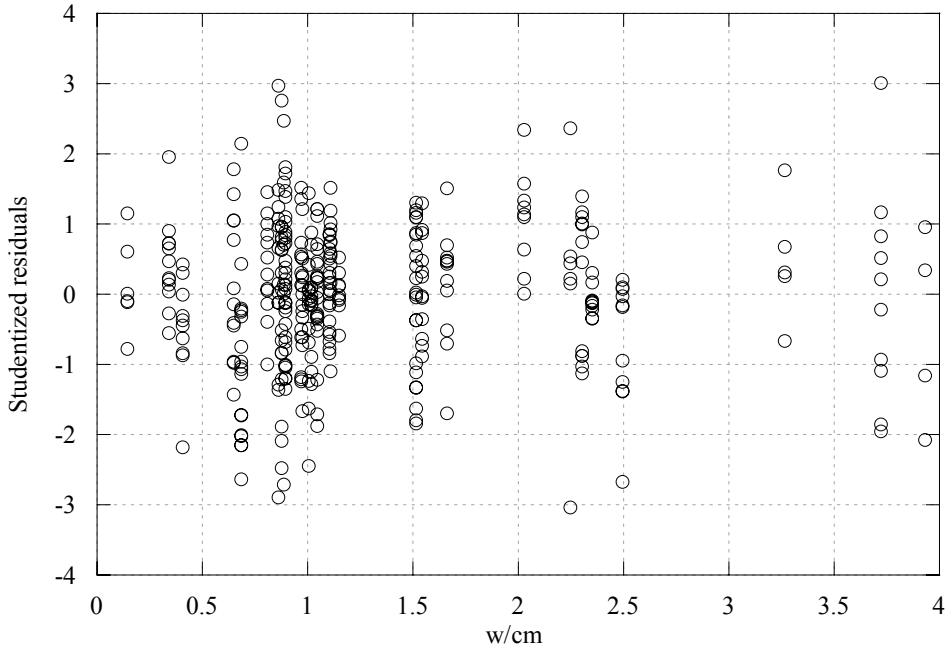

Fig. 5.24--Studentized residuals vs. the water cementitious materials ratio.

The R^2 value for the weighted regression analysis is 67 percent and the root mean square error value is 0.98. The R^2 value is a measure of how much of the variation of the percent mass loss values are explained by the overall model. Table 5.5 shows the ANOVA table for the weighted regression analysis. All of the factors included in the model were statistically significant.

Table 5.5 Analysis of variance table for the weighted regression analysis

Source	DF[1]	Type III SS[2]	Mean Square	F Value	Pr > F
environment	1	42.914977	42.914977	44.33	<.0001
fine aggregate	3	45.4581813	15.1527271	15.65	<.0001
fly ash	3	126.2288401	42.07628	43.47	<.0001
log(Resistivity)	1	27.4008757	27.4008757	28.31	<.0001
pH	1	16.6873769	16.6873769	17.24	<.0001
metal type	1	27.0076031	27.0076031	27.9	<.0001
w/cm	1	15.0677038	15.0677038	15.57	<.0001
fine aggregate*metal type	3	26.8651966	8.9550655	9.25	<.0001
fly ash*metal type	3	80.4483833	26.8161278	27.7	<.0001
environment*fly ash	3	39.6963963	13.2321321	13.67	<.0001
environment*metal type	1	21.1944876	21.1944876	21.9	<.0001
log(Resistivity)*metal type	1	23.8608938	23.8608938	24.65	<.0001
w/cm*metal type	1	6.6172763	6.6172763	6.84	0.0093

[1]Degrees of freedom, [2]Sum of squares

The parameters defined in the model for the main effects of classification variables represent the expected value of the response variable for different levels of the corresponding classification variable, all other factors being the same. The parameters defined in the model for the main effects of continuous variables represent the amount of change in the expected value of the response variable for each unit change of the corresponding continuous variable, all other factors being the same. The interaction parameters in the model define how the response reacts to one variable based on the value or level of another variable. In the case of an interaction of a classification

variable with a continuous variable, the coefficient of the continuous variable is changed based on the level of the classification variable.

Table 5.6 shows the parameters of the model and their standard errors. The parameters for the main effects and interactions that are not shown in the table are zero. The sign of the estimated parameter shows the type of relationship between the effect and the response value for the selected model. If the parameter is positive, it indicates an increasing effect on the response value considering the values of all the variables.

5.4.1.Alkalinity

Research on the corrosion of metals in concrete has established that high alkaline pore water environment (pH between 12 and 13) of concrete leads to the formation of a passive layer on the metal surface protecting the metal from corrosion (Broomfield 1997). Since CLSM is a cementitious material, it also exhibits an environment with higher pH values compared to traditional backfill materials. The mean pH value measured for the CLSM samples in this phase was 9.54 with a minimum of 8.42 and a maximum of 11.56. The mass loss data obtained from the study indicated that pH was significantly negatively correlated to the percent mass loss data. The variable pH was also one of the statistically significant continuous variables in the selected model and the expected LPML decreased with the increasing pH values. These findings are contrary to the point system established by AWWA (discussed in Chapter III) where points were assigned for high pH values of soils. Figure 5.25 shows the box plots of LPML values for different pH ranges observed in this study. The pH ranges are built using the 0, 25, 50, and 100 percent quantiles of the data.

Table 5.6--Values of the coefficients and their standard errors

Main effect		Parameter	Standard Error
Intercept		1.04	0.31
Environment			
	Chloride	0.13	0.12
Fine Aggregate type			
	Bottom Ash	0.03	0.04
	Foundry Sand	0.05	0.07
	None	0.15	0.06
Fly Ash type			
	Class C	-0.10	0.18
	Class F	0.20	0.18
	High Carbon	0.22	0.17
Logarithm of Resistivity		0.01	0.02
pH		-0.06	0.02
Metal type			
	Ductile iron	-3.23	0.66
Water cementitious material ratio		0.09	0.05
Interaction effect		Parameter	Standard Error
Fine Aggregate type & metal type			
Bottom Ash	Ductile iron	-0.21	0.11
Foundry Sand	Ductile iron	0.17	0.19
None	Ductile iron	0.44	0.16
Fly Ash type & metal type			
Class C	Ductile iron	0.84	0.40
Class F	Ductile iron	1.17	0.39
High Carbon	Ductile iron	1.27	0.36
Logarithm of Resistivity & metal type			
	Ductile iron	0.29	0.06
Environment & metal type			
Chloride	Ductile iron	0.50	0.11
Environment & fly ash type			
Chloride	Class C	0.22	0.12
Chloride	Class F	-0.07	0.12
Chloride	High Carbon	-0.14	0.12
w/cm & metal type			
	Ductile iron	0.37	0.14

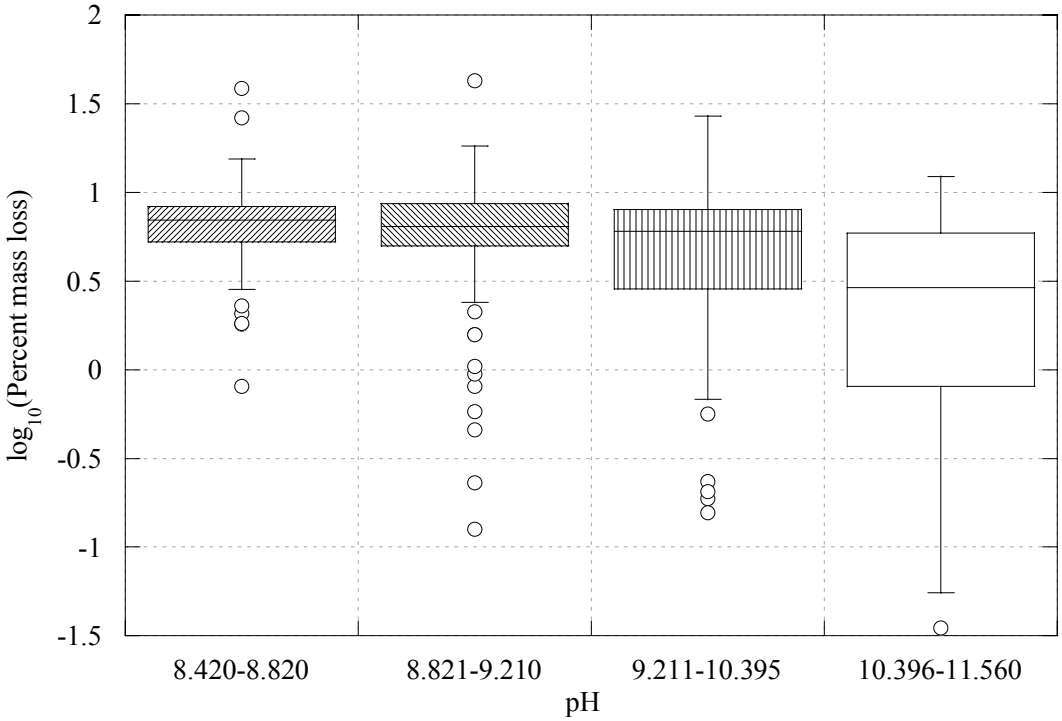

Fig. 5.25--LPML box plots for pH ranges.

5.4.2.Environment

Comparison of transformed percent mass loss means for the different levels of classification variables was performed using the Tukey's comparison of means method. The mean LPML values for the samples exposed to chloride solution and distilled water were 0.76 percent and 0.38 percent, respectively. The comparison for the two levels of environment indicates that the means are significantly different and the mean of samples exposed to chloride solution is higher. The lower and upper limits of the 95 percent confidence interval (CI) for the LPML of the samples exposed to chloride solution was 0.66 percent and 0.86 percent, i.e., there is 95 percent probability that the true mean is inside this interval. The 95 percent CI limits for the transformed mean percent mass loss of the samples exposed to distilled water were 0.25 percent and 0.50 percent. Although previous research has indicated that the alkaline environment would lead to passivation

of metals, research has also indicated that the presence of chloride ions above a certain threshold can cause depassivation of the metal leading to corrosion (Tuutti 1982). The comparison was performed at the mean values of the three continuous explanatory variables, pH, logarithm of resistivity, and w/cm. In order to check the significance of difference of mean LPML values of different levels of environment at different levels of continuous variables, the ranges of continuous variables were divided into four intervals and the comparisons were performed at the midpoints of these intervals. Since there are three continuous variables and four levels of each, the mean LPML values for different environments were compared at 64 possible combinations. Table 5.7 shows the LPML means for chloride and distilled water environment at the 64 combinations and their 95 percent CI's. Results in Table 5.7 indicate that the mean LPML values of samples exposed to chloride environment were significantly higher at all combinations of the three continuous variables (i.e, the p-values of the comparisons are all close to zero).

Table 5.7--LPML comparison for chloride (CL) and distilled water (DW)

No	Environment	LSMean[1]	p-value	Lower CL[2]	Upper CL[3]
1	CL	0.382	<.0001	0.184	0.58
	DW	0.001	-	-0.25	0.252
2	CL	0.643	<.0001	0.56	0.726
	DW	0.262	-	0.104	0.42
3	CL	0.904	<.0001	0.812	0.997
	DW	0.523	-	0.38	0.667
4	CL	1.166	<.0001	0.956	1.376
	DW	0.784	-	0.56	1.008
5	CL	0.508	<.0001	0.324	0.693
	DW	0.127	-	-0.097	0.351
6	CL	0.77	<.0001	0.697	0.842
	DW	0.388	-	0.264	0.512
7	CL	1.031	<.0001	0.93	1.132
	DW	0.649	-	0.529	0.77

Table 5.7—Continued

No	Environment	LSMean[1]	p-value	Lower CL[2]	Upper CL[3]
8	CL	1.292	<.0001	1.07	1.514
	DW	0.911	-	0.693	1.128
9	CL	0.635	<.0001	0.452	0.818
	DW	0.253	-	0.049	0.458
10	CL	0.896	<.0001	0.807	0.985
	DW	0.515	-	0.413	0.616
11	CL	1.157	<.0001	1.03	1.284
	DW	0.776	-	0.663	0.888
12	CL	1.418	<.0001	1.177	1.66
	DW	1.037	-	0.816	1.258
13	CL	0.761	<.0001	0.568	0.954
	DW	0.38	-	0.185	0.574
14	CL	1.022	<.0001	0.9	1.145
	DW	0.641	-	0.543	0.739
15	CL	1.283	<.0001	1.121	1.446
	DW	0.902	-	0.779	1.026
16	CL	1.545	<.0001	1.276	1.813
	DW	1.163	-	0.929	1.397
17	CL	0.331	<.0001	0.135	0.528
	DW	-0.05	-	-0.299	0.199
18	CL	0.592	<.0001	0.513	0.672
	DW	0.211	-	0.057	0.365
19	CL	0.854	<.0001	0.765	0.943
	DW	0.472	-	0.333	0.612
20	CL	1.115	<.0001	0.906	1.323
	DW	0.733	-	0.512	0.955
21	CL	0.458	<.0001	0.274	0.641
	DW	0.076	-	-0.146	0.298
22	CL	0.719	<.0001	0.651	0.787
	DW	0.337	-	0.218	0.457

Table 5.7—Continued

No	Environment	LSMean[1]	p-value	Lower CL[2]	Upper CL[3]
23	CL	0.98	<.0001	0.882	1.078
	DW	0.599	-	0.483	0.714
24	CL	1.241	<.0001	1.021	1.461
	DW	0.86	-	0.645	1.075
25	CL	0.584	<.0001	0.402	0.766
	DW	0.203	-	0	0.405
26	CL	0.845	<.0001	0.759	0.931
	DW	0.464	-	0.367	0.561
27	CL	1.106	<.0001	0.981	1.231
	DW	0.725	-	0.617	0.833
28	CL	1.368	<.0001	1.127	1.608
	DW	0.986	-	0.767	1.205
29	CL	0.71	<.0001	0.518	0.902
	DW	0.329	-	0.136	0.521
30	CL	0.971	<.0001	0.851	1.092
	DW	0.59	-	0.497	0.684
31	CL	1.233	<.0001	1.071	1.394
	DW	0.851	-	0.731	0.971
32	CL	1.494	<.0001	1.226	1.761
	DW	1.112	-	0.88	1.345
33	CL	0.281	<.0001	0.083	0.478
	DW	-0.101	-	-0.35	0.148
34	CL	0.542	<.0001	0.46	0.624
	DW	0.16	-	0.006	0.315
35	CL	0.803	<.0001	0.711	0.894
	DW	0.422	-	0.282	0.561
36	CL	1.064	<.0001	0.855	1.274
	DW	0.683	-	0.461	0.904
37	CL	0.407	<.0001	0.222	0.592
	DW	0.025	-	-0.197	0.248
38	CL	0.668	<.0001	0.596	0.74
	DW	0.287	-	0.166	0.407

Table 5.7—Continued

No	Environment	LSMean[1]	p-value	Lower CL[2]	Upper CL[3]
39	CL	0.929	<.0001	0.829	1.03
	DW	0.548	-	0.432	0.664
40	CL	1.19	<.0001	0.969	1.412
	DW	0.809	-	0.594	1.024
41	CL	0.533	<.0001	0.35	0.717
	DW	0.152	-	-0.051	0.355
42	CL	0.794	<.0001	0.705	0.884
	DW	0.413	-	0.315	0.511
43	CL	1.056	<.0001	0.928	1.183
	DW	0.674	-	0.565	0.783
44	CL	1.317	<.0001	1.075	1.558
	DW	0.935	-	0.716	1.155
45	CL	0.66	<.0001	0.466	0.853
	DW	0.278	-	0.085	0.471
46	CL	0.921	<.0001	0.797	1.044
	DW	0.539	-	0.444	0.634
47	CL	1.182	<.0001	1.018	1.345
	DW	0.8	-	0.68	0.921
48	CL	1.443	<.0001	1.174	1.712
	DW	1.062	-	0.829	1.294
49	CL	0.23	<.0001	0.028	0.431
	DW	-0.152	-	-0.403	0.1
50	CL	0.491	<.0001	0.399	0.582
	DW	0.11	-	-0.049	0.268
51	CL	0.752	<.0001	0.652	0.852
	DW	0.371	-	0.227	0.515
52	CL	1.013	<.0001	0.8	1.227
	DW	0.632	-	0.408	0.856
53	CL	0.356	<.0001	0.167	0.545
	DW	-0.025	-	-0.25	0.2
54	CL	0.617	<.0001	0.534	0.7
	DW	0.236	-	0.11	0.361

Table 5.7—Continued

No	Environment	LSMean[1]	p-value	Lower CL[2]	Upper CL[3]
55	CL	0.878	<.0001	0.77	0.987
	DW	0.497	-	0.376	0.619
56	CL	1.14	<.0001	0.914	1.365
	DW	0.758	-	0.54	0.977
57	CL	0.482	<.0001	0.294	0.671
	DW	0.101	-	-0.105	0.307
58	CL	0.744	<.0001	0.645	0.843
	DW	0.362	-	0.258	0.467
59	CL	1.005	<.0001	0.87	1.139
	DW	0.623	-	0.508	0.738
60	CL	1.266	<.0001	1.021	1.511
	DW	0.885	-	0.662	1.107
61	CL	0.609	<.0001	0.41	0.807
	DW	0.227	-	0.031	0.424
62	CL	0.87	<.0001	0.739	1.001
	DW	0.489	-	0.386	0.591
63	CL	1.131	<.0001	0.962	1.3
	DW	0.75	-	0.623	0.876
64	CL	1.392	<.0001	1.12	1.664
	DW	1.011	-	0.775	1.247

[1]Mean value calculated by the linear statistical module of SAS
[2,3]Lower and upper limits of the 95 percent CI

Although there was a significant difference between the mean LPML of the samples exposed to different environments, analysis indicated a weak correlation between the percent chloride contents and the percent mass loss values among the samples exposed to chloride solution. This could have occurred because the percent chloride contents of these samples were all above the critical chloride threshold value needed to initiate the corrosion, and the actual amount of chloride ions did not have a significant effect.

5.4.3.Fly Ash Type

Comparison of the LPML at the mean values of continuous variables for the four different fly ash types indicated that there were two significantly different groups. The first group consists of the samples containing Class C fly ash and no fly ash, and the second group consisted of samples containing Class F fly ash and high carbon fly ash. The mean LPML values of the second group were significantly higher than the means of the first group. Figure 5.26 shows the LPML box plots separated by the fly ash type. Table 5.8 shows the mean LPML values for the four groups and their 95 percent CIs at the mean values of continuous variables. It should be noted that the variability of the samples without fly ash is much larger than the variability of other groups.

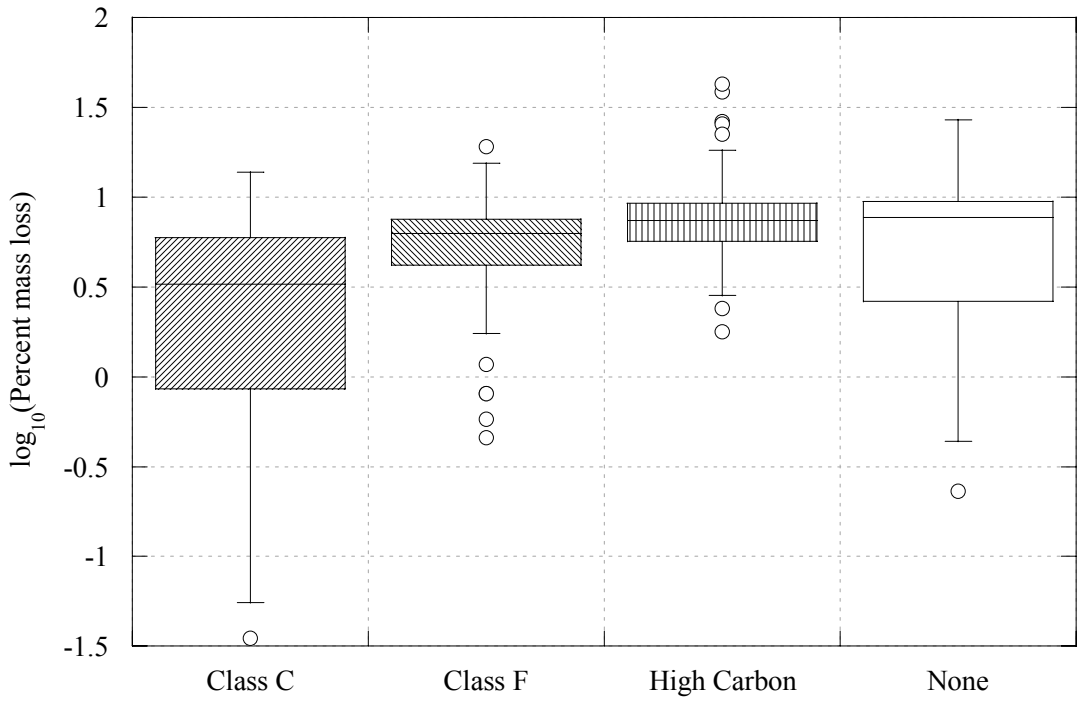

Fig. 5.26--LPML box plots separated by fly ash type.

Table 5.8--Mean LPML values and their 95 percent CIs for different fly ash types

Fly Ash	Mean LPML	95% Confidence Interval	
Class C	0.506	0.436	0.576
Class F	0.828	0.759	0.896
High Carbon	0.862	0.799	0.925
None	0.079	-0.303	0.462

Previous studies reported that some siliceous by-products with pozzolanic properties may potentially decrease the alkalinity of pore solution in concrete. Parameters such as the alkali content of cement and by-product and the absorption capacity of calcium silicate hydrate (C-S-H) like gels for alkalis are believed to be important in determining the effect of byproducts on the alkalinity of pore solution (Lorenzo et al. 1996). Figure 5.27 shows the box plots for the pH values of samples containing sand as the fine aggregate, separated by fly ash type and cement content. Figure 5.28 shows the box plots for the LPML values of samples containing sand as the fine aggregate, separated by fly ash type and cement content. The figures show that among the samples with the same amount of cement content, samples with Class F and high-carbon fly ashes have lower pH values compared to the samples with Class C fly ash. The figures also show that among the samples with the same cement content, samples with Class F and high-carbon fly ashes have higher percent mass loss values compared to the samples with Class C fly ash. The difference between the percent mass loss values of samples containing Class C and the other of fly ash types matches the pH difference of the samples. This may indicate that the difference in percent mass loss values is mainly due to the pH difference of the pore solutions of samples containing different types of fly ashes.

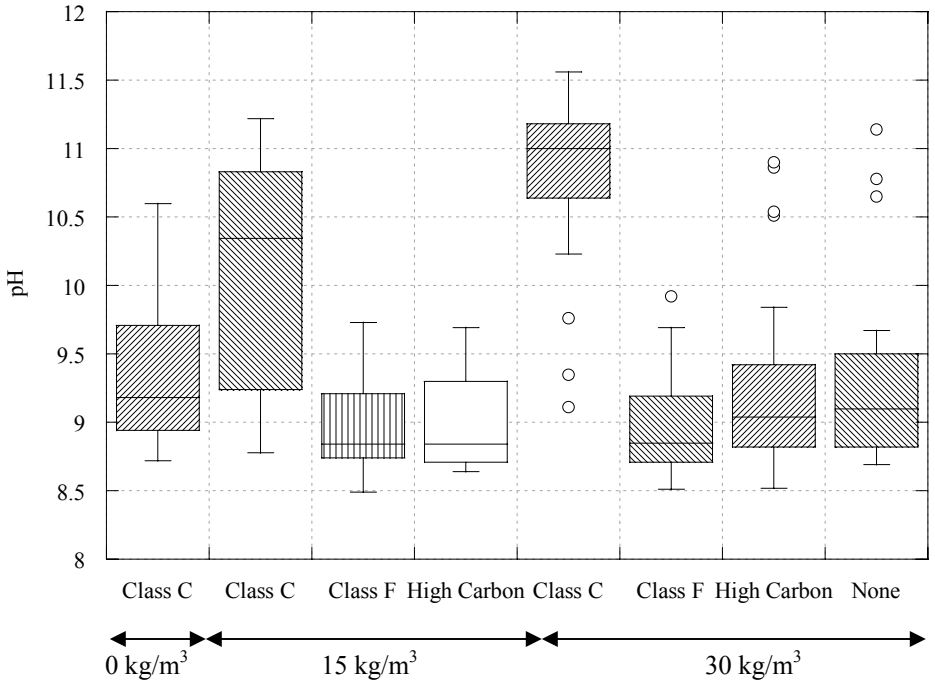

Fig. 5.27--pH of samples with sand separated by cement content and fly ash type.

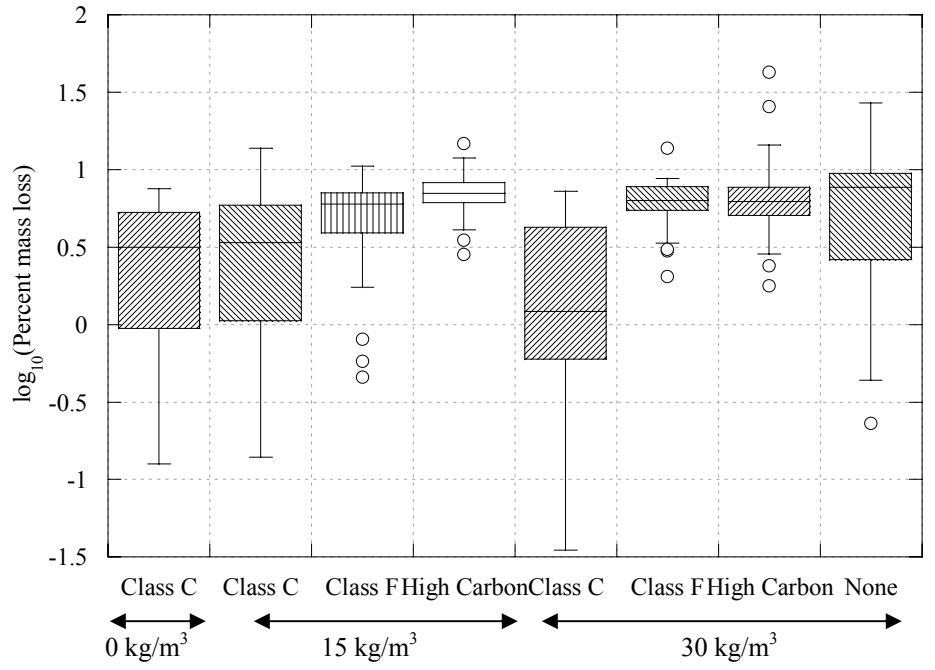

Fig. 5.28--LPML of samples with sand separated by cement content and fly ash type.

The comparison of the mean LPML values for the different types of fly ash was also performed at the 64 combinations of four levels of the three continuous variables as explained earlier. At all combinations the difference between the samples with Class C fly ash and without fly ash and the difference between the samples with Class F fly ash and high carbon fly ash were not statistically significant. The mean values for the first group was higher compared to the mean values of the second group at all combinations. Table 5.9 shows the mean LPML values and their 95 percent CI's at the 64 tried combinations of the continuous variable levels.

Table 5.9--Mean and 95% CI values of LPML for different fly ash levels

No[1]	Fly Ash	Lower CL	LSMean	Upper CL
	Class C	-0.005	0.129	0.262
	Class F	0.309	0.451	0.592
	High Carbon	0.318	0.484	0.651
1	None	-0.794	-0.298	0.198
	Class C	0.285	0.39	0.495
	Class F	0.616	0.712	0.808
	High Carbon	0.649	0.746	0.842
2	None	-0.413	-0.037	0.339
	Class C	0.456	0.651	0.846
	Class F	0.793	0.973	1.153
	High Carbon	0.849	1.007	1.165
3	None	-0.04	0.224	0.489
	Class C	0.597	0.912	1.227
	Class F	0.935	1.234	1.533
	High Carbon	0.995	1.268	1.541
4	None	0.304	0.486	0.667
	Class C	0.145	0.255	0.364
	Class F	0.461	0.577	0.693
	High Carbon	0.47	0.611	0.751
5	None	-0.652	-0.172	0.309

Table 5.9—Continued

No[1]	Fly Ash	Lower CL	LSMean	Upper CL
6	Class C	0.424	0.516	0.608
	Class F	0.76	0.838	0.916
	High Carbon	0.803	0.872	0.941
	None	-0.27	0.09	0.449
7	Class C	0.58	0.777	0.974
	Class F	0.919	1.099	1.28
	High Carbon	0.979	1.133	1.287
	None	0.103	0.351	0.599
8	Class C	0.717	1.038	1.36
	Class F	1.056	1.36	1.665
	High Carbon	1.118	1.394	1.671
	None	0.446	0.612	0.778
9	Class C	0.279	0.381	0.484
	Class F	0.597	0.703	0.81
	High Carbon	0.61	0.737	0.865
	None	-0.515	-0.045	0.424
10	Class C	0.541	0.642	0.744
	Class F	0.88	0.964	1.049
	High Carbon	0.931	0.998	1.066
	None	-0.133	0.216	0.565
11	Class C	0.694	0.904	1.113
	Class F	1.033	1.226	1.418
	High Carbon	1.096	1.26	1.423
	None	0.238	0.477	0.717
12	Class C	0.831	1.165	1.499
	Class F	1.169	1.487	1.804
	High Carbon	1.233	1.521	1.809
	None	0.575	0.738	0.902
13	Class C	0.392	0.508	0.623
	Class F	0.713	0.83	0.946
	High Carbon	0.733	0.863	0.994
	None	-0.381	0.081	0.544

Table 5.9—Continued

No[1]	Fly Ash	Lower CL	LSMean	Upper CL
	Class C	0.641	0.769	0.897
	Class F	0.978	1.091	1.203
	High Carbon	1.031	1.125	1.218
14	None	-0.002	0.342	0.687
	Class C	0.799	1.03	1.261
	Class F	1.138	1.352	1.566
	High Carbon	1.201	1.386	1.571
15	None	0.364	0.603	0.843
	Class C	0.938	1.291	1.644
	Class F	1.277	1.613	1.949
	High Carbon	1.341	1.647	1.953
16	None	0.691	0.865	1.038
	Class C	-0.049	0.078	0.204
	Class F	0.259	0.4	0.541
	High Carbon	0.269	0.434	0.598
17	None	-0.844	-0.349	0.147
	Class C	0.243	0.339	0.435
	Class F	0.565	0.661	0.757
	High Carbon	0.601	0.695	0.789
18	None	-0.462	-0.088	0.287
	Class C	0.41	0.6	0.79
	Class F	0.742	0.922	1.102
	High Carbon	0.8	0.956	1.112
19	None	-0.089	0.174	0.436
	Class C	0.549	0.861	1.173
	Class F	0.884	1.183	1.482
	High Carbon	0.945	1.217	1.489
20	None	0.256	0.435	0.613
	Class C	0.103	0.204	0.305
	Class F	0.41	0.526	0.642
	High Carbon	0.421	0.56	0.699
21	None	-0.702	-0.222	0.257

Table 5.9—Continued

No[1]	Fly Ash	Lower CL	LSMean	Upper CL
	Class C	0.384	0.465	0.547
	Class F	0.71	0.787	0.865
	High Carbon	0.755	0.821	0.887
22	None	-0.32	0.039	0.397
	Class C	0.534	0.726	0.919
	Class F	0.868	1.048	1.229
	High Carbon	0.93	1.082	1.235
23	None	0.054	0.3	0.546
	Class C	0.669	0.988	1.306
	Class F	1.005	1.31	1.614
	High Carbon	1.068	1.344	1.619
24	None	0.398	0.561	0.724
	Class C	0.237	0.33	0.424
	Class F	0.546	0.652	0.759
	High Carbon	0.56	0.686	0.812
25	None	-0.565	-0.096	0.372
	Class C	0.499	0.592	0.684
	Class F	0.828	0.914	0.999
	High Carbon	0.883	0.948	1.012
26	None	-0.183	0.165	0.513
	Class C	0.647	0.853	1.058
	Class F	0.982	1.175	1.367
	High Carbon	1.046	1.209	1.371
27	None	0.189	0.426	0.664
	Class C	0.783	1.114	1.445
	Class F	1.119	1.436	1.753
	High Carbon	1.183	1.47	1.757
28	None	0.527	0.687	0.848
	Class C	0.349	0.457	0.565
	Class F	0.662	0.779	0.896
	High Carbon	0.683	0.813	0.942
29	None	-0.431	0.03	0.492

Table 5.9—Continued

No[1]	Fly Ash	Lower CL	LSMean	Upper CL
30	Class C	0.597	0.718	0.839
	Class F	0.927	1.04	1.153
	High Carbon	0.982	1.074	1.166
	None	-0.052	0.291	0.635
31	Class C	0.752	0.979	1.207
	Class F	1.087	1.301	1.515
	High Carbon	1.151	1.335	1.519
	None	0.315	0.553	0.791
32	Class C	0.89	1.24	1.591
	Class F	1.226	1.562	1.898
	High Carbon	1.291	1.596	1.902
	None	0.643	0.814	0.985
33	Class C	-0.096	0.027	0.15
	Class F	0.204	0.349	0.494
	High Carbon	0.216	0.383	0.55
	None	-0.895	-0.4	0.096
34	Class C	0.197	0.288	0.38
	Class F	0.509	0.61	0.711
	High Carbon	0.547	0.644	0.742
	None	-0.513	-0.138	0.236
35	Class C	0.361	0.549	0.738
	Class F	0.689	0.871	1.054
	High Carbon	0.747	0.905	1.064
	None	-0.14	0.123	0.386
36	Class C	0.5	0.811	1.121
	Class F	0.832	1.133	1.433
	High Carbon	0.893	1.166	1.44
	None	0.205	0.384	0.563
37	Class C	0.056	0.153	0.251
	Class F	0.354	0.475	0.596
	High Carbon	0.368	0.509	0.651
	None	-0.753	-0.273	0.207

Table 5.9—Continued

No[1]	Fly Ash	Lower CL	LSMean	Upper CL
	Class C	0.337	0.414	0.492
	Class F	0.652	0.736	0.821
	High Carbon	0.699	0.77	0.842
38	None	-0.371	-0.012	0.347
	Class C	0.485	0.676	0.866
	Class F	0.814	0.998	1.181
	High Carbon	0.877	1.032	1.186
39	None	0.003	0.249	0.496
	Class C	0.62	0.937	1.254
	Class F	0.952	1.259	1.566
	High Carbon	1.016	1.293	1.57
40	None	0.347	0.51	0.674
	Class C	0.19	0.28	0.37
	Class F	0.489	0.602	0.714
	High Carbon	0.506	0.636	0.765
41	None	-0.616	-0.147	0.322
	Class C	0.452	0.541	0.63
	Class F	0.771	0.863	0.955
	High Carbon	0.826	0.897	0.967
42	None	-0.234	0.114	0.462
	Class C	0.598	0.802	1.006
	Class F	0.928	1.124	1.32
	High Carbon	0.993	1.158	1.323
43	None	0.137	0.375	0.613
	Class C	0.733	1.063	1.394
	Class F	1.066	1.385	1.704
	High Carbon	1.131	1.419	1.708
44	None	0.475	0.637	0.798
	Class C	0.301	0.406	0.511
	Class F	0.606	0.728	0.85
	High Carbon	0.629	0.762	0.895
45	None	-0.482	-0.021	0.441

Table 5.9—Continued

No[1]	Fly Ash	Lower CL	LSMean	Upper CL
	Class C	0.548	0.667	0.786
	Class F	0.87	0.989	1.108
	High Carbon	0.927	1.023	1.119
46	None	-0.103	0.241	0.584
	Class C	0.702	0.928	1.155
	Class F	1.033	1.25	1.468
	High Carbon	1.098	1.284	1.471
47	None	0.263	0.502	0.74
	Class C	0.84	1.19	1.539
	Class F	1.174	1.512	1.849
	High Carbon	1.239	1.545	1.852
48	None	0.591	0.763	0.935
	Class C	-0.149	-0.024	0.101
	Class F	0.146	0.298	0.451
	High Carbon	0.16	0.332	0.504
49	None	-0.947	-0.45	0.046
	Class C	0.144	0.237	0.331
	Class F	0.448	0.559	0.671
	High Carbon	0.487	0.593	0.7
50	None	-0.565	-0.189	0.187
	Class C	0.309	0.499	0.688
	Class F	0.632	0.821	1.009
	High Carbon	0.691	0.855	1.018
51	None	-0.193	0.072	0.337
	Class C	0.449	0.76	1.071
	Class F	0.777	1.082	1.386
	High Carbon	0.839	1.116	1.392
52	None	0.151	0.333	0.515
	Class C	0.003	0.102	0.202
	Class F	0.294	0.425	0.555
	High Carbon	0.31	0.458	0.607
53	None	-0.805	-0.324	0.157

Table 5.9—Continued

No[1]	Fly Ash	Lower CL	LSMean	Upper CL
	Class C	0.284	0.364	0.444
	Class F	0.588	0.686	0.783
	High Carbon	0.636	0.72	0.803
54	None	-0.423	-0.063	0.298
	Class C	0.433	0.625	0.817
	Class F	0.757	0.947	1.137
	High Carbon	0.82	0.981	1.142
55	None	-0.051	0.198	0.447
	Class C	0.568	0.886	1.204
	Class F	0.898	1.208	1.518
	High Carbon	0.962	1.242	1.522
56	None	0.292	0.46	0.627
	Class C	0.136	0.229	0.322
	Class F	0.428	0.551	0.673
	High Carbon	0.448	0.585	0.721
57	None	-0.668	-0.198	0.272
	Class C	0.398	0.49	0.582
	Class F	0.708	0.812	0.916
	High Carbon	0.763	0.846	0.929
58	None	-0.287	0.064	0.414
	Class C	0.546	0.751	0.956
	Class F	0.872	1.073	1.275
	High Carbon	0.936	1.107	1.278
59	None	0.084	0.325	0.566
	Class C	0.681	1.012	1.344
	Class F	1.011	1.334	1.657
	High Carbon	1.076	1.368	1.66
60	None	0.42	0.586	0.751
	Class C	0.247	0.355	0.463
	Class F	0.545	0.677	0.809
	High Carbon	0.571	0.711	0.852
61	None	-0.535	-0.071	0.392

Table 5.9—Continued

No[1]	Fly Ash	Lower CL	LSMean	Upper CL
62	Class C	0.495	0.616	0.738
	Class F	0.809	0.938	1.067
	High Carbon	0.866	0.972	1.079
	None	-0.156	0.19	0.536
63	Class C	0.65	0.878	1.105
	Class F	0.977	1.2	1.422
	High Carbon	1.042	1.233	1.425
	None	0.209	0.451	0.693
64	Class C	0.788	1.139	1.489
	Class F	1.119	1.461	1.802
	High Carbon	1.184	1.495	1.805
	None	0.536	0.712	0.888

5.4.4.Interaction of Fly Ash with Environment

The analysis of variance for the proposed model indicates that the interaction of fly ash type with environment was a statistically significant factor. Figure 5.29 shows the box plots of LPML values separated by environment and fly ash type. Table 5.10 indicates that the effect of fly ash type was significant for samples exposed to both environments. The effect of fly ash in both environments was the same, i.e., samples with Class C fly ash and without fly ash had lower mean LPML values compared to the group of samples with Class F fly ash and high carbon fly ash. The effect of fly ash was more significant in the distilled water environment. Table 5.11 shows the mean LPML values and their 95 percent CI's for the environment and fly ash type combinations.

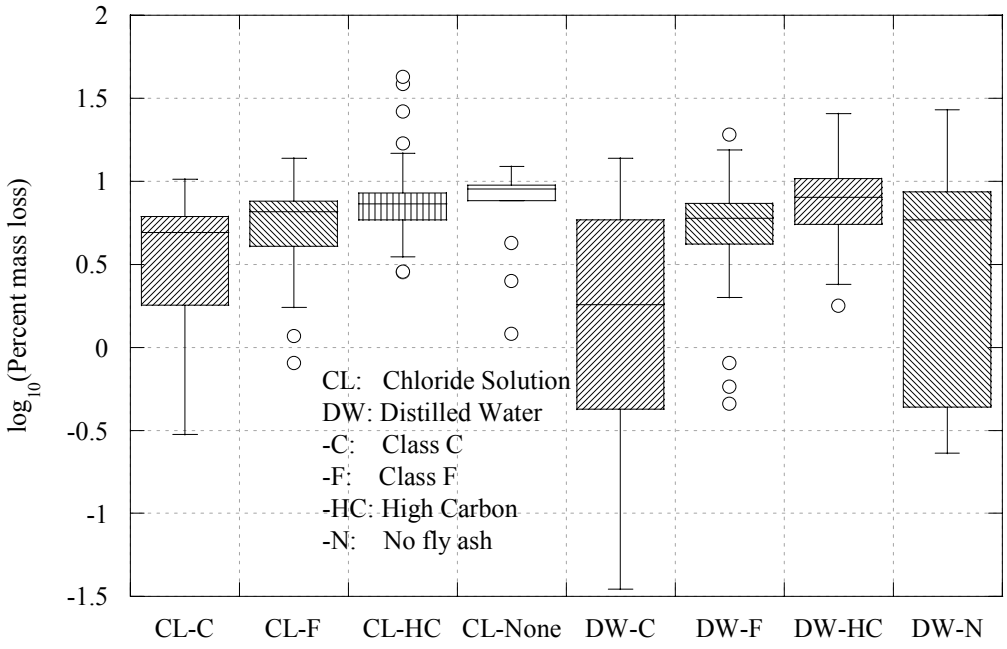

Fig. 5.29--LPML box plots separated by environment and fly ash type.

Table 5.10--The effect of fly ash in different environments

Environment	DF[1]	Sum of Squares	Mean Square	F- Value	Pr > F
Chloride	3	49.69238	16.564127	17.11	<.0001
Distilled water	3	121.481608	40.493869	41.83	<.0001

[1]Degrees of freedom

Table 5.11--The LPML values for environment and fly ash type combinations

Environment	Fly ash	LSMEAN[1]	95% Confidence Limits	
			Low	High
Chloride	Class C	0.804	0.706	0.902
Chloride	Class F	0.984	0.892	1.075
Chloride	High Carbon	0.981	0.904	1.059
Chloride	None	0.269	-0.098	0.636
Distilled water	Class C	0.208	0.120	0.295
Distilled water	Class F	0.672	0.573	0.771
Distilled water	High Carbon	0.742	0.644	0.841
Distilled water	None	-0.110	-0.541	0.321

[1]Mean value calculated by the linear statistical module of SAS

5.4.5.Fine Aggregate Type

The mean LPML values and their 95 percent CIs of the samples containing one of the three different fine aggregate types and of the samples without a fine aggregate are shown in Table 5.12. Figure 5.30 shows the same information graphically. Tukey's comparison at the mean values of the continuous variables indicates that samples with bottom ash have the lowest mean LPML value and the difference is statistically significant compared to all other groups. Samples with sand have a higher mean LPML value compared to bottom ash, however with a lower variability. Both samples with bottom ash and sand have statistically significantly lower mean LPML values compared to the samples without fine aggregates. Samples containing foundry sand exhibited the largest variability and even though they exhibited a mean LPML value lower than the mean of samples without fly ash, the difference was not statistically significant. Results from the uncoupled samples in the Phase I research indicated that using any kind of fine aggregate decreased the percent mass loss of the samples compared to samples without fine aggregates. The findings of this phase support these results and indicate that the difference in LPML may not be statistically significant in the case of foundry sand, due to the high variability observed in samples containing this type of fine aggregate. The pH of spent foundry sand can vary from approximately 4 to 8, depending on the binder and type of metal cast (Johnson 1981) and previous research has reported that some spent foundry sands can be corrosive to metals (MNR 1992).

Table 5.12--The mean LPML values separated by the fine aggregate type

Fine Aggregate	LSMEAN[1]	95 % Confidence Limits	
		Low	High
Bottom ash	0.387	0.242	0.533
Foundry sand	0.597	0.362	0.831
None	0.830	0.699	0.960
Sand	0.461	0.392	0.530

[1]Mean value calculated by the linear statistical module of SAS

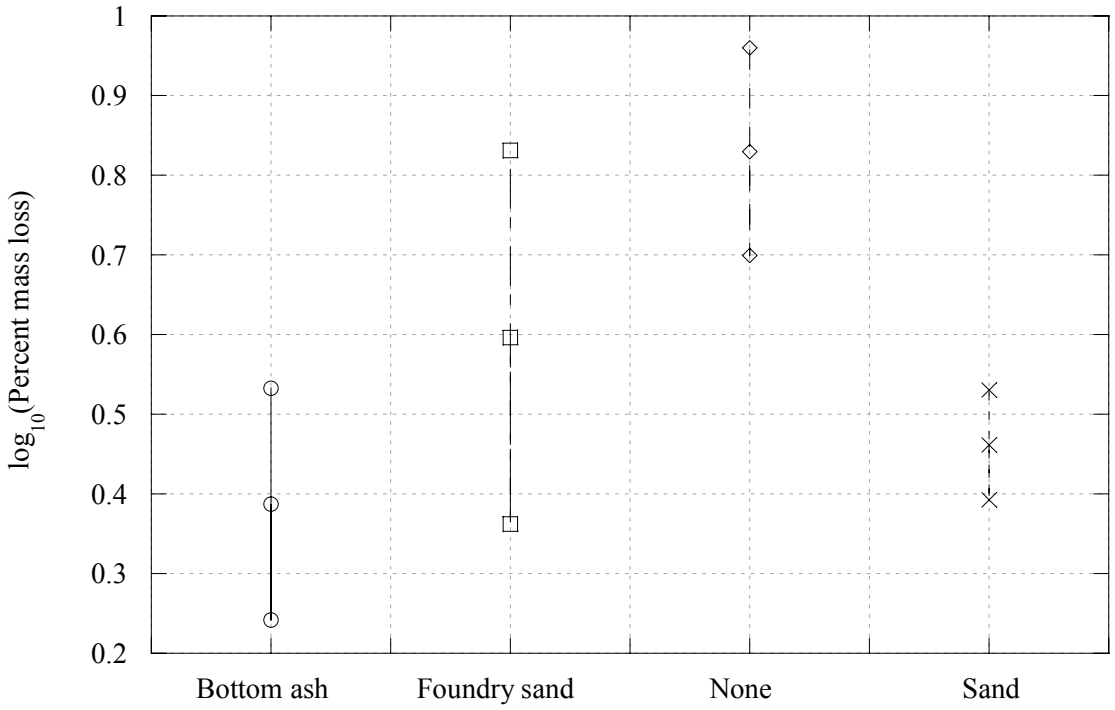

Fig. 5.30--Mean LPML values and their confidence interval of samples containing different fine aggregate types.

Figure 5.31 shows the LPML values of the samples separated by their fine aggregate type. The comparison of the mean LPML values of samples with different fine aggregate types at the 64 combinations of the three continuous variables also indicate that the observed relations between the samples with different fine aggregates are the same over the whole range of the continuous variables. Table 5.13 shows the mean LPML values and the limits of the 95 percent CI at the 64 combinations for samples with different fine aggregate types.

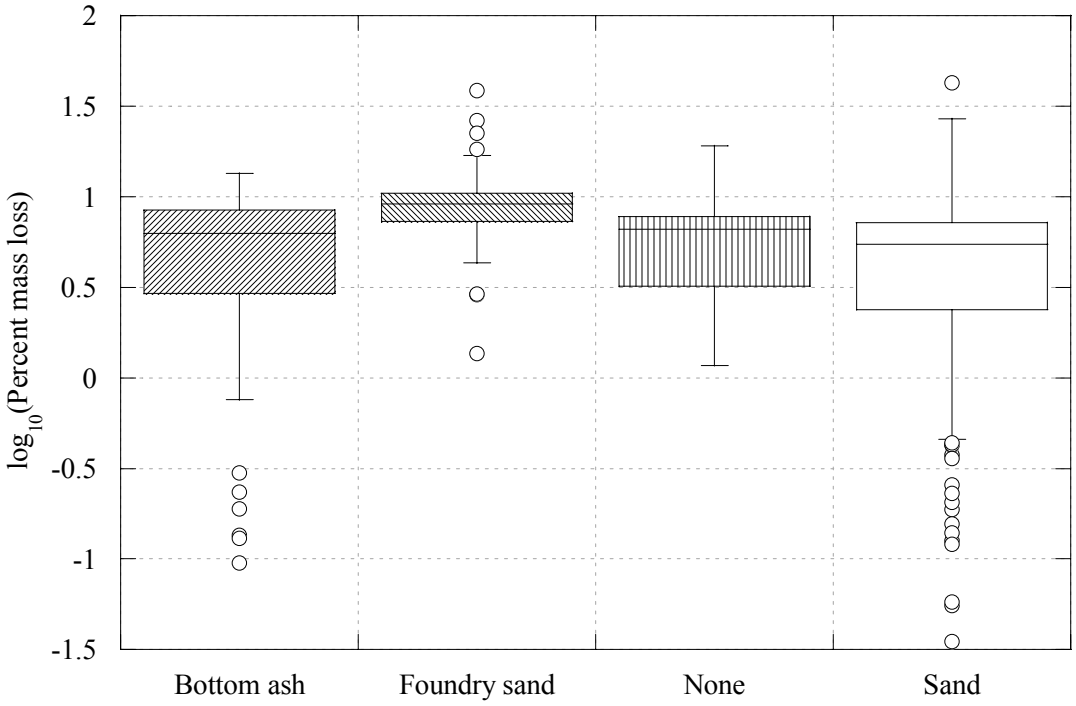

Fig. 5.31--LPML box plots separated by the fine aggregate type.

Table 5.13--LPML means and 95% CI for 64 combinations

No[1]	Fine aggregate	Lower CL[2]	LSMean[3]	Upper CL[4]
1	Bottom ash	-0.247	0.01	0.267
	Foundry sand	-0.129	0.219	0.568
	None	0.302	0.452	0.602
	Sand	-0.116	0.084	0.284
2	Bottom ash	0.123	0.271	0.419
	Foundry sand	0.254	0.481	0.708
	None	0.565	0.713	0.862
	Sand	0.229	0.345	0.461
3	Bottom ash	0.424	0.532	0.64
	Foundry sand	0.617	0.742	0.867
	None	0.739	0.975	1.211
	Sand	0.462	0.606	0.751

Table 5.13—Continued

No[1]	Fine aggregate	Lower CL[2]	LSMean[3]	Upper CL[4]
4	Bottom ash	0.606	0.794	0.982
	Foundry sand	0.886	1.003	1.12
	None	0.885	1.236	1.587
	Sand	0.619	0.868	1.117
5	Bottom ash	-0.101	0.136	0.374
	Foundry sand	0.013	0.346	0.678
	None	0.443	0.579	0.714
	Sand	0.039	0.21	0.381
6	Bottom ash	0.272	0.397	0.523
	Foundry sand	0.397	0.607	0.816
	None	0.693	0.84	0.986
	Sand	0.395	0.472	0.548
7	Bottom ash	0.565	0.659	0.752
	Foundry sand	0.762	0.868	0.974
	None	0.859	1.101	1.342
	Sand	0.604	0.733	0.861
8	Bottom ash	0.731	0.92	1.109
	Foundry sand	1.017	1.129	1.241
	None	1.003	1.362	1.721
	Sand	0.747	0.994	1.241
9	Bottom ash	0.036	0.263	0.489
	Foundry sand	0.15	0.472	0.794
	None	0.568	0.705	0.842
	Sand	0.186	0.337	0.487
10	Bottom ash	0.407	0.524	0.641
	Foundry sand	0.532	0.733	0.935
	None	0.808	0.966	1.125
	Sand	0.547	0.598	0.649
11	Bottom ash	0.685	0.785	0.885
	Foundry sand	0.888	0.994	1.1
	None	0.972	1.227	1.483
	Sand	0.731	0.859	0.988

Table 5.13—Continued

No[1]	Fine aggregate	Lower CL[2]	LSMean[3]	Upper CL[4]
12	Bottom ash	0.845	1.046	1.247
	Foundry sand	1.129	1.256	1.382
	None	1.115	1.488	1.862
	Sand	0.867	1.12	1.374
13	Bottom ash	0.164	0.389	0.613
	Foundry sand	0.28	0.598	0.917
	None	0.678	0.831	0.985
	Sand	0.32	0.463	0.606
14	Bottom ash	0.523	0.65	0.777
	Foundry sand	0.656	0.86	1.063
	None	0.91	1.092	1.275
	Sand	0.663	0.724	0.785
15	Bottom ash	0.785	0.911	1.037
	Foundry sand	0.996	1.121	1.246
	None	1.077	1.354	1.63
	Sand	0.841	0.985	1.13
16	Bottom ash	0.95	1.173	1.395
	Foundry sand	1.228	1.382	1.535
	None	1.222	1.615	2.007
	Sand	0.978	1.247	1.515
17	Bottom ash	-0.298	-0.041	0.216
	Foundry sand	-0.179	0.169	0.516
	None	0.26	0.401	0.543
	Sand	-0.166	0.033	0.232
18	Bottom ash	0.073	0.22	0.368
	Foundry sand	0.204	0.43	0.656
	None	0.523	0.663	0.803
	Sand	0.181	0.294	0.408
19	Bottom ash	0.374	0.482	0.589
	Foundry sand	0.568	0.691	0.814
	None	0.693	0.924	1.154
	Sand	0.413	0.556	0.698

Table 5.13—Continued

No[1]	Fine aggregate	Lower CL[2]	LSMean[3]	Upper CL[4]
20	Bottom ash	0.555	0.743	0.931
	Foundry sand	0.837	0.952	1.067
	None	0.838	1.185	1.532
	Sand	0.569	0.817	1.065
21	Bottom ash	-0.152	0.086	0.323
	Foundry sand	-0.037	0.295	0.626
	None	0.401	0.528	0.654
	Sand	-0.01	0.16	0.329
22	Bottom ash	0.222	0.347	0.472
	Foundry sand	0.348	0.556	0.764
	None	0.651	0.789	0.927
	Sand	0.347	0.421	0.495
23	Bottom ash	0.515	0.608	0.701
	Foundry sand	0.713	0.817	0.921
	None	0.814	1.05	1.287
	Sand	0.555	0.682	0.809
24	Bottom ash	0.68	0.869	1.058
	Foundry sand	0.968	1.078	1.189
	None	0.955	1.311	1.667
	Sand	0.697	0.943	1.189
25	Bottom ash	-0.015	0.212	0.438
	Foundry sand	0.1	0.421	0.743
	None	0.526	0.654	0.782
	Sand	0.137	0.286	0.435
26	Bottom ash	0.355	0.473	0.591
	Foundry sand	0.482	0.682	0.883
	None	0.764	0.915	1.066
	Sand	0.5	0.547	0.595
27	Bottom ash	0.633	0.734	0.835
	Foundry sand	0.839	0.944	1.048
	None	0.926	1.176	1.427
	Sand	0.681	0.808	0.935

Table 5.13—Continued

No[1]	Fine aggregate	Lower CL[2]	LSMean[3]	Upper CL[4]
28	Bottom ash	0.794	0.995	1.197
	Foundry sand	1.08	1.205	1.329
	None	1.067	1.438	1.808
	Sand	0.817	1.07	1.322
29	Bottom ash	0.113	0.338	0.563
	Foundry sand	0.229	0.548	0.866
	None	0.635	0.78	0.926
	Sand	0.27	0.412	0.554
30	Bottom ash	0.472	0.599	0.727
	Foundry sand	0.605	0.809	1.012
	None	0.866	1.042	1.217
	Sand	0.615	0.673	0.732
31	Bottom ash	0.734	0.861	0.987
	Foundry sand	0.946	1.07	1.194
	None	1.03	1.303	1.576
	Sand	0.791	0.935	1.078
32	Bottom ash	0.899	1.122	1.344
	Foundry sand	1.179	1.331	1.484
	None	1.174	1.564	1.954
	Sand	0.928	1.196	1.464
33	Bottom ash	-0.351	-0.092	0.167
	Foundry sand	-0.231	0.118	0.466
	None	0.214	0.351	0.487
	Sand	-0.218	-0.018	0.183
34	Bottom ash	0.018	0.17	0.321
	Foundry sand	0.152	0.379	0.606
	None	0.477	0.612	0.747
	Sand	0.127	0.244	0.36
35	Bottom ash	0.318	0.431	0.544
	Foundry sand	0.514	0.64	0.766
	None	0.645	0.873	1.101
	Sand	0.36	0.505	0.649

Table 5.13—Continued

No[1]	Fine aggregate	Lower CL[2]	LSMean[3]	Upper CL[4]
36	Bottom ash	0.501	0.692	0.883
	Foundry sand	0.784	0.901	1.019
	None	0.789	1.134	1.48
	Sand	0.517	0.766	1.015
37	Bottom ash	-0.205	0.035	0.275
	Foundry sand	-0.089	0.244	0.577
	None	0.356	0.477	0.598
	Sand	-0.063	0.109	0.281
38	Bottom ash	0.166	0.296	0.426
	Foundry sand	0.295	0.505	0.715
	None	0.605	0.738	0.871
	Sand	0.292	0.37	0.448
39	Bottom ash	0.458	0.557	0.657
	Foundry sand	0.659	0.766	0.874
	None	0.766	0.999	1.233
	Sand	0.502	0.631	0.76
40	Bottom ash	0.626	0.818	1.01
	Foundry sand	0.914	1.028	1.141
	None	0.906	1.261	1.615
	Sand	0.645	0.892	1.14
41	Bottom ash	-0.068	0.161	0.39
	Foundry sand	0.048	0.37	0.693
	None	0.48	0.603	0.727
	Sand	0.083	0.235	0.387
42	Bottom ash	0.299	0.422	0.545
	Foundry sand	0.429	0.632	0.834
	None	0.718	0.865	1.011
	Sand	0.441	0.496	0.552
43	Bottom ash	0.577	0.683	0.79
	Foundry sand	0.785	0.893	1.001
	None	0.877	1.126	1.374
	Sand	0.627	0.758	0.888

Table 5.13—Continued

No[1]	Fine aggregate	Lower CL[2]	LSMean[3]	Upper CL[4]
44	Bottom ash	0.74	0.945	1.149
	Foundry sand	1.026	1.154	1.282
	None	1.018	1.387	1.755
	Sand	0.764	1.019	1.273
45	Bottom ash	0.06	0.287	0.515
	Foundry sand	0.177	0.497	0.816
	None	0.588	0.73	0.872
	Sand	0.216	0.361	0.507
46	Bottom ash	0.416	0.549	0.681
	Foundry sand	0.553	0.758	0.963
	None	0.818	0.991	1.163
	Sand	0.557	0.623	0.688
47	Bottom ash	0.678	0.81	0.941
	Foundry sand	0.892	1.019	1.146
	None	0.981	1.252	1.523
	Sand	0.737	0.884	1.03
48	Bottom ash	0.845	1.071	1.297
	Foundry sand	1.125	1.28	1.436
	None	1.125	1.513	1.901
	Sand	0.876	1.145	1.414
49	Bottom ash	-0.406	-0.142	0.121
	Foundry sand	-0.284	0.067	0.418
	None	0.164	0.3	0.435
	Sand	-0.273	-0.068	0.137
50	Bottom ash	-0.04	0.119	0.278
	Foundry sand	0.097	0.328	0.559
	None	0.427	0.561	0.695
	Sand	0.069	0.193	0.317
51	Bottom ash	0.258	0.38	0.502
	Foundry sand	0.457	0.589	0.722
	None	0.595	0.822	1.049
	Sand	0.304	0.454	0.605

Table 5.13—Continued

No[1]	Fine aggregate	Lower CL[2]	LSMean[3]	Upper CL[4]
52	Bottom ash	0.445	0.641	0.838
	Foundry sand	0.726	0.851	0.975
	None	0.738	1.083	1.429
	Sand	0.463	0.715	0.968
53	Bottom ash	-0.261	-0.016	0.229
	Foundry sand	-0.142	0.193	0.529
	None	0.305	0.426	0.547
	Sand	-0.119	0.058	0.235
54	Bottom ash	0.107	0.245	0.384
	Foundry sand	0.24	0.454	0.669
	None	0.555	0.687	0.82
	Sand	0.23	0.319	0.409
55	Bottom ash	0.396	0.506	0.617
	Foundry sand	0.6	0.716	0.832
	None	0.715	0.949	1.182
	Sand	0.444	0.58	0.717
56	Bottom ash	0.57	0.768	0.965
	Foundry sand	0.855	0.977	1.098
	None	0.856	1.21	1.564
	Sand	0.591	0.842	1.093
57	Bottom ash	-0.124	0.11	0.345
	Foundry sand	-0.006	0.32	0.645
	None	0.429	0.553	0.676
	Sand	0.026	0.184	0.343
58	Bottom ash	0.239	0.371	0.504
	Foundry sand	0.374	0.581	0.788
	None	0.667	0.814	0.96
	Sand	0.375	0.446	0.516
59	Bottom ash	0.515	0.633	0.75
	Foundry sand	0.725	0.842	0.959
	None	0.827	1.075	1.323
	Sand	0.569	0.707	0.844

Table 5.13—Continued

No[1]	Fine aggregate	Lower CL[2]	LSMean[3]	Upper CL[4]
60	Bottom ash	0.684	0.894	1.104
	Foundry sand	0.968	1.103	1.238
	None	0.968	1.336	1.705
	Sand	0.71	0.968	1.226
61	Bottom ash	0.003	0.237	0.47
	Foundry sand	0.123	0.446	0.769
	None	0.537	0.679	0.821
	Sand	0.159	0.311	0.463
62	Bottom ash	0.356	0.498	0.64
	Foundry sand	0.497	0.707	0.917
	None	0.768	0.94	1.113
	Sand	0.492	0.572	0.651
63	Bottom ash	0.618	0.759	0.9
	Foundry sand	0.833	0.968	1.103
	None	0.931	1.201	1.472
	Sand	0.68	0.833	0.986
64	Bottom ash	0.789	1.02	1.251
	Foundry sand	1.068	1.23	1.391
	None	1.074	1.462	1.851
	Sand	0.821	1.094	1.367

[1]Combination number
[3]Mean value calculated by the linear statistical module of SAS
[2,4]Lower and upper limits of the 95 percent CI

5.4.6.Metal Type

Analysis of variance also indicates that the metal type was a very significant factor in the magnitude of LPML. Tukey's comparison indicates that the mean LPML value of samples with galvanized steel coupons was significantly higher than the mean LPML value of samples with ductile iron coupons. The mean LPML values and their 95

percent CI limits at the mean values of the three continuous variables are shown in Table 5.14.

Table 5.14--LPML means and confidence intervals for different metal types

Metal type	LSMEAN	95% Confidence Interval	
		Low	High
Ductile iron	0.348	0.166	0.531
Galvanized steel	0.789	0.713	0.865

Previous research on corrosion of metals in concrete indicates that if the pH value of pore water solution is between 12.2 and 13.3, zinc is covered with a protective film of calcium hydroxyzincate, which protects the underlying steel against corrosion. If the pH value is over 13.2, zinc is in an active state and corrodes. If the pH of the surrounding solution is between 11 and 12, zinc is covered with a porous zinc oxide layer that offers no protection against corrosion (Macias and Andrade 1987c, 1987d). The majority of samples had pH values less than 11 as shown in Figure 5.27.

5.4.7.Resistivity and Water Cementitious Material Ratio

The analysis of variance results indicated that the logarithm of resistivity and w/cm were statistically significant factors. Many researchers investigating the corrosion of metals embedded in soils have noted an inverse relationship between the soil resistivity and corrosion (Peabody 1967, Coburn 1978, Palmer 1990, Chaker 1990, Escalante 1992). Previous research has also indicated that there is a nonlinear relationship between the mass loss of metal coupons embedded in soils and resistivity (Edgar 1989, Palmer 1989).

Previous research has shown that for conventional concrete the strength increases and the diffusivity, porosity, and permeability decrease with decreasing w/cm. Thus, for conventional uncracked concrete, the mean LPML value would be expected to be

directly proportional to the w/cm. Although not concrete the correlation coefficients shown in Table 5.2 for the CLSM mixtures support this. The analysis of variance also shows that the interactions between the logarithm of resistivity and metal type, and between the w/cm and metal type were significant. Table 5.15 shows the comparison of mean LPML values for different metal types at the 64 combinations of the three continuous variables; pH, logarithm of resistivity, and w/cm. The p-values of comparisons, where the differences were not significant, are typed bold and with a different font.

Table 5.15--Comparison of LPML for different metal types at 64 combinations of continuous variables (DI: Ductile iron, GS: Galvanized steel)

No	Metal type	t Diff	Pr>t	pH	lRes	w/cm	Lower CL	LSMean	Upper CL
1	DI	-5.12	<.0001	8.813	2.422	0.619	-0.773	-0.373	0.027
	GS	-	-				0.583	0.756	0.929
2	DI	-7.12	<.0001	8.813	2.422	1.566	-0.138	0.061	0.261
	GS	-	-				0.749	0.844	0.939
3	DI	-4.22	<.0001	8.813	2.422	2.513	0.304	0.496	0.688
	GS	-	-				0.851	0.932	1.013
4	DI	-0.43	***0.6693***	8.813	2.422	3.46	0.541	0.93	1.319
	GS	-	-				0.87	1.02	1.17
5	DI	-4.5	<.0001	8.813	3.222	0.619	-0.492	-0.13	0.233
	GS	-	-				0.613	0.765	0.917
6	DI	-6.89	<.0001	8.813	3.222	1.566	0.158	0.305	0.452
	GS	-	-				0.783	0.853	0.923
7	DI	-2.22	0.0272	8.813	3.222	2.513	0.568	0.739	0.911
	GS	-	-				0.871	0.941	1.011
8	DI	0.68	***0.4985***	8.813	3.222	3.46	0.78	1.173	1.566
	GS	-	-				0.876	1.029	1.182
9	DI	-3.54	0.0005	8.813	4.021	0.619	-0.229	0.114	0.457
	GS	-	-				0.636	0.774	0.912

Table 5.15—Continued

No	Metal type	t Diff	Pr>t	pH	lRes	w/cm	Lower CL	LSMean	Upper CL
10	DI	-4.43	<.0001	8.813	4.021	1.566	0.413	0.548	0.684
	GS	-	-				0.805	0.862	0.92
11	DI	0.32	***0.7511***	8.813	4.021	2.513	0.791	0.983	1.174
	GS	-	-				0.873	0.95	1.027
12	DI	1.68	***0.0939***	8.813	4.021	3.46	1.002	1.417	1.832
	GS	-	-				0.874	1.038	1.202
13	DI	-2.29	0.0226	8.813	4.82	0.619	0.014	0.357	0.701
	GS	-	-				0.651	0.783	0.916
14	DI	-0.88	***0.3794***	8.813	4.82	1.566	0.619	0.792	0.964
	GS	-	-				0.805	0.871	0.938
15	DI	2.05	0.041	8.813	4.82	2.513	0.984	1.226	1.468
	GS	-	-				0.861	0.959	1.058
16	DI	2.49	0.0133	8.813	4.82	3.46	1.208	1.66	2.113
	GS	-	-				0.865	1.047	1.23
17	DI	-5.12	<.0001	9.598	2.422	0.619	-0.822	-0.424	-0.026
	GS	-	-				0.532	0.705	0.878
18	DI	-7.12	<.0001	9.598	2.422	1.566	-0.185	0.01	0.206
	GS	-	-				0.7	0.793	0.886
19	DI	-4.22	<.0001	9.598	2.422	2.513	0.256	0.445	0.634
	GS	-	-				0.805	0.881	0.958
20	DI	-0.43	***0.6693***	9.598	2.422	3.46	0.491	0.879	1.267
	GS	-	-				0.823	0.969	1.115
21	DI	-4.5	<.0001	9.598	3.222	0.619	-0.541	-0.18	0.18
	GS	-	-				0.562	0.714	0.866
22	DI	-6.89	<.0001	9.598	3.222	1.566	0.111	0.254	0.397
	GS	-	-				0.735	0.802	0.87
23	DI	-2.22	0.0272	9.598	3.222	2.513	0.52	0.688	0.857
	GS	-	-				0.825	0.89	0.956
24	DI	0.68	***0.4985***	9.598	3.222	3.46	0.73	1.123	1.515
	GS	-	-				0.829	0.978	1.128

Table 5.15—Continued

No	Metal type	t Diff	Pr>t	pH	lRes	w/cm	Lower CL	LSMean	Upper CL
25	DI	-3.54	0.0005	9.598	4.021	0.619	-0.277	0.063	0.404
	GS	-	-				0.585	0.723	0.862
26	DI	-4.43	<.0001	9.598	4.021	1.566	0.367	0.497	0.628
	GS	-	-				0.756	0.811	0.867
27	DI	0.32	***0.7511***	9.598	4.021	2.513	0.743	0.932	1.121
	GS	-	-				0.826	0.899	0.973
28	DI	1.68	***0.0939***	9.598	4.021	3.46	0.952	1.366	1.78
	GS	-	-				0.826	0.988	1.149
29	DI	-2.29	0.0226	9.598	4.82	0.619	-0.035	0.307	0.648
	GS	-	-				0.6	0.733	0.865
30	DI	-0.88	***0.3794***	9.598	4.82	1.566	0.572	0.741	0.91
	GS	-	-				0.756	0.821	0.885
31	DI	2.05	0.041	9.598	4.82	2.513	0.935	1.175	1.416
	GS	-	-				0.813	0.909	1.004
32	DI	2.49	0.0133	9.598	4.82	3.46	1.158	1.61	2.062
	GS	-	-				0.817	0.997	1.176
33	DI	-5.12	<.0001	10.383	2.422	0.619	-0.872	-0.475	-0.078
	GS	-	-				0.478	0.654	0.83
34	DI	-7.12	<.0001	10.383	2.422	1.566	-0.235	-0.04	0.155
	GS	-	-				0.645	0.742	0.84
35	DI	-4.22	<.0001	10.383	2.422	2.513	0.205	0.394	0.583
	GS	-	-				0.751	0.83	0.91
36	DI	-0.43	***0.6693***	10.383	2.422	3.46	0.44	0.828	1.217
	GS	-	-				0.772	0.918	1.065
37	DI	-4.5	<.0001	10.383	3.222	0.619	-0.591	-0.231	0.128
	GS	-	-				0.508	0.663	0.819
38	DI	-6.89	<.0001	10.383	3.222	1.566	0.061	0.203	0.345
	GS	-	-				0.678	0.752	0.825
39	DI	-2.22	0.0272	10.383	3.222	2.513	0.469	0.638	0.807
	GS	-	-				0.77	0.84	0.909

Table 5.15—Continued

No	Metal type	t Diff	Pr>t	pH	lRes	w/cm	Lower CL	LSMean	Upper CL
40	DI	0.68	***0.4985***	10.383	3.222	3.46	0.679	1.072	1.465
	GS	-	-				0.777	0.928	1.078
41	DI	-3.54	0.0005	10.383	4.021	0.619	-0.328	0.012	0.352
	GS	-	-				0.53	0.673	0.815
42	DI	-4.43	<.0001	10.383	4.021	1.566	0.316	0.447	0.577
	GS	-	-				0.698	0.761	0.823
43	DI	0.32	***0.7511***	10.383	4.021	2.513	0.691	0.881	1.071
	GS	-	-				0.772	0.849	0.925
44	DI	1.68	***0.0939***	10.383	4.021	3.46	0.9	1.315	1.73
	GS	-	-				0.775	0.937	1.099
45	DI	-2.29	0.0226	10.383	4.82	0.619	-0.086	0.256	0.597
	GS	-	-				0.544	0.682	0.819
46	DI	-0.88	***0.3794***	10.383	4.82	1.566	0.521	0.69	0.859
	GS	-	-				0.698	0.77	0.841
47	DI	2.05	0.041	10.383	4.82	2.513	0.884	1.125	1.365
	GS	-	-				0.76	0.858	0.956
48	DI	2.49	0.0133	10.383	4.82	3.46	1.106	1.559	2.012
	GS	-	-				0.765	0.946	1.126
49	DI	-5.12	<.0001	11.168	2.422	0.619	-0.923	-0.525	-0.128
	GS	-	-				0.421	0.604	0.786
50	DI	-7.12	<.0001	11.168	2.422	1.566	-0.289	-0.091	0.106
	GS	-	-				0.585	0.692	0.798
51	DI	-4.22	<.0001	11.168	2.422	2.513	0.151	0.343	0.536
	GS	-	-				0.691	0.78	0.868
52	DI	-0.43	***0.6693***	11.168	2.422	3.46	0.387	0.778	1.168
	GS	-	-				0.717	0.868	1.018
53	DI	-4.5	<.0001	11.168	3.222	0.619	-0.642	-0.282	0.078
	GS	-	-				0.45	0.613	0.776
54	DI	-6.89	<.0001	11.168	3.222	1.566	0.007	0.152	0.298
	GS	-	-				0.615	0.701	0.786

Table 5.15—Continued

No	Metal type	t Diff	Pr>t	pH	lRes	w/cm	Lower CL	LSMean	Upper CL
55	DI	-2.22	0.0272	11.168	3.222	2.513	0.414	0.587	0.76
	GS	-	-				0.709	0.789	0.869
56	DI	0.68	***0.4985***	11.168	3.222	3.46	0.626	1.021	1.416
	GS	-	-				0.722	0.877	1.031
57	DI	-3.54	0.0005	11.168	4.021	0.619	-0.38	-0.038	0.303
	GS	-	-				0.471	0.622	0.772
58	DI	-4.43	<.0001	11.168	4.021	1.566	0.261	0.396	0.531
	GS	-	-				0.633	0.71	0.787
59	DI	0.32	***0.7511***	11.168	4.021	2.513	0.637	0.83	1.024
	GS	-	-				0.711	0.798	0.885
60	DI	1.68	***0.0939***	11.168	4.021	3.46	0.848	1.265	1.682
	GS	-	-				0.72	0.886	1.052
61	DI	-2.29	0.0226	11.168	4.82	0.619	-0.138	0.205	0.548
	GS	-	-				0.485	0.631	0.777
62	DI	-0.88	***0.3794***	11.168	4.82	1.566	0.467	0.639	0.812
	GS	-	-				0.634	0.719	0.804
63	DI	2.05	0.041	11.168	4.82	2.513	0.83	1.074	1.318
	GS	-	-				0.7	0.807	0.914
64	DI	2.49	0.0133	11.168	4.82	3.46	1.053	1.508	1.963
	GS	-	-				0.711	0.895	1.08

The analysis of the LPML values from this research phase indicates that, as noted earlier, the effect of pH is inversely proportional to the LPML. For constant logarithm of resistivity and w/cm, increasing the pH always decreases the LPML for both ductile iron samples and galvanized samples which again is contradictory to the AWWA spec. The effect of logarithm of resistivity and the w/cm on the mean LPML of ductile and galvanized coupons and on the significance of their difference is the same at every pH level.

In order to explain the effects of w/cm and the logarithm of resistivity, the pH level of 8.813 will be examined. Figure 5.32 shows the mean LPML values and their 95 percent CI limits at w/cm of 0.619 for increasing resistivity. The difference between the mean LPML values of ductile iron and galvanized steel coupons is statistically significant and the mean LPML values of galvanized steel coupons are higher. Figure 5.33 shows the mean LPML values and their 95 percent CI limits at the second w/cm of 1.566 for increasing resistivity. The behavior of the LPML values is almost the same, the mean LPML values of galvanized steel coupons are higher, but the difference at the highest logarithm of resistivity value is statistically not significant. Figure 5.34 shows the mean LPML values and their 95 percent CI limits at the third w/cm of 2.513 for increasing resistivity. It can be seen that this level of w/cm is like a transition level. At the lowest and second level of logarithm of resistivity the mean LPML of galvanized steel is higher than the ductile iron. At the third level of logarithm of resistivity the difference is not statistically significant and at the fourth level of logarithm of resistivity the mean LPML of ductile iron coupons is significantly higher than the mean LPML value of galvanized steel coupons. Figure 5.35 shows the mean LPML values and their 95 percent CI limits at the fourth w/cm of 3.460 for increasing resistivity. For the first three levels of logarithm of resistivity differences between mean LPML values of galvanized steel and ductile iron coupons are insignificant. At the fourth level of logarithm of resistivity, the mean LPML value of ductile iron coupons is significantly higher than the galvanized steel samples.

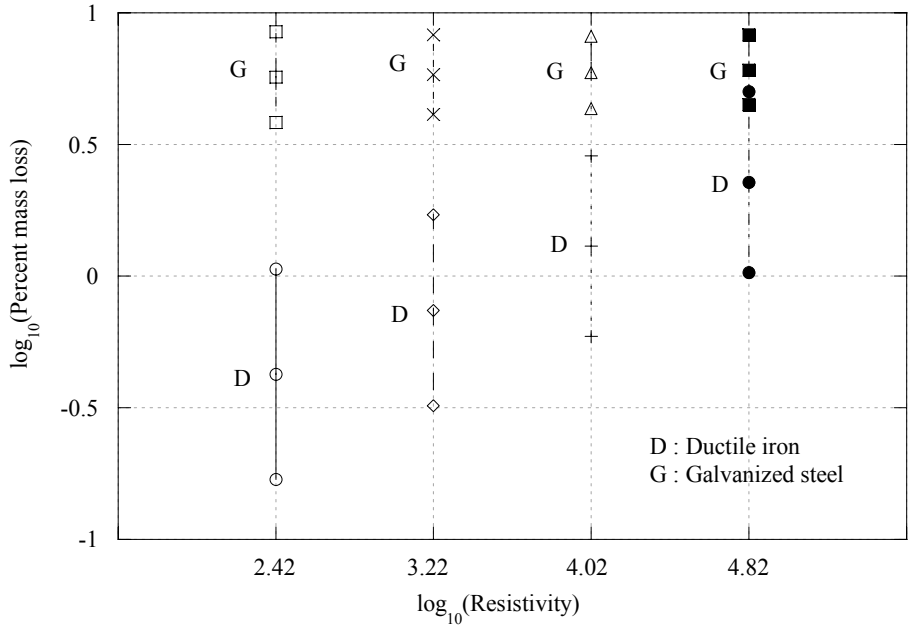

Fig. 5.32--Mean and 95% CI limits of LPML at pH=8.813 and w/cm=0.619.

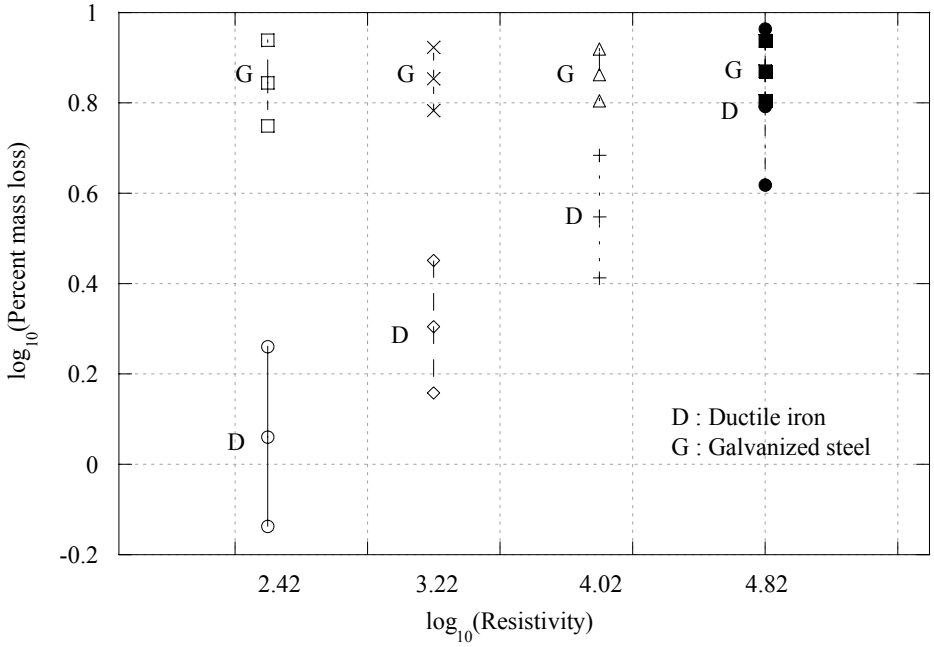

Fig. 5.33--Mean and 95% CI limits of LPML at pH=8.813 and w/cm=1.566.

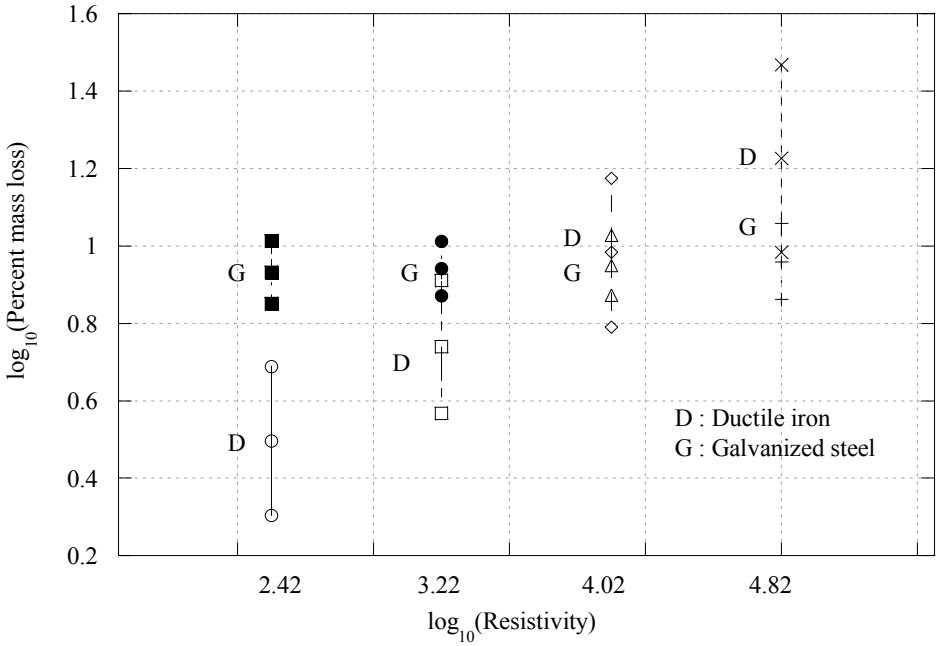

Fig. 5 34--Mean and 95% CI limits of LPML at pH=8.813 and w/cm=2.513.

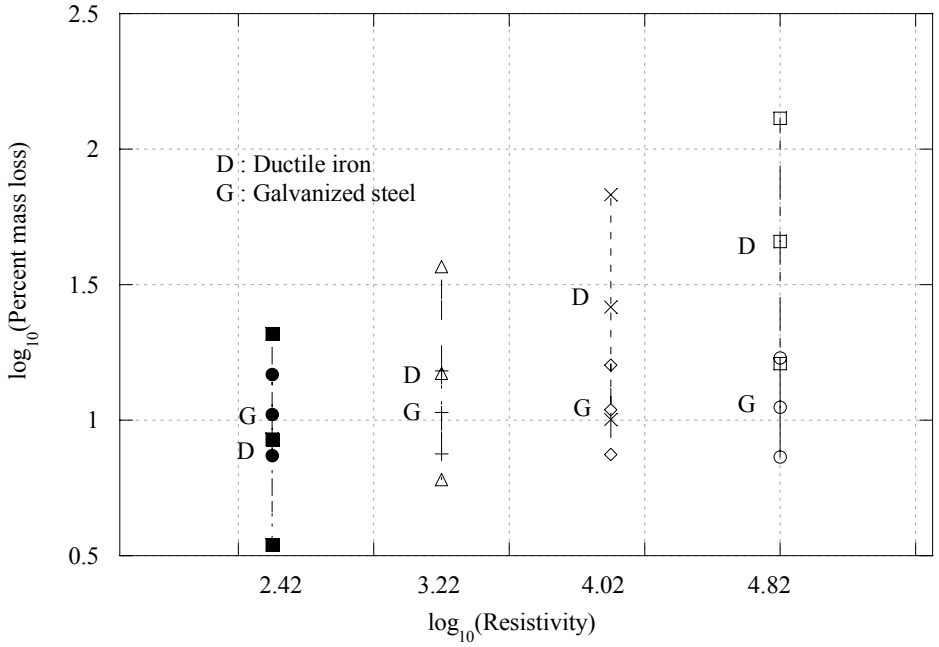

Fig. 5.35--Mean and 95% CI limits of LPML at pH=8.813 and w/cm=3.460.

As mentioned earlier the relation between the w/cm, logarithm of resistivity, and the mean LPML value of ductile iron and galvanized steel coupons is the same for all four examined pH levels, however the mean LPML values of both types of metal coupons decrease with increasing pH values. The results indicate that the mean LPML values of ductile iron coupons are lower compared to the mean LPML values of galvanized steel coupons at low w/cm and logarithm of resistivity. As the w/cm increases the difference gets smaller, and at sufficiently high values of the logarithm of resistivity the mean LPML values of ductile iron coupons significantly exceed the mean LPML values of galvanized steel coupons.

5.4.8.Interactions with Metal Type

The last three significant factors of the model were the interactions of fine aggregate type, fly ash type, and the environment with metal type. Table 5.16 shows the effects of fine aggregate type in sample groups separated by the metal type. The results indicate that the effect of fine aggregate type was significant for both metal types. Figure 5.36 shows the mean LPML values and their 95 percent CIs of samples with ductile iron coupons separated by their fine aggregate type. Samples with ductile iron coupons separated by their fine aggregate type exhibit the same relation as described earlier for the whole data. Samples containing bottom ash and sand have significantly lower mean LPML values compared to the samples without fine aggregates. Although the mean LPML value of samples with foundry sand is lower compared to the samples without fine aggregates, due to the high variability of the results, their difference is not statistically significant at the 95 percent level. Figure 5.37 shows the mean LPML values and their 95 percent CIs of samples with galvanized steel coupons separated by their fine aggregate type. For these samples, the effect of fine aggregate type is much less significant compared to the samples with ductile iron coupons. The mean LPML values of samples containing bottom ash, foundry sand, and sand are lower compared to the samples without fine aggregates; however, Tukey's comparison shows that the

differences are not significant. Samples with foundry sand still exhibit the largest variation.

Table 5.16--Effect of fine aggregate type on samples separated by metal type

Metal type	DF	Sum of Squares	Mean Square	F-Value	Pr > F
Ductile iron	3	41.68846	13.896153	14.36	<.0001
Galvanized steel	3	9.725724	3.241908	3.35	0.0193

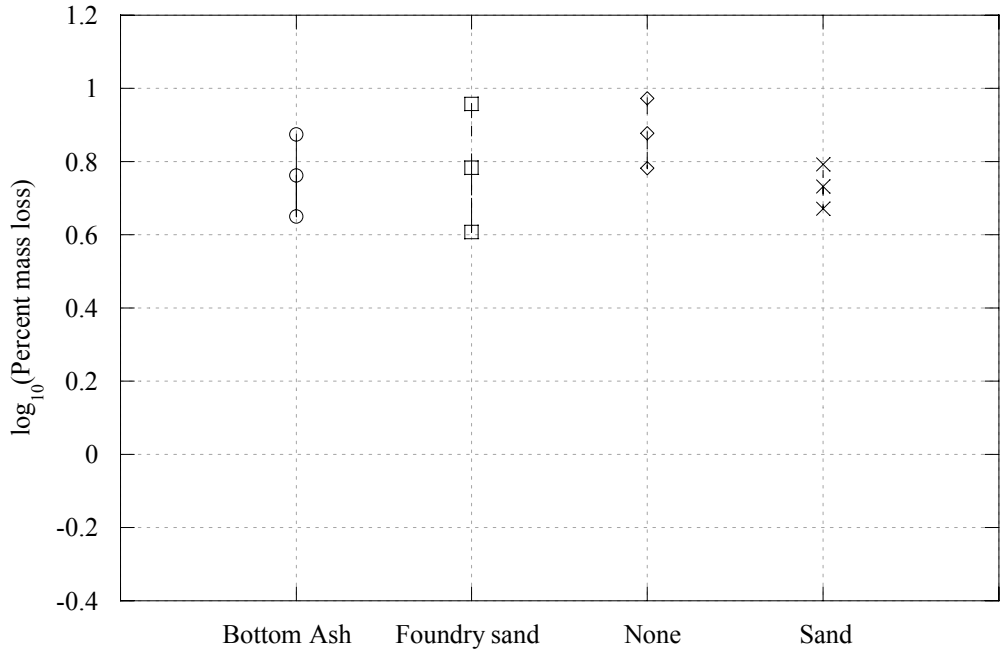

Fig. 5.36-- LPML of samples with ductile iron coupons by fly ash type.

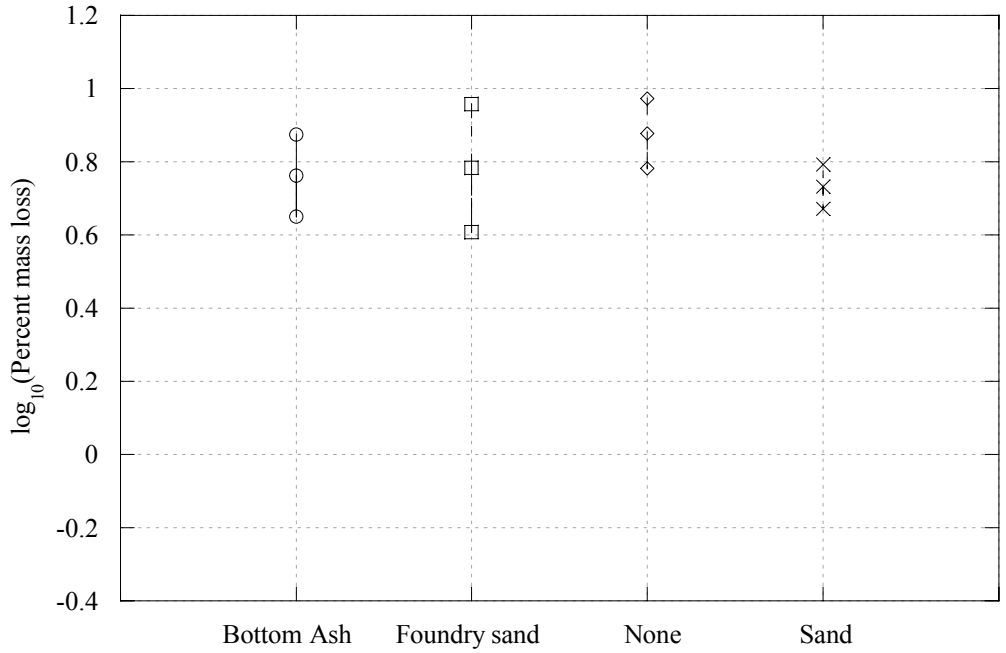

Fig. 5.37--LPML of samples with galvanized steel coupons by fly ash type.

Table 5.17 shows the effects of fly ash type in sample groups separated by the metal type. The results indicate that the effect of fly ash type was significant for both metal types. Figure 5.38 shows the mean LPML values and their 95 percent CIs of samples with ductile iron coupons separated by their fly ash type. Samples with ductile iron coupons separated by their fly ash type exhibit the same relation as described earlier for the whole data set. Samples with Class C fly ash and without fly ash have significantly lower mean LPML values compared to the samples with Class F and high carbon fly ash. Samples without fly ash have the largest variation. Figure 5.39 shows the mean LPML values and their 95 percent CIs of samples with galvanized steel coupons separated by their fly ash type. Among these samples, the samples containing Class C fly ash still have a significantly lower mean LPML value compared to the samples with Class F and high carbon fly ash. The mean LPML value of the samples without fly ash is higher compared to the samples without fly ash and ductile iron coupons. Again, the samples without fly ash exhibit the highest variability and therefore

the differences between the samples without fine aggregates and all other samples are statistically not significant.

Table 5.17--Effect of fly ash type on samples separated by metal type

Metal type	DF[1]	Sum of Squares	Mean Square	F- Value	Pr > F
Ductile iron	3	132.7558	44.25194	45.71	<.0001
Galvanized steel	3	24.28616	8.095386	8.36	<.0001

[1]Degrees of freedom

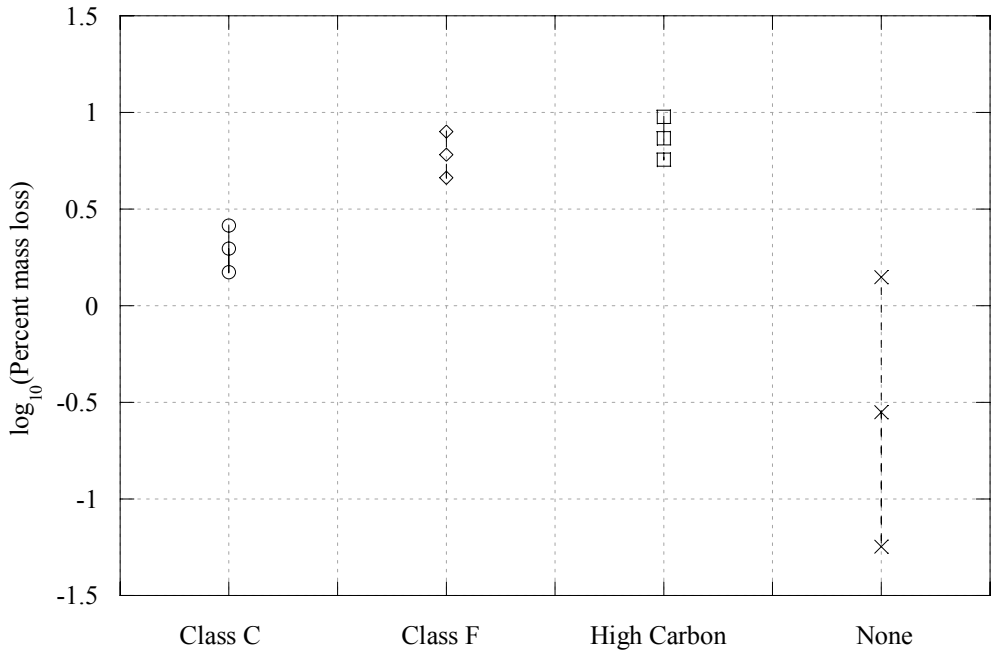

Fig. 5.38--LPML of samples with ductile iron coupons by fine aggregate.

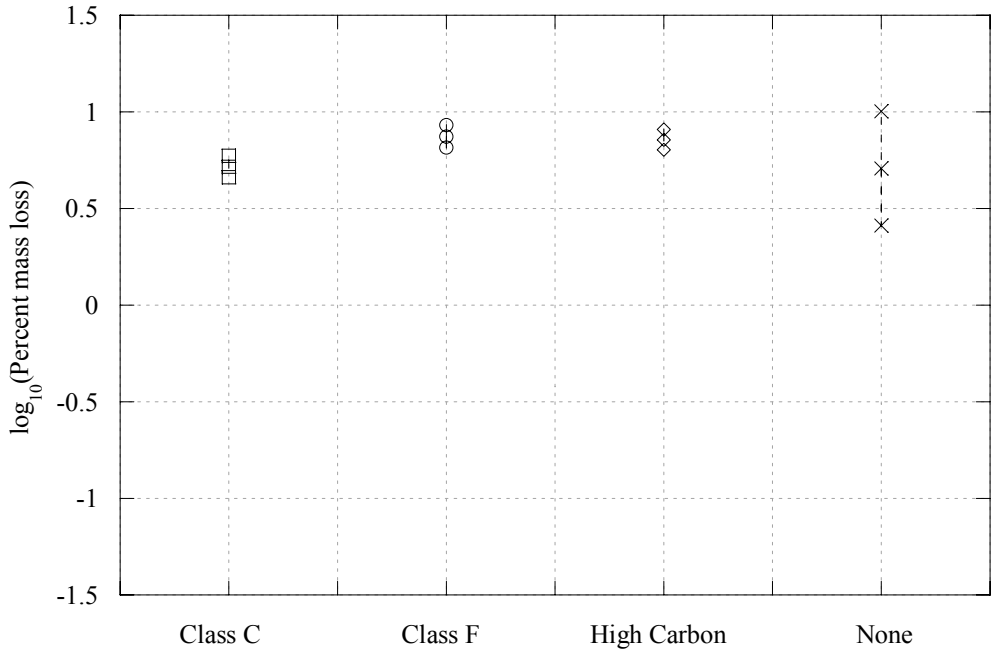

Fig. 5.39--LPML of samples with galvanized steel coupons by fine aggregate.

Table 5.18 shows the effects of the environment on the samples separated by their metal type. The results indicate that the effect of the environment was statistically significant for both samples with ductile iron coupons and samples with galvanized steel coupons. For both metal types, the samples exposed to chloride environment exhibited a higher mean LPML value compared to the samples exposed to distilled water environment. Figure 5.40 shows the mean LPML values and their 95 percent CI limits for samples separated by their metal type and environment. The difference between the samples exposed to different environments is larger for the galvanized steel samples.

Table 5.18--Effect of environment on samples separated by metal type

Metal type	DF	Sum of Squares	Mean Square	F- Value	Pr > F
Ductile iron	1	38.88268	38.88268	40.17	<.0001
Galvanized steel	1	7.205301	7.205301	7.44	0.0067

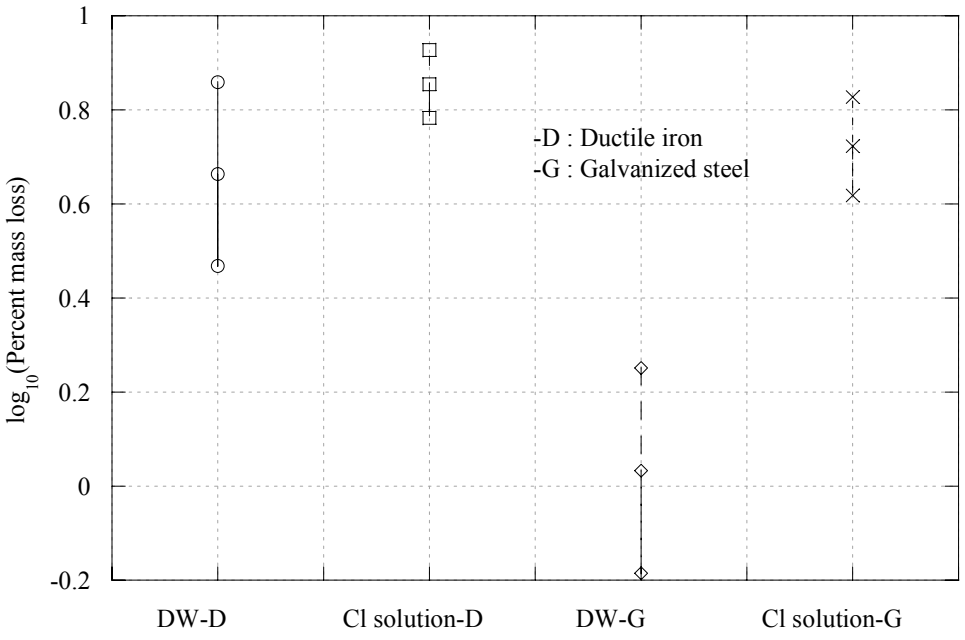

Fig. 5.40--Mean and 95% CI of LPML of samples with galvanized steel and ductile iron coupons.

5.5.Phase II – Coupled Samples

The histogram showing the percent mass of ductile iron and galvanized steel coupons embedded in CLSM and soil sections of coupled samples exposed to distilled water and chloride solution are shown in Figure 5.41.

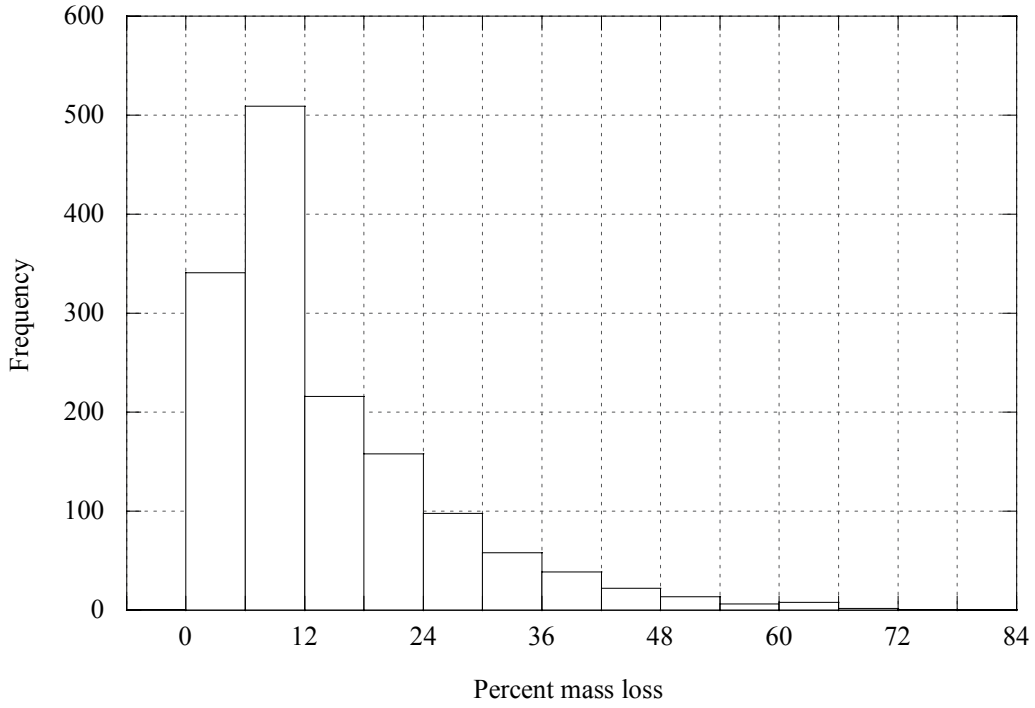

Fig. 5.41--Percent mass loss of metallic coupons.

Analyses indicates that the percent mass loss values of metallic coupons embedded in CLSM and soil were significantly correlated. The mass loss values of coupons embedded in the soil section of the coupled samples were higher compared to the mass loss values of coupons embedded in the CLSM section of samples. Table 5.19 shows the correlation coefficients and significance of correlations between the mass loss values of coupons embedded in the two sections of the coupled samples. Figure 5.42 shows the percent mass loss box plots of metallic coupons embedded in soil section and CLSM section of the coupled samples separately.

Table 5.19 Phase II coupled samples correlation table

	CLSM	Soil
CLSM	1	0.25091
(significance)		<0.0001
Soil	0.25091	1
(significance)	<0.0001	

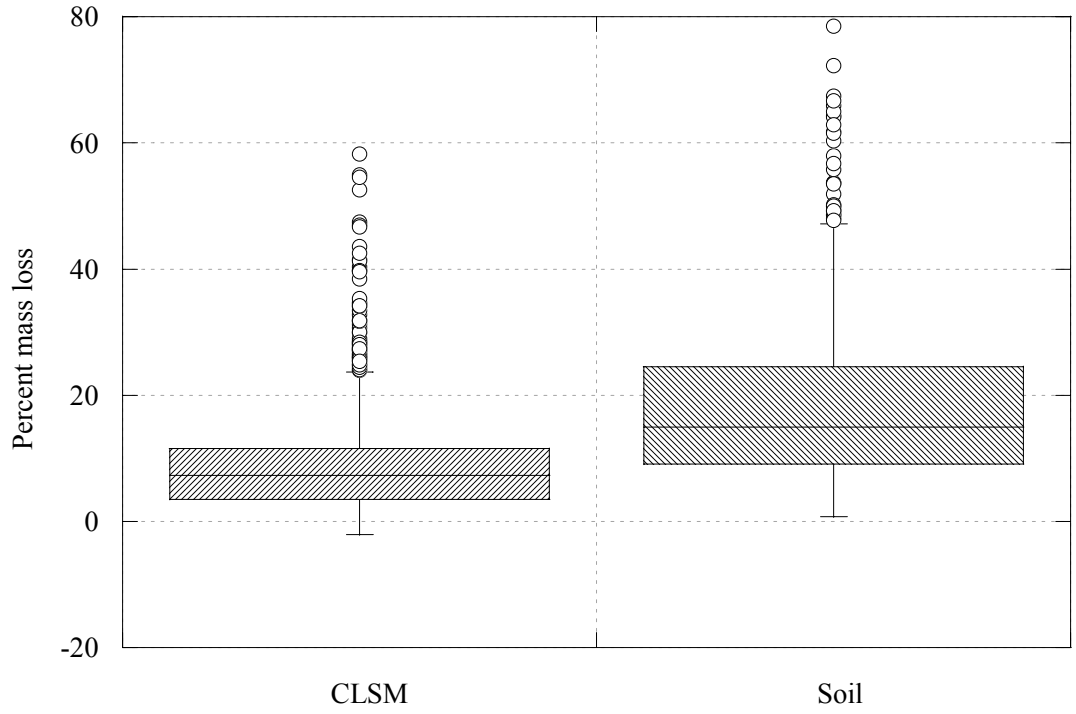

Fig. 5.42--Percent mass loss values separated by the CLSM and soil sections.

In the coupled samples the mass loss is believed to be mainly due to galvanic corrosion taking place between the metallic coupons embedded in different sections. The significantly higher mean percent mass loss values exhibited by the metallic coupons in the soil section compared to the metallic coupons embedded in the CLSM section indicate that these coupons were behaving like anodes and the coupons in the CLSM section were behaving like cathodes. Since the metallic coupons embedded in the soil sections of coupled samples represent the critical anodic areas of pipes for

corrosion damage, further statistical analysis will be performed on the percent mass loss (PML) data of these coupons.

The explanatory variables evaluated for the PML of coupons included environment, metal type, soil type, fine aggregate type, fly ash type, resistivity of CLSM, resistivity of soil, pH of CLSM, chloride content of the CLSM, and chloride content of the soil. Table 5.20 shows the correlation coefficients and the significance of the coefficients between the continuous explanatory variables and the response variable, PML. Results in Table 5.20 indicate that the percent mass loss was correlated directly to the chloride content in CLSM and soil, the w/cm and that it was indirectly correlated to the pH of CLSM and the resistivity of the soil.

Table 5. 20 Phase II variables correlation table (coupled samples)

Response PML	Chloride in CLSM	Chloride in Soil	Cement content	w/cm	pH of CLSM	R_{CLSM}[1]	R_{SOIL}[2]
Correlation	0.42829	0.41373	0.04088	0.21043	-0.125	-0.0716	-0.33512
p-value	<0.0001	<0.0001	0.2683	<0.0001	0.0007	0.0523	<0.0001

[1]Resistivity of CLSM
[2]Resistivity of Soil

Different possible models consisting of main effects and single interaction effects of the explanatory variables were applied to the data to find the best parsimonious model. Different models were compared using their adjusted coefficient of multiple determination (R^2) and root mean square values. Models were applied to the observed percent mass loss values, to their square root transformation, and to their logarithm. Trials indicated that a logarithmic transformation was more effective in decreasing the observed dependence of variability of residuals on the values of the response variable. Among the models tried for the logarithm of percent mass loss values (LPML), the below given model had the highest R^2 value and smallest root means square error;

$$\log_{10}(\%mass\,loss) = 0.97 + \alpha + \beta + \delta + \varepsilon + \gamma + \phi + \varphi + \eta + \lambda \qquad (5.7)$$

The coefficients α, β, δ, ε, and γ are assigned values for the different levels of the classification variables: environment (α), soil type (β), fine aggregate type (δ), fly ash type (ε), and metal type (γ), respectively. The coefficients ϕ, φ, η, λ are assigned values for the two factor interactions of classification variables: environment with metal type (Φ), environment with soil type (φ), fly ash type with metal type (η), and fine aggregate type with soil type (λ). Table 5.21 shows the results of the multiple regression analysis and Table 5.22 is the analysis of variance table. Table 5.21 shows that the probability of getting an F-statistic higher than the one calculated is almost zero, which indicates that the overall model was statistically significant. The analysis of variance was used to detect which model factors had an effect on the LPML that was significantly greater than the background level of noise.

Table 5. 21—Phase II coupled samples multiple regression analysis

Source	DF[1]	Sum of squares	Mean Square	F-value	Pr > F
Model	17	25.3947	1.49381	22.79	<.0001
Error	720	47.1847	0.06553		
Total	737	72.5794			

[1]Degrees of freedom

Table 5.22--Analysis of variance table (coupled)

Source	DF[1]	Sum of squares	Mean Square	F-value	Pr > F
environment	1	14.441	14.441	220.36	<.0001
soil	1	1.740	1.740	26.55	<.0001
metal type	1	0.086	0.086	1.31	0.2531
fine aggregate	3	1.965	0.655	10	<.0001
fly ash	3	1.883	0.628	9.58	<.0001
environment · metal type	1	0.808	0.808	12.33	0.0005
environment · soil	1	0.646	0.646	9.85	0.0018
metal type · fly ash	3	0.528	0.176	2.69	0.0456
soil · fine aggregate	3	0.719	0.240	3.66	0.0123

[1]Degrees of freedom

The probability values shown in Table 5.22 indicate that all of factors included in the model had statistically significant effects on the LPML values of metallic coupons except the metal type. However, since two factor interactions of metal type with other factors is significant, this factor was left in the model for hierarchical completeness.

Examination of the studentized residuals indicated that there were two points with a studentized residual greater than 3. This indicates that these two points were outliers. Calculation of Dffit statistics indicated that none of the data points was an influential data point. Figures 5.43 and 5.44 show the residuals plotted against the predicted values of LPML and against their normal quantiles. Although the distribution of residuals in Figure 5.44 exhibits some skewness on the left side, the normality assumption of residuals is acceptable.

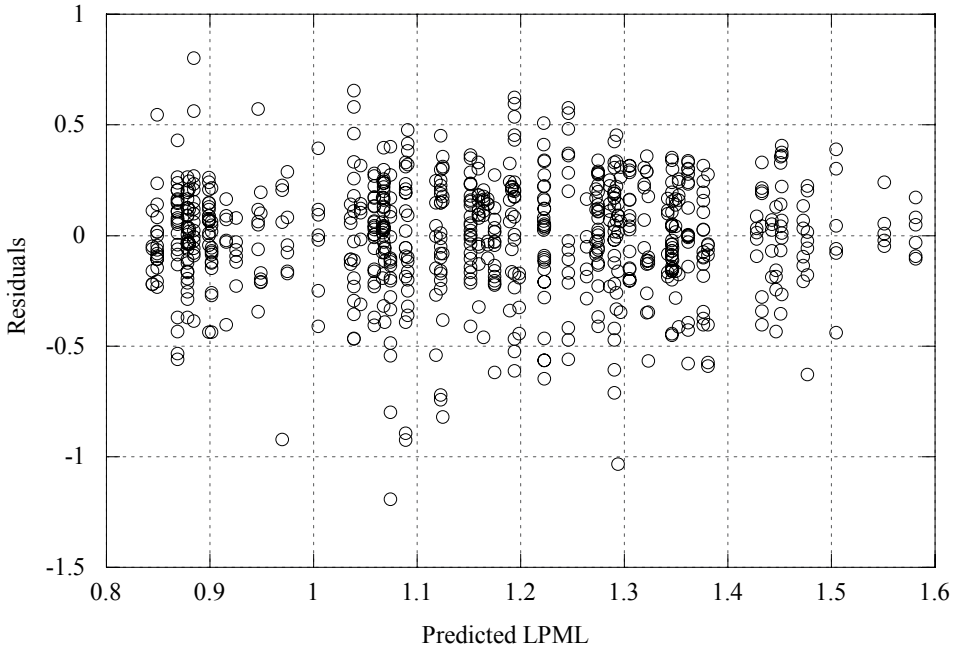

Fig. 5.43--Residuals plotted against the predicted LPML values.

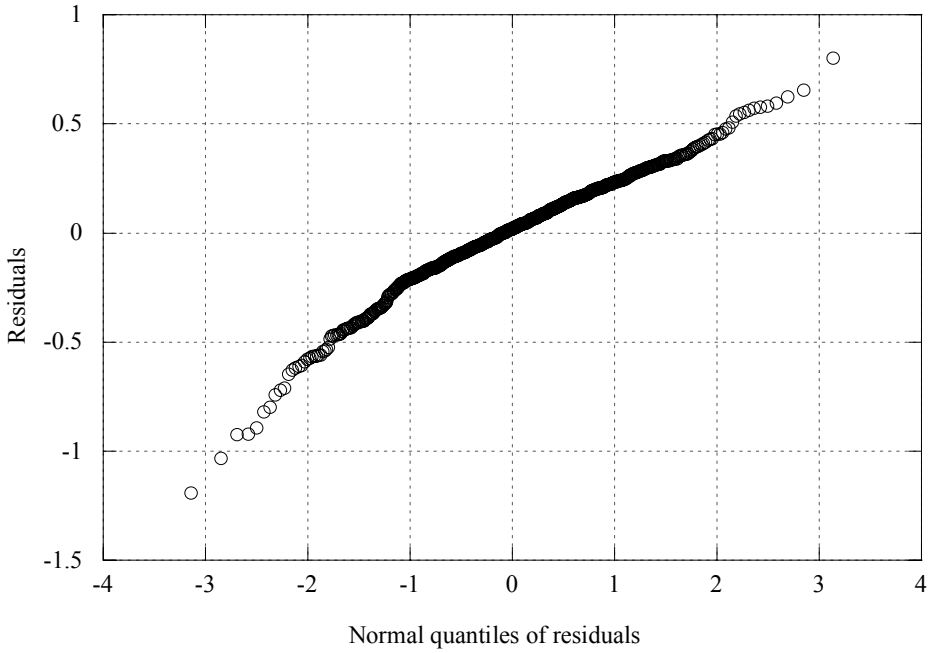

Fig. 5.44--QQ plot of residuals.

Table 5.23 shows the values of coefficients and their standard errors. The value of the coefficients not shown for a level of its variable in the table is zero.

Table 5. 23--Parameter estimates and standard errors

Parameter		Estimate	Standard error
Intercept		0.975	0.052
Environment			
	Chloride	0.406	0.032
Soil type			
	Clay	0.190	0.030
Metal type			
	Ductile	0.185	0.071
Fine aggregate			
	Bottom ash	0.047	0.041
	Foundry sand	0.167	0.042
	None	-0.005	0.056
Fly ash type			
	Class C	-0.106	0.053
	Class F	-0.090	0.055
	High Carbon	-0.076	0.054
Environment & metal type			
Chloride	Ductile	-0.133	0.038
Environment & soil type			
Chloride	Clay	-0.118	0.038
Metal type & fly ash type			
Ductile	Class C	-0.175	0.075
Ductile	Class F	-0.220	0.078
Ductile	High Carbon	-0.183	0.077
Soil type & fine aggregate			
Clay	Bottom ash	0.158	0.058
Clay	Foundry sand	-0.067	0.058
Clay	None	-0.065	0.075

Figure 5.45 shows the observed percent mass loss values against the percent mass loss values obtained from the model. The overall model is statistically significant and the R^2 is 35 percent (R=59 percent). An R value ranging from about 40 percent to 60 percent may be regarded as indicating a moderate degree of correlation (Franzblau 1958). This correlation coefficient is lower compared to the 82 percent obtained for the model established to estimate the corrosion of metallic coupons that were completely embedded in CLSM (uncoupled samples). This indicates that although the investigated CLSM properties and environment factors were good indicators for the amount of corrosion of coupons embedded completely in CLSM, a model built solely from these variables cannot be used to estimate the corrosion of metallic coupons with great accuracy if they are galvanically coupled.

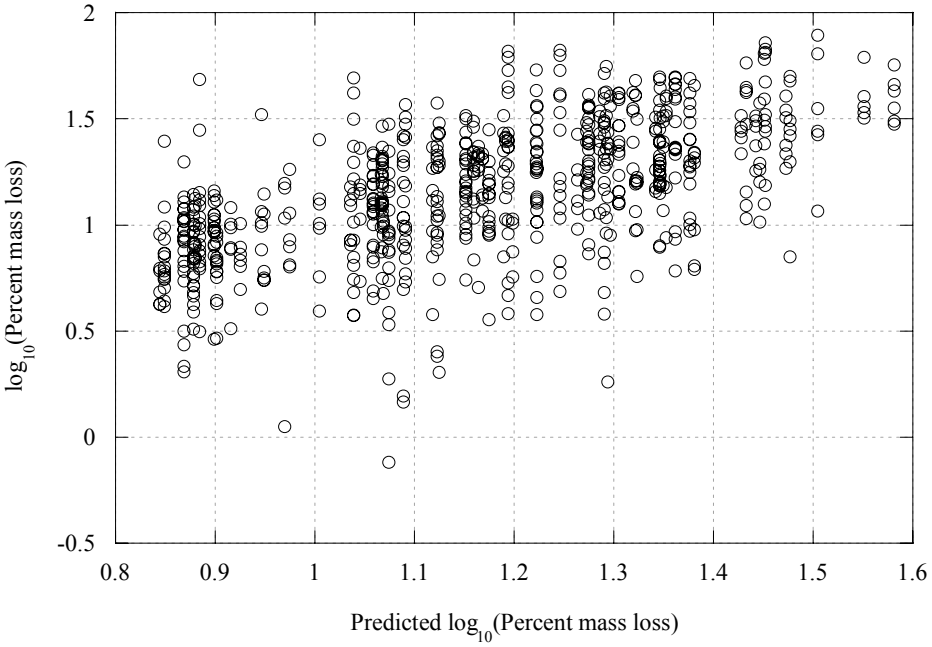

Fig. 5.45--Predicted vs. observed LPML.

The model shows that the type of environment is a statistically significant factor. Tukey's comparison at 95 percent level of the mean LPML values for samples exposed to different environments indicates that the difference of means is statistically significant. The samples exposed to chloride environment exhibit higher mean LPML compared to the samples exposed to distilled water. Table 5.24 shows the comparison results and the 95 percent confidence intervals for the mean LPML values of samples exposed to both environments.

Table 5.24--Comparison and confidence intervals of mean LPML values

Environment	Mean LPML	t-Value	Pr > |t|	95% CI	
				Lower limit	Upper limit
Chloride	1.358	14.84	<.0001	1.323	1.394
Distilled water	1.078			1.042	1.114

Figure 5.46 shows the LPML box plots of the metallic coupons separated by the environment type, and soil type.

There could be two reasons for higher corrosion in the chloride environment. First, previous studies have shown that the existence of chlorides above a threshold level in the vicinity of the steel surface can disturb the passivation of steel surface and increase corrosion (Tuutti 1982). This could be increasing the corrosion on the coupon surface. Another explanation could be found in the significant correlation between the environment type and the logarithm of resistivity of CLSM and soil. The CLSM and soil samples exposed to the chloride environment exhibited significantly lower resistivity values that may increase the galvanic corrosion between the embedded coupons of coupled samples by increasing the flow of ions between the coupons. Figure 5.47 shows the logarithm of resistivity box plots for soils and CLSM samples exposed to the different environments.

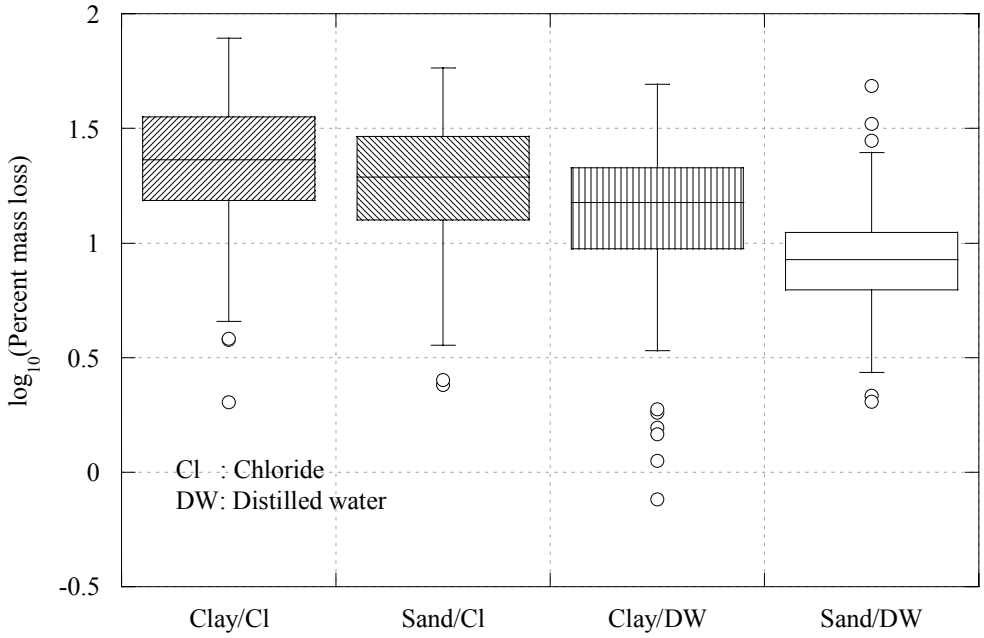

Fig. 5.46--LPML box plots separated by soil type and environment.

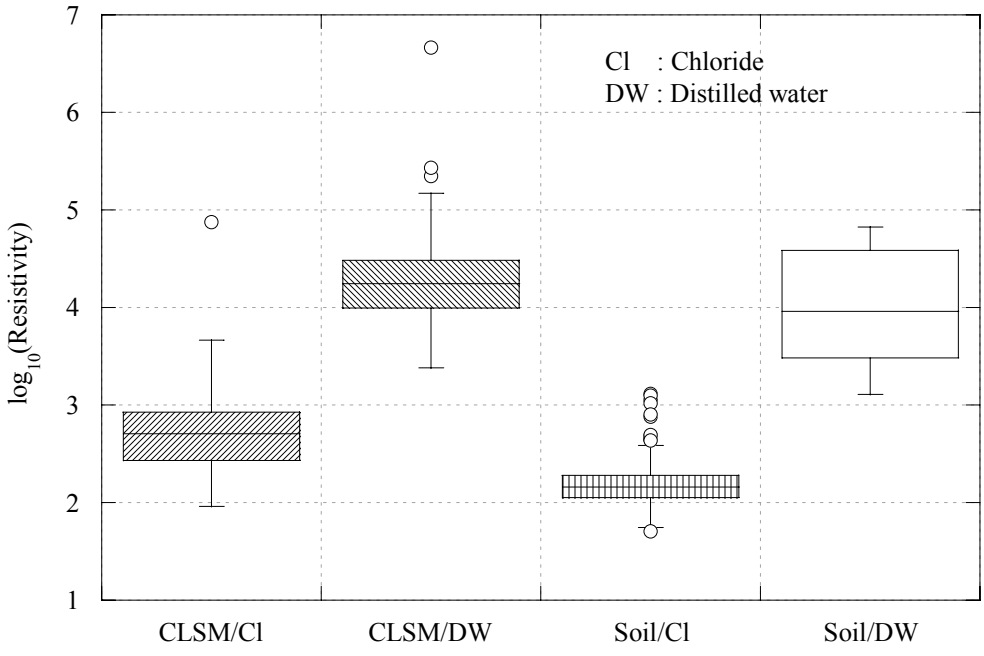

Fig. 5.47--Logarithm of resistivity of CLSM and soil separated by environment.

The analysis results in Table 5.25 also show that both the logarithm of CLSM resistivity and the logarithm of soil resistivity values were negatively correlated to the LPML values and the correlations were statistically significant. The table also indicates that there was a great direct and significant correlation between the logarithm of CLSM resistivity values and the logarithm of soil resistivity values and both were significantly and indirectly correlated to the chloride content measured in CLSM and soil samples. This indicates that based on the environment the resistivity of CLSM and soils decreased with increasing chloride content and the logarithm of percent mass loss increased with decreased logarithm of resistivity.

Table 5.25—Phase II correlation of model variables (coupled samples)

	ClC	ClS	LPML	lresC	lresS
ClC[1]	1	0.77148	0.42256	-0.8598	-0.7863
significance		<0.0001	<0.0001	<0.0001	<0.0001
ClS[2]	0.77148	1	0.37091	-0.7134	-0.7437
significance	<0.0001		<0.0001	<0.0001	<0.0001
LPML	0.42256	0.37091	1	-0.4235	-0.4596
significance	<0.0001	<0.0001		<0.0001	<0.0001
lresC[3]	-0.8598	-0.7134	-0.4235	1	0.81788
significance	<0.0001	<0.0001	<0.0001		<0.0001
lresS[4]	-0.7863	-0.7437	-0.4596	0.81788	1
significance	<0.0001	<0.0001	<0.0001	<0.0001	

[1]ClC : Chloride content in CLSM, [2]ClS : Chloride content in soil, [3]lresC : logarithm of CLSM resistivity, [4]lresS : logarithm of soil resisitivity,

One other factor that was shown to have a positive correlation with the response was the w/cm. Table 5.26 shows that w/cm has a significant but small correlation with the chloride content in CLSM and a negative correlation with the logarithm of resistivity of CLSM.

Table 5.26--Correlation table with water cementitiouis materials ratio

	ClC[1]	ClS[2]	lresC[3]	lresS[4]
w/cm	0.08437	-0.0038	-0.1212	0.00888
significance	0.022	0.9184	0.001	0.8098

[1]ClC : Chloride content in CLSM, [2]ClS : Chloride content in soil, [3]lresC : logarithm of CLSM resistivity, [4]lresS : logarithm of soil resisitivity

The Tukey's comparison at 95 percent level of mean LPML values of samples embedded in different soil types indicates that the means were significantly different and the mean LPML of coupons embedded in clay was higher. Table 5.27 shows the mean LPLM values for soil types, their comparison, and their 95 percent CI limits. The box plots of the LPML values of coupons separated by the soil type and environment were shown in Figure 5.46. The figure also shows that the mean LPML values of coupons embedded in clay were higher compared to the coupons embedded in sand in both environments.

Table 5.27--Comparison of mean LPML by soil type

Soil type	mean LPML	t Value	Pr > |t|	95% Confidence limits	
				Lower	Upper
Clay	1.28641076	5.15	<.0001	1.246057	1.326765
Sand	1.14938586			1.109401	1.18937

The model also indicates that the interaction of soil type and environment was a significant factor. Figure 5.48 shows the mean LPML values and their 95 percent CI's for different soil types exposed to different environments. The slopes of the lines indicate that the magnitude of the effect of changing the soil type was different in different environments, i.e., the soil type and environment type interaction was significant. Additionally, the analysis shown in Table 5.28 indicates that the effect of

soil type was significant for samples in both environments (probabilities of F values calculated for the comparisons are close to zero).

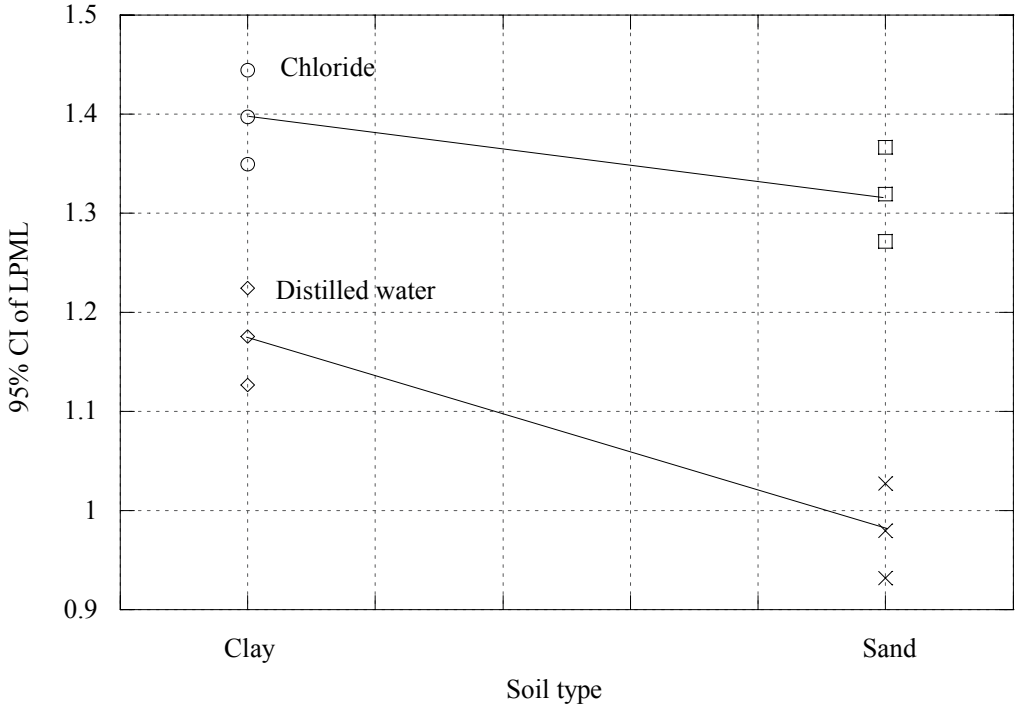

Fig. 5.48--Interaction effect of soil and environment on LPML.

Table 5.28 Effect of soil type in different environments

Environment	DF[1]	Sum of squares	Mean Square	F-value	Pr > F
Chloride	1	0.380	0.380	5.8	0.0163
Distilled water	1	2.330	2.330	35.56	<.0001

[1]Degrees of freedom

Analysis indicates that the resistivity values of clay samples were significantly lower compared to the sand samples exposed to both environments. This could be one

of the reasons why the coupled coupons embedded in clay were corroding more than the coupled coupons embedded in sand. Figure 5.49 shows the logarithm of soil resistivity box plots for coupons separated by soil type and environment. The figure clearly shows that even though the environment type had the main effect on the soil resistivity, the mean resistivity values of sand samples were higher compared to the clay samples exposed to the same environment

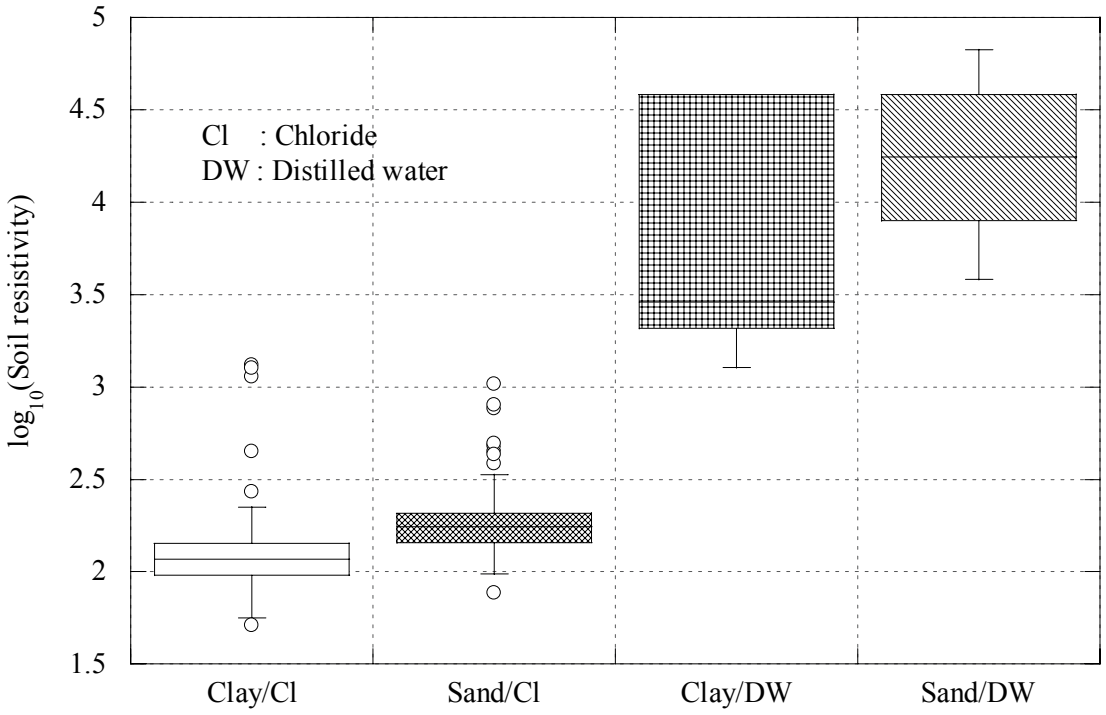

Fig. 5.49--Logarithm of soil resistivity separated by soil and environment type.

The observed lower mean pH values in clay compared to sand exposed to the same environment could also be another cause for the higher mean LPML values of coupons embedded in clay. The 95 percent CI of pH values obtained from the testing of randomly selected soil samples were 9.33 ± 0.14, 8.08±0.19, 8.17±0.16, and 7.95±0.29 for sand exposed to distilled water, clay exposed to distilled water, sand exposed to

chloride solution, and clay exposed to chloride solution, respectively. The pH value of the same sand was measured as 7.46 before it was used in testing. The observed higher pH values measured from sand samples after they were used in coupled samples exposed to different environments could be due to the interaction of pore solutions at the CLSM/soil interface of the coupled samples.

Metal type was one of the factors included in the model. Although analysis of variance indicated that this factor was not significant, it had statistically significant interactions with other factors. Table 5.29 shows the mean LPML values for metal types, their comparison, and their 95 percent CI limits. Figure 5.50 shows the LPML box plots of coupons separated by the metal type.

Table 5.29 LPML comparison by metal type

Metal type	mean LPML	t Value	Pr > |t|	95% Confidence limits	
				Lower	Upper
Ductile	1.205	-1.14	0.2531	1.167	1.243
Galvanized	1.231			1.194	1.268

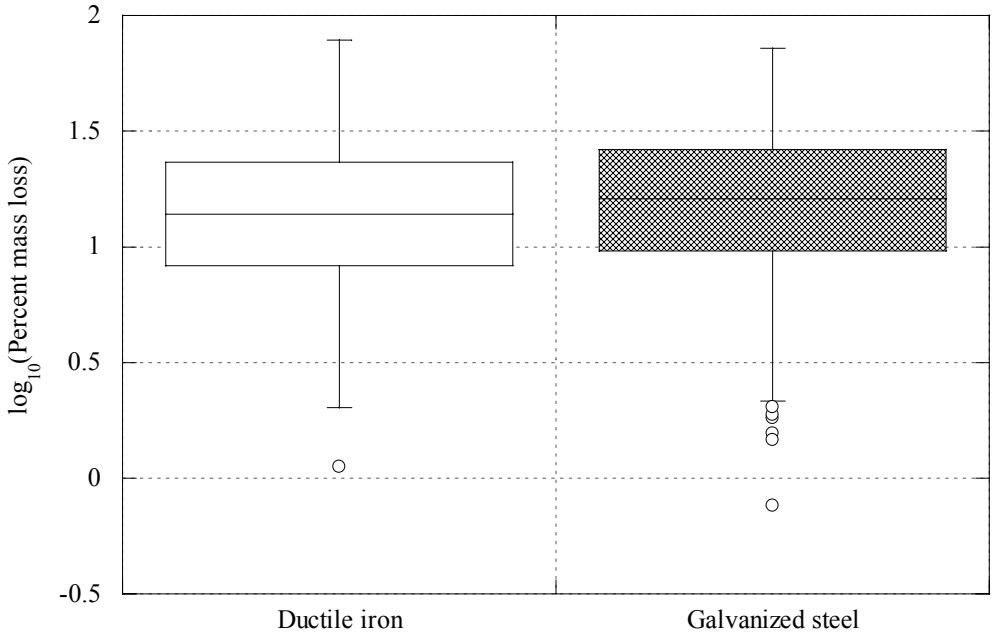

Fig. 5.50--LPML box plots separated by metal type.

The first of two significant interactions of the metal type is the interaction with environment. Figure 5.51 shows the mean LPML values and their 95 percent CIs for different metal types exposed to different environments. Table 5.30 shows the test results for the effect of sample type in different environments. Results indicate that although the effect of metal type was not significant in distilled water, it had a significant effect among the samples exposed to chloride solution. The galvanized steel samples exhibited a statistically higher mean LPML value compared to the ductile iron samples in chloride environment.

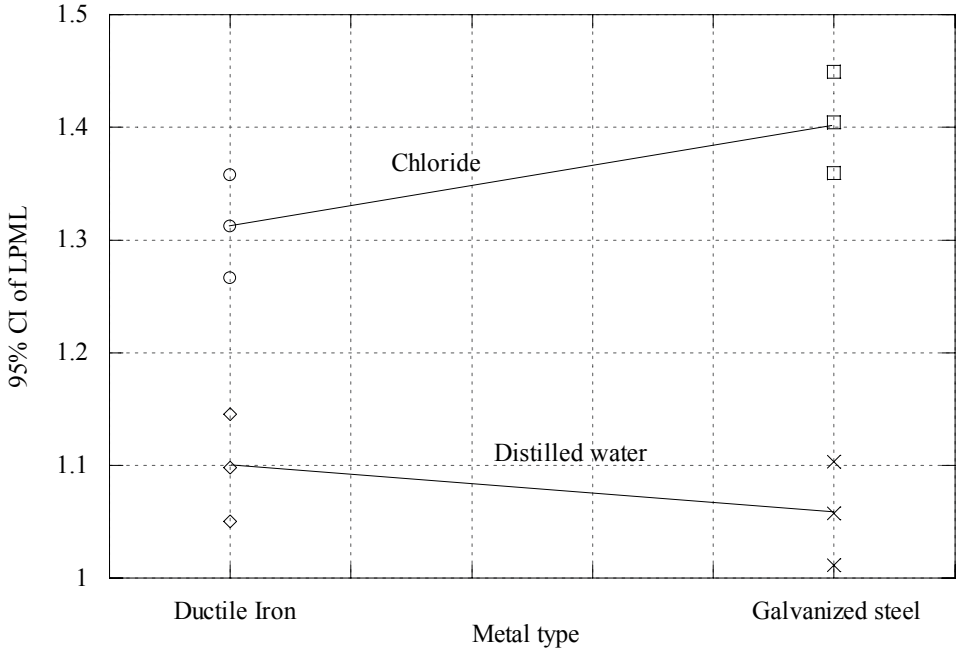

Fig. 5.51--95% CI of LPML separated by metal type and environment.

Table 5.30 Effect of metal type in different environments

Environment	DF	Sum of squares	Mean Square	F Value	Pr > F
Chloride	1	0.665	0.665	10.14	0.0015
Distilled water	1	0.118	0.118	1.8	0.18

Galvanized steel has zinc-iron alloy layers on the base steel with a relatively pure outer layer of zinc. The zinc coating should protect the steel surface from any direct contact with the environment by oxidizing and providing a physical barrier. However, research on galvanized steel cooling towers indicated that the basic zinc carbonate barrier will form on galvanized steel surfaces within eight weeks of operation with water of neutral pH (6.5-8.0). If the galvanized steel is exposed to water with pH greater than 8 for an extended period of time before the zinc carbonate barrier can form, this can lead to the formation of a white, waxy, porous adherent deposit (white rust) which offers no

protection (Marley Manual 92-1184A). The Association of Water Technologies (AWT) also reported that during the initial exposure of galvanized steel to water, the pH should be controlled between 6.5 and 8, and chlorides and sulfates should be maintained at levels not corrosive to steel to allow for the formation of a protective oxide layer (AWT 2002). The high alkalinity of CLSM and soil environments (8 or greater) and the observation of white, waxy layer during the cleaning of galvanized steel coupons in this study may indicate that the observation of high LPML values of galvanized steel coupons in uncoupled and coupled conditions was due to the disruption of protective oxide layer formation on the galvanized steel surface (Figure 5.52).

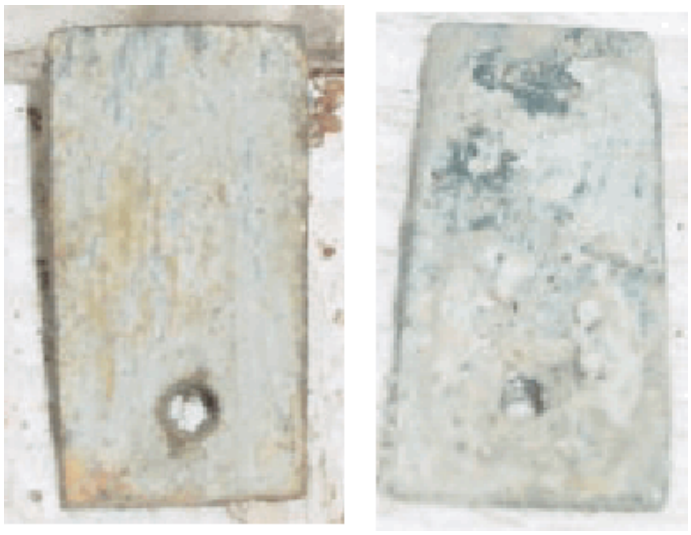

Fig. 5.52--Corroded galvanized steel samples extracted from CSLM.

The examination of the LPML values of the metallic coupons in coupled samples with different types of fly ash showed that there were two statistically different sets. The mean LPML value of the coupled samples that contained no fly ash in their CLSM section was statistically significantly higher compared to the rest of the samples (i.e., fly ash reduced the corrosion susceptibility of metallic materials). The 95 percent CIs of the

mean LPML values for samples with and without fly ashes are shown in Table 5.31. Figure 5.53 shows the LPML box plots separated by the fly ash type.

Table 5.31--Mean LPML values and 95% CI for samples with and without fly ashes

Fly ash	mean LPML	95% CI limits	
		Lower	Upper
Class C	1.164	1.127	1.202
Class F	1.158	1.114	1.201
High Carbon	1.191	1.151	1.232
None	1.358	1.284	1.432

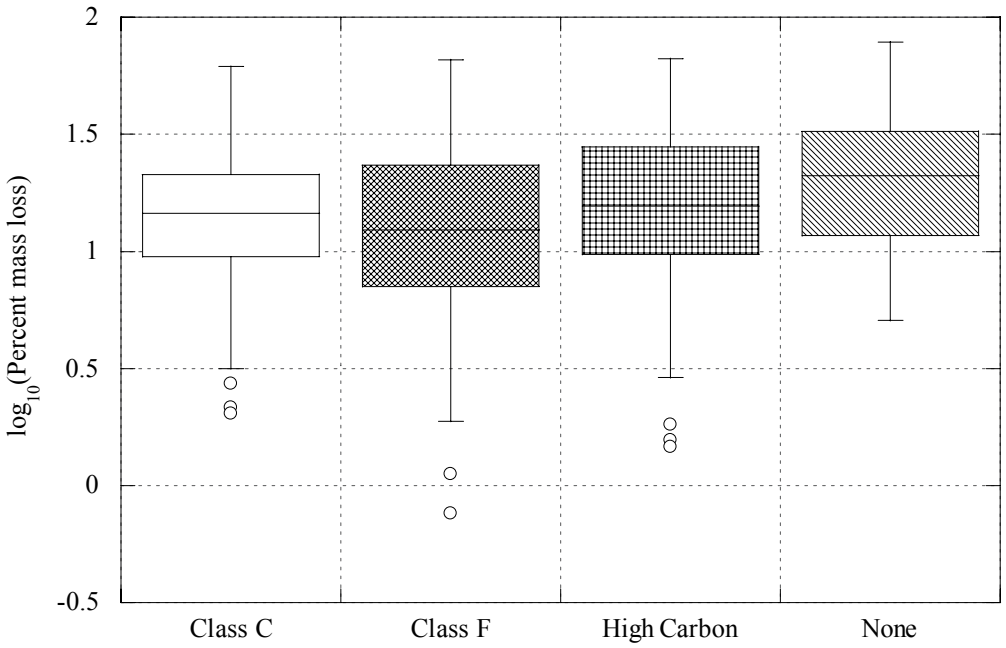

Fig. 5.53--LPML box plots separated by fly ash type.

The lower mean LPML values of the samples containing fly ash compared to the samples without fly ash are contradictory to the results obtained from the Phase II

uncoupled samples. The results obtained from the uncoupled samples indicated that the samples with Class F and high carbon fly ashes had significantly higher mean LPML values compared to the samples without fly ash and the difference between the mean LPML values of samples without fly ash and samples with Class C fly ash was not statistically significant. The reason of the lower mean LPML values among the coupled samples could be the densification of the CLSM structure of the samples containing fly ashes.

The second significant interaction of metal type was with fly ash. Table 5.32 shows the results of the analysis of the effect of fly ash on different metal types and it indicates that the effects of fly ash were not significant for the galvanized steel samples. Figure 5.54 shows the 95 percent CI of LPML for ductile iron samples separated by fly ash type and Figure 5.55 show the 95 percent CI for galvanized steel samples separated by fly ash type. The figures show the general effects of fly ash were observed for both groups, i.e., samples with fly ash has lower mean LPML values compared to samples without fly ash. However, the differences were only significant for the ductile iron samples.

Table 5.32--Significance of fly ash effects for different metal types

Metal type	DF	Sum of squares	Mean Square	F Value	Pr > F
Ductile iron	3	2.082	0.694	10.59	<.0001
Galvanized steel	3	0.281	0.094	1.43	0.2328

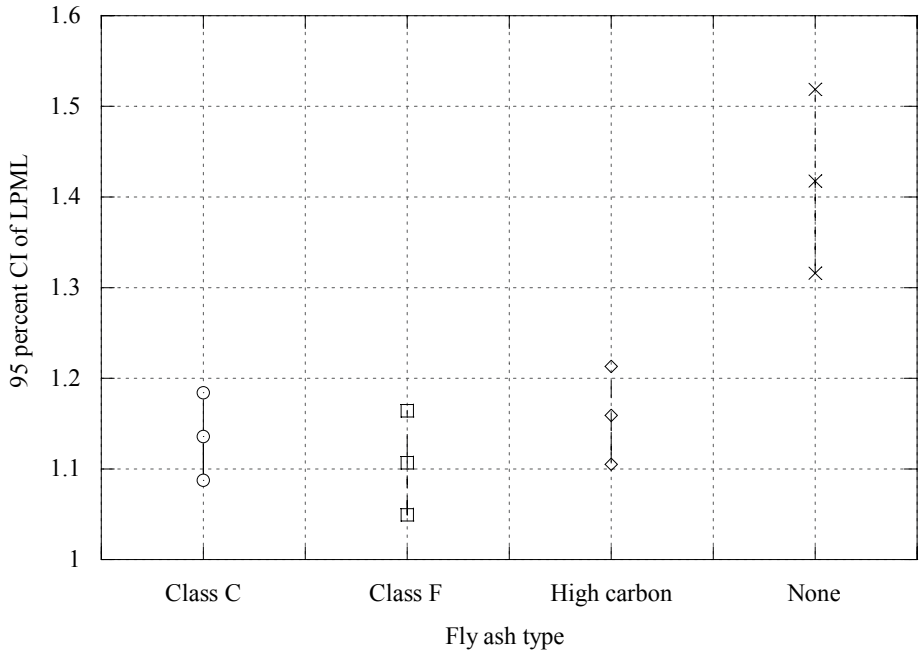

Fig. 5.54--LPML confidence intervals for ductile iron samples separated by fly ash.

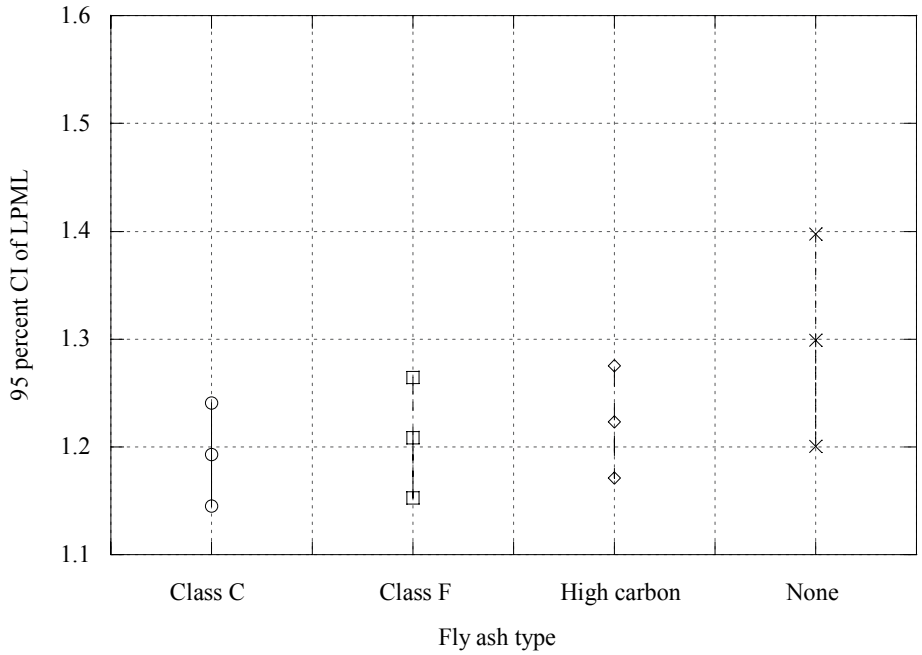

Fig. 5.55--LPML confidence intervals for galvanized steel samples separated by fly ash.

Fine aggregate type and the interaction between fine aggregate type and soil type were the last significant factors included in the model. Table 5.33 shows the mean LPML values of samples containing different fine aggregates and their 95 percent CIs. Analysis indicates that there were two separate groups. Samples with bottom ash or foundry sand exhibited significantly higher LPML values compared to the samples with sand or without fine aggregates. Figure 5.56 shows the box plots of LPML separated by fine aggregate type.

Table 5.33--Mean LPML values and 95% confidence limits by fine aggregates

Fine aggregate	mean LPML	95% Confidence limits	
		Lower	Upper
Bottom ash	1.288	1.230	1.346
Foundry sand	1.296	1.238	1.354
None	1.125	1.045	1.205
Sand	1.162	1.137	1.187

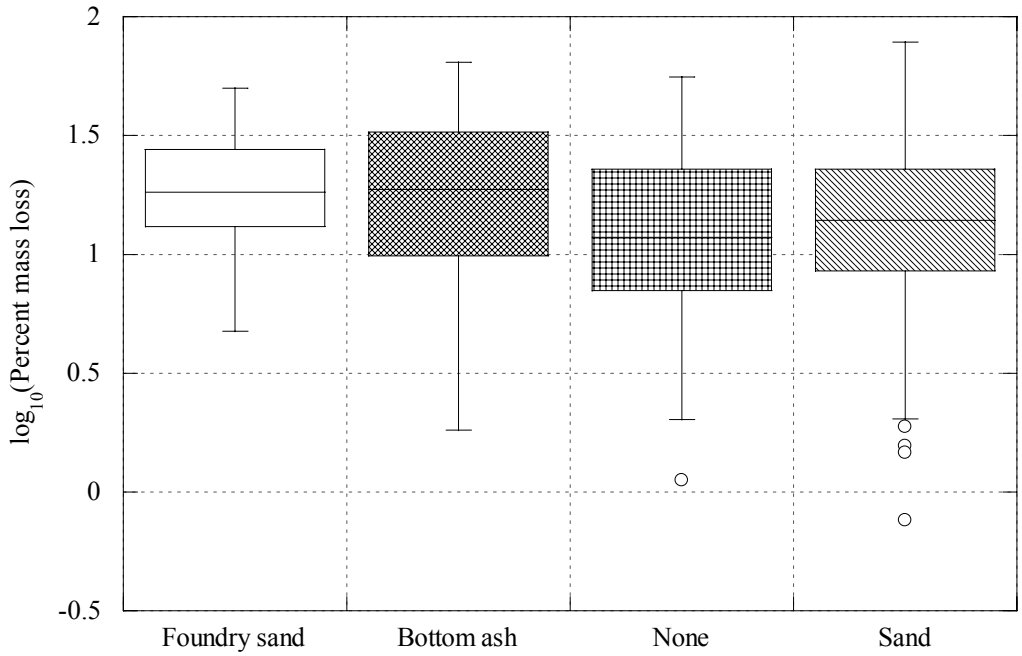

Fig. 5.56--LPML box plots separated by fine aggregate.

Results in Table 5.34 show that the effects of fine aggregates were significant for both soil types. Although in general the mean LPML values of samples with foundry sand or bottom ash were higher compared to the samples with sand or without fine aggregates for both soil types samples with bottom ash exhibited the highest mean LPML value for clay samples. For sand samples foundry sand had a significantly higher mean LPML value compared to the all other samples which had similar mean LPML values. Figures 5.57 and 5.58 show the 95 percent confidence intervals of LPML values separated by the fine aggregate type for clay and sand samples, respectively.

Table 5.34--Significance of fine aggregate effects for different soil types

Soil type	DF	Sum of squares	Mean Square	F Value	Pr > F
Clay	3	1.797	0.599	9.14	<.0001
Sand	3	1.035	0.345	5.27	0.0013

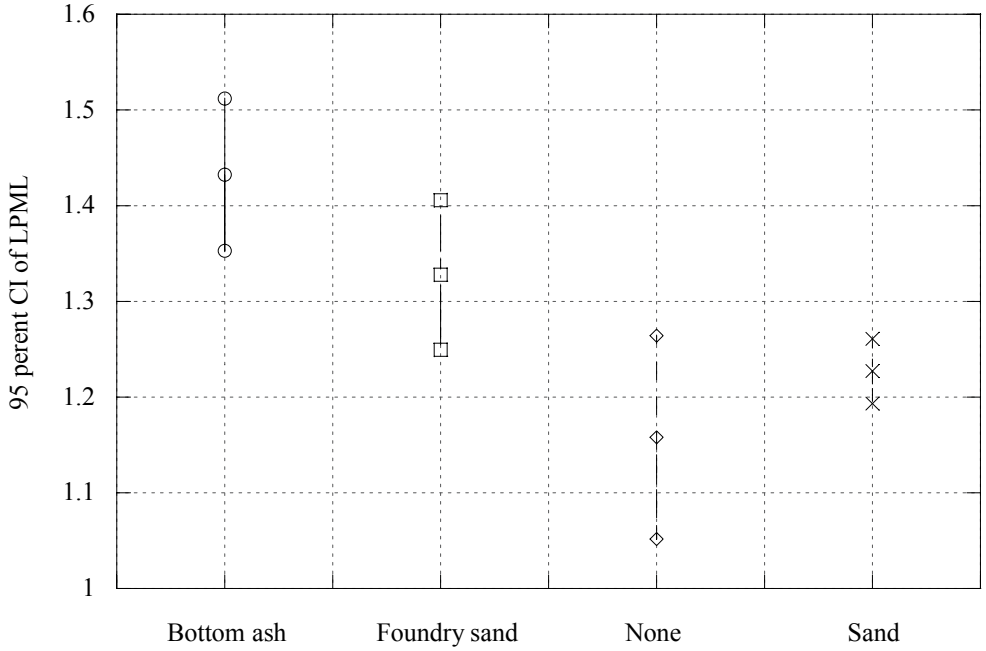

Fig. 5.57--95% CIs of LPML values separated by fine aggregates for clay samples.

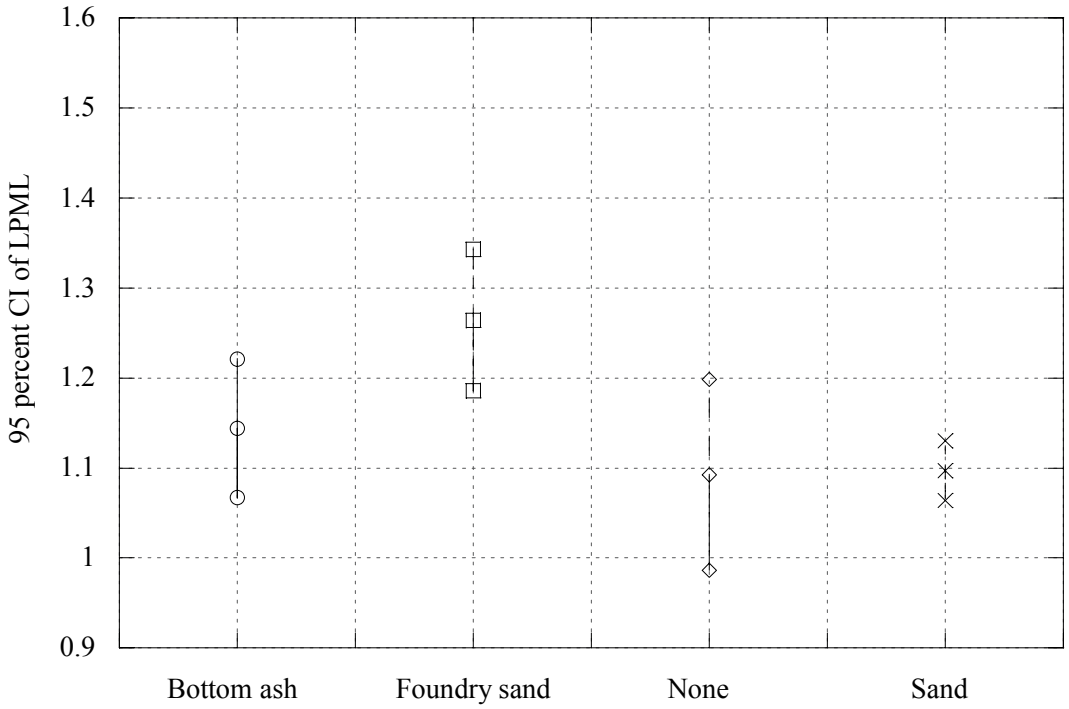

Fig. 5.58--95% CIs of LPML values separated by fine aggregates for sand samples.

In this chapter the data obtained from the uncoupled and coupled samples from both phases and its statistical analysis were presented. Statistically significant factors affecting the corrosion of galvanized steel and ductile iron coupons in different environments were determined. Through data analysis empirical models were obtained to estimate the logarithm of percent mass loss values of metallic coupons embedded in CLSM and exposed to different environments. In Chapter VI these empirical models will be used to derive service life models for the galvanized steel and ductile iron pipes embedded in CSLM.

CHAPTER VI

SERVICE LIFE OF GALVANIZED AND DUCTILE IRON PIPES EMBEDDED IN CSLM

6.1.Introduction

The deterioration of the aging pipeline infrastructure and the increasing need for repair or rehabilitation of pipelines is a critical issue for many state agencies. Although many state agencies invest a significant amount of their budget into pipeline systems every year, there are no standard guidelines used to select materials for new pipeline construction and to select appropriate repair or rehabilitation methods.

According to a survey among transportation agencies performed by NCHRP in 2002, only 7 percent of the agencies had established guidelines to select pipe rehabilitation methods and 27 percent of the agencies replied that they considered different factors such as hydraulic capacity, traffic volume, height of fill, service life, and risk assessment in making pipe rehabilitation decisions (NCHRP 2002). Of these agencies, 24 percent used service life estimates.

To select a backfill material for corrugated steel pipes most state agencies consider pH and resistivity (measures of corrosion resistance) as suggested by the National Corrugated Steel Pipe Association (NCSPA). To assess the corrosivity of environment for ductile iron pipes most agencies use the 10-point system developed by the Cast Iron Pipe Association. The 10-point system is included in the ANSI/AWWA C.105/A21.5, *Polyethylene Encasement for Ductile Iron Pipe Systems* and ASTM A674, *Polyethylene Encasement for Ductile Iron Pipe for Water and Other Liquids* standards and also uses pH, resistivity, moisture content, redox potential, and sulfides content. for predicting soil corrosivity. The points assigned to a soil for different levels of considered corrosion factors in the AWWA method was shown earlier.

The probabilistic percent mass loss models established in Chapter V of this dissertation for ductile iron and galvanized steel pipes embedded in CLSM can further be used to make service life estimates based on the CLSM mixture and environmental properties. These useful service life estimates can provide important data for pipeline management systems to compare and select materials and rehabilitation methods.

6.2.Service Life of Ductile Iron Pipe and Galvanized Steel Embedded in CLSM

The model established for the logarithm of percent mass loss (LPML) of ductile iron coupons and galvanized steel coupons completely embedded in CLSM was provided in Chapter V and is repeated below for reader's convenience:

$$\log_{10}(\%mass\,loss) = 1.04 + \alpha + \beta + \gamma + (\delta + \kappa)\cdot \log_{10}(resistivity) + \varepsilon \cdot pH + \phi + (\tau + \omega)\cdot \frac{w}{cm} + \varphi + \eta + \lambda + \sigma \quad (6.1)$$

The model includes;

- The main effects of classification variables; environment (α), fine aggregate type (β), fly ash type (γ), and metal type (ϕ).
- The main effects of continuous variables; logarithm of electrical resistivity (δ), pH (ε), and water cementitious material (w/cm) ratio (τ).
- The interaction effects of classification variables with classification variables; fine aggregate type with metal type (φ), fly ash type with metal type (η), and environment with metal type (λ), and fly ash type with environment (σ).
- The interaction effect of a classification variable with a continuous variable; logarithm of electrical resistivity with metal type (κ) and w/cm with metal type (ω).

Analysis indicated that a weighted regression analysis was appropriate to satisfy the assumptions of regression analysis and the values of the coefficients determined

through weighted multiple regression analysis were provided in the corrosion study results section. The model includes four classification variables with different numbers of levels and three continuous variables. The variables, their type and levels are shown in Table 6.1.

Table 6.1--Variables and their levels used in the analysis

Variable	Type	Levels
Environment	Classification	2
Fine aggregate type	Classification	4
Fly ash type	Classification	4
Metal type	Classification	2
pH	Continuous	-
Resistivity	Continuous	-
Water/cementitious material	Continuous	-

The two levels of environment were distilled water and chloride solution. The four levels of fine aggregate type were sand, foundry sand, bottom ash, and no fine aggregates. The four levels of fly ash were Class C, Class F, High Carbon, and no fly ash. The two levels of the metal type were ductile iron and galvanized steel.

As a first step to calculate a service life estimate, the mean LPML values needs to be estimated by placing the appropriate coefficients into the model. These values can then be placed into the formula provided in ASTM G1, *Standard Practice for Preparing, Cleaning, and Evaluating Corrosion Test Specimens,* to predict the corrosion rate. The formula converts mass loss values to corrosion rates based on the Faraday's principle discussed in Chapter III and is shown below:

$$CR = \frac{K \times W}{A \times T \times \rho} \tag{6.2}$$

where:

CR, is the corrosion rate in mm/yr (mpy),
K, is a constant 8.76×10^4 (3.45×10^6)
T, is time of exposure in hours,
A, is area in cm^2,
W, is mass loss in grams, and
ρ, is the density in g/cm^3.

The formula indicates that percent mass loss, mass loss, and the corrosion rate are all directly proportional. The useful service life of non pressurized metallic pipe is assumed to be when complete perforation of the pipe occurs. The definition of useful service life as the required time for first perforation is adopted by representative states such as California, Florida, Louisiana, New York, Mississippi, Pennsylvania, and Wisconsin (NCHRP 1998). After determining the mean corrosion rates, and knowing the pipe wall thickness the number of years until perforation (mean service life) can be calculated by dividing the wall thickness by the corrosion rate. It should be noted that the obtained service life estimate would be correct for a uniform corrosion assumption.

The initial weight, W_i, and its area, *A*, of a pipe of length, L, as shown in Figure 6.1 can be calculated as shown in Equation 6.3 and 6.4

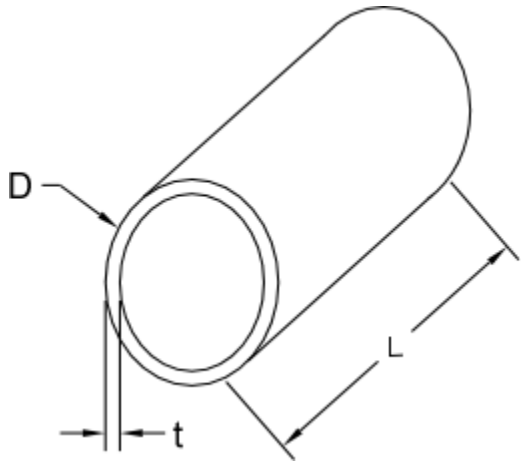

Fig. 6.1--Pipe with unit length.

$$W_i = \pi \left[D^2 - (D - t)^2 \right] \cdot L \cdot \rho \tag{6.3}$$

where

D is the outside radius of the pipe in cm
t is the pipe wall thickness in cm
ρ is the density of the material in g/cm^3

$$A = 4\pi DL \tag{6.4}$$

where

A is the area of the pipe in cm^2

The mass loss of the pipe due to corrosion can be calculated by multiplying the percent mass loss value with the initial mass of the pipe. Using the model shown in Equation 6.1 the mass loss can be calculated as shown in Equation 6.5

$$W = 10^{LPML()} \cdot W_i \cdot 10^{-2} \tag{6.5}$$

where:

W is the mass loss in grams

The time of exposure in hours used in this study to calculate the LPML values was 17,462. By substituting equation 6.3, 6.4, and 6.5 into equation 6.2 we obtain the corrosion rate formula shown below

$$CR = \frac{K \cdot 10^{-2} \cdot 10^{LPML()} \pi \left[D^2 - \left(D - t \right)^2 \right] \cdot L \cdot \rho}{4\pi DL \cdot 17,472 \cdot \rho} \tag{6.6}$$

The expression for service life can then be established by dividing the pipe wall thickness by the corrosion rate formula shown in Equation 6.6 as shown below

$$SL = \frac{D \cdot t \cdot 7978x10^{-2}}{10^{LPML()} \left[D^2 - (D - t)^2 \right]} \tag{6.7}$$

where:

SL is the service life in years
D is the outside radius in cm
t is the pipe wall thickness in cm
LPML() is the logarithm of percent mass loss obtained from Equation 6.1

The formula in Equation 6.7 indicates that the service life and the LPML values are indirectly proportional. To obtain the LPML value from Equation 6.1 one must specify the values of the classification variables and the values of the three continuous variables (w/cm, resistivity, and pH) must be specified. The evaluation of the data indicated that the values of the three continuous variables were not independent of the selected levels of the classification variables. Therefore, different service life values can be obtained for the same values of classification variables based on the different combinations of the values of the continuous variables. In the following sections three different service life values (shortest, median, and longest) were calculated for each combination of the classification variables using the values of the continuous variables. The median service life value was calculated using the mean values of the observed range of the three continuous variables. The shortest service life was calculated using the minimum or maximum values of the observed range of the three continuous variables that will result in the highest possible LPML. The longest service life was calculated using the minimum or maximum values of the observed range of the three continuous variables that will result in the lowest LPML possible.

It should also be noted that the coefficients of the LPML model were determined using a weighted regression analysis. The weights were obtained by separating the residuals into groups by the environment type and the metal type. The reciprocal of the variance of each residual group was used as a weight variable for that group. Therefore the variance of the group of the estimated condition can be used to obtain a distribution around the obtained service life value. Equation 6.8 shows how to obtain the required percentile of the LPML value using the variance and the LPML value obtained from Equation 6.1

$$LPML_{\text{Pr.}} = LPML + \Phi^{-1}(\text{Pr.}) \times \sqrt{Variance} \tag{6.8}$$

where:

$LPML_{Pr.}$, is the LPML for which probability of LPML<$LPML_{Pr.}$ is Pr.
Φ^{-1}, is the inverse standard normal distribution function

Considering the levels of the four classification variables used in this study, 64 (2x4x4x2) different LPML estimates can be calculated. Also as explained earlier for each of the 64 cases 3 different service life distributions can be calculated.

An example of the calculation of three different service life distributions for one specific case following the described procedure is as follows. Assume a ductile iron pipe with 6.35 mm (0.25 in) wall thickness and 76.2 mm (3 in) outside radius will be completely embedded in a CLSM mixture containing sand and Class C fly ash with a spread of approximately 200 mm (7.87 in) (This was the target spread of the CLSM mixtures used in this study). Also assume existence of substantial amounts of chlorides in the environment. Based on the data obtained in this study the mean resistivity, pH, and w/cm for the described conditions are estimated to be approximately 6049 Ω-cm (15.36 kΩ-in), 10.13, and 0.81, respectively. If these values are entered into the model together with the levels of environment (chloride), fine aggregate type (sand), fly ash type (Class C), and the metal type (ductile iron), a mean LPML of 0.299 is obtained. The variance of the group of samples containing ductile iron coupons and exposed to chloride environment was 0.075. The median service life obtained by substituting these values into Equation 6.7 is 21 years as shown below:

$$SL = \frac{7.62 \cdot 0.635 \cdot 7978x10^{-2}}{10^{0.299}\left[7.62^2 - (7.62 - 0.635)^2\right]} = 21\,years \qquad (6.9)$$

Using the LPML and its variance, one can also calculate the service life for which there will be only 20 percent chance of having a shorter service life. To find this service life we need to use the LPML value for which the probability of having a larger LPML is only 20 percent, since the LPML value and the service life are indirectly proportional. This LPML value can be calculated using Equation 6.8 as shown below:

$$LPML_{80} = 0.299 + 0.842 * \sqrt{0.075} = 0.530 \qquad (6.10)$$

The service life calculated based on this corrosion rate would be 12.3 years, i.e. the probability of having a service life shorter than 12.3 years is 20 percent. This entire process can be repeated for different probabilities to obtain a service life distribution as shown in Figure 6.2.

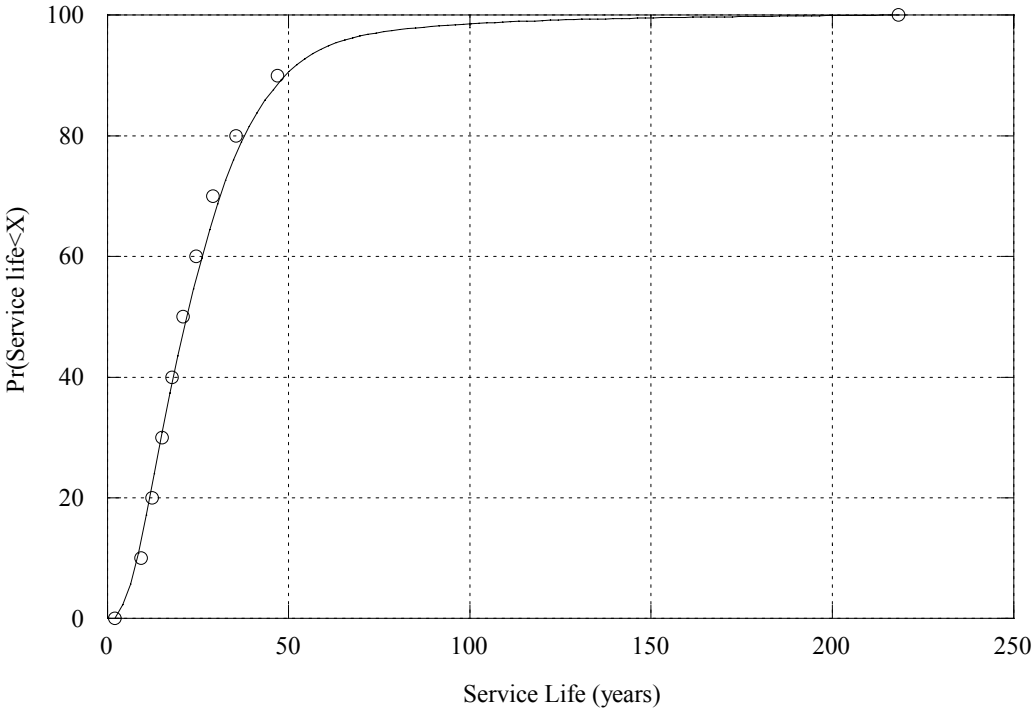

Fig. 6.2--Probability distribution of service life.

It should be noted that the distribution in Figure 6.2 was generated for the assumed levels of the classification variables and the mean values of the corresponding ranges of the three continuous variables. As noted earlier by selecting the minimum and maximum values of the appropriate ranges of the three continuous variables a

distribution for the shortest service life and a distribution for the longest service life can be generated as shown in Figure 6.3.

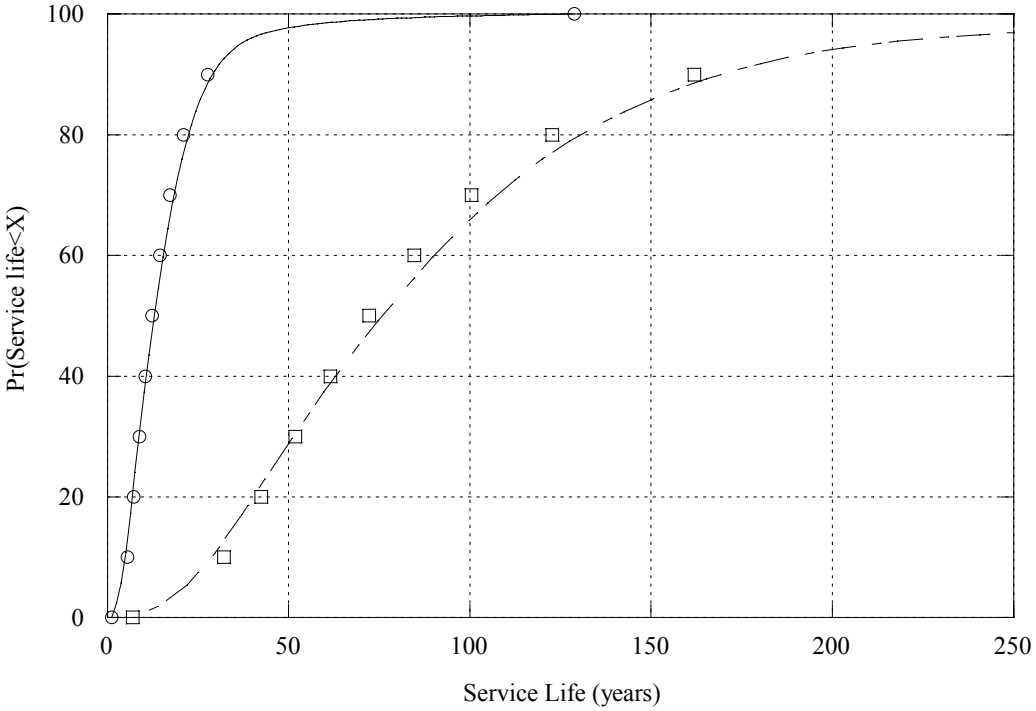

Fig. 6.3--Shortest and longest service life distributions.

This procedure was used to calculate the service life of the 64 different cases at the mean values of their corresponding continuous variables. The service life values were calculated for a wall thickness of 6.35 mm (0.25 in) for both galvanized and ductile iron pipes for comparability, even though galvanized steel pipes generally have thinner walls. The calculated service life values are shown in Table 6.2. Also the service life value for which the probability of having a shorter service life is 20 percent is given in column 6 of Table 6.2.

Table 6.2--Median and 20th percentile of service life

Case No	Environment*	Fine Aggregate**	Fly Ash	Metal Type***	Service Life	Service Life Pr(SL<X)=20
1	CL	Sand	None	GS	6	5
2	CL	Sand	None	DI	16	9
3	CL	Sand	Class C	GS	9	8
4	CL	Sand	Class C	DI	30	18
5	CL	Sand	Class F	GS	7	6
6	CL	Sand	Class F	DI	9	5
7	CL	Sand	High Carbon	GS	8	7
8	CL	Sand	High Carbon	DI	4	2
9	CL	BA	None	GS	10	8
10	CL	BA	None	DI	344	202
11	CL	BA	Class C	GS	7	6
12	CL	BA	Class C	DI	38	22
13	CL	BA	Class F	GS	6	5
14	CL	BA	Class F	DI	15	9
15	CL	BA	High Carbon	GS	7	6
16	CL	BA	High Carbon	DI	14	8
17	CL	FS	None	GS	9	8
18	CL	FS	None	DI	87	51
19	CL	FS	Class C	GS	7	6
20	CL	FS	Class C	DI	10	6
21	CL	FS	Class F	GS	5	4
22	CL	FS	Class F	DI	3	2
23	CL	FS	High Carbon	GS	6	5
24	CL	FS	High Carbon	DI	3	2
25	CL	None	None	GS	7	5
26	CL	None	None	DI	14	8
27	CL	None	Class C	GS	5	4
28	CL	None	Class C	DI	2	1
29	CL	None	Class F	GS	8	6
30	CL	None	Class F	DI	17	10
31	CL	None	High Carbon	GS	9	7
32	CL	None	High Carbon	DI	15	9
33	DW	Sand	None	GS	9	5
34	DW	Sand	None	DI	50	22
35	DW	Sand	Class C	GS	21	13
36	DW	Sand	Class C	DI	102	46
37	DW	Sand	Class F	GS	9	6
38	DW	Sand	Class F	DI	18	8
39	DW	Sand	High Carbon	GS	8	5
40	DW	Sand	High Carbon	DI	7	3
41	DW	BA	None	GS	11	7

Table 6.2—Continued

Case	Environment*	Fine Aggregate**	Fly Ash	Metal type ***	Service Life	Service Life Pr(SL<X)=20
42	DW	BA	None	DI	491	221
43	DW	BA	None	GS	11	7
44	DW	BA	Class C	DI	89	40
45	DW	BA	Class F	GS	7	5
46	DW	BA	Class F	DI	13	6
47	DW	BA	High Carbon	GS	7	4
48	DW	BA	High Carbon	DI	10	4
49	DW	FS	None	GS	10	6
50	DW	FS	None	DI	100	45
51	DW	FS	Class C	GS	12	8
52	DW	FS	Class C	DI	18	8
53	DW	FS	Class F	GS	6	4
54	DW	FS	Class F	DI	3	2
55	DW	FS	High Carbon	GS	6	4
56	DW	FS	High Carbon	DI	3	1
57	DW	None	None	GS	9	6
58	DW	None	None	DI	36	16
59	DW	None	Class C	GS	11	7
60	DW	None	Class C	DI	7	3
61	DW	None	Class F	GS	8	5
62	DW	None	Class F	DI	10	4
63	DW	None	High Carbon	GS	5	3
64	DW	None	High Carbon	DI	1	1

*CL: Chloride solution, DW: Distilled water
**BA: Bottom ash, FS: Foundry sand
***GS: Galvanized steel, DI: Ductile iron

6.3.Comparison with Estimated Ductile Iron Service Life in Soils

DIPRA has performed extensive corrosion studies to determine the corrosion characteristics of gray cast iron and ductile iron since 1928. A recent DIPRA study investigated a subset of their data consisting of 1379 specimens embedded in more than

300 different soils to evaluate the expected service life of bare, shop coated, and polyethylene encased gray and ductile iron pipes (Bonds et al. 2004).

The DIPRA study results indicated that the average corrosion rate of sandblasted and bare ductile iron pipes embedded in corrosive soils, i.e. soils with more than 10 points following the AWWA system, were 0.6426 and 0.3835, respectively. For a ductile iron pipe with 6.35 mm (0.25 in) wall thickness (the thinnest ductile iron pipe wall available in the market) the DIPRA study estimates the service life of sandblasted and bare ductile iron pipe to be 10 and 17 years, respectively. The study also estimates the service life of sandblasted and bare ductile iron pipe in uniquely severe corrosive environments to be 7 and 6 years, respectively. The results shown in Table 6.2 indicated that CLSM mixtures can be designed to provide a service life in the range of 15 to 87 years for ductile iron pipes embedded in CLSM in similar corrosive conditions. The results also indicated that in non-corrosive conditions some CLSM samples can provide a median service life of 100 years or more. The largest expected median service life value was 491 years.

Different agencies may be expected to have different minimum design service life requirements. Because the results of this study show that CLSM samples can be designed to provide the same or better minimum service life values for ductile iron pipes, the expected service life due to external corrosion becomes less of an important factor for choosing between the use of soils and CLSM as a backfill material. In this case it can be concluded that other factors such as material cost, construction cost, construction time, and long-term settlement should be the considered factors in material selection decisions.

6.4.Comparison with Estimated Galvanized Steel Pipe Service Life in Soils

Corrugated steel has been used as a pipe material for storm sewers and culverts for many years. Many studies on the internal and external corrosion of corrugated steel pipes have been performed and many coating materials, such as zinc, aluminum, asphalt, etc., have been used to improve its corrosion performance.

Most states accept the resistivity and pH of soil (external) and water (internal) as the main factors affecting the corrosion of galvanized steel pipes. Instead of estimating minimum useful service life they have defined upper and lower bounds for pH and resistivity, between which galvanized steel pipes can be used. In arid and semi-arid western states (Arizona, Idaho, Nevada, and Wyoming) that have alkaline soils, galvanized steel pipes can be used in soils with lower resistivity values compared to heavy and moderate rainfall eastern states that have acidic soils (NCHRP 1998).

States such as Florida, Illinois, Louisiana, Maine, Mississippi, and Washington use the California Test Method 643 (C643 1993) or a modification of it to estimate service life based on the pH and minimum resistivity. Figure 6.4 shows the California test method chart that uses years to perforation of 1.32 mm (0.05 in) thick steel culvert to define useful service life. The method uses a multiplier for increased wall thickness.

It should be noted that many state agencies through their own research determined that the California Test Method underestimates the average service life of galvanized steel pipes (Ault and Ellor 2000). Research performed by the State of Idaho indicated that the method estimated service life conservatively in all but a few installations (State of Idaho 1965). Research performed by the State of Georgia indicated that the service life was 50 percent greater than that predicted by the California method (NCSPA 1977). Research performed in Oklahoma reported that the California method predicted a shorter life time than observed in the western two thirds of the State. However, the method was very accurate for the high plains area of the state (Hayes 1971).

The main reason for the conservative estimates of the method is the definition of the useful service life used by the California method. A gravity drainage structure can perform adequately well beyond the first perforation, which was the criteria used by the California method to define the end of the useful service life. Also the structures surveyed in California were in mountainous areas where structures were affected by above average abrasion. Also the original study used to develop the California test

method indicated a standard error of ±12 years, which could be the result of many different climatic regions observed in California (Ault and Ellor 2000).

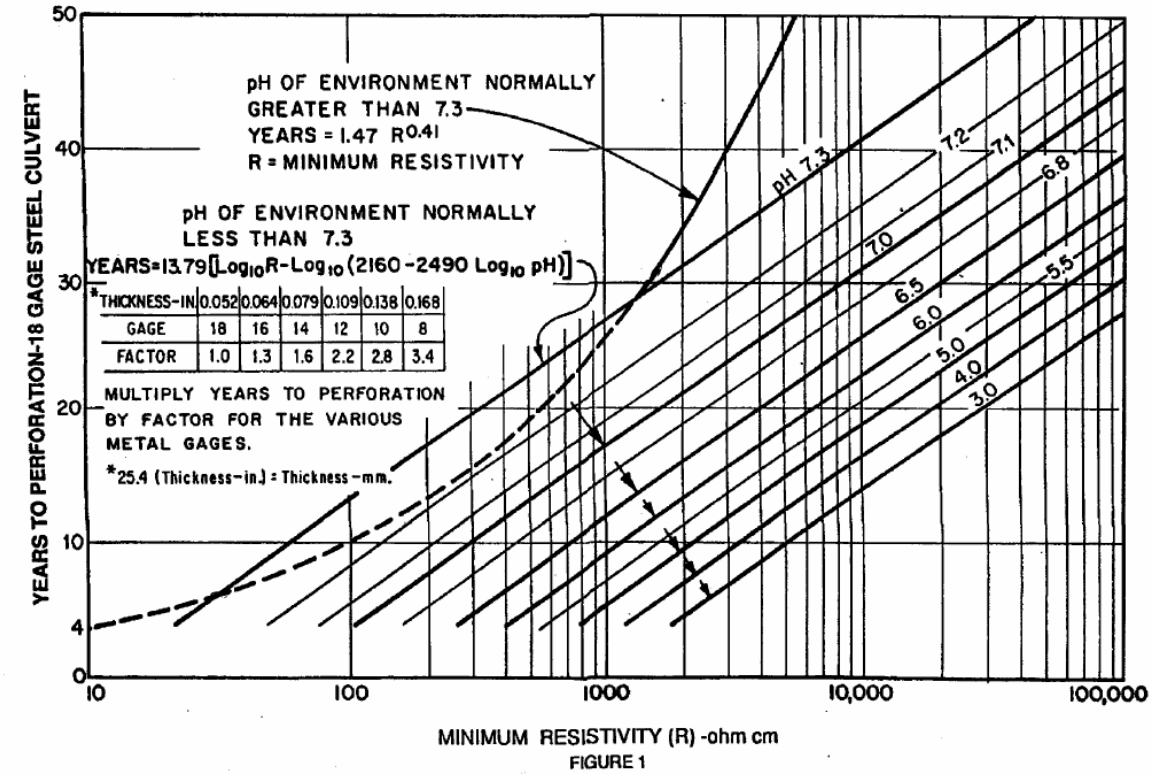

Fig. 6.4--Caltrans 643 service life estimation chart for galvanized pipe.

The AISI developed a similar method to the California 643 method to estimate the service life of galvanized steel pipes. AISI assumes that at the time of first perforation of the galvanized steel pipe, 13 percent average metal loss occurs in the invert of the pipe and that the useful service life of the pipe ends at the 25 percent metal loss in the invert. Therefore, AISI predicts the service life twice as long as that of the California 643 method. The chart used by the AISI was shown in Chapter III and is repeated in Figure 6.5.

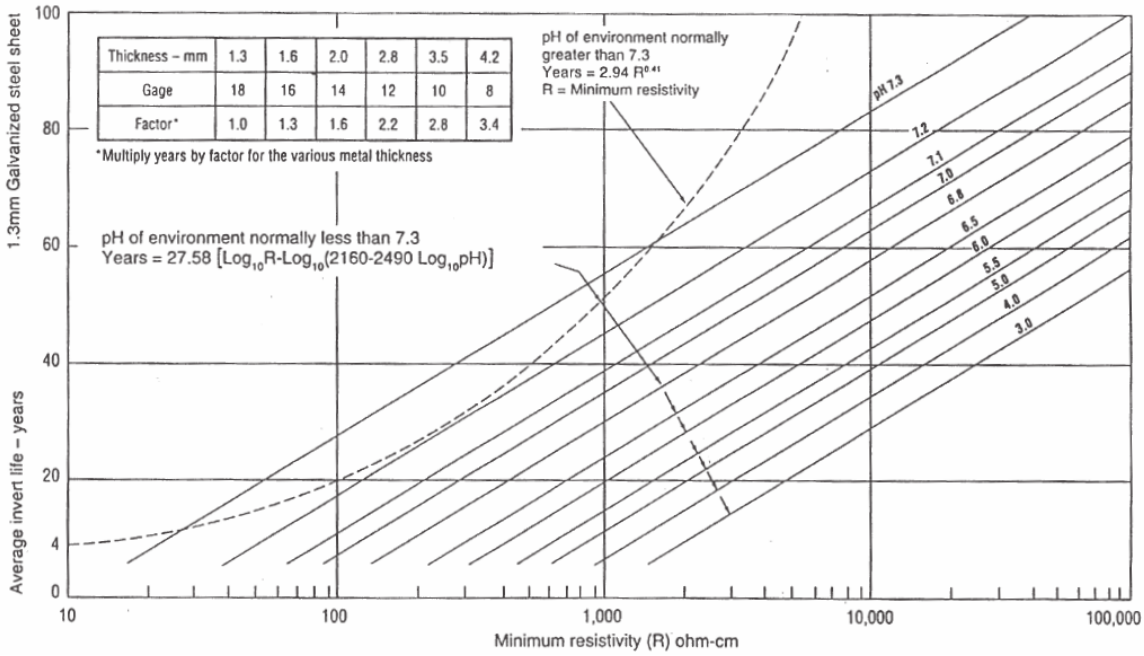

Fig. 6.5--AISI service life estimation chart (Highway Task Force 2002).

The National Corrugated Steel Pipe Association (NCSPA) also published a CSP durability guide that includes the AISI chart to predict service life of corrugated steel pipe and provides a table with additional service life durations for different coatings (CSP Durability Guide 2000).

The Federal Lands Highway Division of FHWA uses a modified version of the California 643 method to estimate the service life of galvanized pipes. The FHWA method estimates the service life 25 percent longer compared to the California method (FHWA 1996).

The State of Missouri defines the end of useful service life as the time of replacement of the pipe due to structural failure or erosion of the roadway bed (NCHRP 1998). A field survey performed by the Missouri Highway and Transportation Department estimates the replacement time of galvanized steel pipes as 45 to 50 years (MoDOT 1990).

Even though different organizations modified the California 643 method to estimate longer service life values, a study performed in Louisiana indicated that the service life estimates obtained using the California method overestimated the service life (Bednar 1989).

Because in this study the end of useful service life was calculated assuming complete perforation of the pipe, the service life values of galvanized steel coupons given in Table 6.2 should be compared with service life estimates obtained from the California 643 method that uses the same criteria. Control samples used in this study had metallic coupons embedded in sand and were exposed to the same chloride environment as the CLSM samples. The results indicated that the sand had a pH and resistivity of 7.46 and 31,000 Ω-cm, respectively, after exposure. The California 643 method estimates the useful service life of gage 18 pipe until perforation in these conditions as 102 years. The median service life values shown in Table 6.2 were calculated for a wall thickness of 0.635 mm (0.25 in). To convert those values to comparable values for estimates obtained from the California 643 chart, they need to be divided by 4.8 (factor for 18 gage). Results indicate that the service life of galvanized steel coupons embedded in CLSM varied from a minimum average service life of 5 years to a maximum average service life of 21 years. These values are low considering that a galvanized steel pipe embedded in sand and exposed to the same moisture and corrosive environment would be expected to have a service life of 102 years. It should also be noted that California Test Method is assumed to make conservative estimates for the service life.

The NCSPA classifies soils into different corrosiveness categories based on their resistivity values as shown in Table 6.3 (NCSPA 1949). Even though different states have different pH boundaries for the usage of galvanized steel pipes, a range of pH between 6 and 9.5 appears to be generally accepted for uncoated galvanized steel pipes (NCHRP 1998).

Table 6.3--Soil corrosivity assessment based on resistivity

Soil Corrosiveness	Resistivity (ohm-cm)
Very low	10000>R>6000
Low	6000>R>4500
Moderate	4500>R>2000
Severe	2000>R

Table 6.4 shows the typical resistivity ranges of different soil types and estimated service life values of galvanized steel pipes (18 gage) in these soils at different pH values using the California 643 method.

Table 6.4--Service life estimates using Caltrans 643 method

Soil type	Resistivity (ohm-cm)		Corrosiveness	Service life (years) at pH					
				6	6.5	7	7.3	7.5	9
Clay	min	750	Severe	7	10	16	26	22	22
	max	1999	Severe	13	16	21	32	33	33
Loam	min	2000	Moderate	13	16	21	32	33	33
	med	5000	Low	19	22	27	37	48	48
	max	9999	Very low	23	26	31	41	64	64
Gravel	min	10000	Very low	23	26	31	41	64	64
	max	29999	Very low	29	32	38	48	101	101
Sand	min	30000	Very low	29	32	38	48	101	101
	max	50000	Very low	32	35	41	51	124	124

Figure 6.6 shows the calculated service life values in Table 6.4 as box plots separated by different corrosiveness classifications and the box plots of the estimated average service life values in chloride and distilled water environments for an 18 gage galvanized steel pipe embedded in CLSM. The service life values for CLSM were estimated using the model established in this research. The results indicate that

galvanized steel pipes embedded in CLSM mixtures evaluated in this study could be expected to have a useful service life (until perforation) comparable to the service life of galvanized steel pipes in severely or moderately corrosive soils with low resistivity and pH values. Based on the results of this study, backfill of bare galvanized steel pipes with CLSM is not warranted.

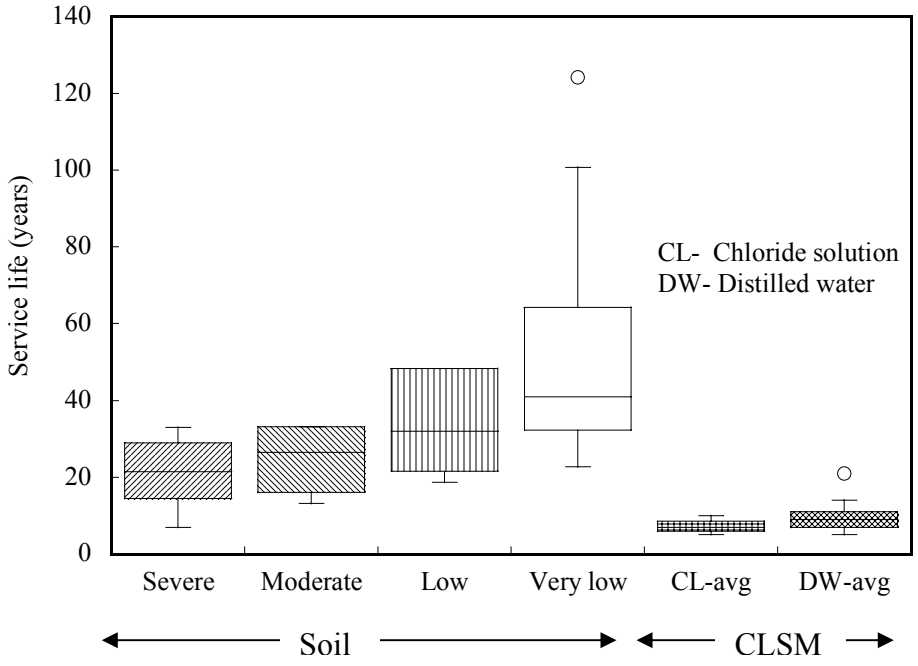

Fig. 6.6--Service life comparison between soil and CLSM.

All service life estimates obtained in this chapter for galvanized steel and ductile iron pipes were calculated using the service life model shown in Equation 6.7. This model was developed based on the probabilistic percent mass loss models developed in Chapter V. Results indicated that equal or better service life periods can be expected from ductile iron pipes embedded in appropriately designed CLSM mixtures even in corrosive environments. Results also indicated that the use of galvanized steel in CLSM

can provide service life values similar to service life values observed in severely corrosive soils.

CHAPTER VII

SUMMARY AND CONCLUSIONS

CLSM has unique characteristics that make it an ideal alternative material for conventional, compacted bedding and backfilling materials. Because limited work has been performed on the influence of CLSM on the corrosion of embedded metallic materials, engineers and owners are often reluctant to use CLSM. An extensive research program has been carried out to extend the knowledge on the corrosivity of CLSM on metallic pipe materials.

The corrosion of corrugated galvanized steel and ductile iron pipes embedded in CLSM was investigated in a laboratory environment by determining the mass loss of metallic coupons embedded in different CLSM mixtures. Exposing coupons from actual pipe materials to controlled environments to evaluate the mass loss of coupons due to corrosion is a commonly used and reliable technique. In this study several hundreds of metallic coupons were embedded in more than 40 different CLSM mixtures and exposed to two different environments. Coupons were exposed to distilled water and chloride solutions for 18 and 21 months in two phases of this study.

As a result of an extensive literature survey, factors that were thought to be influential on the corrosion of metallic materials embedded in soils and CLSM materials were determined. Several of these factors were used in designed experiments as variables with multiple levels to determine their influence on the corrosion of galvanized steel and ductile iron pipe embedded in CLSM mixtures. These factors included cement content, water content, fly ash type, fly ash content, fine aggregate type, fine aggregate content, pH, resistivity, and existence of chloride ions in the environment. Because there are no standard guidelines to measure the pH and resistivity of CLSM mixtures reliable measurement techniques were identified.

Corrugated galvanized steel and ductile iron are two of the most commonly used metallic pipe materials for water distribution mains, sewer, and storm drains. Besides providing general information on different factors that can influence the corrosivity of CLSM mixtures, important specific information on the durability and service life of these materials when embedded in CLSM was obtained. Currently there are no guidelines available for practitioners or researchers to estimate the service life of these materials embedded in CLSM mixtures. The results of this study provide empirical service life estimation models for ductile iron and galvanized steel pipelines embedded in CLSM mixtures. The models consider constituent materials of CLSM mixtures as well as environmental factors.

7.1.Conclusions

Results of the phase I study indicated the following:

- The corrosion activity for metallic coupons completely embedded in CLSM was significantly lower than that of ductile iron pipe embedded in sand.
- CLSM may provide more protection against corrosion initiation and propagation when metallic structures are completely embedded in CLSM compared to compacted sand.
- Examination of the effects of the constituent materials on corrosion with limited number of samples indicated that there was no significant difference between the fly ash types and the fine aggregate types used in this study. However, the corrosion of metal coupons in uncoupled samples that contained a fine aggregate or a fly ash was lower compared to the coupons in uncoupled samples without a fine aggregate or a fly ash.

The results of the Phase II study that used different measurement methods for pH and resistivity and used more samples for a better statistical analysis resulted in slightly

different conclusions. Analysis of the results of uncoupled samples in the Phase II research indicated the following:

- pH was significantly and inversely correlated to the observed logarithm of percent mass loss (LPML) values.
- Environment was a significant variable for all the samples.
- The samples exposed to a chloride solution exhibited significantly higher LPML values compared to the samples exposed to the distilled water.
- The effect of environment for galvanized steel coupons was larger compared to the ductile iron coupons.
- There was a significant difference in the LPML values of different metal types.
- For low w/cm and logarithm of resistivity values ductile iron coupons exhibited significantly lower LPML values.
- At higher w/cm and with increasing logarithm of resistivity the difference in values became less and at sufficiently high values, ductile iron coupons exhibited higher LPML values.
- The effects of different fly ash types and fine aggregate types were more important for samples with ductile iron coupons.
- Samples that contained a fine aggregate exhibited lower LPML values compared to the samples without fine aggregates regardless of the type of the fine aggregate.
- The difference between the mean LPML values of samples containing bottom ash and sand as fine aggregates was statistically not significant.
- The samples containing foundry sand as fine aggregate exhibited a mean LPML value between the samples with bottom ash or sand and the samples without fine aggregates.

- Due to the high LPML variability of samples containing foundry sand the difference between these samples and the samples without fine aggregates was not statistically significant.
- The use of fly ashes may have adverse effects on the corrosion of embedded galvanized steel or ductile iron coupons, especially for the ductile iron coupons.
- Samples containing a high carbon fly ash or Class F fly ash exhibited higher LPML values compared to the samples without fly ashes, but the samples without fly ashes exhibited much larger variation.
- The mean LPML value of the samples containing Class C fly ash was lower than the samples with Class F or high carbon fly ash but higher than the samples without fly ash. However, due to the high variance of the samples without fly ash, the difference between the samples containing Class C fly ash and samples without fly ash was not statistically significant.

The general conclusions obtained from the research performed in both phases indicated the following:

- The metallic coupons embedded in the soil section of coupled samples exhibited significantly higher percent mass loss values compared to the coupons embedded in uncoupled samples.
- Because the main driving force of corrosion is the potential difference in the coupled samples, the significance of the factors that affected the corrosion in uncoupled samples was generally lower for coupled samples.

Past research has shown that the corrosion activity is increased when metallic materials are placed in soils with significantly different characteristics, and good engineering could prevent this. For instance, various utilities are taking precautions to

prevent pipes from traversing dissimilar soils, such as wrapping of pipes or junctions with polyethylene or the use of electrical decouplers. It is logical to conclude that precautions typically taken by engineers to avoid corrosion of metals embedded in dissimilar soils should also mitigate corrosion when CLSM is considered as one of the dissimilar mediums. However, the usefulness of the different approaches used to minimize galvanic coupling was not assessed in this dissertation.

Comparison of the service life models obtained in this study with available service life models for pipelines embedded in conventional backfill materials provided important and needed guidance. Results indicated that CLSM mixtures could provide an equal or longer service life for ductile iron pipes as conventional backfill materials that are rated non-corrosive following the AWWA standard (uncoupled case). However, results also indicated that in highly corrosive environments that contain high amounts of chloride ions some CLSM mixtures tested in this study could provide a minimum average service life of 50 years or more. The case was different for galvanized steel pipes. The results of the empirical service life model indicated that galvanized steel pipes embedded in CLSM mixtures evaluated in this study could be expected to have a useful service life only comparable to the service life of galvanized steel pipes in severely or moderately corrosive soils with low resistivity and pH values.

Data and analysis provided in this dissertation extends the limited knowledge of the corrosion performance of metallic materials embedded in CLSM that may be a better alternative to conventional backfill materials because of its inherent characteristics. With future research work that builds on the findings presented in this dissertation, CLSM can become one of the common construction materials that can be used to decrease construction time, improve durability, and provide cost savings for all parties involved.

REFERENCES

AASHTO, 1986, *AASHTO Guide for Design of Pavement Structures*, American Association of State Highway and Transportation Officials, Washington, D.C.

Abelleira, A., Berke, N.S., and Pickering, D.G., 1998, "Corrosion Activity of Steel in Cementitious Controlled Low-Strength Materials vs. That in Soil." *The Design and Application of Controlled Low-strength Materials (Flowable Fill)*, A.K. Howard and J.L. Hitch, eds., American Society for Testing and Materials (ASTM), West Conshohocken, PA, pp. 124-134.

ACAA, 1997, *1996 Coal Combustion Product-Production and Use*, American Coal Ash Association, Alexandria, VA.

ACI, 1994, "Controlled Low Strength Materials (CLSM)", American Concrete Institute Committee 229, ACI 229R-94 Report, *Concrete International*, V. 16, No. 7, pp. 55-64.

Adaska, W.S., and Krell, W.S., 1992, "Bibliography on Controlled Low Strength Materials (CLSM)," *Concrete International*, V. 14, No. 10, pp. 42-43.

Adaska, W.S., 1997, "Controlled Low Strength Materials," *Concrete International*, V. 19, No. 4, pp 41-43.

AGA, retrieved on Feb. 2, 2000, "Zinc Coatings," American Galvanizers Association, <http://www.galvanizeit.org/resources/files/AGA%20PDFs/T_ZC_00.pdf>.

Andrade, C., and Alonso, C., 2001, "On-site Measurements of Corrosion Rate of Reinforcements," *Construction and Building Materials*, V. 15, pp. 141-145.

Ault, J.P., and Ellor, J.A., 2000, "Durability Analysis of Aluminized Type 2 Corrugated Metal Pipe," Report FHWA-RD-97-140, Federal Highway Administration, McLean, VA, 106 pp.

AWT, retrieved on Oct. 13, 2002, "White Rust: An Industry Update and Guide Paper 2002," Association of Water Technologies, <http://www.awt.org/ AWT_WHITE %20RUST% 20PAPER_2002.pdf>.

AWWA, 1996, *Manual M41, Ductile-Iron Pipe and Fittings*, American Water Works Association, Denver, CO

AWWA, 1990, *Manual M36, Water Audits and Leak Detection*, American Water Works Association, Denver, CO

AWWA, 2004, *Manual M11, Steel Water Pipe: A Guide for Design and Installation*, 4th ed., American Water Works Association, Denver, CO

Ayers, P.H., Charlton, C.B., and Frishette, C.W., 1995, "Investigation of Flash Fill® as a Thermal Backfill Material," 57th American Power Conference Proceedings, Chicago, IL.

Baker, T.H.W. and Goodrich, L.E., 1995, "Trench Backfill and Reinstatement", Proceedings of the American Water Works Association Distribution Systems Symposium, Nashville, TN, Session 9.4, pp. 160-169.

Balogh, A., 1994, "Flowable Fill Gets Even Better," *Report* No. J940601A, The Aberdeen Group, Boston, MA, 2 pp.

Bednar, L., 1989, "Plain Galvanized Steel Drainage Durability Estimation with a Modified California Chart," *Transportation Research Record,* No. 1231, pp. 70-79.

Bernard, H., 1981, "A Statistical Probability Method for Soil Resistivity Determination," *Underground Corrosion*, ASTM STP 741, Edward Escalante, ed., American Society for Testing and Materials, West Conshohocken, PA, pp. 53-60.

Bhat, S.T., and Lovell, C.W., 1996, "Design of Flowable Fill: Waste Foundry Sand as a Fine Aggregate," *Transportation Research Record*, No. 1546, pp. 70-78.

Bhat, S.T., and Lovell, C.W., 1997, "Flowable Fill Using Waste Sand: A Substitute for Compacted or Stabilized Soil," *Testing Soil Mixed with Waste or Recycled Materials*, ASTM STP 1275, Mark A. Wasemiller and Keith B. Hoddinott, eds., American Society for Testing Materials, West Conshohocken, PA., pp. 26-41.

Birks, A., and Green, R., 1991, "Ultrasonic Testing," *Nondestructive Testing Handbook,* 2nd edition, American Society For Nondestructive Testing, Columbus, Ohio , V. 7.

Bonds, R.W., 1992, Letter from Ductile Iron Pipe Research Association Research and Technical Director to Mr. Bill Chin from Virginia Beach Public Utilities Engineering, VA.

Bonds, R.W., Barnard, L.M., Horton, A.M., and Oliver, G.L., 2004, "Corrosion and Corrosion Control Research of Iron Pipe," *Pipeline Engineering and Construction: What's on the Horizon?*, Pipelines 2004 International Conference Proceedings CD, August 1-4, San Diego, CA.

Bonds, R.W., Horton, A.M., Oliver, G.L., and Barnard, L.M., 2005, "Corrosion Control Statistical Analysis of Iron Pipe," *Journal of Materials Performance*, V. 44, No. 1, pp. 30-34.

Brewer, W.E., and Hurd, J.O., 1991, "Economic Considerations When Using Controlled Low Strength Material (CLSM) as Backfill," *Transportation Research Board*, Committee A2K04, Session Presentation.

Brewer, W.E., 1992, *The Design and Construction of Small Span Bridges and Culverts Using Controlled Low Strength Material (CLSM)*, Ohio Department of Transportation, Columbus, OH.

Brewer, W.E., 1993, *Special Report Controlled Low Strength Material (CLSM) for Construction Contractors,* Cincinnati Gas and Electric Company, Cincinnati, OH.

Brewer, W.E., 1994,. "Durability Factors Affecting CLSM," *Controlled Low-Strength Materials*, ACI SP 150, W.S. Adaska, ed., American Concrete Institute, Detroit, MI, 113 pp.

Brinkley, D., and Mueller, P.E., 1998, "Ten-Year Performance Record of Non-Shrink Slurry Backfill," *The Design and Application of Controlled Low-Strength Materials (Flowable Fill)*, ASTM STP 1331, A.K. Howard and J. L. Hitch, eds., American Society for Testing and Materials, West Conshohocken, PA, pp. 231-237.

Broomfield, J.P., 1997, *Corrosion of Steel in Concrete*, London and New York: E& FN Spon.

Brown, R., 1995, retrieved on Sept. 10, 2004, "Class notes," University of Rhode Island, <http://www.egr.uri.edu /che/course/CHE534w/chapter4PittingCorrosion.htm>.

Byfors, K., 1987, "Influence of Silica Fume and Fly Ash on Chloride Diffusion and pH Values in Cement Paste," *Cement and Concrete Research*, V. 17**,** pp. 115-130.

Cady, P., and Gannon, E., 1992, "Condition Evaluation of Concrete Bridges Relative to Reinforcement Corrosion," in *Report* No. SHRP-S/FR-92-110, Transportation Research Boar, Washington, DC

CALTRANS, 1993, "Method for Estimating the Service Life of Steel Culverts," *California Test 643*, State of California DOT, Division of New Technology and Material Research, Sacramento, CA.

Camitz, G., and Vinka, T., 1989, "Corrosion of Steel and Metal-Coated Steel in Swedish Soil Effects of Soil Parameters," *Effects of Soil Characteristics on Corrosion*, ASTM STP 1013, V. Chaker and J.D. Palmer, eds., ASTM, Philadelphia, PA, pp. 37-53.

Cao, L.B., Wortley, B., and Sirivivatnanon, V., 1994, "Corrosion Behaviours of Steel Embedded in Fly Ash Blended Cements," *Durability of Concrete,* Third International Conference Proceedings CD, American Concrete Institute, Nice, France.

Chaker, V., 1990, "Corrosion Testing in Soils – Past, Present, and Future," *Corrosion Testing and Evaluation*; Silver Anniversary Volume, ASTM STP 1000, R. Baboian and S. W. Dean, eds., American Society for Testing and Materials, Philadelphia, PA., pp. 95-111.

Compton, K.G., 1981, "Corrosion of Buried Pipes and Cables, Techniques of Study, Survey, and Mitigation," *Underground Corrosion*, ASTM STP 741, Edward Escalante, Ed., American Society for Testing and Materials, Philadelphia, PA., pp. 141-155.

Caproco Ltd., 1985, "Underground Corrosion of Water Pipes in Canadian Cities, Case: The City of Calgary", Caproco Corrosion Prevention Ltd., CANMET Contract *Report* No. 0SQ81-0096, Catalogue No. M38-17/2-1-1985E, Edmonton, Alberta.

Chesner, W.H., 1998, "User Guidelines for Waste and Byproduct Materials in Pavement Construction," Federal Highway Administration, Turner-Fairbank Highway Research Center, Washington, D.C.

CIPRA, 1964, *Soil Corrosion Test Report: Ductile Iron Pipe*, Cast Iron Pipe Research Association, Birmingham, Ala.

Coburn, S.K., 1978, "Soil Corrosion," *Metals Handbook*, 9th ed., V. 1: "Properties and Selection: Irons and Steels", Bruce P. Bardes, ed., American Society for Metals International, Metals Park, OH, pp. 725-731.

Corrpro, 1991, "Condition and Corrosion Survey: Soil Side Durability of CSP," *Report* by Corrpro Companies, Medina, OH.

Corrosion Doctors, retrieved on Sept. 14, 2005, "Pipeline Stress Corrosion Cracking (SCC)," Kingston Technical Software, <http://www.corrosion-doctors.org /Forms/scc-pipeline.htm>.

Costanzo, F.E., and McVey, R.E., 1958, “Development of the Redox Probe Field Technique,” *Corrosion Journal*, V. 14, No. 6, pp. 26-30.

Cox, G.J., 1983, "Developments in Alloy Cast Irons," *British Foundryman*, V. 76, No. 9, pp. 129-144.

Craft, G., 1995, “Corrosion Protection – A Cost Comparison”, *U.S. Piper*, V.65, No. 2, Fall-Winter, pp.14.

Crouch, L.K., Gamble, R., Brogdon, J.F., and Tucker, C.J., 1998, “Use of High-Fines Limestone Screenings as Aggregate for Controlled Low Strength Material (CLSM),” *The Design and Application of Controlled Low-Strength Materials (Flowable Fill)*, ASTM STP 1331, A.K. Howard and J. L. Hitch, eds., American Society for Testing and Materials, Philadelphia, PA, pp. 45-59.

Dandria, G.G., Frost, D.J., Ashmawy, A., and Patterson, K.R., 1997, “Potential Factors Affecting Flow Consistency Test Method for Controlled Low Strength Materials,” *Transportation Research Record*, No. 1589, pp. 29-35.

De Rosa, P.J., and Parkinson, R.W., 1985, "Corrosion of Ductile Iron Pipe", *Report* TR241, Water Research Center, Swindon, UK., 249 pp.

Diamond, S., 1981, "Effects of Two Danish Fly-ashes on Alkali Contents of Pore Solutions of Cement Fly-ash Pastes," *Cement and Concrete Research*, V. 2**,** pp. 383-394.

DIPRA, 1994, “Ductile Iron Solutions," *Ductile Iron Pipe News*, Ductile Iron Pipe Research Association, Fall/Winter Issue.

DIPRA, 1997, “Ductile Iron Solutions," *Ductile Iron Pipe News*, Ductile Iron Pipe Research Association, Fall/Winter Issue.

DIPRA , retrived on Sept. 5, 2003, "Ductile Iron Pipe General Info," DIP-GEN/3/03/5M, Ductile Iron Pipe Research Association, Birmingham, AL, <http://www.dipra.org/pdf/generalBrochure.pdf>.

Docter, B.A., 1998, “Comparison of Dry Scrubber and Class C Fly Ash in Controlled Low Strength Material (CLSM) Applications,” *The Design and Application of Controlled Low-Strength Materials (Flowable Fill)*, ASTM STP 1331, A.K. Howard and J. L. Hitch, eds., American Society for Testing and Materials, Philadelphia, PA, pp. 13-26.

Doherty, B.J., 1989, “Controlling Ductile-Iron Water Main Corrosion”, *NACE Corrosion/89 Conference Proceedings*, New Orleans, LA, Paper no. 588.

Dolen, T.P and Benavidez, A.A., 1998, “Properties of Low Strength Concrete for Meeks Cabin Dam Modification Project, Wyoming,” Ohio Department of Transportation, Columbus, OH.

Du, L., 2001, "Laboratory Investigations of Controlled Low-Strength Material," Ph.D. Dissertation, The University of Texas at Austin.

Du, L., Folliard, K.J., and Trejo, D., 2002, "Effects of Constituent Materials and Quantities on Water Demand and Compressive Strength of Controlled Low Strength Material," *ASCE Journal of Civil Engineering Materials*, V. 14, No. 6., pp. 485-495.

Dunham, B., 1988, “Controlled Low Strength Material: Sample Specifications and Project Evaluation,” November 1988, City of Peoria Department of Public Services, IL.

Duritsch, D., 1993, “The Use of Non-Toxic Spent Foundry Sand into Controlled Low Strength Materials in Ohio,” The Institute of Advanced Manufacturing Sciences, , The Ohio Department of Development, Columbus, OH.

Edgar, T.V., 1989, “In Service Corrosion of Galvanized Culvert Pipe,” *Effects of Soil Characteristics on Corrosion*, ASTM STP 1013, V. Chaker and J.D. Palmer, eds., American Society for Testing and Materials, Philadelphia, PA, pp. 133-143.

Elsener, B., 2002, “Macrocell Corrosion of Steel in Concrete – Implications for Corrosion Monitoring,” *Cement and Concrete Composites*, V. 24, pp. 65-72.

EPA, 1998, "Back Document for Proposed CPG III and Draft RMAN III," in *EPA Report EPA530-R-98-003*, Environmental Protection Agency, Washington, D.C.

Escalante, E., 1992, “Measuring the Corrosion of Steel Piling at Turcott Yard, Montreal, Canada- A 14 Year Study,” *Corrosion Forms and Control for Infrastructure*, ASTM STP 1137, Victor Chaker, ed., American Society for Testing and Materials, Philadelphia, PA, pp. 339-355.

Evans, U.R., 1960, *The Corrosion and Oxidation of Metals: Scientific Principles and Practical Applications*, Edward Arnold, London, 272 pp.

Ferguson, P.H., and Nicholas, D.M.F., 1992, "External Corrosion of Buried Iron and Steel Water Mains," Corrosion Australasia, V. 17, No. 4, Aug., pp.7-10.

FHWA, 1996, "Federal Lands Highway Project Development and Design Manual," Publication No. FHWA-DF-88-03, June, Federal Highway Administration, Washington, D.C., pp. 7-42.

Fitzgerald, J.H., 1984a, “Fundamentals of Corrosion”, Basic Text for the Twenty Ninth Annual Appalachian Underground Corrosion Short Course, West Virginia University, College of Minerals and Resources, Morgantown, WV.

Fitzgerald III, J.H., 1984b, *Corrosion of Various Type of Pipe*, PSG Corrosion Engineering, Inc., Detroit, MI.

Folliard, K.J., Trejo, D., Du, L., and Sabol, S.A., 1999, "Controlled Low-Strength Material for Backfill, Utility Bedding, Void Fill, and Bridge Approaches," in *NCHRP 24-12 Interim Report,* National Cooperative Highway Research Project, Washington, D.C.

Folliard, K.J., Trejo, D., Du, L., and Sabol, S.A., 2001, “Controlled Low Strength Material for Backfill, Utility Bedding, Void Fill, and Bridge Approaches,” *NCHRP 24-12(1) Interim Report*, National Cooperative Highway Research Project, Washington, D.C.

Fox, T.A., 1989, “Use of Coarse Aggregate in Controlled Low-Strength Materials,” *Transportation Research Record*, No. 1234, Transportation Research Board, Washington, D.C.

Franzblau, A., 1958, *A Primer of Statistics for Non-Statisticians*, Harcourt, Brace & World, Orlando, FL.

Fuller, A.G., 1981, "Corrosion Resistance of Ductile Iron Pipe", *BCIRA Report 1442,* 109 pp.

Gandham, S., Seals, R.K., and Foxworthy, P.T., 1996, “Phosphogypsum as a Component of Flowable Fill,” *Transportation Research Record*, No. 1546, pp. 79-87.

Gas Res. Inst., 1996, "Pipe Inspection: Adapting Technology to Inspect “Live” Mains for Metal Loss," *Report,* Department of Energy, Gas Research Institute, Washington, D.C.

Gill, S., 1923, "Locating Pipe Line Inspection Points," *Oil Weekly*, (May 30, 1923), pp. 12-24.

Goldbaum, J. E., Hook, W., and Clem, D. A., 1997, "Modification of Bridges with CLSM." *Concrete International*, V.19, No 5, pp. 44-47.

Gray, D.D., Reddy, T.P., Black, D.C., and Ziemkiewics, P.F., 1998, "Filling Abandoned Mines with Fluidized Bed Combustion Ash Grout," *The Design and Application of Controlled Low-Strength Materials (Flowable Fill)*, ASTM STP 1331, A.K. Howard and J. L. Hitch, eds., American Society for Testing and Materials, Philadelphia, PA, pp. 180-193.

Green, B.H., Staheli, K., Bennett, D., and Walley, D.M., 1998, "Fly Ash Based Controlled Low Strength Material (CLSM) Used for Critical Microtunneling Applications," *The Design and Application of Controlled Low-Strength Materials (Flowable Fill)*, ASTM STP 1331, A.K. Howard and J. L. Hitch, eds., American Society for Testing and Materials, Philadelphia, PA, pp. 151-164.

Green, B.M., and De Rosa, P.J., 1994, "'Retrocat' and 'Retrovac': In-situ Cathodic Protection of Existing Ductile Iron Pipe", *Proceedings of the 19th International Water Supply Conference*, Budapest, Hungary.

Gress, D., 1996, "The Effect of Freeze-Thaw and Frost Heaving on Flowable Fill." *Report* HPR 93-8(X2712), New Hampshire Department of Transportation, Concord, NH, 102 pp.

Guan, S., 1995, *Wasteliner Test Report,* Madison Chemical Industries Inc., Milton, ON.

Gummow, R.A., 1984, "The Corrosion of Municipal Iron Watermains", *Materials Performance*, Vol. 23, No. 3, 1984, pp. 39-46.

Hadley, R.F., 1939, "Microbiological Anaerobic Corrosion of Steel Pipe Lines," *Oil Gas J.,* Vol. 38, No. 19, pp. 92-110.

HAMCIN, 1996, *A Performance Specification for Controlled Low Strength Material Controlled Density Fill (CLSM-CDF)*, Hamilton County and the City of Cincinnati, OH.

Hamilton, W.A, 1985, "Sulphate Reducing Bacteria and Anaerobic Corrosion," *Annu. Rev. Microbiol.*, V. 39, pp. 195-217.

Harry, T., and Baker, W., 1998, "Frost Penetration in Flowable Fill Used in Pipe Trench Backfill." *The Design and Application of Controlled Low-Strength Materials (Flowable Fill)*, A. K. Howard and J. L. Hitch, eds., American Society for Testing and Materials (ASTM), West Conshohocken, PA, pp. 275-282.

Hawn, D.E., and Davis, J.R., 1975, "Special Corrosion Investigation," *Report* for the City of Calgary, Water Transmission and Distribution System, Caproco Corrosion Prevention Ltd., Edmonton, Alberta.

Hayes, C. J., 1971, *Durability of Corrugated Steel Culvert in Oklahoma*, Oklahoma Department of Highways, Oklahoma City, OK.

Hegarty, J.R., and Eaton, S.J., 1998, "Flowable Fill Promotes Trench Safety and Supports Drainage Pipe Buried 60 ft Under New Runway," *The Design and Application of Controlled Low-Strength Materials (Flowable Fill)*, ASTM STP 1331, A.K. Howard and J. L. Hitch, eds., American Society for Testing and Materials, West Conshohocken, PA, pp. 255-264.

Highway Task Force (HTF), 2002, *Handbook of Steel Drainage & Highway Construction Products*, American Iron and Steel Institute (AISI), Washington, D.C.

Ho, D.W.S., and Lewis, R.K., 1987, "Carbonation of Concrete and its Prediction," *Cement and Concrete Research*, Vol. 17, pp. 489-504.

Hoar, T.P., and Farrer, T.W., 1961, "The Anodic Characteristics of Mild Steel in Dilute Aqueous Soil Electrolytes," *Corrosion Science*, Vol. 1, pp. 49-61.

Holden, W.R., C.L. Page, and N.R. Short, 1983, "The Influence of Chlorides and Sulphates on Durability of Reinforcement in Concrete," *Corrosion of Reinforcement in Concrete Construction*, A.P. Crane, ed., Ellis, Horwood, Chichester, pp. 143-150.

Hook, W., and Clem, D.A., 1998, "Innovative Uses of Controlled Low Strength Materials (CLSM) in Colorado," *The Design and Application of Controlled Low-Strength Materials (Flowable Fill)*, ASTM STP 1331, A.K. Howard and J. L. Hitch, eds., American Society for Testing and Materials, West Conshohocken, PA, pp. 137-150.

Hoopes, R.J., 1998, "Engineering Properties of Air-Modified Controlled Low Strength," *The Design and Application of Controlled Low-Strength Materials (Flowable Fill)*, ASTM STP 1331, A.K. Howard and J. L. Hitch, eds., American Society for Testing and Materials, West Conshohocken, PA, pp. 87-101.

Horn, L.G., 1993, *Product Advisory: Tape Coat*, Ductile Iron Pipe Research Association, Birmingham, AL.

Horton, A.M., 1988, "Protecting Pipe with Polyethylene Encasement, 1951-1988", *Waterworld News*, V. 12, pp. 26-33.

Howard, A, 1998, "Proposed Standard Practice for Installing Buried Pipe Using Flowable Fill," *The Design and Application of Controlled Low-Strength Materials (Flowable Fill)*, ASTM STP 1331, A.K. Howard and J. L. Hitch, eds., American Society for Testing and Materials, West Conshohocken, PA, pp. 285-295.

ICC, 1937, *Valuation Docket 1203*, Interstate Commerce Commission, Washington, DC

Jackson, R.Z., Pitt, C., and Skabo, R., 1992, *Nondestructive Testing of Water Mains for Physical Integrity*, American Water Works Association Research Foundation, Denver, CO.

Janardhanam, R., Burns, F., and Peindl, R.D., 1992, "Mix Design for Flowable Fly Ash Backfill Material," *Journal of Materials in Civil Engineering*, Vol. 4, No. 3, pp. 252-263.

Janik-Czakor, M., Szummer, A., and Szklarska-Smialowska, Z., 1975, "Effect of Nitrogen Content in a 18Cr-5Ni-10Mn Stainless Steel on the Pitting Susceptibility in Chloride Solutions," Corrosion Science, Vol. 15, No. 11, pp. 394-398.

Javed, S., 1994, "Use of Waste Foundry Sand in Highway Construction," *Final Report*: Project N. C-36-50N, School of Engineering, Purdue University, West Lafayette, IN.

Javed, S., and Lovell, C.W., 1995, "Use of Waste Foundry Sand in Civil Engineering," *Transportation Research Record*, No.1486, pp. 109-113.

Johnson, C.K., 1981, "Phenols in Foundry Waste Sand," *Modern Casting*, Vol. 71, No. 1, pp. 48-49.

Jones, D.A., 1982, *Corrosion Processes*, R.N. Parkins, ed., Applied Science, Englewood, NJ.

Jones, M.R., and Giannakou, A., 2004, "Thermally Insulating Foundations and Ground Slabs Using Highly-Foamed Concrete," *Journal of ASTM International*, Vol. 1, No. 6, 13 pp.

Kabonov, B., Burstien, R., and Frumkin, A., 1947, "Kinetics of Electrode Processes on the Iron Electrode," *Discussions of the Faraday Society*, V. 1, p.259-265.

Kane, R.D., Eden, D.C., and Eden, D.A., 2005, "Real-Time Solutions Integrate Corrosion Monitoring with Process Control," *Materials Performance*, V. 44, No. 2, pp. 36-41

Kaneshiro, J., Navin, S., Wendel, L., and Snowden, H., 2001, "Controlled Low Strength Material for Pipeline Backfill-- Specifications, Case Histories, and Lessons Learned," ASCE *Pipelines 2001: Advances in Pipeline Engineering & Construction*, July 15-18, Castronovo, J.P., ed., San Diego, CA, 13 pp.

Katz, A., and Kovler, K., 2004, “Utilization of Industrial By-products for the Production of Controlled Low Strength Materials (CLSM),” *Waste Management*, V. 24, No. 5, pp. 501-512.

King, R.A., Moosavi, A.N., and Dawson, J.L., 1986, "Corrosion Behavior of Ductile and Gray Iron Pipes in Environments Containing Sulphate-Reducing Bacteria," *Proceedings of Biologically Induced Corrosion Conference*, Gaithersburg, MD, Dexter, S.C., ed., NACE, Houston, TX, pp. 83-92.

Kozhushner, G., Brander, R., and Ng, B., 2001, "Use of Pipe Recovery Data and the Hydroscope "NDT" Inspection Tool for Condition Assessment of Buried Water Mains," *AWWA Infrastructure Conference 2001*, Orlando, FL, American Water Works Association, Denver, CO.

Krell, W.C., 1989, “Flowable Fly Ash,” *Concrete International*, V. 11, No.11, pp. 54-58.

Kroon, D.H., Lindemuth, D., Sampson, S., and Vincenzo, T., 2005, “Corrosion Protection of Ductile Iron Pipe,” *Journal of Materials Performance*, V. 44, No. 1, pp. 24-30.

Landwermeyer, J. S., and Rice, E. K., 1997, "Comparing Quick-set and Regular CLSM," *Concrete International*, V. 19, No. 5, pp. 34-39.

Larsen, R.L., 1988, “Use of Controlled Low Strength Materials in Iowa,” *Concrete International*, V. 10, No. 7, pp. 22-23.

Larsen, R.L., 1990, “Sound Uses of CLSMs in the Environment,” *Concrete International*, V. 12, No. 7, pp. 26-29.

LaQue, F.L., 1995, “The Corrosion Resistance of Ductile Iron,” *Corrosion of Ductile Iron Piping*, Proceedings of the NACE International Conference, Baltimore, MD, Michael J. Szeliga, ed., NACE International, Houston, TX.

Levlin, E., 1996, “Aeration Cell Corrosion of Carbon Steel in Soil: In Situ Monitoring Cell Current and Potential,” *Corrosion Science*, V. 38, No. 12, pp. 2083-2090.

Lisk, I., retrieved on Jan. 14, 1997, “The Use of Coatings and Polyethylene for Corrosion Protection”, Water Online, Erie, PA, http://www.wateronline.com /content/news/article.asp?docid={cd207494-f4fb-11d2-a405-00c04f4f7c39}.

Logan, K.H., 1939, "Engineering Significance of National Bureau of Standards Soil Corrosion Data," *NBS Journal of Research,* V. 22, pp. 109-117.

Logan, K.H., and Koenig, A.E., 1939, "Methods of Inspecting Pipe Lines," *J. Am. Water Works Assoc.*, V. 31, pp. 1451-1455.

Lorenzo, P., Goni, S., and Hernandez, S., 1996, "Effect of Fly Ashes with High Total Alkali Content on the Alkalinity of the Pore Solution of Hydrated Portland Cement Paste," *Journal of the American Ceramic Society*, V. 79, pp. 470-474.

Lucht, D.A., 1995, "Thermal Performance of Flowable Fill Mixtures for Horizontal GSHP System," M.S. thesis, South Dakota State University, Brookings.

Macias, A., and Andrade, C., 1987a, "Corrosion of Galvanized Steel Reinforcements in Alkaline Solutions. Part 1. Electrochemical Results," *British Corrosion Journal*, V. 22, No. 2, pp. 113-118.

Macias, A., and Andrade, C., 1987b, "Corrosion of Galvanized Steel Reinforcements in Alkaline Solutions, Part 2. SEM Study and Identification of Corrosion Products," *British Corrosion Journal*, V 22, No. 2, pp. 119-129.

Macias, A., and Andrade, C., 1987c, "Corrosion of Galvanized Steel in Dilute $CaOH_2$ Solutions," *British Corrosion Journal*, V. 22, No. 3, pp. 162-171.

Macias, A., and Andrade, C., 1987d, "Galvanized steel behaviour in $Ca(OH)_2$ saturated solutions containing $SO_4^{=}$ ions," *Cement and Concrete Research*, V. 17, No. 2, pp. 307-316.

Mackintosh, D.D., Atherton, D.L., Schmidt, T.R., and Russell, D.E., 1996, "Remote Field Eddy Current for Examination of Ferromagnetic Tubes," *Materials Evaluation*, V. 54, No. 6, pp. 652-657.

Mailliard, J., 1985, "Polyurethane Resin Base External Coating for the Protection of Buried Ductile Iron Mains", *Proceedings of the 6th International Conference on the Internal and External Protection of Pipes*, Nice, France, R. Pickford, ed., British Hydraulic Research Association, Cranfield, UK, pp. 236-242.

Makar, J., and Chagnon, N., 1999, "Inspecting Systems for Leaks, Pits, and Corrosion," *AWWA Journal,* V. 91, No. 7, p. 36-42.

Malloy, C., retrieved on Nov. 1, 1998, "EPA Cites Recovery Potential in Flowable Fill," *Concrete Products*, Skokie, IL, <http://concreteproducts.com/mag/concrete_epa_cites_recovery/>.

Mason, T.F., 1998, “Use of Controlled Density Fill to Fill Underslab Void,” *The Design and Application of Controlled Low-Strength Materials (Flowable Fill)*, ASTM STP 1331, A.K. Howard and J. L. Hitch, eds., American Society for Testing and Materials, West Conshohocken, PA, pp. 210-212.

McCarthy, D.F., 2002, *Essential of Soil Mechanics and Foundations – Basic Geotechnics*, 3rd ed., Prentice Hall, Englewood Cliffs, NJ.

McDonald, S. and Makar, J., 1996, "Assessment of the Hydroscope 201 TM Condition Index Evaluation of Gray Cast-Iron Pipe From Gatineau, Que," *Report* A-7015.3, Natl. Res. Council, Ottawa, Ont.

DiGioia, A.M., Brendel, G.F., McLaren, R.J., Balsamo, N.J., Glogowski, P.E., Kelley, J.M., 1992, "Fly Ash Design Manual for Road and Site Applications," *Report* EPRI-TR-100472-Vol. 2, Electric Power Research Institute, Palo Alto, CA, 181 pp.

Mehta, P.K., 1991, “Durability of Concrete-Fifty Years of Progress?” *Durability of Concrete*, *Second International Conference*, Montreal, Canada, ACI SP-126, V.M. Malhotra, ed., American Concrete Institute, Farmington Hills, MI, Vol. 1, pp. 1-31.

Mehta, P.K., 1994, “Concrete Technology at the Crossroads – Problems and Opportunities,” *Concrete Technology: Past, Present, and Future*, V. M. Malhotra, ed., , American Concrete Institute, Farmington Hills, MI, pp.1-30.

Melton, J. S., Nourse, W. A., Gardner, K. H., and Seager, T. P., 2005, "A Rational Mix Design for Flowable Fill Containing Contaminated Sediment." *Third International Conference on Remediation of Contaminated Sediments*, Jan. 24-27, New Orleans, LA.

MoDOT, 1990, “Life Expectancy Determination of Zinc-Coated Corrugated Steel and Reinforced Concrete Pipe Used in Missouri,” *Report* MR91-1, Missouri Highway and Transportation Department, Division of Materials and Research, Jefferson City, MO.

MNR, 1992, "Mineral Aggregate Conservation – Reuse and Recycling," *Report* prepared by John Emery Geotechnical Engineering Limited for Aggregate and Petroleum Resources Section, Ontario Ministry of Natural Resources, Queen’s Printer for Ontario.

NACE, 1992, “Corrosion Control of Ductile and Cast Iron Pipe,” *Task Group T-10A-21 Report* 54293, NACE Publication 10A292, NACE, Houston, TX.

Naik, T.R., and Ramme, B.W., 1990, "High Early Strength Fly Ash Concrete for Precast/Prestressed Products," *Precast/Prestressed Concrete Institute Journal*, V. 35, No. 6, pp. 72-78.

Naik, T., and Singh, S., 1997, "Permeability of Flowable Slurry Materials Containing Foundry Sand and Fly Ash," *Journal of Geotechnical and Geoenvironmental Engineering*, V. 123, No. 5, pp. 446-452.

Naik, T.R., Kraus, R.N., Sturzl, R.F., and Ramme, B.W., 1998, "Design and Testing Controlled Low Strength Materials (CLSM) Using Coal Ash," *The Design and Application of Controlled Low-Strength Materials (Flowable Fill)*, ASTM STP 1331, A.K. Howard and J. L. Hitch, eds., American Society for Testing and Materials, West Conshohocken, PA, pp. 27-45.

Nantung, T.E., 1993, "Design Criteria for Controlled Low Strength Materials," Ph.D. dissertation, Purdue University, West Lafayette, IN.

NCHRP, 1998, *Synthesis of Highway Practice 254: Service Life of Drainage Pipe*, Transportation Research Board, National Research Council, Washington, D.C.

NCHRP, 2002, *Synthesis of Highway Practice 303: Assessment and Rehabilitation of Existing Culverts*, Transportation Research Board, National Research Council, Washington, D.C.

NCSPA, 1949, *Sewer Manual for Corrugated Steel Pipe*, National Corrugated Steel Pipe Association, Washington, D.C.

NCSPA, 1977, "Performance Evaluation of Corrugated Metal Culverts in Georgia," *Report*, National Corrugated Steel Pipe Association (southeastern region), Dallas, TX.

NCSPA, retrieved on Aug. 2, 2000, "CSP Durability Guide," National Corrugated Steel Pipe Association, <http://www.cspi.ca/english_files/technical_bulletins/durability_guide.pdf>.

Nicholson, P., 1991, "Corrosion of Municipal Water Systems", *Proceedings of NACE Corrosion'91conference*, NACE, Houston, TX, Paper No. 592.

NRMCA, 1989, "What, Why, and How? Flowable Fill Materials," *Concrete in Practice No. 17*, National Ready Mixed Concrete Association, Silver Spring, MD.

Ohlheiser, T., 1998, “Utilization of Recycled Glass as Aggregate in Controlled Low Strength Material (CLSM),” *The Design and Application of Controlled Low-Strength Materials (Flowable Fill)*, ASTM STP 1331, A.K. Howard and J. L. Hitch, eds., American Society for Testing and Materials, West Conshohocken, PA, pp. 60-64.

Okpala, D.C., 1989, "Pore Structure of Hardened Cement Paste and Mortar," *International Journal of Cement Composites and Lightweight Concrete*, V. 11, No. 4, pp. 245-254.

OSHA, 2005, “Safety and Health Regulations for Construction- Excavations,” *Code of Federal Regulations Title 29*, Ch. XVII, U.S. Department of Labor, Occupational Safety & Health Aministration, Washington, D.C.

Palmer, J.D., 1989, “Environmental Characteristics Controlling the Soil Corrosion of Ferrous Piping,” *Effects of Soil Characteristics on Corrosion*, ASTM STP 1013, V. Chaker and J. D. Palmer, eds., American Society for Testing and Materials, West Conshohocken, PA, pp. 5-17.

Palmer, J. D., 1990, “Field Soil Corrosivity Testing – Engineering Considerations,” *Corrosion Testing and Evaluation*, Silver Anniversary Volume, ASTM STP 1000, R. Baboian and S. W. Dean, eds., American Society for Testing and Materials, PA, pp. 125-138.

Peabody, A. W., 1967, *Control of Pipeline Corrosion*, National Association of Corrosion Engineers International, Houston, TX.

Pennington, W. A., 1966, “Corrosion of Steel and Two Types of Cast Iron in Soil”, *Highway Research Record No. 140 Corrosion and Protection of Metals*, Division of Engineering, National Research Council – National Academy of Sciences – National Academy of Engineering, Washington, D.C.

Pons, F., Landwermeyer, J.S., and Kerns, L., 1998, “Development of Engineering Properties for Regular and Quick-set Flowable Fill,” *The Design and Application of Controlled Low-Strength Materials (Flowable Fill)*, ASTM STP 1331, A.K. Howard and J. L. Hitch, eds., American Society for Testing and Materials, West Conshohocken, PA, pp. 67-85.

Puckorius, P.R., 1983, "Ozone for Cooling Tower Systems- Current Guidelines-Where it Works," *Materials Performance,* V. 22, No. 12, pp. 19-22.

Rajani, B., McDonald, S., and Felio, G., 1995, “Water Mains Breaks Data on Different Pipe Materials for 1992 and 1993”, *Report,* National Research Council Canada, Ottawa, Ontario.

Riggs, E.H., and Keck, R.H., 1998, "Specifications and Use of CLSM by State Transportation Agencies," *The Design and Application of Controlled Low-Strength Materials (Flowable Fill)*, ASTM STP 1331, A.K. Howard and J. L. Hitch, eds., American Society for Testing and Materials, West Conshohocken, PA, pp. 298-305.

Rodriguez, J., Ortega, L.M., Casal, J., and Diez, J. M., 1996, "Corrosion of Reinforcement and Service Life of Concrete Structures," *Seventh Int. Conference on Durability of Building Materials and Components*, Stockholm, Sweden.

Romanoff, M., 1957, "Underground Corrosion", *National Bureau of Standards Circular No. 579*, U.S. Government Printing Office, Washington, D.C.

Romanoff, M., 1968, "Performance of Ductile Iron Pipe in Soils", *J. AWWA*, V. 60, No. 6, pp. 645-653.

Rossum, J.R., 1969, "Prediction of Pitting Rates in Ferrous Metals from Soil Parameters," *Journal of American Water Works Association*, V. 61, pp. 305-310.

Samadi, A., and Herbert, R., 2003, "Corrosiveness of Controlled Low Strength Material vs. That of Encasement Sand," *Journal of New Pipeline Technologies, Security, and Safety*, Vol. 1, pp 514-523.

Sears, E.C., 1964, "Comparison of the Soil Corrosion Resistance of Ductile Iron Pipe and Gray Cast Iron", *Materials Protection*, V. 7, No. 10, pp. 33-37.

Schmidt, T.R., Atherton, D.L., and Sullivan, S., 1989, "Experience with the Remote Field Eddy Current Technique," *Proc. of the Third Natl. Seminar on Nondestructive Evaluation of Ferromagnetic Materials*, Houston, TX.

Shreir, L.L., 1963, *Corrosion*, John Wiley & Sons, Inc., New York.

Smith, A., 1991, "Controlled Low Strength Material," *Aberdeen's Concrete Construction*, V. 36, No. 5, pp. 389-391.

Smith, W.H., 1968, "A Report on Corrosion Resistance of Cast Iron and Ductile Iron Pipe", *Cast Iron Pipe News*, V. 35, No. 3, pp. 16-22.

Smith, W.H., 1972, "Corrosion Prevention With Loose Polyethylene Encasement", *Water & Sewage Works*, V. 119, pp. 14-21.

Spangler, M.G., 1941, *The Structural Design of Flexible Pipe Culverts*, Iowa Engineering Experiment Station, Bulletin No. 153, Ames, IA

Spickelmire, B., 2002, "Corrosion Considerations for Ductile Iron Pipe," *Journal of Materials Engineering and Performance*, V. 11, pp. 16-23.

Snethen, D.R., and Benson, J.M., 1998, "Construction of CLSM Approach Embankment to Minimize the Bump at the End of the Bridge," *The Design and Application of Controlled Low-Strength Materials (Flowable Fill)*, ASTM STP 1331, A.K. Howard and J. L. Hitch, eds., American Society for Testing and Materials, West Conshohocken, PA, pp. 165-179.

Stansbury, E.E., and Buchanan, R.A., 2000, *Fundamentals of Electrochemical Corrosion*, ASM International, Materials Park, OH.

Starkey, R.L., and Wight, K.M., 1945, "Anaerobic Corrosion of Iron in Soils." *Final Report of the American Gas Association Corrosion Research Fellowship*, Monograph, American Gas. Association, Washington, D.C.

Starkey, R. L. and Wight K. M., 1947, "Anaerobic Corrosion of Iron in Soil – A Condensation," *Corrosion*, V. 3, No. 5, pp. 227-233.

State of Idaho, 1965, *Durability of Metal Pipe Culverts*, Department of Highways, Boise.

Stern, K., 1995, "The Use of Spent Foundry Sand in Flowable Fill in Ohio," *Foundry Management and Technology*, V. 23, No. 9, pp. 78-86.

Stetler, F.E., 1980, "Accelerating Leak Rate in Ductile Cast Iron Water Mains Yields to Cathodic Protection", *Materials Performance*, V. 19, No. 10, p.15-20.

Stoecker, J.G., 1984, "Microbiological Influence and Electrochemical Types of Corrosion: Back to Basics," *Materials Performance*, V. 23, No. 8, pp. 48-55.

Stroud, T.F., 1989, "Corrosion Control Measures for Ductile Iron Pipe", *Proceedings of the NACE Corrosion/1989 Conference*, New Orleans, LA, Paper No. 585.

Sullivan, J.P., 1990, "Leak Detection and Repair: Boston's Conservation Success Story," *Proceedings of the 1990 AWWA Ann. Conference,* Cincinnati, OH.

Sullivan, R.W, 1997, "Boston Harbor Tunnel Project Utilizes CLSM," *Concrete International*, V. 19, No. 5, pp 40-43.

Swaffar, K.M. and Price, H.R., 1987, "Tunnel Saved by Fly Ash," *ASCE Materials Journal*, V. 57, No. 9, pp. 68-70.

Tatnall, R.E, 1981, "Case Histories: Bacteria Induced Corrosion," *Materials Performance,* V. 22, No. 8, pp. 41-48.

Tikalsky, P., Gaffney, M., and Regan, R., 2000, "Properties of Controlled Low Strength Materials Containing Foundry Sand," *ACI Materials Journal*, V. 97, No. 6, pp. 698-702.

Trejo, D., 1997, "Microstructural Design and Electrochemical Evaluation of Fe/2Si/0.1C Dual-phase Ferritic Martensitic Steel for Concrete Reinforcement," Ph.D. dissertation, University of California, Berkeley.

Trejo, D., Folliard, K.J., and Du, L., 2004, "Sustainable Development Using Controlled-Low Strength Material," *International Workshop on Sustainable Development and Concrete Technology Conference Proceedings*, Beijing, China.

Tuutti, K., 1982, *Corrosion of Steel in Concrete*, Swedish Cement and Concrete Institute, Stockholm, Sweden.

Uhlig, H. H. and Revie, R. W., 1985, *Corrosion and Corrosion Control: An Introduction to Corrosion Science and Engineering*, 3rd ed., John Wiley and Sons, Inc., New York.

USACE, 1986, "Laboratory Soils Testing," *Report* EM 1110-2-1906, US Army Core of Engineers, Washington, D.C.

Walker, M.P., and Ash, J.R., 1998, "Flowable Fill Backfill for Use in Sequential Excavations in Contaminated Soil," *The Design and Application of Controlled Low-Strength Materials (Flowable Fill)*, ASTM STP 1331, A.K. Howard and J. L. Hitch, eds., American Society for Testing and Materials, West Conshohocken, PA, pp. 200-209.

Williams, J., 1982, "Bibliography of Underground Corrosion," *Materials Performance*, Vol. 21, No. 1, pp. 40-43.

Won, J.P., Lee, Y.S., Park, C.G., and Park, H.G., 2004, "Durability Characteristics of Controlled Low Strength Materials Containing Recycled Bottom Ash," *Concrete Research*, V. 56, No. 7, pp. 429-436.

Vrabs, J.B., 1972, "External Corrosion and Protection of Ductile Iron Pipe," *Materials Protection and Performance*, V. 11, No.3, pp. 26-33.

APPENDIX A

CASE HISTORIES

1. The U.S. Bureau of Reclamation used a CLSM mixture, a combination of blow sand and cement paste, as a bedding material from 1964 to 1966 for the construction of Canadian River Aqueduct from Amarillo to South of Lubbock, Texas. Bedding costs reduced by 40 percent and production increased from 122 to 305 meters per shift (Adaska 1997).
2. In 1972 CLSM was used as pavement base material in Monroe, Michigan. Two 5.18 m (17 ft) wide, 30.5 m (100 ft) long, 0.15 m (15 in) thick test sections with compressive strength of 3.4 MPa (500 psi) and 6.8 MPa (1000 psi) were prepared. Test sections outperformed 25.4 cm (10 in) conventional base material. 48.2 m^3 (63 cy) of CLSM with a cost of \$20/m^3 (\$15/cy) was used (Brewer 1993).
3. In 1973 CLSM was used to backfill 1.83 m diameter (72 in) concrete cooling pipes of a generating station in Avoca, Michigan. Different filler materials were utilized in CLSM production as long as the flowability and strength gain was controlled (for later excavability). Considering factors such as trench width reduction, climate, testing, and safety the cost of CLSM was less than the cost of conventional materials. 9,175 m^3 (12,000 cy) of CLSM with a cost of \$18.3/m^3 (\$14/cy) was used (Brewer 1993).
4. In 1974 CLSM was used to build a 5.5 m (18 ft) wide and 3 m (10 ft) high pipe arch for access over a drainage creek in Toledo, Ohio. Instead of excavating a trench 1½ times the pipe arch's diameter which also required the use of sheet piling adjacent to a highway on one side, CLSM was used to backfill to an elevation approximately ½ the pipe height and the remaining backfill was completed with conventional materials. 612 m^3 (800 cy) of a CLSM mixture with a compressive strength of 0.68 MPa (100 psi) was used. The cost of CLSM was \$20/m^3 (\$15/cy) (Brewer 1993).
5. In 1974 stones were placed along the shoreline banks of Lake Erie in Toledo, Ohio to prevent erosion. Later a CLSM mixture with a compressive strenth of

3.4 MPa (500 psi) was used around the stones to prevent their displacement by high water and wind. Application was very successful. 1147 m^3 (1500 cy) of CLSM with a cost of \$22.2/m^3 (\$17/cy) was used (Brewer 1993).

6. In 1975 due to the poor bearing capacity of upper level soil, 3 to 5 m (10 to 18 ft) of extra excavation was required below designed bottom grade of strip footings of a parking structure in Columbus, Ohio. A CLSM mixture with compressive strength of 3.4MPa (500 psi) was used to fill the extra excavations below the footings. CLSM provided required strength to transfer loads to good bearing capacity soil, no worker was required to get into the excavation, quick setup and pouring of CLSM eliminated the need of shoring/sheeting and their expense. Each excavation section was filled before nightfall every day. 688 m^3 (900 cy) of CLSM with a cost of \$33.7/m^3 (\$25/cy) was used (Brewer 1993).
7. In 1975 CLSM was used in the construction of a utility pit wall at high ground water table site of the Standard Oil Company Refinery in Oregon, Ohio. After excavating a 5 m x 6 m (16 ft x 20 ft) pit, water was pumped out and wall forms were placed at the outside wall line. CLSM was poured between the soil and wall form to cut off water flow and the wall form was moved to the inside wall line. After the placement of reinforcements, concrete wall was poured between CLSM and wall forms. Only one wall form was used with no ties, the continuous pumping of the pit was eliminated and the project was finished 3 days early. 191 m^3 (250 cy) of CLSM with a cost of \$21/m^3 (\$16/cy) was used (Brewer 1993).
8. In 1975 floor construction equipment was getting stuck during the construction of a building's interior due to poor soil conditions in Toledo, Ohio. The exterior walls of the building were already erected and the equipment access for lime stabilization of the soil was limited. A CLSM mixture with compressive strength of 3.4 MPa (500 psi) was placed that was able to support the construction equipment. 382 m^3 (500 cy) of CLSM with a cost of \$25/m^3 (\$19/cy) was used (Brewer 1993).

9. In 1975 Ohio Department of transportation tested CLSM as a possible replacement for deteriorated transverse joints on the southbound lane of USR 33 instead of Portland cement concrete. Compressive strength, wetting and drying tests (ASTM D-559), freeze-thaw tests (ASTM D-560) were conducted and a mixture with compressive strength of 11.7 MPa (1700 psi) was used. Based on the test data and visual inspection of the pavement, ODOT report indicated that the CLSM mixture was an acceptable replacement (Brewer 1993).
10. In 1975 two 2 m (7 ft) high, 4 m (13 ft) wide, and 15 m (50 ft) long metal pipe arch roadways were built in Monroe, Michigan. One of the roadways was built with conventional backfill and CLSM was used to build the other one. The labor and equipment cost for the conventional backfill was $1,317.76 and the material cost was $765 (Total $2,082.76). The labor and equipment cost for the CLSM backfill was $434 and the material cost was $1,335 (Total $1,769). The conventional backfill was not placed and tested according to the specifications which later resulted in the vertical displacement of the roadway. The cost of the CLSM used was $20/$m^3$ ($15/cy) (Brewer 1993).
11. In 1976 a CLSM mixture containing fly ash (27 percent) and bottom ash (59 percent) was used to backfill twin fiberglass cooling tower lines 4.7 m (15.5 ft) in diameter and 0.4 km (0.25 mile) long in Masontown, Pennsylvania. Both filler materials were available on site, and due to floatation of pipe concerns the initial lift of CLSM was restricted to 0.8 m (2.67 ft) per day. The project was completed successfully. 53,519 m^3 (70,000 cy) of CLSM was used and the cost varied between $12.4 to $18.3/$m^3$ ($9.50 to $14/cy) (Brewer 1993).
12. In 1976 CLSM was used to backfill a 3.7 m x 3.7 m x 13.7 m (12 ft x 12 ft x 40 ft) excavation for a 12,000 gal. Fiberglas gasoline tank in Toledo, Ohio. The 1406 kg (3100 lbs) tank was suspended 0.45 m (18 in) above the ground and the first lift of CLSM up to 0.2 m (8 in) above the bottom of the tank was placed. After 3 hours, CLSM was poured up to 0.6 m above the bottom of the tank. Next day the tank was filled up to the spring line and after a wait of two hours the fill

was completed to the elevation of pavement subbase. CLSM placement speed was limited due to the tank floatation tendency. The use of CLSM eliminated the need of a concrete mat and tank straps called for in the original specifications and no construction personnel was required to go into the excavation. 153 m^3 (200 cy) of CLSM with a cost of \$23.3/m^3 (\$18/cy) was used (Brewer 1993).

13. In 1976 CLSM was used to rehabilitate the lift span bridge on state route 163 in Port Clinton, Ohio. CLSM was poured successfully into the cells below the deteriorated concrete spans in winter time without any delays due to weather. 863 m^3 (1129 cy) of CLSM with a cost of \$20/m^3 (\$15/cy) was used (Brewer 1993).
14. In 1980 a CLSM mixture with 7 days strength in the range of 0.34 to 0.68 MPa (50 to 100 psi) was used as a bedding material for pipes in California. The mixture provided an equivalent material to Class B pipe bedding material. The pipe laying productivity was increased from 30.5 m (100 ft) to 305 m (1000 ft) per day and the cost was reduced by 30 percent (Brewer 1993).
15. In 1988 due to severe settlement problems with conventional backfill materials in utility trenches, the Department of Public Services of Peoria, Illinois started a research program with the Illinois Concrete Council. A CLSM mixture containing 22.6 kg/m3 (50 lbs/cy) Portland cement, 90.7 kg/m3 (200 lbs/cy) fly ash, 1356 kg/m3 (2990 lbs/cy) fine aggregate was used to fill trenches with depths ranging from 0.9 m to 2.7 m (3 ft to 9 ft). Minimal shrinkage was observed and material set quickly and could support the weight of a person within 2 to 3 hours. Pavements could be placed within 3 to 4 hours. The Department decided to change its backfilling specifications to require the use of CLSM (Dunham 1988, Brewer 1993).
16. Since 1988 Iowa uses CLSM to rehabilitate existing bridges by placing culverts under the existing bridge and then pouring CLSM through holes cut in the bridge deck. Culverts were wrapped with polypropylene to keep out CLSM. This method costs approximately ¼ of the cost of removing and replacing the existing

bridge structure and can be performed under normal traffic conditions. One example was a bridge on wooden pilings in Cedar Rapids damaged by a grass fire. The bridge was rehabilitated using 2600 m^3 (3400 cy) CLSM without closing the street. Iowa has rehabilitated 65 bridges with this method between 1988 and 1993 (Larsen 1988, Brewer 1993).

17. In 1989 Ohio Department of Transportation and the Federal Highway Administration built a pipe arch as a replacement for a concrete culvert for a research project. CLSM was placed above the pipes up to the top of base elevation and a bituminous asphalt wearing surface was placed directly on CLSM. The use of CLSM cut the estimated construction time for this project by 10 days (Brewer 1993).
18. In 1990 a street cave in caused by the collapse of a storm sewer was filled with a 0.68 MPa (100 psi) CLSM mixture. After cleaning the hole and repairing the sewer the hole was filled with CLSM and paved. The project was so successful that the city decided to use CLSM for future maintenance work and received bids approximately for \$36.6/m^3 (\$28/cy) of CLSM containing concrete sand as filler material (Brewer 1993).
19. Following the example of Iowa Department of Transportation (IDOT), Colorado Department of Transportation used CLSM in four bridge rehabilitation projects in 1991 and 1993. Two wooden structures and one steel girder structure were converted to a corrugated metal culvert system and a concrete girder structure was converted into pre-cast concrete box culvert. The culverts used in these projects need to be able to handle the water-carrying capacity and they must fit the existing bridge structure and flow line of the channel. Same construction sequence was followed as the one used by IDOT. In three separate filling operations, the trench around the culverts up to the spring line of the culverts, the gap between the spring line of culverts up to 30 cm (1 foot) below the bridge deck, and the 30 cm below the bridge deck were filled. The culverts beyond the limits of bridge deck were backfilled with conventional backfill materials. The

total project cost in 1991 for the conversion of one of the bridges using CLSM was $170,000. In the same year on a nearby project a similar structure was removed and replaced with a box culvert for $400,000. CDOT saved more than 50% of the total bridge replacement cost by using CLSM. The delivered cost for CLSM ranged from $130.8/m^3 ($100/cy) for the initial project in 1991 to $50/m^3 ($38/cy) in 1993. The total in place cost including furnishing, placing, flange filler material, drilling, and filling core holes, and labor varied from $65 to $183 per cubic meter ($50 to $140 per cubic yard). On conventional bridge replacement projects a temporary asphalt-on-base course must be constructed which may require acquisition of additional right of way. The right of way cost may vary from $100 per acre in eastern Colorado to $500,000 per acre in the Denver metropolitan area. The acquisition may last up to three years. By eliminating the need for detour construction CLSM reduces the total traffic control costs substantially. On a typical CDOT project the total cost of traffic control was approximately one tenth the cost of traffic control for a conventional bridge replacement project (Goldbaum et al. 1997).

20. Boston's new Central Artery/Tunnel (CA/T) project to solve the complex traffic problems of Boston was started in 1992 and utilized CLSM for backfilling purposes. CLSM was used to backfill around corridors for complete consolidation and elimination of future settlement problems. CLSM was used to backfill between the slurry walls and the existing terrain and the space between the tunnel boxes and supporting walls for the cut and cover tunnels. In all these applications space was very limited and difficult to properly backfill using conventional backfill materials. CLSM was successfully utilized during harsh winter months and it was reported that CLSM was the only type of material placement able to be conducted in some very cold days. A CLSM mixture utilizing a large amount of fly ash was designed by the manufacturers to lower the cost of CLSM to ½ the price of 1 cy of ready mixed concrete as specified by the project managers. Thousands of cubic yards of CLSM was used in the

project and the use of CLSM was beneficial for construction and design companies, power companies, ready mixed concrete producers, and the state of Massachusetts that expects a low number of calls for repairs and failures due to backfill settlement problems (Sullivan 1997).

21. Wisconsin Electric Company used a high fly ash content CLSM mixture with a 28 days compressive strength greater than 690 kPa (100 psi) to fill two obsolete steam service tunnels in downtown Milwaukee in December of 1983. One tunnel was 1.8 m in diameter by 88 m long (6 ft x 290 ft). The other tunnel had an ellipsoid section with 1.5 m height and 1.2 m width (5 ft x 4 ft). The tunnels had a cover depth of 4.6 m and 2.1 m (15 ft and 7 ft) and 249 m^3 (420 cy) of CLSM was used to fill the tunnels. Bulkheads made out of concrete blocks were used to limit the flow of CLSM. Small openings were left at the top of the bulkheads for venting air during backfill. CLSM was mixed in ready mixed concrete trucks and was placed using a truck-mounted concrete pump, rated at 27 m per hour (30 yd/hr). The maximum length of pipeline was 61 m (200 ft) and no pumping problems were experienced. The maximum distance of CLSM flow was about 40 m (130 ft) (Naik and Ramme 1990).
22. In 1984 Wisconsin Electric Company used CLSM to backfill a hollow sidewalk cavity containing locker room facilities in downtown Milwaukee. 230 m^3 (300 cy) of CLSM with a 28 days compressive strength of 1172 to 2206 kPa (170 to 320 psi) was used to fill the 24.4 m long, 4.3 m wide, and 2.1 m deep section. The CLSM mixture was placed directly from trucks into the cavity and the CLSM flowed along the whole cavity. CLSM was excavated with a backhoe several months later to install a water supply line. CLSM could be ripped and the excavation had straight walls on each side (Naik and Ramme 1990).
23. In 1984 CLSM was used to fill abandoned steam utility facilities in the Menomonee River Valley of Milwaukee. A 114 m (375 ft) long main with 76 cm (30 inch) diameter, a 104 m (340 ft) long main and trench box with double 76 cm (30 inch) diameter, a 72 m (235 ft) long steel tunnel with 2.9 m diameter (91/2

ft), two 20 m deep (65 ft) concrete shafts with 5.5 m (18 ft) diameter, and associated valve bunkers and manholes were filled. 1178 m^3 (2324 cy) of CLSM with 28 days compressive strength of 276 kPa (40 psi) was placed directly from the trucks into the cavities. The material flowed freely and filled the cavities completely (Naik and Ramme 1990).

24. In 1987 Iowa Department of Transportation (IDOT) used CLSM to fill two abandoned underground fuel tanks near Ames. The removal of tanks was estimated to cost $8000 and could endanger the foundation of an adjacent garage structure. The two 7.6 m^3 and 3.8 m^3 (2000 gal. and 1000 gal.) tanks were filled with CLSM at a cost of $1140 (Larsen 1990).
25. In Toledo, Ohio CLSM was used to protect pipes installed under railroad tracks. Originally when a pipe had to be installed under tracks, tracks were removed, the soil was excavated to the bedding line elevation, pipes were placed, and backfilled and compacted to the original elevation, and tracks were placed back. Instead of this labor intensive plan, when CLSM was used, the tracks were left in place and the road bed was excavated to the level of pipe bedding. Pipes were installed and CLSM was used to backfill the trench. A train was able to pass over the tracks in 23 hours (Larsen 1990).
26. In 1980s CLSM was used in Burlington, Iowa to prevent erosion. Due to the runoff from an adjacent parking lot, the riprap in a 3.7 to 4.3 m deep (12 to 14 ft) V-shaped ditch was washed away. 31 m^3 (40 cy) of 3448 kPa (500 psi) CLSM was used after relining the ditch wall with riprap to fill the voids and to place a 0.6 to 0.9 m (2 to 3 ft) wide and 100 mm (4 inch) deep cap over the riprap (Larsen 1990).
27. In 1980s the flood wall in Burlington built to protect Burlington from Mississippi River flood waters started to tilt towards the river due to a void eroded by the river in front of the deadman that was connected to the wall. The deadman was replaced and 321 m^3 (420 cy) CLSM was used to fill the voids behind and in front of the deadman (Larsen 1990).

28. In 1980s the erosion of Iowa River bank was threatening the Iowa's business district Wapello. The city installed 306 m^3 (400 cy) of 690 kPa (100 psi) CLSM as an erosion control mat. The project was so successful that the city installed a second mat of similar size a year later (Larsen 1990).
29. The Minnesota District #9 Maintenance Department used CLSM to fill voids caused by erosion under bridge pier footings of the Robert Street Bridge in St. Paul, Minn. A 100 mm (4 inch) diameter pipe was used to place riprap into the voids and then CLSM was placed to the bottom of the voids through riprap. 126 m^3 if CLSM was used and the cost of the project was $107,000 (Larsen 1990).
30. In Hutchinson County, South Dakota when spring flooding washed the entire fill from over and around a multiplate steel arch pipe CLSM was used to rehabilitate the pipe. The pipe had a span of 5.2 m (17 ft 2 inch) and 3.4 m (11 ft 4 inch) rise and was anchored to cutoff walls at both ends. The washout under the pipe was about 0.9 m (3 ft) and the center of the pipe sagged putting pressure on the cutoff walls. The pipe was drilled in the middle and jacked until the bottom of the pipe was brought to the original flow line elevation. Then CLSM was used to displace the water and fill the void. After setting of the CLSM jacks were cut, holes were grouted and CLSM was placed around the pipe to a depth of 0.6 m (2 ft). The pipe was repaired in nine days at a cost of $12,000 using 69 m^3 (90 cy) of CLSM. The estimated cost of pipe replacement was $40,000 (Larsen 1990).
31. In 1995 during the construction of Kent County International Airport in Grand Rapids, Michigan engineers decided to enclose a stream in a 1500 mm (60 inch) diameter reinforced concrete pipe before building the embankment for a crosswind runway. To minimize earth loads on the concrete pipe the engineers specified a narrow 3 m (10 ft) trench, however the safety authorities demanded a wider trench. Since a wider trench would place unacceptable loads on the reinforced concrete pipe, instead of modifying the pipe, the designers decided to use a narrow trench and to backfill it with CLSM. The use of CLSM made it unnecessary for workers to get between the pipe and the trench wall to compact

conventional backfill material. CLSM was placed to the springline of the pipe and the rest was backfilled with compacted clay. The culvert had been inspected three times after the construction and is performing well (Hegarty and Eaton 1998).

32. In late 1980s the City of Prescott, Arizona started to use a non-shrink slurry (CLSM) to backfill pipelines. A sewer project that required a 5.2 m (17 ft) cut and backfilling across a major arterial street was estimated to last 24 to 48 hours due to standard backfilling and compaction of thin lifts. The project required also extensive shoring due to instability of the fill. Through the use of CLSM the project was completed and the roadway opened to traffic in 7 hours. Also a 152.5 m (500 ft) conduit bank which contained many conduits in close proximity was backfilled through a continuous operation in less than 4 hours. The city of Prescott reported that over a ten year period the rate of backfill failure declined to 1% from 80percent since the start of use of CLSM (Brinkley and Mueller 1998).
33. In 1991-1993 the City of Denver constructed a new international airport that covered 137 km^2 (53 square miles) at a cost of $3 billion. 32000 m (105000 ft) of reinforced concrete pipe ranging in diameter from 0.4 m to 2.4 m (15 in to 96 in) were placed on CLSM bedding and backfilled with CLSM up to 152 mm (6 in) above the spring line of the pipe, i.e., completely embedded in CLSM. The use of CLSM allowed the contractor to use a narrow trench width (152 mm on both sides of the pipe). Workers connected pipes in the trench using a trench shield and no compaction work was necessary. CLSM easily flowed under the pipes that were placed on 152 mm (6 in) high blocks. Slump, unit weight, temperature, and compressive strength of CLSM were measured as part of the quality control program (Hook and Clem 1998).
34. Colorado Department of Transportation used CLSM to fill an abandoned 1.52 m (60 inch) diameter pipeline beneath interstate 70 east of Copper Mountain, Colorado. The job required the pumping of CLSM uphill a distance of 61 m (200 ft) through the pipe that had 305-457 mm water (12-18 inch) constantly

running through it. The first three CLSM mixtures were unsuccessful due to observed segregation, however a fourth mixture prepared using an anti-wash admixture was pumped successfully and filled the pipe completely. 367 m^3 (480 cy) of CLSM was used for the project (Hook and Clem 1998).

35. In 1995 CLSM was used to fill the abutments of a bridge located along the Colorado State Highway 135 near Crested Butte, Colorado. 306 m^3 (400 cy) of CLSM was placed in two lifts, a 96 m^3 (125 cy) lift followed by a 210 m^3 (275 cy) lift. The use of CLSM to fill bridge abutments in Colorado cuts time and labor costs and eliminates the rough transition due to settlement of conventional backfill materials from pavement to bridge, known as the bump at the end of the bridge (Hook and Clem 1998).
36. In late 1990s contractors in Denver area used CLSM in tilt-up construction projects. In regular tilt-up construction, floor forms are placed on the foundation 1.15 m (4 ft) inside the exterior wall line and the floor is formed. After the placement of the floor, wall panels are tilted on the foundation and the foundation excavation is filled with conventional backfill materials and the 1.15 m strip between the floor and the wall panels is filled with concrete. However, the use of CLSM to backfill foundation excavation before the placement of the floor allows contractors to form the floor right to the line of wall panels that allows the placement of floor in one pour. The estimated time saving through the use of this method is approximately 2 days (Hook and Clem 1998).
37. In 1991 CLSM was used to backfill exterior foundation walls of a commercial distribution center construction in Loveland, Colorado. The average backfill cavity adjacent to the foundation wall was 1.52 m (5 ft) deep and 457-610 mm wide (18-24 inch). 3058 m^3 (4000 cy) of a regular Colorado DOT mix was used. CLSM was placed in two lifts to prevent extra pressure on the foundation walls and the typical backfilling was performed by one person guiding the chute of the ready mixed truck. Typical placement ranged from 153 to 344 m^3 (200-450 cy) per day and the discharge time changed from 5 minutes to under 1 minute.

Overall the use of CLSM cut two weeks off of the construction schedule (Hook and Clem 1998).

38. In 1994 a CLSM mixture developed by the US Army Engineer Waterways Experiment Station (WES) was used for soil stabilization during the Newark Subbasin Lower Relief Sewer Project construction in Newark, California. The CLSM was a combination of fly ash, bentonite, cement, and water. Class C fly ash was used in the mixture for high early strength. The project required the installation of approximately 2377 m (7800 ft) of 610 to 914 mm (24-36 inch) sanitary sewer using microtunneling techniques. The tunneling machine was to be launched from shafts that were constructed with driven piles and required a hole to be cut in the sheet pile material. The instability of the soil and the high ground water table made the cut of the sheet pile material without soil stabilization impossible. Due to the close proximity of the project to the Oakland bay dewatering equipment used to lower the ground water table was not successful and the use of a chemical stabilization also proved to be ineffective. A CLSM mixture was injected into the soil through six 51 mm (2 in) diameter nipples welded to the inside of the sheet piles at a pressure of 0.17 to 0.34 MPa (25 to 50 psi). After 4 days of curing the sheet piles were cut and the microtunneling equipment was launched. The equipment was able to operate at tunnel progression rates through the CLSM comparable to the rates through the native sand material on the project. The material cost for the CLSM was $54.80 and the associated labor cost was $700. The cost of the chemical stabilization method that was found to be ineffective was $17,000. The total savings due to the use of CLSM in the project was approximately $100,000 that represented 40percent of the total projected profit margin of the project (Green et al. 1998).
39. In 1998 the Oklahoma Department of Transportation constructed three new bridges on US 177 north of Stillwater, Oklahoma. One of the abutments were constructed using a CLSM mixture to compare its performance with conventional backfill and as a possible solution for the bump at the end of the

bridge problem. A total volume of 158 m^3 (207 cy) of CLSM was placed in 4.5 hours using ready mixed trucks. Two ready mixed trucks were placing CLSM simultaneously. The total cost for the CLSM and its placement, including the preparation of the abutment area and the finishing, was $14,560 compared to $1,500 for the conventional backfill. The duration of the construction was 2 days while the construction with conventional backfill materials lasted 4 days. Measurements indicated that the lateral earth pressure and settlement of the approach embankment were generally less compared to the conventional backfill materials (Snethen and Benson 1998).

40. In 1996 a CLSM mixture comprised of water, ash, and bentonite was used to fill part of an abandoned room and pillar coal mine in Preston County, West Virginia. The coal seam had a thickness of 1.5 m (4.9 ft) and was about 70 m (230 ft) below the ground surface. 765 m^3 (1000 cy) of CLSM was injected into the mine which solidified in one week. CLSM flowed approximately 120 m (394 ft) from the borehole and filled the mines satisfactorily (Gray et al. 1998).
41. In 1991 a CLSM mixture comprised of cement, water, ash, sand, and 18-20percent air was used to fill in from the top of the arch of an underground bus tunnel to the subgrade below paving level at downtown Seattle on a busy arterial. A total of 38000 m^3 (49702 cy) of CLSM with a compressive strength of 0.6 MPa (87 psi) was used. CLSM at the consistency of pancake batter was placed directly from chutes and flowed over a city block without aid. 9.18 m^3 (12 cy) of CLSM was placed in 45 seconds where fast production was necessary (Gardner 1998).
42. In 1990s during the construction of a cast in place parking garage with spread footings in Seattle the contractor found out that the areas that were supposed to be bearing soil were an old landfill. Instead of over excavating and backfilling, trenches with vertical walls were cut and filled with a CLSM mixture that had a compressive strength of 0.83 MPa (120 psi). A total of 750 m^3 of CLSM was poured in two pours (Gardner 1998).

43. In 1990s during the update construction of a manufacturing plant in Seattle, manufacturing was being continued around the construction site. The equipment on the site was very expensive and sensitive, therefore cutting the construction time, traffic, and pollution was very important. The use of CLSM cut the time, pollution, and traffic as required by the owner. The mixture was line pumped over 305 m (1000 ft) on some placements (Gardner 1998).
44. About 305 m (1000 ft) of a 914 mm (36 inches) in diameter water main that went under numerous train tracks of a massive switching yard in Seattle had to be replaced. Two fast setting CLSM mixtures with compressive strengths of 0.34 and 0.83 MPa (49 and 120 psi) were used for the project. The mixture with higher compressive strength was used for areas where CLSM was paved over. The tracks were left in place and trenches were cut under the trucks. The contractor poured CLSM in the afternoon and the next day CLSM was covered with railroad ballast and the tracks were opened to use (Gardner 1998).
45. A manufacturing plant was going to be constructed on a Superfund cleanup site in Seattle. Instead of excavating contaminated soil and hauling it to a landfill 640 km (398 miles) away, the owner decided to encapsulate the contaminated soil in CLSM. A design using higher values of cement and fly ash compared to regular CLSM mixtures and the contaminated soil was prepared and tested and found to be satisfactory for EPA requirements (Gardner 1998).
46. CLSM was used to backfill excavations conducted to remove oil contaminated soil adjacent to foundations of existing structures at a former rope manufacturing facility in Plymouth, Massachusettes. The primary goal of the project was to remove as much contaminated soil as possible without damaging the adjacent foundations. CLSM was used to backfill sequential narrow excavations perpendicular to the foundations. CLSM allowed narrow, controlled excavations beneath the groundwater table with limited dewatering and uniform placement of material into the trenches using a pipe like a tremie. CLSM supported excavation equipment after one day of curing, provided support to the sidewalls

of the excavation, and limited the slumping of clean soil into the excavation (Walker and Ash 1998).

47. During the removal of a portion of a warehouse slab for the United States Navy at Rough & Ready Island, Stockton, California, a large void was discovered that was caused by erosion due to tidal and current action of San Joaquin River. Use of compacted conventional backfill was dismissed due to limited space. A CLSM mixture comprised of cement, fly ash, water, sand, and pea gravel was injected through holes drilled along the exterior of the warehouse. 92 m^3 (120.3 cy) of CLSM was delivered by ready mixed concrete trucks and placed in two days to prevent excessive pressures. Total costs were less than 20percent of the amount authorized by the owner for the placing and compaction of conventional granular backfill (Mason 1998).

VITA

CEKI HALMEN
Zachry Department of Civil Engineering
Dwight Look College of Engineering
Texas A&M University
3136 TAMU
College Station, TX 77843-3136

EDUCATION

Ph.D., December 2005
Major: Civil Engineering
Texas A&M University, College Station

M.S., 2000
Major: Construction Management
Texas A&M University, College Station

B.S., 1998
Major: Civil Engineering
Bogazici University, Istanbul, Turkey

PUBLICATIONS

Trejo, D., Halmen, C., Folliard, J. K., and Du, L., 2005, "Corrosion of Metallic Pipe in Controlled Low-Strength Materials – Parts 1 and 2," *ACI Materials Journal*, V. 105, No. 3, pp. 192-201.

Halmen, C., Trejo, D., Folliard, J. K., and Du, L., (forthcoming), "Corrosion of Metallic Materials in Controlled Low-Strength Materials – Part 3," *ACI Materials Journal*

Halmen, C., Trejo, D., Folliard, J. K., and Du, L., (forthcoming), "Corrosion of Metallic Materials in Controlled Low-Strength Materials – Part 4," *ACI Materials Journal*